

# **The Use of GIS and Remote Sensing Techniques to Evaluate the Impact of Land use and Land Cover Change on the Hydrology of Luvuvhu River Catchment in Limpopo Province**

Report to the  
**WATER RESEARCH COMMISSION**

by

**PM KUNDU, FI MATHIVHA & TR NKUNA**  
Department of Hydrology and Water Resources  
University of Venda

**WRC Report No. 2246/1/15**  
**ISBN 978-1-4312-0705-3**

**October 2015**

**Obtainable from**

Water Research Commission  
Private Bag X03  
Gezina, 0031

[orders@wrc.org.za](mailto:orders@wrc.org.za) or download from [www.wrc.org.za](http://www.wrc.org.za)

**DISCLAIMER**

This report has been reviewed by the Water Research Commission (WRC) and approved for publication. Approval does not signify that the contents necessarily reflect the views and policies of the WRC nor does mention of trade names or commercial products constitute endorsement or recommendation for use

## EXECUTIVE SUMMARY

The Luvuvhu River Catchment is one of the regions in South Africa which is undergoing rapid land cover and land use change. Due to the increase in population growth and associated developments in Vhembe District, the catchment has been subjected to considerable land use change over the past decades which are causing accelerated environmental degradation and impacting negatively on the hydrology and water availability in the area. Land use and land cover changes in a catchment can impact water supply by altering hydrological processes such as infiltration, groundwater recharge, base-flow and runoff. Studies that link anthropogenic factors and land cover to hydrology and water resources have not been widely conducted in the catchment. This study was therefore conducted to evaluate the impact of land cover and land use change on the hydrology of Luvuvhu River catchment. The results of this study will be of significance by way of detecting the cause-effect relationships of human induced changes to the hydrology and water resources in the catchment. The information derived will help prevent the potential for human conflict over diminishing resources and disease outbreaks related to waterborne vectors.

Remotely sensed data and ground survey methods were used to evaluate the changes. A combination of multi-date fine, medium and coarse resolution remotely sensed imagery was used to detect and quantify changes. Vegetation data was captured and automated in a GIS-compatible format, which provided flexibility in mapping, data analysis, data management and utilisation. A statistical sampling methodology based on area frame sampling was adopted for this study. The method relied on satellite imagery, orthophoto maps and topographic maps to divide the study area into sample segments. Frequency distributions models (Generalized Extreme Value distributions, the Gumbel or Extreme Value type I distribution, the Lognormal distribution and the Log Pearson type III distribution) were used to describe historical characteristics and magnitudes of floods.

This study found that there had been considerable land use and land cover change over the past decades in the catchment. The 2008 revealed that the most dominant land cover was forest/bushlands/woodlands covering 32.95% of the catchment while water bodies only covered 0.29% of the catchment. Build up areas covered 9.86% of the land as of 2008. These developments were concentrated on hillsides and hilltops in the catchment and they were of concern as they were impacting on the hydrological processes. Developments on slopes had disrupted the hydrologic processes by reducing infiltration, interflow, surface runoff and prevented rainwater from reaching natural water ways. The diversity of the land use in the catchment was related to the diversity of the agroclimatic zones and landscape ecology. The dominant land use categories concentrated specifically on the agricultural application, which was considered the most important human economic activity of the area.

SWAT was applied to the upper part of the LRC in the Levubu-Tshakhuma area. It enabled the delineation of 502 Hydrological Response Unit. The latter aids in efficient management of water resources at catchment. This is because each hydrological response unit is different

from the other in terms of catchment properties. A sensitivity analysis was conducted using the SWAT tool to identify parameters that most influenced predicted flow, sediment, and nutrient outputs. By means of the LH-OAT sensitivity analysis, the dominant hydrological parameters were determined and a reduction of the number of model parameters was performed.

The study made it possible to evaluate the impact of the dynamic geomorphic processes and environmental degradation due to deforestation and intensive land use on stream flows. The impacts of land use and land cover change were determined by the cause-effect relationships of human activity, landscape dynamics and hydrology. Through time series analysis of remotely sensed data and ground survey, it was ascertained that significant change in land cover and land use, particularly the conversion of forest and woodlands to arable and build-up land had occurred. The results showed that an increase in the peak discharges was to be expected, especially for the discharge range corresponding to smaller and medium flood magnitudes.

The study recommends the following:

- The re-afforestation of hills and management of forests;
- The use of image synergism to monitor land cover and land use in the catchment;
- Refurbishment of existing and establishment of new weather and river gauging station;
- Use of suitable land use management practices;
- Concurrent application of biological and physical measures should be promoted depending on the validation of such combinations under given circumstances from engineering, agronomic, and socioeconomic points of view;
- Cultural practices to minimize soil loss should be practiced by selecting vegetative plant materials such as Vetiver grass (*Vetiveria ziz savendara*) that can thrive in the same ecosystem;
- The conservation strategy must involve a package of conservation measures that are economically beneficial to the land owners;
- Settlements and build up areas should mimic natural functions and minimize disruption to hydrologic processes.

## ACKNOWLEDGEMENTS

We acknowledge the support we received from various individuals, organisations and agencies by way of services and products that enabled us to execute this project. Specifically, we acknowledge the South African Weather Services for providing rainfall data; the Department of Water and Sanitation for providing hydrological data; the South African National Space Agency for providing satellite images; the Agricultural Research Council for land cover and land use data as well as soil maps. We acknowledge the Water Research Commission of South Africa for funding the project and highly appreciate the support and guidance that was provided by the reference committee which comprised of the following:

Mr W Nomqophu (Chair)	Water Research Commission
Prof A Taigbenu	University of Witwatersrand
Prof T Abrahams	Council of Geosciences
Prof M Illunga	University of South Africa
Dr T Sawunyama	IWR Water Resources Pty Ltd
Dr W Nyabeze	WR Nyabeze & Associates
Prof B Mwaka	Department of Water and Sanitation

We acknowledge the following individuals for the invaluable support they provided towards this project: Mr T Masakona of Vhembe District Municipality for organizing a stakeholders meeting with officials from the Municipality; Mr Piesanghoek of Piesanghoek macadamia cropland for allowing us to conduct tests and collect samples on his farm; the Mhinga and Tsianda communities for giving access and permission to test and collect samples on their small scale farms; Ms LR Singo, a PhD student in the Department of Hydrology and Water Resources for her invaluable support in helping to organize and analyze large volumes of hydrometeorological data sets.

We acknowledge both the Directorate of Research and Innovations and the Research and Publications Committee of the University of Venda for providing funds for us to attend and participate in International conferences where we presented partial results from the research findings.



## TABLE OF CONTENTS

EXECUTIVE SUMMARY	iii
ACKNOWLEDGEMENT	v
TABLE OF CONTENTS	vi
LIST OF FIGURES	ix
LIST OF TABLES	xi
LIST OF PLATES	xii
LIST OF ACRONMYS	xiii
LIST OF APPENDICES	xv
<b>Chapter 1: Introduction</b>	1
1.1 Background	1
1.2 Rationale	1
1.3 Aims of the study	3
1.4 Location and size of the catchment	3
1.5 Conceptual Framework and Scope	4
<b>Chapter 2: Detection of land cover and land use change</b>	6
2.1 Land cover change between 1986 and 2006	6
2.2 Land use classification in 2006	9
2.3 Land cover change in Lwamondo-Tshakhuma-Tsianda area	10
2.4 Nandoni Dam	11
2.5 Developments on hill sides, Saddles and Bottom lands	12
2.6 Riparian lands	13
2.7 Image registration and analysis for land cover mapping	14
<b>Chapter 3: Land cover and land use mapping</b>	16
3.1 Field Survey for land cover and land use mapping	16
3.2 Area by direct expansion	18
3.3 Land use and Land cover mapping	19
3.4 Dominant land use and land cover types	20
3.4.1 Large scale agriculture	20
3.4.2 Subsistence agriculture	21
3.4.3 Agroforestry	21
3.4.4 Urban/Built-up Area	22
3.4.5 Water	24
3.4.6 Wetlands	24
3.4.7 Eucalyptus forest	26
3.4.8 Woodland, Grassland and Bushland	26
3.5 Pressure on land	28
3.5.1 Land cover and land use statistics for 2013 based on direct expansion and regression estimation	28
3.6 Environmental Monitoring in the catchment	29
<b>Chapter 4: Hydrometeorological data analysis</b>	34
4.1 Rainfall	34
4.2 Temperature and Solar radiation	37

4.3 Evaporation	39
4.4 Evapotranspiration	40
4.4.1 <i>Potential Evapotranspiration</i>	40
4.4.2 <i>Actual Evapotranspiration</i>	40
4.5 The CROPWAT Model analysis	41
4.6 Humidity	42
4.7 Winds	44
4.8 Model Performance	46
4.9 Stream discharges	47
4.9.1 <i>Changes in Flow Regimes</i>	48
<b>Chapter 5: Soil data analysis</b>	51
5.1 Sampling at a test site	52
5.2 Soil texture	53
5.3 Soil moisture	56
5.4 Infiltration	57
5.4.1 <i>Tsianda sampling and test site</i>	58
5.4.2 <i>Mhinga sampling and test site test site</i>	58
5.4.3 <i>Univen School of Agriculture test site</i>	59
5.4.4 <i>Thengwe sampling and test site</i>	60
5.4.5 <i>Mukula sampling and test site</i>	61
5.4.6 <i>Levubu at Dandani/Lakomkom farm sampling and test site</i>	61
5.4.7 <i>Mpheni village at Elim test site</i>	62
5.4.8 <i>Levubu at Tshakuma Village test site</i>	62
5.4.9 <i>Matiyani village at Punda Maria test site</i>	63
5.5 Spatial variability of infiltration rates	64
<b>Chapter 6: Automated Catchment Delineation</b>	67
6.1 Digital Elevation Model	67
6.1.1 <i>DEM generation</i>	67
6.1.2 <i>Threshold</i>	68
6.1.3. <i>Extraction of morphologic and hydrologic properties</i>	68
6.1.4 <i>Catchment delineation</i>	71
<b>Chapter 7: Soil Water Assessment Tool (SWAT) analysis for Levubu-Tsakhuma sub-catchment</b>	78
7.1 Description of the SWAT model	78
7.2 Levubu-Tshakhuma sub-catchment	79
7.3 SWAT soil classification	82
7.4 Hydrologic Response Units	83
7.5 Sensitivity analysis	85
<b>Chapter 8: Impact of Land cover and Land use change in the catchment</b>	88
8.1 Streamflow	89
8.2 Surface runoff	90
8.2.1 <i>Runoff simulation by Curve Number (CN) method</i>	91
8.3 Suspended sediment discharge	94
8.4 Flood frequency and magnitude	96



8.5 Quality controls	101
<b>Chapter 9: Conclusion and Recommendations</b>	102
9.1 Conclusion	102
9.2 Recommendations	103
<b>References</b>	105
<b>Appendix 1: SWAT Report Statistics</b>	110
<b>Appendix 2: Climate/ <math>ET_0</math> data for selected stations in the catchment</b>	133

## LIST OF FIGURES

FIGURE 1.1: Luvuvhu and Letaba Water Management Area	3
FIGURE 1.2: Luvuvhu River Catchment	4
FIGURE 1.3: Conceptual framework of the study	5
FIGURE 2.1: Land cover and land use	7
FIGURE 2.2: Classified image for 2008 showing 8 classes	7
FIGURE 2.3: LRC land use and land cover 2008	8
FIGURE 2.4: Estimated quantities of the various land cover types in the catchment	8
FIGURE 2.5: Land cover change in LRC	10
FIGURE 2.6: Land cover change in Lwamondo Village	11
FIGURE 2.6a: Topo map for period before 1999: No built up in the selected area	11
FIGURE 2.6b: Orthophoto for 2008: New built up in the selected area	11
FIGURE 2.7a: Landsat image for 1986 before construction of Nandoni Dam	11
FIGURE 2.7b: Landsat image for 2008 showing Nandoni Dam	11
FIGURE 3.1: GIS generated sampling grid	17
FIGURE 3.2: Land cover by CAMP project	23
FIGURE 3.3: Water bodies in the catchment	24
FIGURE 3.4: Developments on a large wetland in Thohoyandou	25
FIGURE 3.5: Monthly trends for rainfall and NDVI	32
FIGURE 3.6: Locations and sites for environmental monitoring	32
FIGURE 4.1: Mean annual rainfall	35
FIGURE 4.2: Rainfall trends for Nooitgedacht and Palmaryville: 1960-1985	36
FIGURE 4.3: Rainfall trends for Nooitgedacht and Palmaryville: 1985-2010	36
FIGURE 4.4: Total and effective rainfall distribution for six stations in the study area	37
FIGURE 4.5: Temperature and Solar radiation	38
FIGURE 4.6: Average monthly minimum and maximum temperatures for selected Station in the study area	38
FIGURE 4.7: Spatial variation of evaporation	39
FIGURE 4.8: Average monthly ETo for selected stations in the study area	42
FIGURE 4.9: Average monthly humidity for selected stations in the study area	43
FIGURE 4.10: Average annual humidity for Levubu	43
FIGURE 4.11: Average annual humidity for Thohoyandou	44
FIGURE 4.12: Average monthly wind speed for selected stations in the study area	45
FIGURE 4.13: Average annual wind speed for Thohoyandou	45
FIGURE 4.14: Average annual wind speed for Levubu	46
FIGURE 4.15: Linear regression of estimated ETo over observed ETo	47
FIGURE 4.16: Model validation	47
FIGURE 4.17: Location of gauging stations used in the study	48
FIGURE 4.18: Stream discharge from 1960 to 2012	50
FIGURE 5.1: The spatial distribution of sampling and test sites	51
FIGURE 5.2: Soil map for LRC	54
FIGURE 5.3: Gradational curves for Levubu settlement test site	54
FIGURE 5.4: Gradational curves for various selected sites in the catchment	55

FIGURE 5.5: The soil triangle for LRC	56
FIGURE 5.6: Soil moisture for selected sites in the catchment	57
FIGURE 5.7: Infiltration curves for Tsianda test site	58
FIGURE 5.8: Infiltration curves for Mhinga test site	59
FIGURE 5.9: Infiltration curves for Univen school of Agriculture farm test site	60
FIGURE 5.10: Infiltration curves for Thengwe test site	60
FIGURE 5.11: Infiltration curves for Mukula test site	61
FIGURE 5.12: Infiltration curves for Dandani/Lakomkom test site	61
FIGURE 5.13: Infiltration curves for Elim test site	62
FIGURE 5.14: Infiltration curves for Tshakuma test site	62
FIGURE 5.15: Infiltration curves for Punda Maria test site	63
FIGURE 5.16: Infiltration rates at selected sampling sites	64
FIGURE 5.17: Spatial variability of infiltration rates	66
FIGURE 6.1: Hydrologically corrected DEM	70
FIGURE 6.2: Frequency distribution of heights in the LRC	71
FIGURE 6.3: Sub-catchment delineation	72
FIGURE 6.4: Spatial distribution of local slope for LRC	72
FIGURE 6.5: Automated extraction of the drainage pattern	73
FIGURE 6.6: Longest flow path model for Luvuvhu River catchment	74
FIGURE 6.7: Profile for Luvuvhu River	75
FIGURE 6.8: The spatial distribution of flow direction	76
FIGURE 6.9: Flow accumulation	77
FIGURE 7.1: Hydrologically corrected DEM with buffer zone for the catchment	79
FIGURE 7.2: Location of Leveubu-Tsakhuma sub-catchment	79
FIGURE 7.3: A 2008 Landsat ETM+ image clip for Levubu-Tsakhuma sub-catchment	80
FIGURE 7.4: Levubu-Tsakhuma sub-catchment drainage system	81
FIGURE 7.5: The spatial distribution of local slopes for Levubu-Tsakhuma sub-catchment	81
FIGURE 7.6: Soil-landscape relationship for Levubu-Tshakhuma sub-catchment	83
FIGURE 7.7: The SWAT delineated sub-catchments for Levubu-Tsakhuma	84
FIGURE 7.8: The hydrologic response units for Levubu-Tsakhuma sub-catchment	84
FIGURE 7.9: The default parameters for sensitivity analyse	86
FIGURE 7.10: Trend of NH4 chemical component in the subcatchment	87
FIGURE 8.1: Annual maximum stream flow series for the study area	90
FIGURE 8.2: Runoff trends at A9H016 and A9H003:1960-1985	90
FIGURE 8.3: Runoff trends at A9H016 and A9H003 during the 1985-2010	91
FIGURE 8.4: Observed rainfall and simulated runoff upstream: 1960-1984	93
FIGURE 8.5: Observed rainfall and simulated runoff upstream: 1985-2010	93
FIGURE 8.6: Return periods for annual maximum stream flow	98
FIGURE 8.7: Computed peak flows for the 2, 5, 10, 25, 50, 100 and 200 year	99
FIGURE 8.8: Computed peak flood for the 2, 5, 10, 25, 50, 100 and 200 year return	99

## LIST OF TABLES

TABLE 2.1: Major land cover classes	10
TABLE 3.1: The major land cover classes based on Anderson (1977)	19
TABLE 3.2: Land cover and land use statistics for 2013	29
TABLE 4.1: Location of weather stations and elevations in the LRC	34
TABLE 4.2: Gauging stations used in the study	48
TABLE 6.1: Derivation of primary and secondary attributes	69
TABLE 7.1: Hydrologic response units report	85
TABLE 8.1: Curve Numbers for different sub-catchments	91
TABLE 8.2: Suspended sediment sampling sites	96
TABLE 8.3: Estimated Discharges for GEV distribution	100
TABLE 8.4: Estimated discharges for EV1 distribution	100
TABLE 8.5: Estimated discharges for Log-Normal distribution	100
TABLE 8.6: Computed Discharges for LP3 distribution	101

## LIST OF PLATES

Plate 1: New developments on hills and summits in Thohoyandou	12
Plate 2: New developments on hills at Tsianda village	12
Plate 3: Clearing hills for subsistence farming at Tsianda Village	12
Plate 4: Bush clearing for plantation farming along R524 at Levubu	12
Plate 5: Cleared hill tops for cultivation in Piesanghoek croplands	13
Plate 6: Riverine vegetation in Levubu	14
Plate 7: Macadamia Cropland in Piesanghoek	21
Plate 8: Subsistence crop of maize in Lwamondo	21
Plate 9: Agroforestry in Tsianda Village	22
Plate 10: Eucalyptus tree plantation at Ratombo	26
Plate 11: Wood/bushland at Levubu	27
Plate 12: Mopane trees at KNP	27
Plate 13: The acacia trees at KNP	27
Plate 14: Luvuvhu River at KNP	49
Plate 15: Flooding in Luvuvhu River at KNP	49
Plate 16: Collecting samples for determining the texture and moisture content	52
Plate 17: Infiltration test at Mhinga site	59
Plate 18: Suspended sediment in Tshinane River at Gondeni	95
Plate 19: Flood water levels in February 2000 in KNP	97

## LIST OF ACRONYMS

ACRU	Agricultural Catchments Research Unit
AMC	Antecedent Soil Moisture Content
ARC-ISCW	Agricultural Research Council's Institute for Soil Climate and Water
CAMP	Catchment Management and Poverty Alleviation
CEP	California Environmental Protection
CLUE-s	Conversion of Land Use and its Effects
CN	Curve Number
CROPWAT	Crop Water
DEM	Digital Elevation Model
DFID	Department for International Development
DWA	Department of Water Affairs
DWAF	Department of Water Affairs and Forestry
ETM	Enhanced Thematic Mapper
ET <sub>o</sub>	Reference Evapotranspiration
EV1	Extreme Value
FAO	Food and Agricultural Organisation
GCM	Global Circulation Model
GEV	Gumbel Extreme Value
GIS	Geographical Information Systems
HRU	Hydrological Response Unit
HSG	Hydrological Soil Groups
HYLUC	Hydrological Land Use Change
ISRIC	International Soil Reference Information Centre
ISSS	International Soil Science Society
ITCZ	Inter-tropical Convergence Zone
IUSS	International Union of Soil Sciences
KNP	Kruger National Park
LandSat	Land Satellite
LH-OAT	Latin-Hypercube One-factor-At-a-Time
LN	Log Normal
LP III	Log Pearson type III
LRC	Luvuvhu River Catchment
MERIS	Medium Resolution Imaging Spectrometer
MODIS	Moderate Resolution Imaging Spectrometer
MSS	Multispectral Scanner
MUKEY	Map Unit Key
NDVI	Normalized Difference Vegetation Index
NOAA	National Oceanic and Atmospheric Administration
NRCS	Natural Resources Conservation Service
NSE	Nash-Sutcliffe
RCMRD	Regional Centre for Mapping of Resources for Development
RS	Remote Sensing

SANSA	South African National Space Agency
SAWS	South African Weather Services
SCS	Soil Conservation Services
SOTER	Soil and Terrain
SRTM	Shuttle Radar Topographic Mission
SWAT	Soil Water Assessment Tool
TIN	Triangulated Irregular Network
TM	Thematic Mapper
UNESCO	United Nations Educational, Scientific and Cultural Organization
UNIVEN	University of Venda
USDA	United States Department of Agriculture
USP	Unit Stream Power
VDM	Vhembe District Municipality
WRS	World Reference System
WWAP	World Water Assessment Programme





## **CHAPTER 1**

### **INTRODUCTION**

#### **1.1 Background**

Luvuvhu River catchment (LRC) is one of the regions in South Africa which is undergoing rapid land cover and land use change. Due to the increase in population growth and associated developments in Vhembe District Municipality (VDM), the catchment has been subjected to considerable land use change over the past decades which are causing accelerated environmental degradation and impacting negatively on the hydrology and water availability in the area. The changes have had a significant impact on the hydrology by altering hydrological processes such as infiltration, surface runoff, base-flow and stream discharges.

A fundamental but largely unresolved problem in the hydrology of LRC is to establish relationships between the physical attributes and the flow characteristics of the streams and rivers leaving the catchment. These relationships are sought to improve model-based predictions of stream discharges by the procedure of extrapolating research results obtained from intensively studied catchments that are similar to a broader region. Flow characteristics such as total storm flow and base flow volumes, base flow recession rates and peak storm flow volumes have major implications for downstream water supply, risk of flood damage, flood exposure, water quality and catchment erosion potential, and need to be predicted accurately if water resources are to be effectively managed. Predicting flow characteristics is especially important where changes in land use is anticipated and where alterations to the flow regime need to be assessed.

Studies that link anthropogenic factors and land cover to hydrology and water resources have not been widely conducted in the catchment. Thus, the results of this study will be of significance by way of detecting the cause-effect relationships of human induced changes to the hydrology and water resources in the catchment. The information derived will help prevent the potential for human conflict over diminishing resources and disease outbreaks related to waterborne vectors.

#### **1.2 Rationale**

Land use and land cover changes have a significant impact on the hydrology of a catchment and hence also influence available water resources in a catchment. Land use and land cover changes in a catchment can impact water supply by altering hydrological processes such as infiltration, groundwater recharge, base-flow and runoff (Calder, 1992; Miller *et al.*, 2002; Jewitt *et al.*, 2004). Due to the rapid population growth and development in the VDM, the LRC in northern eastern Limpopo Province covering 3500 km<sup>2</sup> (DWAF, 2004) has been subjected to considerable land use and land cover changes over the past decades. Rapid land use change is causing accelerated environmental degradation and impacting negatively on the hydrology and water resources availability of the area. There is potential for human conflict over diminishing resources.

Studies have been conducted on the impacts of land use and land cover change on hydrology and water resources using different models and computer software's. Recent studies demonstrated the potential of an integrated modelling approach to evaluate the impact of land use changes on water resources (Lin *et al.* 2006; Bithell and Brasington, 2009). Lin *et al.* (2006) combined the Conversion of Land Use and its Effects (CLUE-s) land use change model and a distributed/lumped hydrological model developed by Haith and Shoemaker (1987) to evaluate the impacts of land use change scenarios on the hydrology and land use patterns in the Wu-Tu watershed in Northern Taiwan. The study found that the impact on hydrological processes was very significant and cumulatively influenced by land use changes.

Studies that link land use and land cover to hydrology and water resources have not been widely conducted in South Africa. Jewitt *et al.* (2004) conducted a study in the LRC on water resources planning and modelling for the assessment of land use changes. This study made use of the ACRU (Agricultural Catchments Research Unit) and HYLUC (Hydrological Land Use Change) models and concentrated more on the upper Mutale quaternary catchment which is dominated by rural settlements and therefore the results of the study are not representative of the state of the entire river catchment. Thus, a study that will assess the changes in land use and land cover and their impacts on hydrology and water resources of the entire LRC is of significance. However, the current study aims at classifying and analyzing land use and land cover between 1970 and 2010 from both aerial photos and satellite images, where land use data by Griscom *et al.* (2009) will also be used as part baseline data. This is imperative because they might have been changes that occurred in five years after Griscom *et al.* (2009) study period (this is important for hydrological studies such as this to cover a period of at least 30 years). In addition previous studies did not include the urban/ build up area in their land uses classification. There are numerous developments occurring in the LRC and it is important that these are included in the land use analysis. SWAT also requires data that is collected in a certain format, therefore the data collected will be in line with the SWAT requirements. The use of Quickbird images will enhance the validation the results obtained from other imagery of low resolution.

The advantage of utilizing high resolution imagery (Quickbird images) especially in built up areas, is the utilization of segmentation tools with a hybrid classification technique (a rather new trend in image classification) and a rule-based thematic categorization depending on information both at pixel and object level. A variety of images will be utilized depending on the area being interpreted. For example, the LandSat Enhanced Thematic Mapper Plus (ETM+) supplies high resolution visible and infrared imagery, with thermal imagery available at pixel resolution of 30 m and 60 m respectively. Spot is available in 2.5 to 10 m while Geo eye which is an advancement of Ikonos is available at 0.5 m and 1.65 m resolution. To model river flow and water quality, where rivers/ streams are temporally dynamic, the resolution of Spot (10 m) may be too coarse for such small rivers and streams.

The automated extraction of morphologic properties will provide landform information showing hills, slopes and valleys, all of which are important components in development planning for catchments (Kundu and Olang, 2011). Morphologic and hydrologic properties of

a catchment gives information on how different hydrological parameters such as infiltration rate will behave after hydrologic events such as rainfall and hence the results will aid in better management of water resources in a catchment. Furthermore geomorphic characteristics will improve the quality of the model and enhance the accuracy level of the findings. Previously, characteristics have been derived with the use of conventional techniques like contour lines or field survey data from levelling.

This study assessed and modeled the impacts of land use and land cover changes over a period of 40 years on the hydrology of the rivers in the study area and the effects on water resources availability. The results will enhance water resources planning and management to ensure that there is adequate water supply during the both the wet and dry seasons.

### 1.3 Aims of the study

- To classify and quantify the land use and land cover changes in the LRC between 1970 and 2010
- To determine the hydrology of the LRC
- To extract the geomorphologic and hydrologic properties of the study area from Digital Elevation Models (DEMs)
- To model the impact of land use and land cover changes on the hydrology of the LRC

### 1.4 Location and size of catchment

The study area is located in Luvuvhu and Letaba water management area as shown in Figure 1.1.

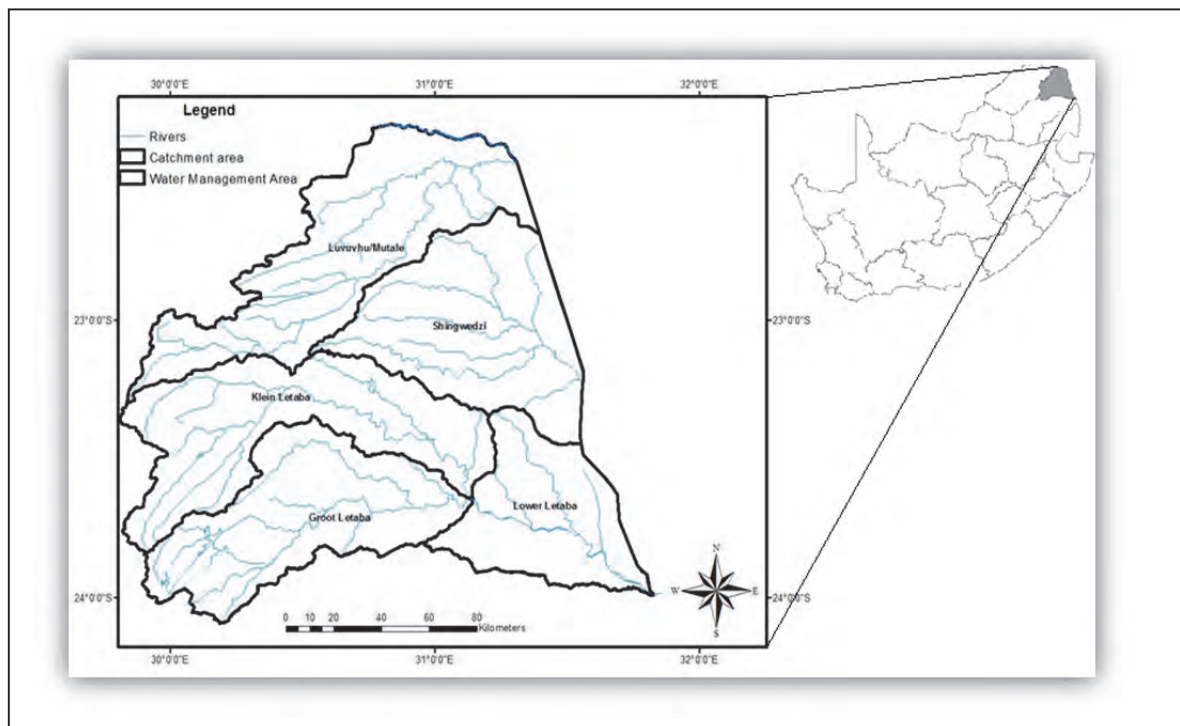


Figure 1.1: Luvuvhu and Letaba Water Management Area

LRC which was the study area is located in VDM of the Limpopo Province in North-eastern South Africa, between latitudes 22°17'34"S and 23°17'57"S and longitudes 29°49'46"E and 31°23'32"E, as shown in Figure 1.2. The relief for the catchment consists of a land system comprising of a landscape of plains, hills and mountains and covers an area of about 5941 km<sup>2</sup> (DWAF, 2002).

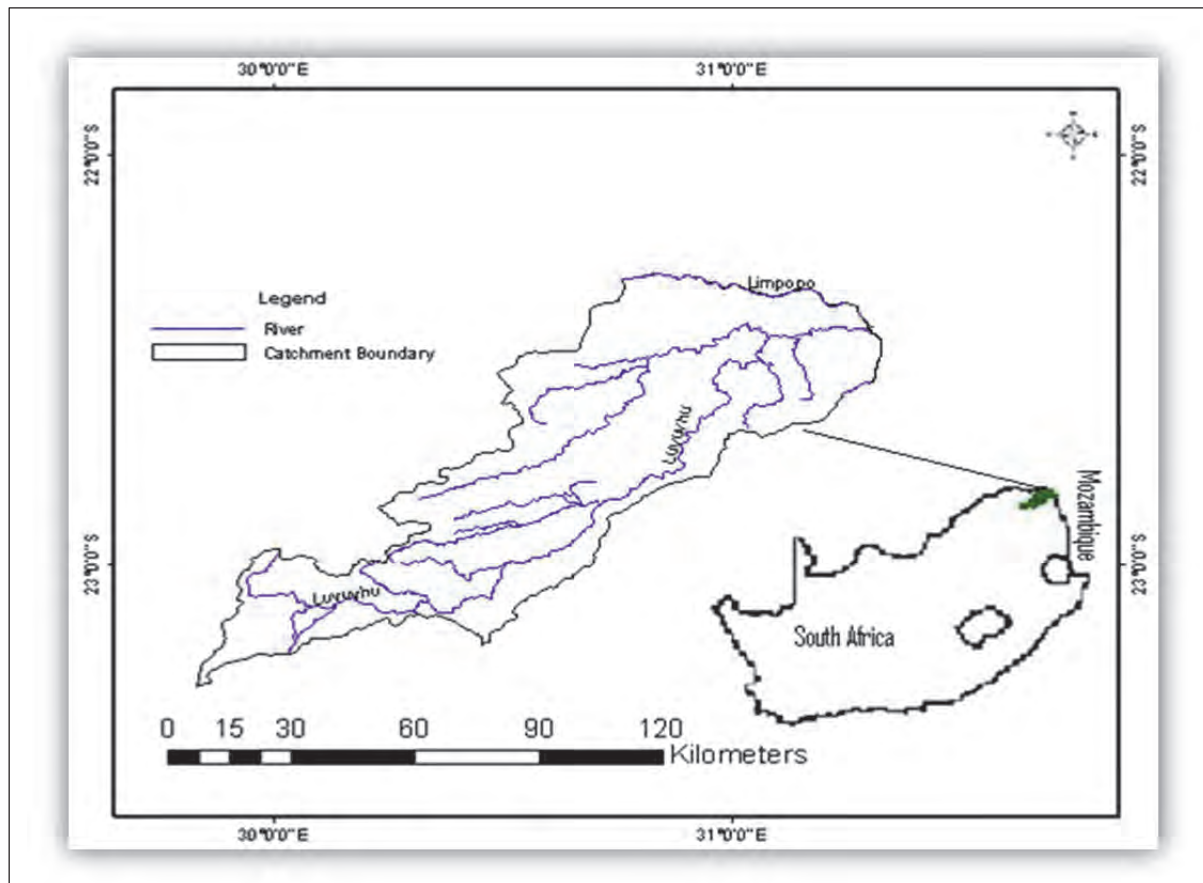


Figure 1.2: Luvuvhu River Catchment

The river originates from Soutpansberg Mountains and drains into the Limpopo River, which extends into Mozambique. The climate of the area is largely influenced by the Inter-tropical Convergence Zone (ITCZ), modified by local orographic effects. Rainfall distribution in the catchment is classified as unimodal, having a rainy season predominantly between the months of October to January with the average annual rainfall of about 200-400 mm (Reddy, 1985).

### 1.5 Conceptual Framework and Scope

In order to achieve the objectives of the study, a conceptual framework was formulated. The main theme was broken into concepts and then broken down into constructs and furthermore into variables. The frameworks are presented in Figure 1.3.

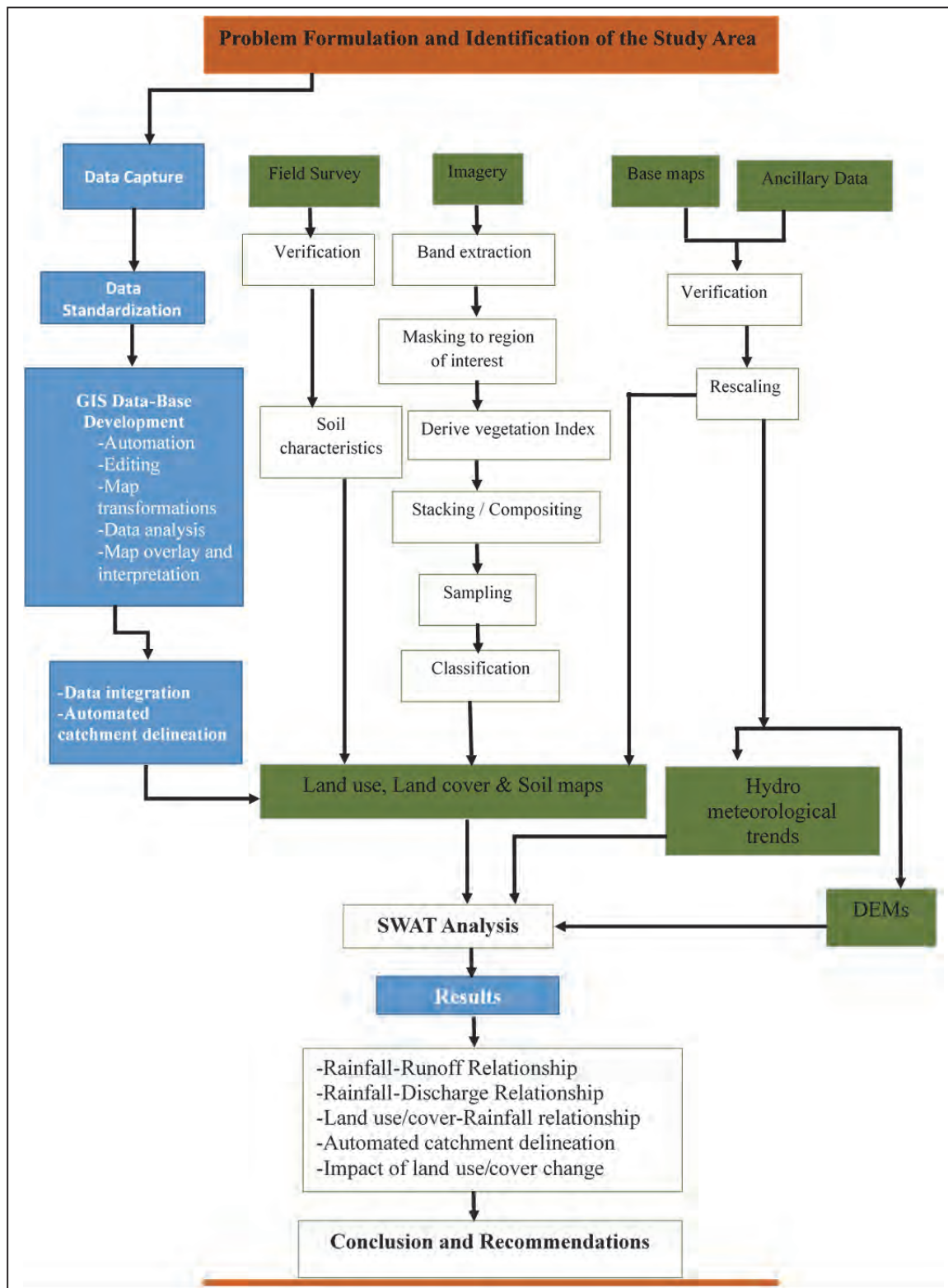


Figure 1.3: Conceptual framework of the study

## **CHAPTER 2**

### **DETECTION AND ANALYSIS OF LAND USE AND LAND COVER CHANGE**

Remotely sensed data and ground survey methods were used to detect and evaluate the land cover and land use change which occurred in the catchment. A combination of multi-date fine, medium and coarse resolution remotely sensed imagery was used to detect and quantify changes.

Vegetation data were captured and automated in a GIS (Geographical Information System)-compatible format, which provided flexibility in mapping, data analysis, data management and utilisation. The use of GIS protocols had the advantage to facilitate effective resource inventory for LRC by ensuring compatibility and widespread use of the information by various stakeholders. The vegetation maps and associated information will support a wide variety of planning concerns, and address issues about vegetation types and their relationship to environmental processes across the landscape. The data will provide a consistent means for the inventory and monitoring of plant communities and, will support environmental management by providing a consistent basis for the characterization of the biological components of different ecosystem units.

#### **2.1 Land use classification for 2006**

The objective of classification was to group together a set of observational units on the basis of their common attributes. The baseline data for land cover and land use showing 27 different classes as described in the legend in Figure 2.1 was obtained from ARC (Agricultural Research Council).



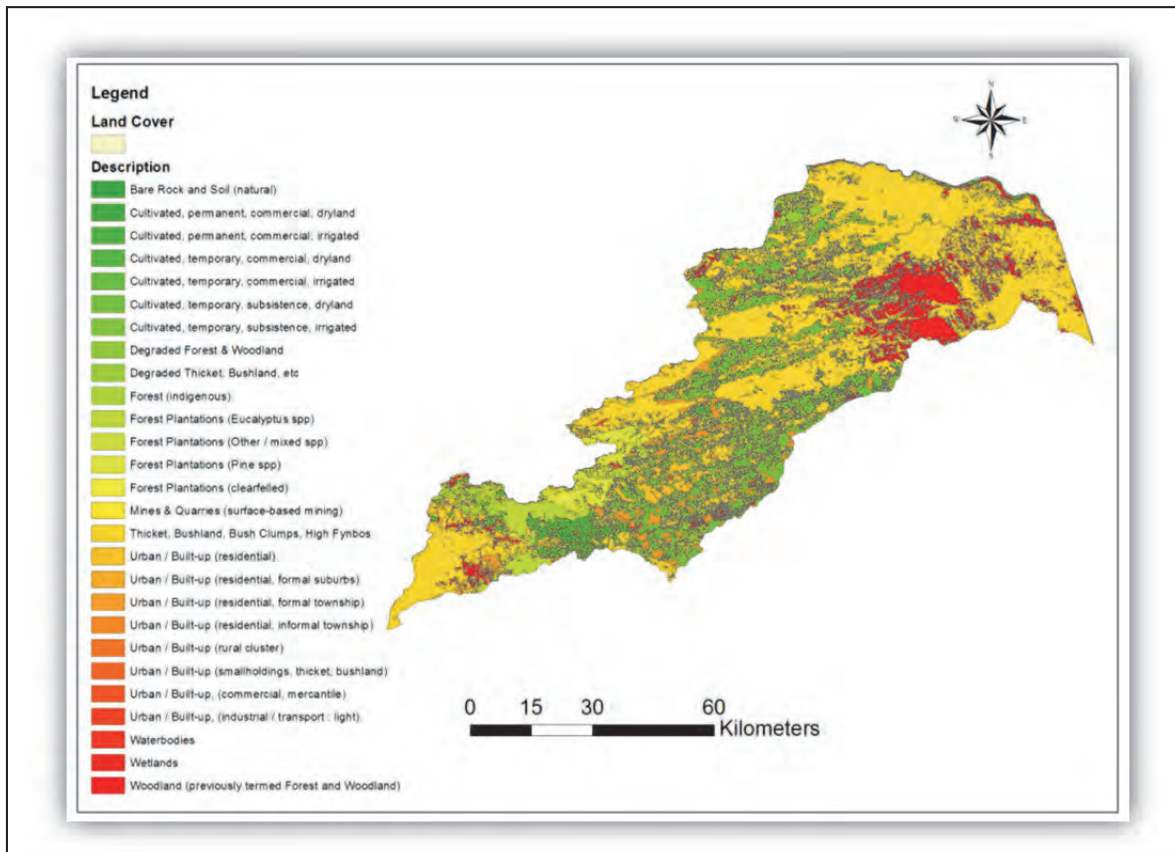


Figure 2.1: Land use and Land cover (Source: ARC, 2006)

Figures 2.2 and 2.3 show a classified full scene image for 2008 showing the dominant land cover classes and the land use and land cover map of the LRC respectively. The dominant land cover classes included herbaceous vegetation, cropland, water, forest-bushland-woodland, urban/built up, open grassland, and riverine vegetation.

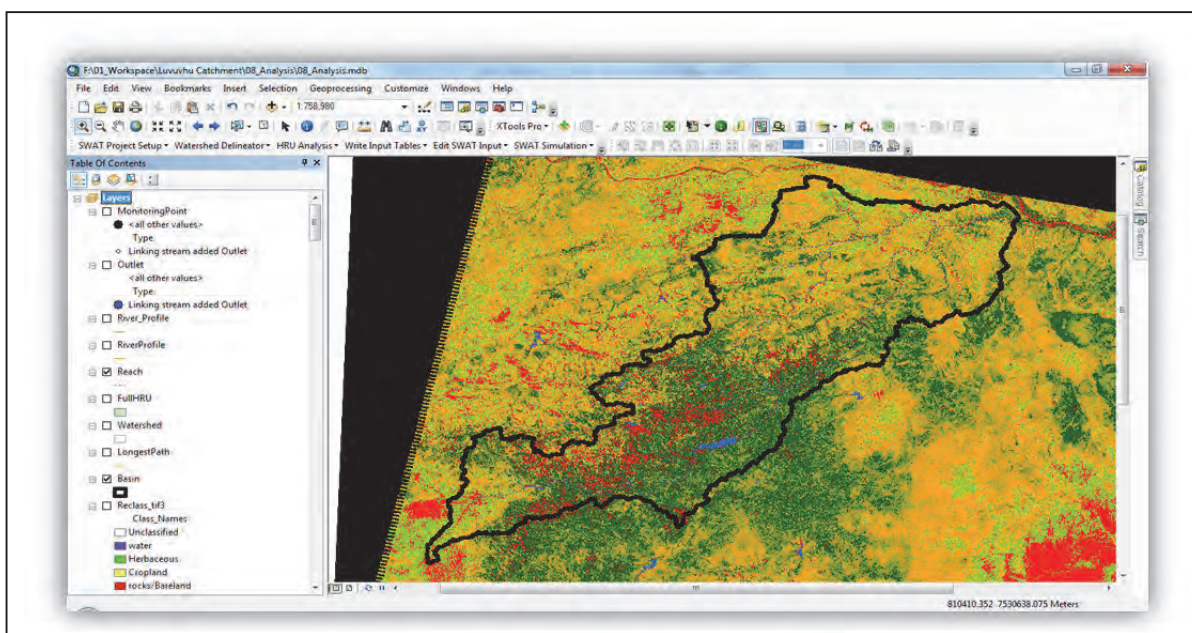


Figure 2.2: Classified image for 2008 showing 8 classes (Image: Path 169, Row 76)

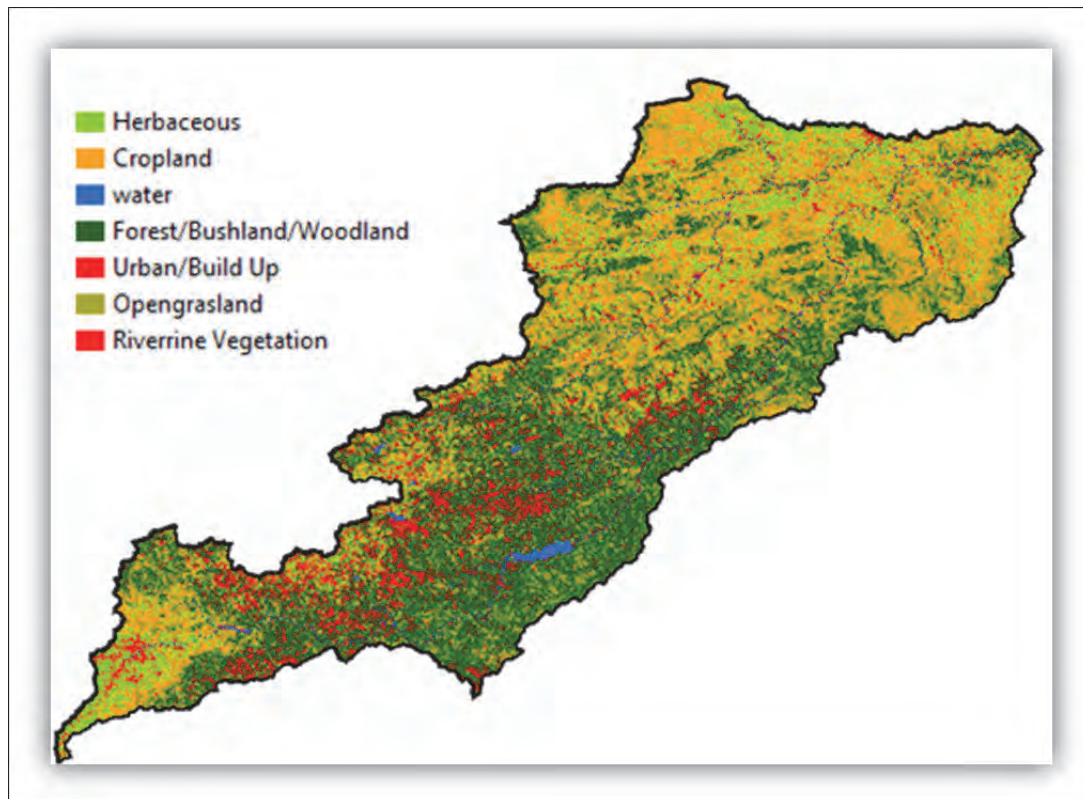


Figure 2.3: LRC land use and land cover for 2008

Figure 2.4 showed the estimated quantities of the various land cover types in the catchment from the classified 2008 image. The most dominant land cover is estimated to be that of forest/bushlands/woodlands covering 32.95% of the catchment while water bodies only covers 0.29% of the catchment. There is therefore a need to conserve the water bodies in the catchment so that they do not degrade as they are already small in term of catchment coverage.

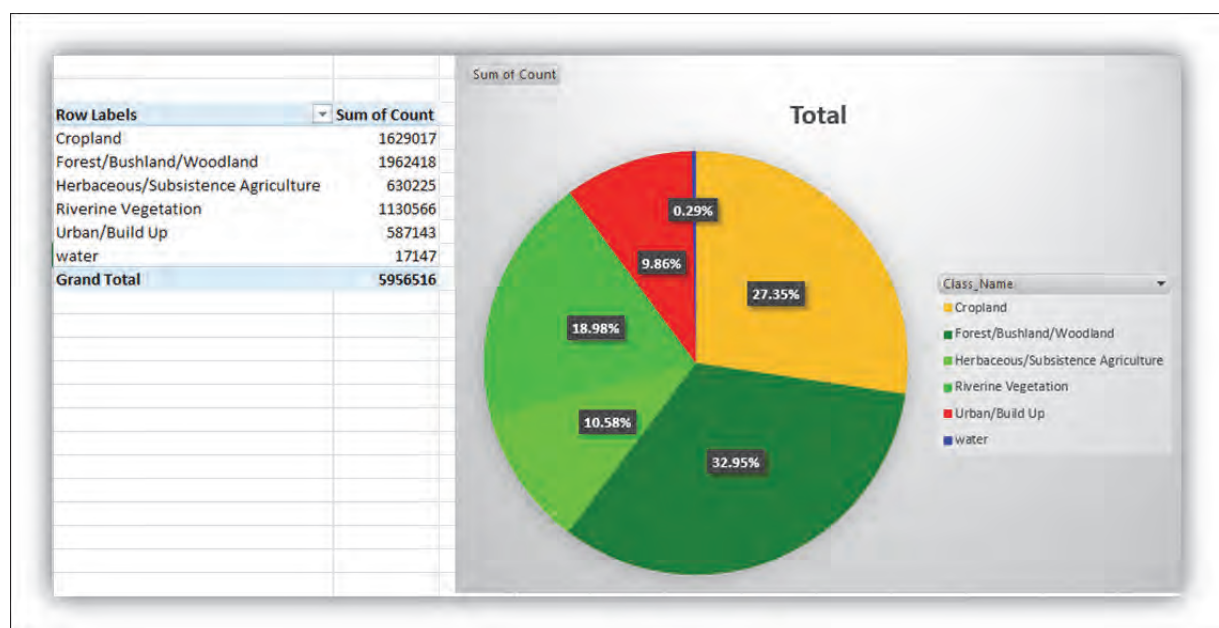


Figure 2.4: Estimated quantities of the various land cover types in the catchment



## 2.2 Land cover change between 1986 and 2006

Baseline land cover data was obtained from Landsat MSS, Landsat TM and land sat ETM+ for Path 169 Row 76 (P169R76) on the World Reference System (WRS) which were acquired from the Regional Centre for Mapping of Resources for Development (RCMRD). SPOT images were provided by the South African National Space Agency (SANSA). Topographic sheets obtained from the National Geospatial Information were used to provide ancillary data which assisted in image analysis and classification.

In order to obtain consistent land cover datasets for semi-distributed hydrological modelling, a per-pixel image classification approach is preferred. The images were classified based on a procedure called guided clustering by Yuan *et al.* (2005). The accuracy of the quantified land cover changes were assessed with the help of reference datasets based on the standard measures for assessing the accuracy of remotely sensed data known as the overall accuracy and the kappa index (Congalton and Green, 1999).

Changes in land cover were detected through classifications of Landsat Multispectral Scanner (MSS) images, Landsat Thematic Mapper (TM) images and Landsat Enhanced Thematic Mapper plus (ETM+) images in ERDAS environment. In order to assess the land cover changes, together with other spatial datasets, a 7 x 7 majority filter was applied to remove small isolated pixels arising out of the classification. The images were later converted into vector coverages and used to derive the required land cover statistics with the derived sub-catchments.

Topological and morphometric characteristics of the catchment were derived from the global digital elevation model developed by the Shuttle Radar Topographic Mission (SRTM). Tiles at a spatial resolution of 90 m x 90 m were obtained in GeoTiff image format, pre-processed and later registered. A DEM was subsequently resampled to a nominal pixel resolution of 30 m by 30 m using the bilinear interpolation technique and hydrologically corrected through a DEM burn-in procedure and sink removal.

To minimize distorting spectral characteristics caused by mosaicking multi-date images before classification, the scenes were independently classified. The multi-temporal satellite images were first resampled to a common spatial resolution of 80 m using the nearest neighbour interpolation technique as described by Jensen (2005).

There was significant land cover change from forest land, woodland and open grassland to medium size farms, subsistence agriculture and built-up land from a classified image showed the land cover change for the catchment between the 1980s and 2000 as shown Figure 2.5 while Table 1 showed the major land cover classes.

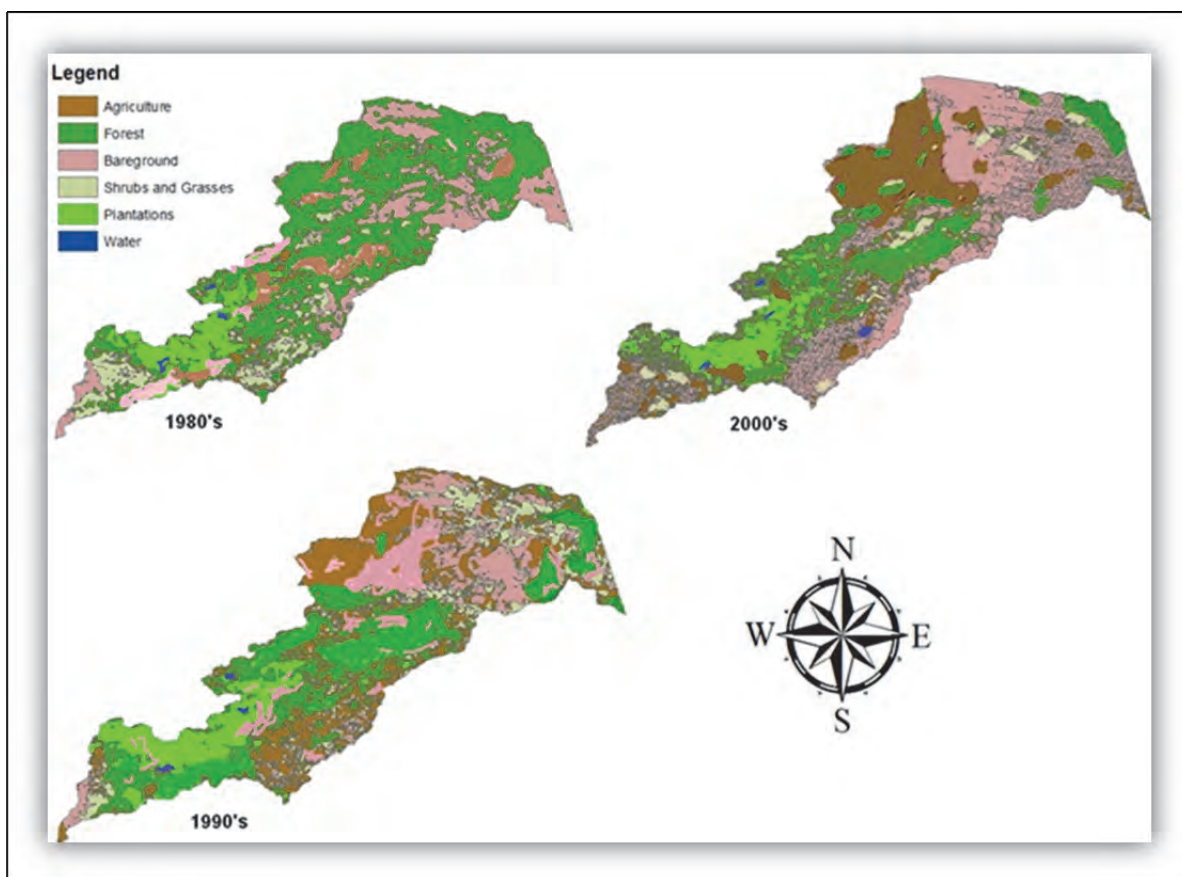


Figure 2.5: Land cover change in LRC

Table 2.1: Major land cover classes

Class Name	Description
Agriculture	This included cumulative land under different crops
Natural forest	Included the natural vegetation and shrubs
Bare ground	This represented virgin land, unoccupied land, settlements and other buildings, including all residential areas in rural and peri-urban
Water bodies	This class included all the dams and other bodies containing clear open water
Plantation	These were mainly planted commercial trees.
Shrub and Grass	Represented all the areas covered by tall grass and bushes of all types

### 2.3 Land cover change in Lwamondo-Tshakhuma-Tsianda area

The Lwamondo-Tshakhuma-Tsianda area shown in Figure 2.6 is an important headwater catchment area for rivers in Limpopo water resources management region. Figure 2.6a and 2.6b are showing the land cover change over the area. The selected area showed the land use before change in 1999 and after change in 2008. Land cover data prior to change was obtained from a topographical map and the after change data was obtained from an orthophoto map of 2008. Before change, the area was open grassland with scattered trees. After change, the area is under cultivation, open clearing and built-up. The latter changes are evident from the below images. In 2008 there were more settlements along the Lwamondo

road both on the left and the right hand side of the road, these settlements where not present in the topographical map that was produces before 1999.

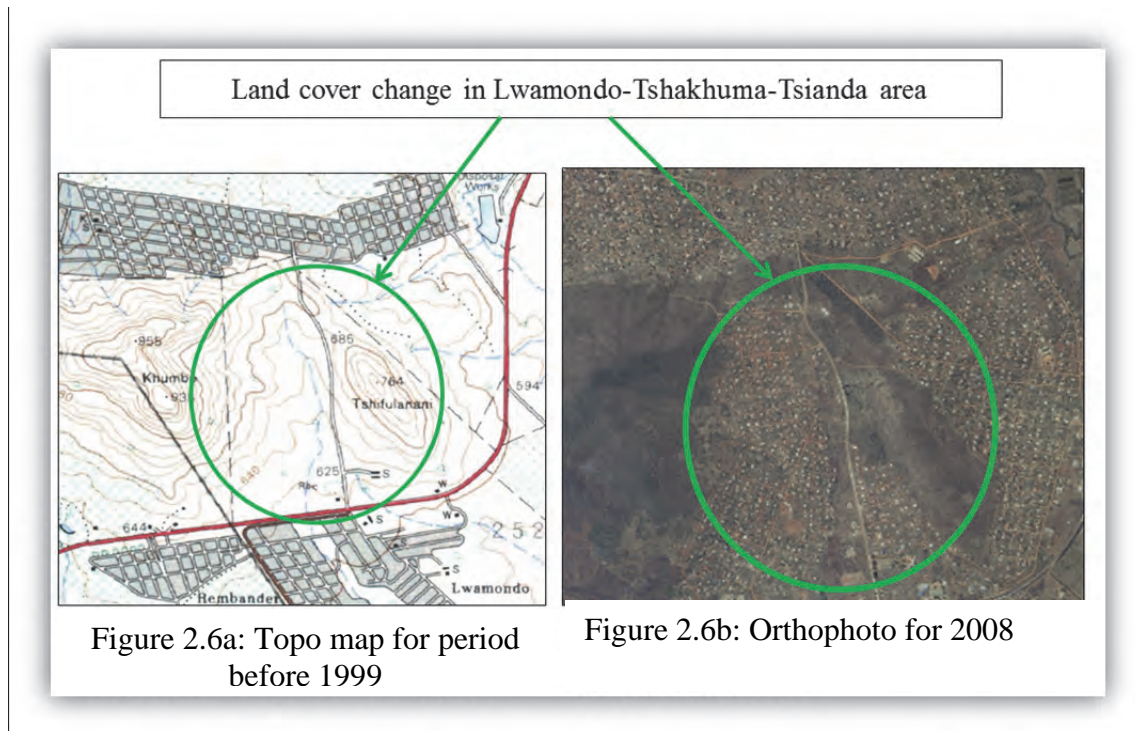


Figure 2.6 Land cover change in Lwamondo Village

## 2.4 Nandoni Dam

Nandoni Dam did not exist in 1986 and does not appear in the Landsat image for that year. Figure 2.7a and 2.7b clearly shows that the water body did not exist in 1986 as can be noted from the 1986 image and is only present in the 2008 image.

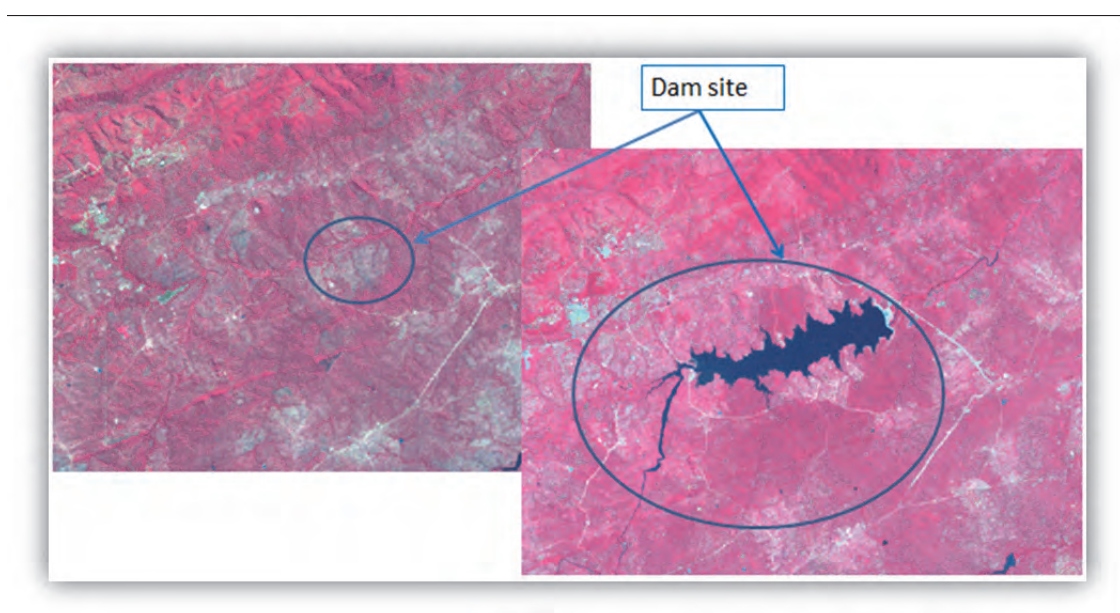


Figure 2.7a: Landsat image for 1986, before construction of Nandoni Dam

Figure 2.7b: Landsat image for 2008 showing Nandoni Dam



## 2.5 Developments on hill sides, Saddles and Bottom lands

Developments on hill sides, saddles and bottom lands were found in Tshakhuma, Lwamondo, Tsianda, Thohoyandou and Mhinga. The major land use in Tshakhuma and Tsianda was agroforestry and built up land, whereas Thohoyandou and Mhinga were mainly under built up which extended up to summit surfaces. The main landform elements were moderately inclined to steep slopes and hillcrests ranging from 5-58% and level to gently inclined valley bottoms of inclination of between 2-5%. Hill sides comprised of land elements that were moderately inclined to steep. Plates 1 to 5 depicts treatment of the land in some parts of the catchment.

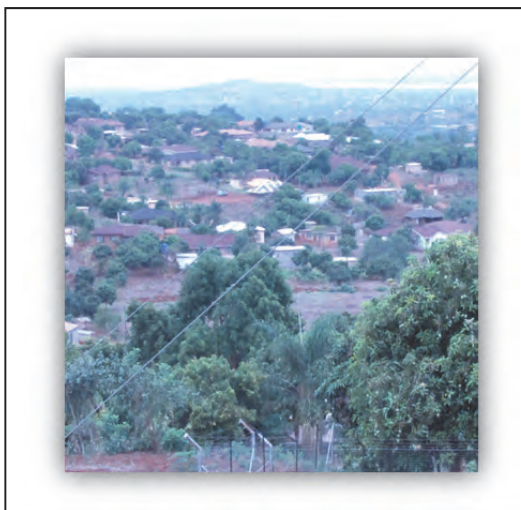


Plate 1: New developments on hills and summits in Thohoyandou

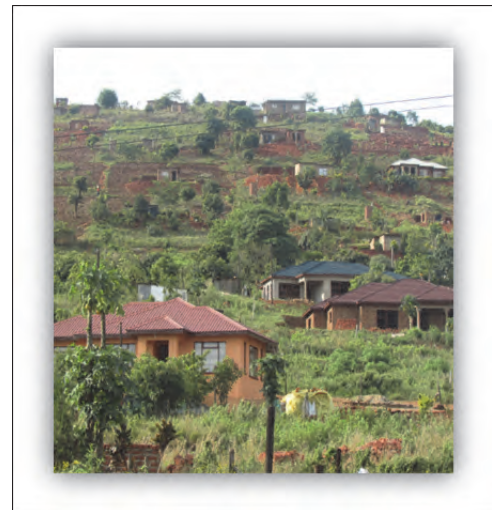


Plate 2: New developments on hills at Tsianda Village



Plate 3: Clearing hills for subsistence farming at Tsianda Village



Plate 4: Bush clearing for plantation farming along R524 at Levubu



Plate 5: Cleared hill tops for cultivation in Piesanghoek croplands

The bottom lands could contain soils developed on infill from volcanic ashes. Such soils will be poorly drained, moderately deep, dark greyish brown, mottled, very firm clay loam, abruptly underlying a topsoil of acid humic friable loam (Planosols). They could also contain soils developed on infill from intermediate igneous rocks (phonolites). These are poorly drained soils, moderately deep, dark grey to grey, mottled, firm clay, with a humic topsoil. They could also be soils developed on infill mainly from undifferentiated basement system rocks (predominantly gneisses). They are imperfectly drained, very deep, dark grey to dark brown, very firm, slightly to moderately calcareous, moderately sodic clay, with a saline deeper subsoil (chromic Vertisols).

## 2.6 Riparian lands

Riparian zones are complex systems composed of aquatic ecosystems which perform vital environmental functions. Riparian lands had been encroached upon in the catchment, especially in middle and lower catchment areas. There was systematic thinning of the riverine vegetation in the upper catchment as shown in Plate 6. It is required that the riparian zones be managed properly and the necessary environmental laws applied and enforced. The sun System and the Integrated Riparian System are the most preferred for LRC. The sun system involves the planting of woody perennials with annual or other crops that require full sunlight (Rudd, 2006). The integrated riparian system is the management of areas bordering water bodies and watercourses to enhance and protect aquatic resources while generating economic benefits



Plate 6: Riverine vegetation in Levubu

## 2.7 Image registration and analysis for land cover mapping

The actual process of land cover mapping required the identification and delineation of homogeneous cover types on orthophoto maps and satellite images. Once identified, the polygons were labelled with the cover units identified in the classification.

To georeference and register raster orthophoto maps and satellite images, which were at different resolutions a definition of how the data was situated in map coordinates was made. The process included assigning a coordinate system to collected datasets such as weather stations in the catchment that associated them with a specific location with known geographic coordinates. Georeferencing raster data allowed it to be viewed, queried, and analyzed with other data in point and vector formats such as gauging stations and drainage lines. The raster data was aligned to existing spatial data such as a road junction that resided in the desired map coordinate system. The basic principle for georeferencing was to move the raster data into the same space as the target data by identifying a series of ground control points of known  $x$ ,  $y$  coordinates that linked locations on the raster with locations in the target data in map coordinates. A combination of one control point on the raster and the corresponding control point on the target data formed a link. The number of links needed to create depended on the method to be used to transform the raster to map coordinates. Typically, having at least one link near each corner of the raster and a few throughout the interior produced the best results. In general, the greater the overlap between the raster and target data, the better the alignment results because more widely spaced points with which to georeference the raster enhance the process.

It is important to note that remote sensing techniques have limitations based on technical constraints such as the scale of observation. Therefore identification of objects will not be the same such that what is observed and mapped at 1:10 000 will be different from what is observed and mapped at 1:250 000. To avoid misrepresentation of land cover types mapped at different scales, ground truthing and field verification should be carried out before the final compilation of reports.

The primary objective of land cover mapping was to produce quality, standardized maps of the land use and other land cover types occurring within the catchment. The end product of a classification was a set of groups derived from the units of observation where, typically, units within a group shared more attributes with one another than with units in other groups. For vegetation classification, the unit of observation was typically the *stand*, defined as a relatively homogeneous area with respect to species composition, structure, and function.

## **CHAPTER 3**

### **LAND USE AND LAND COVER MAPPING**

#### **3.1 Field Survey for land use and land cover mapping**

The methods used were based on integration of Remote sensing, GIS and ancillary data. The compilation of the land use and land cover map was performed essentially as a Geospatial project based on visual interpretation and digital image classification of satellite images, aerial photographs and ground truthing. Fields defined by roads and fence lines were used within grids to classify land use in each sample segments.

Land cover classification and mapping is primarily intended for land resources planning and management. The method emphasizes conspicuous features of the land surface to convey an overall perspective of what is visually present on the land. Degradation of vegetation can be noticed in terms of decreased biodiversity, decreased woody biomass, loss of useful species and increased presence of invader species. A typical problem in land cover and land use mapping is the problem of mixed objects. The three types of mixtures that exist include first, the juxtaposition, where many objects may be observed simultaneously; second, the superposition where various land uses are found on top of each other or crops under tree cover; and third, the mixtures in time, where there is frequent succession of crops. In general, a pro-rata or dominance rules were applied for superposed objects. This technique has the advantage of limiting the number of classes for statistical and cartographic purposes.

A statistical sampling methodology based on area frame sampling was adopted for this study. The method relied on satellite imagery, aerial photographs and maps to divide the study area into sample segments (Gallego, 1995). The unaligned area frame sampling scheme was preferred for the area because of the heterogeneous land use cover found in the catchment. A high densification of for sample sites was preferred in order to validate the consistency of the land cover and land use database. Individual land parcels and ground cover classes were identified in each sample segment. Unaligned systematic random samples were chosen with 1 km<sup>2</sup> fixed size ground segments. A 10 km x 10 km grid corresponding to the 1:50 000 map sheet shown in Figure 3.1 was overlaid upon the image, after which the locations of ground segments were chosen randomly from each block of 10 km x 10 km. Figures 3.1 showed the GIS generated segment sampling grids for the LRC. Each segment had unique and identifiable boundaries outlined on aerial photographs, Landsat images and maps. The total number of ground segments were 430, which produced a sampling frequency of 7.24 % of the 5941 km<sup>2</sup> study area.



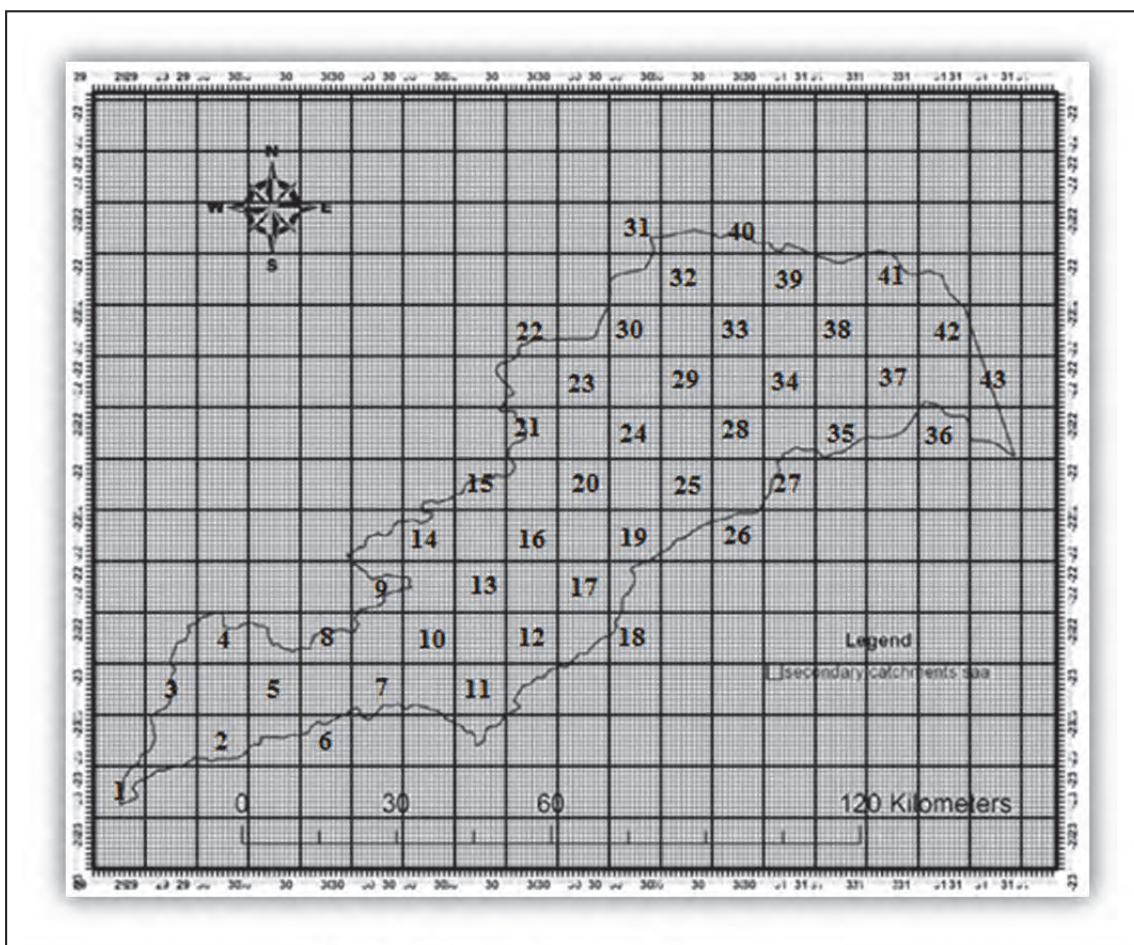


Figure 3.1: GIS generated sampling grid

Field investigators under capacity building visited the segments and recorded information about agricultural activity within the segment boundaries. The area frame technique was used to collect information about crops, homesteads, livestock and other environmental factors. Individual land parcels, land use and ground cover classes were identified in each sample segment. Their locations were accurately determined by using conspicuous land marks and features such as road junctions and planted Eucalyptus and first-hand knowledge of the area by the researcher. By the method of direct expansion, the area for each land use and land cover class was determined for the entire study area. Data verification processes involved rechecking photographs and images to determine if the interpretation was correct, and where questions existed, the site was field verified. At least 2% of the segments were field checked, results tabulated and compared to the original interpretation.

### 3.2 Area by direct expansion

The estimated areas were calculated by the formulas given below (Taylor *et al.*, 2002):

Mean proportion:

$$\bar{y}_c = 1/n \sum_{i=1}^n y_i \quad (3.1)$$

where,  $\bar{y}_c$  = Mean proportion of each coverage area,  $y_i$  = Coverage proportion for each segment and  $n$  = number of segments in the sample. The total area under coverage was obtained using Equation 3.2 given below:

$$Z_c = D\bar{y}_c \quad (3.2)$$

where,  $Z_c$  = Estimate of the coverages area and  $D$  = Total study area. The variance of area estimator was calculated using equation 3.3:

$$Var(\bar{y}_c) = (1 - n/N)1/(n(n-1)) \sum_{i=1}^n (y_i - \bar{y}_c)^2 \quad (3.3)$$

$$Var(Z_c) = D^2 Var(\bar{y}_c) \quad (3.4)$$

where,  $N$  = Total number of segments in the study area

The estimation of land cover and land use was done at level I and level II where categories which were spatially and temporally similar were grouped under one class. Seven classes were distinguished at level one as shown in Table 3.1. The agriculture class was listed first at the top because it is the major human activity that has expanded more rapidly than any other in the catchment. It was followed by the built-up area, being an important physical feature since the extent of its imperviousness affects the response of the catchment to storm events. This was followed by the water class which is the main objective in any hydrological study. The forest class was divided into coniferous, Eucalyptus and mixed classes given their different characteristics regarding storm runoff generation, evapotranspiration and interception. Grass and bush occupy a substantial area and it was necessary to give a class at level I. Level II classes were refinements of level I in recognition of differences among subclasses. For example, the agriculture class was refined into six classes according to crops, subsistence farming and urban agriculture. The built-up area was refined into five classes according to their imperviousness. Forests were refined into classes according to their stands.

The diversity of the land use in the catchment was related to the diversity of agroclimatic zones, landform, water resources, topography, and human activities. The dominant land use categories concentrated specifically on the agricultural application, which was considered the most important human economic activities of the area. Table 3.1 showed the major land cover classes identified in 2013, based on modified Anderson (1977).

Table 3.1: The major land cover classes based on Anderson (1977)

Level I		Level II	
Code	Class Name	Code	Class Name
1.	Agriculture	11 12 13 14 15 16	Maize Bananas Subsistence agriculture Agroforestry Macadamia Avocados, Guavas, Mangos
2.	Urban/Built-up Area	21 22 23 24 25	High density residential (above 90% imperviousness) Middle density residential (65-90% imperviousness) Low density residential (55-65% imperviousness) Industrial areas Rural villages (< 55% imperviousness)
3.	Water	31 32 33 34	River Pond, pool Lake/Dam Wetlands
4.	Coniferous forest	41 42 43	Dense Stand (above 80% tree coverage) Middle Stand (60-80% tree coverage) Loose Stand (40-40% tree coverage)
5.	<i>Eucalyptus</i> forest	51 52 53	Dense Stand (above 80% tree coverage) Middle Stand (60-80% tree coverage) Loose Stand (40-40% tree coverage)
6.	Mixed forest	61 62 63 64	Dense Stand (above 80% tree coverage) Middle Stand (60-80% tree coverage) Loose Stand (40-40% tree coverage) Brushwood (20-40% tree coverage)
7.	Woodland, Grassland and Bushland	71 72 73 74	Improved Pasture Meadow Open grassland with Individual trees Dense bush and thickets Woodland

### 3.3 Land use and land cover mapping

Natural land cover has various properties that help to regulate water flows both above and below the ground surface. Forest canopy and leaf litter help to attenuate the impact of rain drops on the earth's surface, thereby reducing splash erosion. Surplus water moves from the earth's surface through infiltration into underground aquifers and as overland flow to natural depressions, lakes and oceans. Roots hold the soil in place, especially on steeper slopes, and also absorb water. Openings in leaf litter and soil pores permit the infiltration of water, which is carried through the soil into the ground water. Where ground cover is insufficient, sheet, rill and/or gully erosion may result. Soil erosion reduces the productivity of the land and may

result in sedimentation of water courses downstream. Streams eventually carry excess surface water to the lakes and wetlands. In their natural states, the network of streams in a catchment slows down water flow so that there is a significant lag-time between a period of peak precipitation and peak runoff further downstream. Riparian forests serve as important buffers, reducing sediment loads and keeping runoff from moving too quickly into streams.

Land use and land cover mapping distinguished class types according to their dominant characteristics such as rural characteristics, urban characteristics or sub-urban characteristics. The cropland comprises of rolling land and hills with shallow valleys.

Specifically, the following features were checked and expanded or collapsed to produce the land cover and land use classes in Table 3.1 above:

1. Agriculture
  - cropland (cultivation of maize, potatoes, vegetables, mixed subsistence, plantations)
2. Livestock
  - pasture fields
3. Built-up land
  - schools, market centres, factories, urban lands, villages, residential houses, hospitals, etc.
4. Communication
  - roads, railways, etc.
5. Forest (indigenous, plantation)
6. Woodland (open woodland, closed woodland, Acacia, Eucalyptus)
7. Bush and shrub land
8. Riverine vegetation
9. Grassland (open grassland, wooded grassland)
10. Water (dams, reservoirs)

### **3.4 The dominant land use and land cover types**

#### ***3.4.1 Large scale agriculture***

The cropland comprises rolling land and hills with shallow valleys. The cropping pattern for macadamia was divided into blocks of nearly equal size and spread to cover all the entire land area as shown in Plate 7. The blocks carried crops at different stages of maturity and were separated by farm tracks which served as access into the farms. The farms were mechanized, hence the spacing between tree lines could accommodate tractors hitched with various farm machinery.



Plate 7: Macadamia Cropland in Piesanghoek

#### 3.4.2 Subsistence agriculture

The most common farming system involved the production of mostly maize and vegetables. The crops that were incorporated in this farming system served both as food crops for own consumption and as crops that could be sold locally. Plate 8 showed a crop of maize under subsistence farming in Lwamondo area.



Plate 8: Subsistence crop of maize in Lwamondo Village

#### 3.4.3 Agroforestry

Agroforestry was prominent in the Tsianda area where the main tree crops include mangoes, guavas and litchis. This is a land management approach that deliberately combines the



production of trees with other crops and/or livestock. The system is designed to yield a variety of marketable crops and environmental benefits and blends agriculture and forestry with conservation practices and strives to optimize economic, environmental and social benefits. It involves intensive management of trees, non-timber forest crops, agricultural crops and animals on traditional agricultural and forest lands. Agroforestry systems vary depending on the available resources and the outcomes desired. Different management practices will yield different products or functions such as wind protection or soil conservation. Plate 9 showed a section of agroforestry blended with homesteads.



Plate 9: Agroforestry in Tsianda Village

#### *3.4.4 Urban/Built-up Area*

Vhembe District Municipality is undergoing rapid urbanization, where rural land is being converted into urban land. This is evident in the catchment area around Thohoyandou, Elim and Mhinga. Urban areas differ from rural areas in the fraction of total area that is impervious. With development, the spatial flow pattern of water is altered and the hydraulic efficiency of flow is increased through artificial channels, curbing, and storm drainage and collection systems. The net effect of these changes is an increase in the volume and velocity of runoff and larger peak flood discharges.

Urbanization often has more severe hydrologic effects than other forms of land use. When vegetation is replaced with impervious surfaces in the form of paved roads and parking lots, more surface runoff occurs, groundwater levels drop and baseflow decreases accordingly. Accordingly, urbanization results in increased surface runoff and correspondingly higher peak flows following storms.

Recent developments on hillsides and hilltops in the catchment area are of concern as they are impacting on the hydrological processes. Developments on slopes and saddles as shown in section 2.4 disrupts the hydrologic processes by reducing infiltration, interflow surface runoff and prevent water from reaching natural water ways such as streams and rivers. On steep slopes, the net stabilising effect of trees is usually positive and when combined with vegetation cover, they prevent the occurrence of shallow landslides.

The importance of alleviating poverty within LRC attracted the attention of the national government and together with development partners, a Catchment Management and Poverty Alleviation (CAMP) project, supported by the United Kingdom Department for International Development (DFID), was conceived. The project which was under the direction of a stakeholder group comprising forest, water and poverty interests investigated how different scenarios of forest cover, could affect the hydrological regime and water availability, which in turn, would affect economic production and people's livelihoods. The land cover map produced by the project was as shown in Figure 3.2.

The map clearly showed that built-up areas were mainly concentrated in the upper catchment, where the anthropogenic activities would negatively impact on the headwaters. This study established that the urban centres had expanded in size from what they were in 2003 and new ones introduced. Furthermore, there was rapid urbanization which was converting rural land into urban land use, especially between Lwamondo and Thohoyandou.

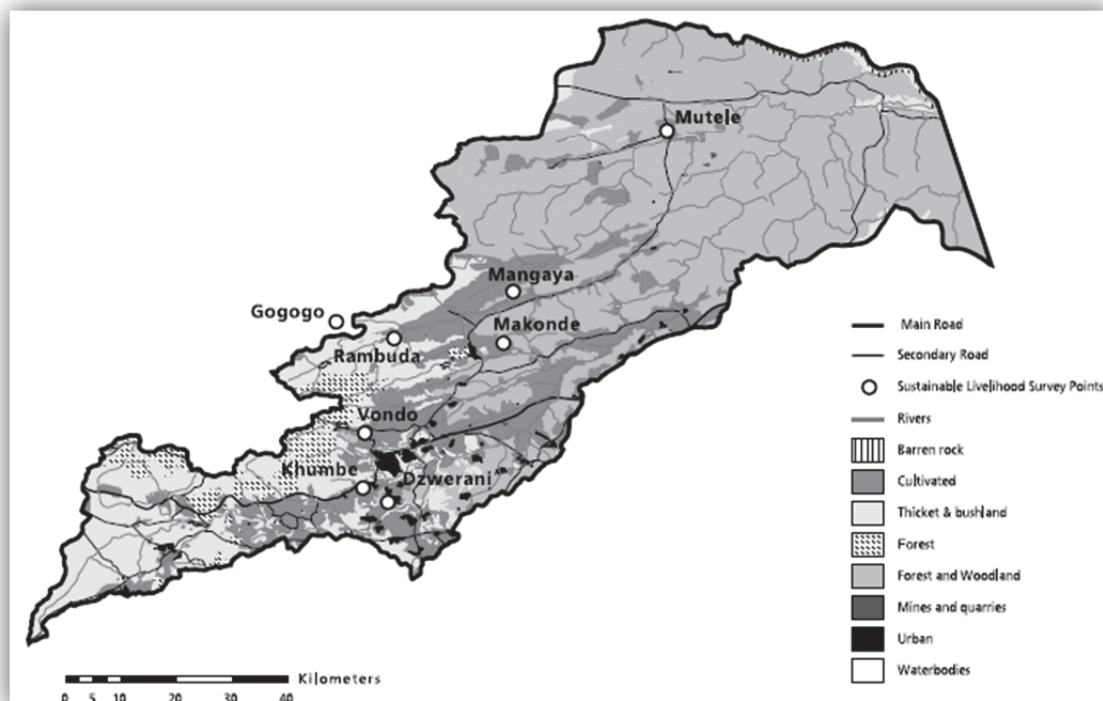


Figure 3.2: Land cover (Source: Calder, 2003)

It was evident that loss of forest cover in the reserves was by both clear cut and progressive thinning. Subsistence agriculture in deforested areas was dominant on higher grounds while remnants of wooded grassland occupied the depressions and lowlands. Land cover classification according to Anderson (1977) and Calder (2003) in the LRC were comparable. Both classifications showed agriculture was the dominant land cover followed by build-up areas.

#### 3.4.5 Water

Water in the catchment was considered in terms of rainfall, rivers and dams. Figure 3.3 showed the main water bodies in the catchment. Stream discharges were monitored at several gauging stations along the river. Nandoni Dam, with a capacity of 150.18 million m<sup>3</sup>, is the latest dam along the river and has been operational since 2006. Albasini Dam is located upstream along Luvuvhu River, while Vondo Dam is located in Mutshundudi River which is a tributary of the Luvuvhu River.

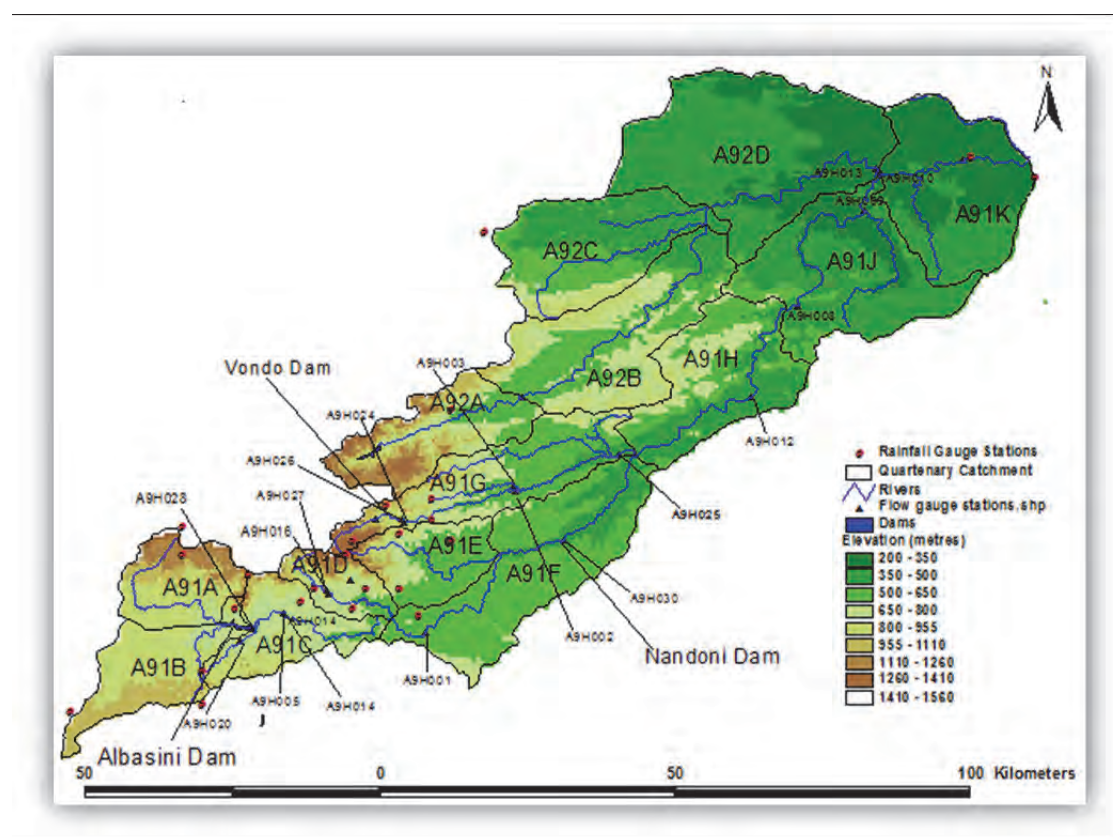


Figure 3.3: Water bodies in the catchment

#### 3.4.6 Wetlands

Many wetlands were found to have been drained for agriculture especially around Tshakhuma and Lwamondo and for commercial development in Thohoyandou town where a shopping complex was constructed on the edge of a large wetland as can be seen in Figure 3.4. Today, however, there is increasing recognition of the valuable ecosystem services provided by wetlands, ranging from flood control to biotic regeneration environments.



Wetlands are natural depressions of the landscape where water collects. They act like sponges, absorbing water during periods of high runoff, and gradually releasing it. Wetlands also serve as natural water filters, removing impurities and sediments.



Figure 3.4: Developments on a large wetland in Thohoyandou

#### 3.4.7 *Eucalyptus* plantations

Eucalyptus plantations were mainly found in the upper catchment area of Luvuvhu River and also in the upper reaches of the Mutshundudi River sub-catchment where they replaced the native vegetation. The expansion of the area under Eucalyptus plantations had the potential to reduce stream flow and water levels in the Vondo Dam on Mutshundudi River which is essential for the supply of water to the community of Thulamela Municipality.

Eucalyptus plantations are commercial forest plantations established to supply raw materials to pulp mills, sawmills and for construction and commercial markets. Eucalyptus plantations are planted because they produce up to 10 times as much timber per hectare than native species (Bate *et al.*, 1999). By virtue of their physiology, extent of coverage and location in the catchment areas, the trees undeniably have an impact on the hydrology of water catchments. The plantations pose a threat of reducing of stream flows during the dry seasons and changing the river from being perennial to intermittent-flow state, and also resulting in an unsustainable supply of water to irrigation schemes, human settlements and other water users. Plate 10 showed a typical Eucalyptus tree plantation at Ratombo.



Plate 10: Eucalyptus tree plantation at Ratombo

#### 3.4.8 *Woodland, Grassland and Bushland*

Woodland, grassland and bushland occurred throughout the catchment, comprising of different species of vegetation. They were found on hills, rolling land and in lowlands where



the vegetation was generally low, with shrubby thicket and bushland occurring as isolated shrubs, bushes and thickets along with subsistence agriculture. Plate 11 showed a typical wood/bushland found in Levubu near Tshakhuma Village in the upper catchment area.



Plate 11: Wood/bushland at Levubu

There were distinct transition zones between different dominant vegetation cover types from the upper to the lower catchment landscape ecology. Such transition zones could comprise of open woodland, grassland or shrubby thicket. The Mopane trees were the dominant land cover type in the lower catchment in segment 38 while segment 41 was dominated by the Acacia Trees within Kruger National Park (KNP). For the exact location of the latter mentioned segments, refer to Figure 3.1 in section 3.1. Plates 12 and 13 showed the typical cover type which could be categorized as open woodland savannah locally referred to as Mopane shrubveld and the Acacia Tree species respectively.



Plate 12: Mopane trees in KNP



Plate 13: Acacia trees in KNP

The acacia trees were the dominant land cover type near Crooks corner in the KNP. Plate 13 showed the typical acacia tree species found in the area

### 3.5 Pressure on land

Indicators in this category included those activities that related to the degree of intensification and diversification of agricultural land use. This included the number of crops in a cropping system per year or per hectare, type and intensity of tillage, degree of removal of biomass, integration with livestock systems and number of food and fibre products produced annually. These indicators were seen within the context of major socio-demographic factors such as population pressures and land tenure systems. The situation could be contained when such lands are rehabilitated with the introduction of agro-forests and wood lots. In the case of transforming degraded lands, it is of great importance to consider the land use capabilities of the landscape to preclude environmental hazards while rehabilitating such lands.

#### *3.5.1 Land use and land cover statistics for 2013 based on direct expansion and regression estimation*

Systematic sampling on a regular grid is better because the sample points are more independent, with no points being close together by chance as in random sampling (Scott and Dixon, 2008). The Physiognomic Class is based on the structure of the vegetation. This is determined by the height and relative percentage of cover of the existing tree, shrub, dwarf shrub, and herbaceous strata. This level has nine mutually exclusive classes:

Forest	Woodland	Sparse Woodland
Shrubland	Sparse Shrubland	
Dwarf Shrubland	Sparse Dwarf Shrubland	
Herbaceous	Sparse Vascular/Non-Vascular	

The area under different land use and land cover in expanded square kilometres was determined. The results obtained by direct expansion and regression estimation were as shown in Table 3.2. At the level of individual classes, the best results were obtained for bananas with a coefficient of variation of 10.22% and a regression coefficient of 5.07%. This could be due to the structure of the banana plant where the broad leaves provided a smooth texture and tone hue that gave a distinct feature class under supervised classification. The other crops and tree plantations had smaller leaves which provided mottled structure and poor tone hue that led to mixed and sometimes unidentifiable classes on imagery.

The Eucalyptus plantations had the lowest reliability with a coefficient of variation of 70.65. This could be due to the mixed reflectance from fire corridors and the contiguous woodlots and tree crops such as avocados, guavas and macadamia. The error matrices developed to assess the accuracies of the classifications indicated values between 78-86% for the overall accuracy, and 65-80% for Kappa index. These values were used as the measure of actual

agreement and the expected output in the sense that values within these ranges normally indicated good representations of the actual land use and land cover.

Table 3.2: Land use and land cover statistics for 2013

Land cover and land use within segments		Total surface area (ha)	Variance	$\sigma$	CV	RE
Maize	direct expansion	3,352	4,815,101	2245	60.12	
	regression estimation	3,009	883,650	950	29.90	4.95
Macadamia	direct expansion	3,799	4,896,099	1989	58.85	
	regression estimation	3,298	899,795	918	30.52	5.08
Bananas	direct expansion	25,664	9,984,885	3170	10.22	
	regression estimation	28,727	2,369,960	1447	5.07	3.98
Agroforestry	direct expansion	3,144	581,419	893	30.53	
	regression estimation	2,945	286,655	623	25.22	1.95
Eucalyptus	direct expansion	2,005	1,887,722	155	70.65	
	regression estimation	2,442	52,354	219	8.06	21.88
Built up area	direct expansion	12,558	15,554,215	3979	38.76	
	regression estimation	8,009	1,340,942	1255	18.32	15.11
Grass/ bushland	direct expansion	34,550	16,868,711	3766	13.08	
	regression estimation	35,537	14,174,091	1473	11.74	2.90

Based on secondary data (ARC, 2006), the results showed that during the 1980s, land cover patterns constituted of 15.81% agriculture, 29.34% natural forest, 32.15% bare ground, 0.06% water bodies, 8.28% plantations and 14.36% shrubs and grasses. During this period, natural forests and bare ground dominated the study area covering almost 60%. During the 1990s, a decrease in forest cover was noted with a major increase in bare ground revealing change in land use in the area.

Forest cover declined from 29.34% to 16.8%. Notable was agriculture and bare ground which rose from 15.81% to 21.73% and from 32.15% to 37.16 respectively. The area covered by plantations also increased by about 1.7% from 8.28% to 9.93%. Insignificant change was noted in water bodies, shrubland and grassland. Throughout the 2000s, land use change revealed a decrease in natural forest from 32.15% to 20.67 and giving rise to agriculture which rose to 38.57% in 2010. An increase in water bodies from 0.06% to 0.08% was observed. This may be due to the construction of Nandoni Dam which started operating in 2005 with the mandate to supply water to rural and peri-urban communities within the catchment. Originally, only Lake Fundudzi, Vondo dam and Albasini dams as well as some tributaries of Luvuvhu River were the dominant water bodies in the catchment.

### 3.6 Environmental Monitoring in the catchment

Environmental monitoring for LRC can be done using satellite remote sensing in combination with the Soil Water Assessment Tool (SWAT) tool. The tool has the advantage to monitor the complete nutrient cycle for nitrogen and phosphorus as well as the degradation of any

pesticides applied at HRU (Hydrological Response Unit) levels. The tool also accounts for the time lag in sub-basins with a time of concentration greater than one day, where only a portion of the surface runoff and lateral flow will reach the main channel on the day it is generated. To account for the time lag, SWAT incorporates a storage feature to lag a portion of the surface runoff and lateral flow release to the main channel from sub-tributaries like Dzindi, Mutshundudi, Latonyanda and Mbwedi rivers. This way, pesticides in the surface runoff and lateral flow are lagged as well. In addition to sediments, nutrients and pesticides, SWAT calculates the amount of algae, dissolved oxygen and carbonaceous biological oxygen demand entering the main channel with surface runoff.

The transport of nutrients and pesticides from agricultural land areas in Levubu, Elim, Tshakhuma and Piesanghoek into streams, dams and other water bodies like farm ponds is a normal result of erosion processes by water. Nitrate however may be transported by surface runoff, lateral flow or percolation. Yet, excessive delivery of nutrients into streams and water bodies will accelerate water pollution and eutrophication and render the water unfit for human consumption and also produce toxic conditions that harm aquatic life. It is therefore very important that continuous monitoring is conducted to determine the amounts being loaded in the streams especially from Levubu, Elim, Tshakhuma and Piesanghoek areas which are under intense commercial agricultural production and from Tshakhuma, Lwamondo, Tsianda and Thohoyandou areas which are undergoing rapid expansion in urbanisation. Nitrogen is an extremely reactive element and its ability to vary its valence state makes it a highly mobile element. Therefore, predicting its movement in the soil is critical to environment management.

Multi-date and spatial-temporal satellite remote sensing offers an alternative option for monitoring and tracking variations in suspended sediment concentration in LRC. Analysis and interpretation of the satellite data using image processing techniques can help in monitoring patterns of suspended sediment movements. Such data can be obtained from SANSA free of charge and would be especially useful in remote and complex hydrologic environments like the Soutpansberg Mountains and KNP where in situ monitoring would be insufficient or impractical.

The transport of fine sediment, carried in suspension by water, is central to the hydrology, geomorphology, and ecological functioning of Luvuvhu River floodplains. Observation of spatial and temporal patterns in sediment transport would be helpful in understanding the formation and function of these environments and how they may respond to natural and anthropogenic activities and perturbations in the future. Monitoring sediment quality is an important environmental concern because sediment may act as a sink for various contaminants and, under certain conditions, as a source of contaminants to the overlying water column and biota. Once in the food chain, some sediment-derived contaminants may be of concern because of bioaccumulation and the tendency to persist in the environment. Furthermore, information on sediment quality is important for reconstructing historical conditions in the catchment, providing a baseline for future assessments, providing a warning

of potential problems, understanding effects of human activity, and providing guidance for management.

It is also important to monitor soil moisture in the catchment because root density is greatest near the soil surface and decreases with depth. The water uptake from the upper layers is assumed to be much greater than that in the lower layers. As the water content of the soil decreases, the water in the soil is held more and more tightly by the soil particles and it becomes increasingly difficult for the plant to extract water from the soil. This will impact negatively on agricultural production where crops require soil moisture at field capacity to go through the growth cycle.

South Africa has prepared a National Action Programme to combat land degradation, and this requires assessment and monitoring to be conducted in a systematic, cost effective, objective, timely and geographically-accurate way (Gibson, 2006). By time series analysis of a sequence of images, which are available at 10-daily and monthly intervals, the status and progress of vegetation and crop growing seasons can be monitored. The data can be analyzed by comparing historical images with current ones to show how rainfall was distributed over the areas as indicated by good or poor vegetation development. The annual maximum of greenness typically occurs during the period of peak vegetation of the primary growing season of a given year which therefore, reveals the level of greenness that would normally be expected at the peak of season. The minimum of the annual maximums for any location generally represents the worst growing seasons of the period.

It is now a common practice to use NDVI (Normalized Difference Vegetation Index) to estimate the cumulative effect of rainfall on vegetation over a given time period, determine the rangeland carrying capacity, crop yields for different crop types, and the quality of the environment as a habitat for different animals, pests and even diseases. Furthermore, monitoring can help create grazing capacity maps in the middle and lower catchment areas like Tsianda, Dumasi, Sidou amongst other villages where grazing is prominent by correlating the maximum NDVI images for different years with animal unit values from earlier grazing capacity maps.

The trend analysis between rainfall and NDVI for Vhembe for 2013/2014 in Figure 3.5 showed a linear relationship where an increase in rainfall resulted in an increase in NDVI. In some cases, NDVI remained high during periods of no rainfall, meaning that temporal water shortage did not affect vegetation cover.

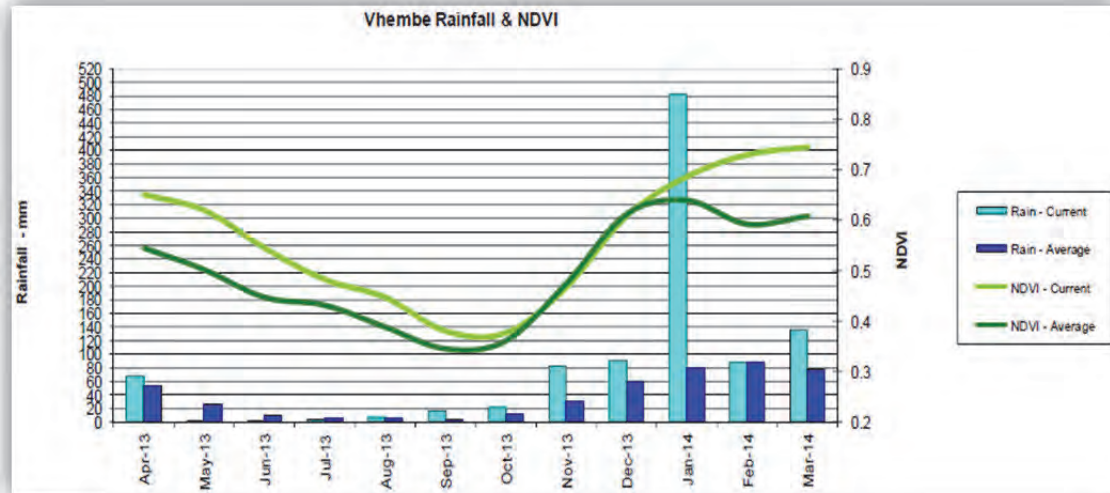


Figure 3.5: Monthly trends for rainfall and NDVI (Source: SAWS, 2014)

For purposes of continuous environmental monitoring in catchment long-term average NDVI should be calculated from the yearly images for use in the degradation analysis. Significant trends in NDVI values over the time series would indicate the potential influence of factors such as rainfall and human-induced changes in vegetation productivity.

Three hot spot areas in the context of rapid developments on hills and saddles were identified for continuous environmental monitoring. The hot spot locations shown in Figure 3.6 included site 1 in Tshakhuma-Tsianda, site 2 in Thohoyandou and site 3 in Mhinga.

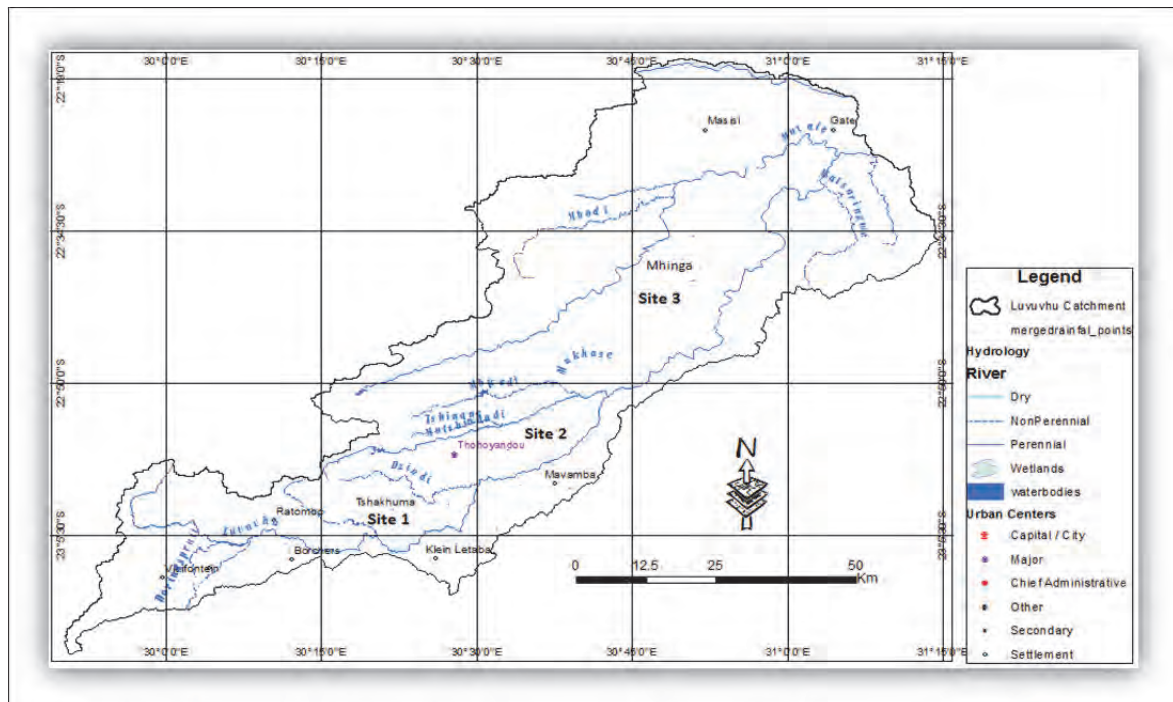


Figure 3.6: Locations and sites for environmental monitoring



Advances in remote sensing and GIS techniques have broadened the scope of data acquisition, providing the capacity to quantify and estimate the spatial-temporal distribution of vegetative cover. Satellite sensors including Landsat Enhanced Thematic Mapper plus (ETM+), SPOT HRV (High Resolution visible), Moderate Resolution Imaging Spectrometer (MODIS), Medium Resolution Imaging Spectrometer (MERIS) and National Oceanic and Atmospheric Administration (NOAA) among others, now provide repetitive land surface data and have made it possible to quantify multi-temporal variability of land cover.

## CHAPTER 4

### HYDROMETEOROLOGICAL DATA ANALYSIS

To determine the hydrological effects of land cover and land use change over large areas, an analysis of the catchment was carried out over two different periods of time. The pre-change period was taken to be between 1960-1986 while the post-change period was taken from 1992-2013. The five years in between was taken to be the transition to change period.

Luvuvhu catchment is a predominantly semi-arid region where precipitation is the limiting factor for agricultural production on one hand and on the other hand is responsible for flash floods due to short-duration and high intensity rainfall in the upper part of the catchment. Meteorological data was collected from fourteen weather stations shown in Table 4.1

Table 4.1: Location of weather stations and elevation in the LRC

Station Name	Latitude	Longitude	Elevation (m)
Levubu	23°05'27"	30°18'09"	610
Lwamondo	23°00'44"	30°37'36"	648
Elim Hosp.	23°15'0"	30°05'0"	808
Entabeni Bos	23°00'0"	30°27'0"	1376
Klein Australie	23°05'0"	30°22'0"	702
Nooitgedacht	23°07'0"	30°20'0"	762
Palmaryville	22°98'0"	30°43'0"	570
Rambuda	22°78'0"	30°43'0"	762
Tshakhuma	23°05'0"	30°30'0"	1158
Tsianda	23°00'0"	30°35'0"	671
Madzivhandila	22°98'62"	30°55'48"	517
Thohoyandou	22°94'62"	30°48'80"	730
University of Venda	22°58'24"	30°27'02"	712
Mhinga-Xikundu	22°46'45"	30°52'46"	460

#### 4.1 Rainfall

Rainfall generally occurs during summer (November through March), although in the southwest, rainfall often occurs in winter (June through August). Rainfall is highly variable, both in space and time, often resulting in severe droughts and extreme flooding. The spatial distribution of mean annual rainfall showed that rainfall was higher on the western side and lower on the eastern side ranging from a maximum of 1400 mm to a minimum of 400 mm. The western side corresponded to the upstream while the eastern corresponded to the downstream parts of the catchment. The rainfall received upstream is crucial within the catchment because it impacts on the flow of the river downstream. Variations in inter-annual rainfall may result in low river flows for much of the year with periodic high flows, thereby limiting the availability of water resources through the dry season (Mukheibir and Sparks, 2003).

The main weather systems that are responsible for rainfall are the tropical-temperate troughs; tropical lows; cut-off lows and tropical cyclones. These weather systems are associated with ITCZ which is linked to atmospheric disturbances and can lead to rainfall anomalies. The spatial distribution of mean annual rainfall for the rainy season was as shown in Figure 4.1. The distribution showed higher amounts in the regime which is undergoing rapid land use change. The negative effects of such changes may have manifested in increased runoff, which led to the recent increase in flood frequency and magnitude in the lower catchment areas. The estimation of areal rainfall in the lower catchment had uncertainties arising from the spatial variation of precipitation. The estimation was further complicated by the fact that the distribution of active rain gauges in the catchment was uneven with the majority located in the upper reaches of the catchment.

The spatial distribution of rainfall showed higher amounts in the region which was undergoing rapid land cover and land use change. There is need for mitigation measures to control the negative impacts associated with such changes in a catchment.

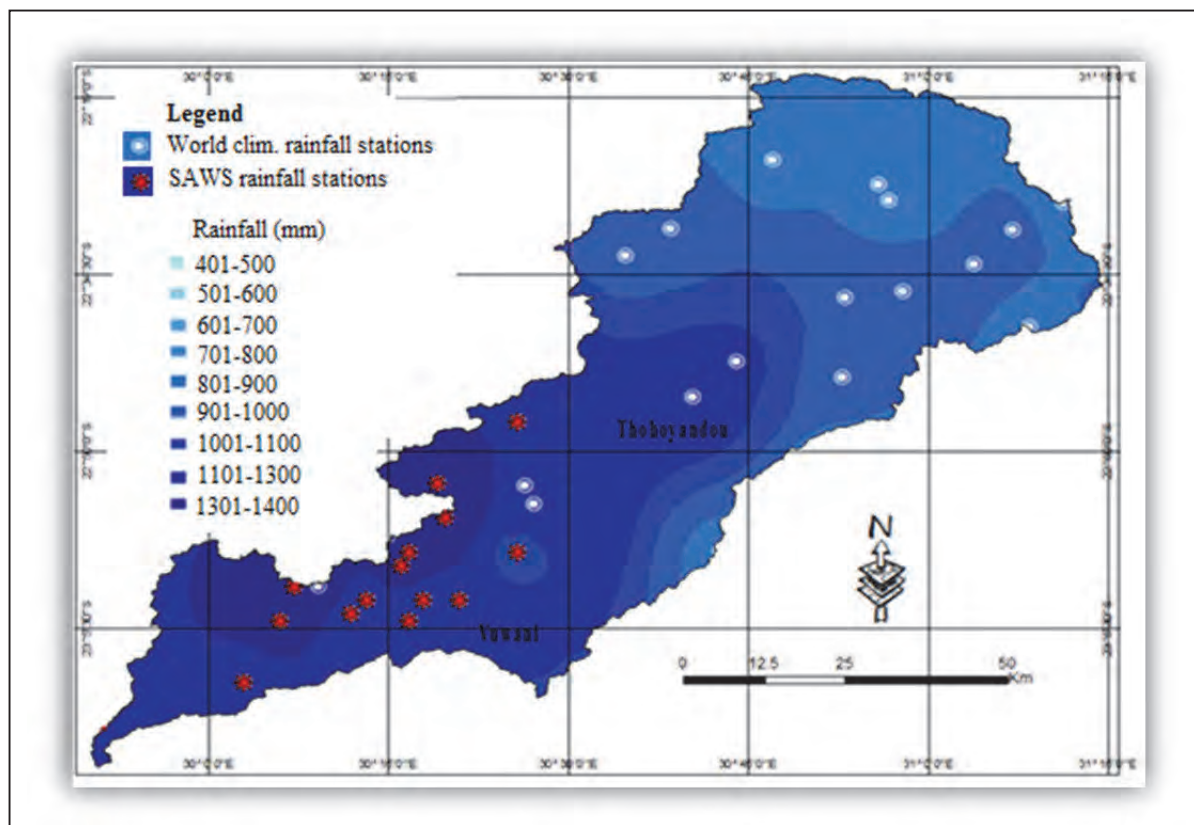


Figure 4.1: Mean annual rainfall

The trend analysis of the rainfall time series showed that the annual rainfall differed across the catchment. Some stations displayed a decreasing trend while others showed increasing trends. The trends during the 1960-1986 phase revealed an increase in rainfall upstream of catchment at Nooitgedacht and a decrease in rainfall downstream at Palmmaryville as shown in Figures 4.2 and 4.3. Other stations which indicated an increasing trend included Klein

Australie, Entabeni Bos, Tshakhuma and Tsianda. Three peaks were observed in 1976/77 at Palmaryville and at Nooitgedacht in 1977/78, revealing the spatial and temporal fluctuations. A study by Mukheibir (2005) has shown that South African regions experience seasonal and interannual variations in rainfall. These variations have a great impact on the agricultural sector in the country. For example, the timing of rainfall during the onset of rainfall in October is crucial for planting of crops whereas the timing of rainfall in early February is crucial for the growth of crops (Jury *et al.*, 1997).

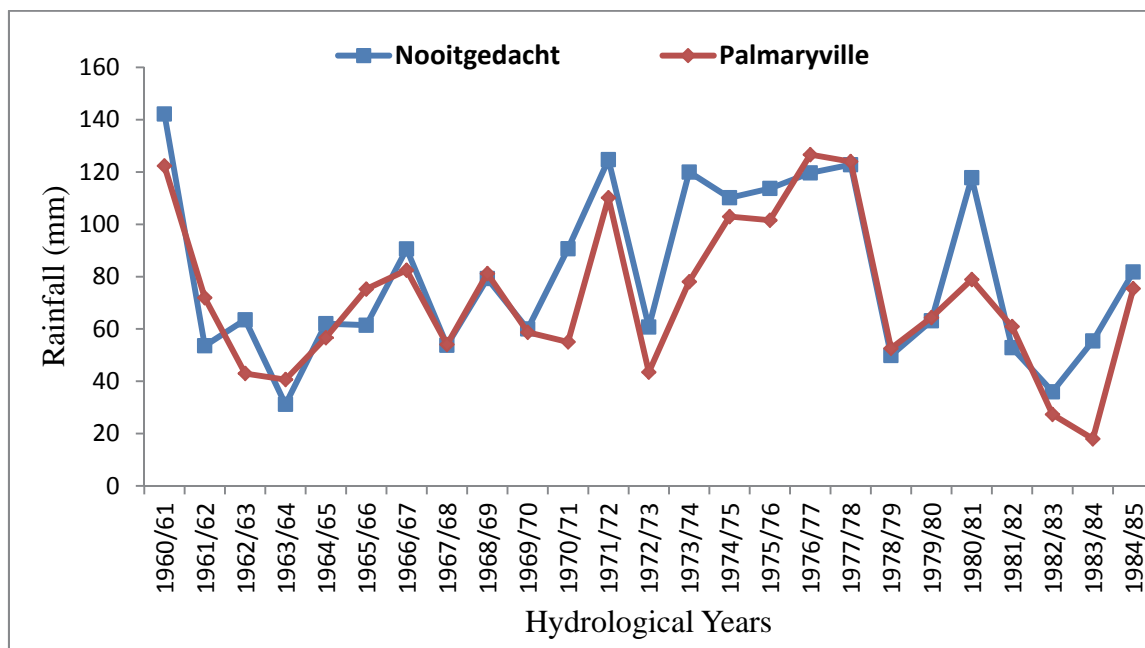


Figure 4.2: Rainfall trends for Nooitgedacht and Palmaryville: 1960 -1985

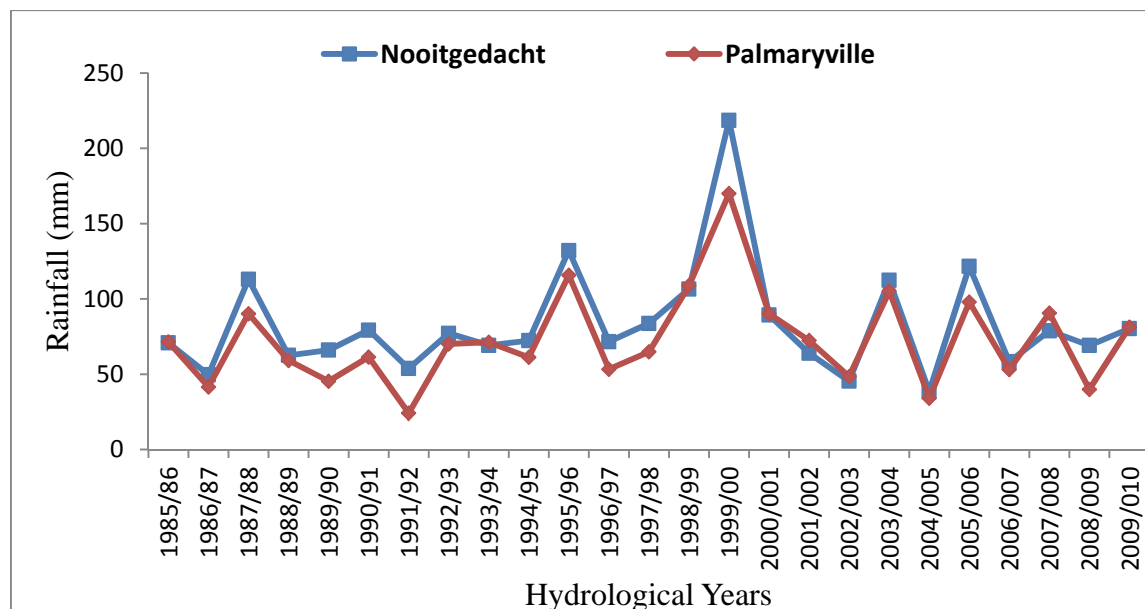


Figure 4.3: Rainfall trends for Nooitgedacht and Palmaryville: 1985-2010

Figure 4.4 showed the total and effective rainfall distribution for six stations in the study area as estimated by the CropWat model. Effective rainfall which is neither retained on the land

surface nor infiltrated into the soil (Chow *et al.*, 2010). Thus, effective rainfall is useful or utilizable rainfall, since all rainfall is not necessarily useful or desirable at the time, intensity and amount in which it is received. Some of it is unavoidably wasted while some may even be destructive as flood water. Knowledge of effective rainfall is importance for the catchment because the agricultural sector relies mainly on rainfall for irrigation water. Since most rainwater is used in agriculture for crop production, the issue which arises is whether the available rainfall is adequate and well distributed for crop production. It is important to know the water requirements of crops during the growing season as well as during different periods of growth and development and how far these needs are met by rainfall. Several factors affect effective rainfall including rainfall characteristics, land characteristics, soil characteristics, crop characteristics and management practices. Farming activities should be based on precise interpretation of long-term data on rainfall patterns in order to realise greater efficiency of water utilization in the catchment.

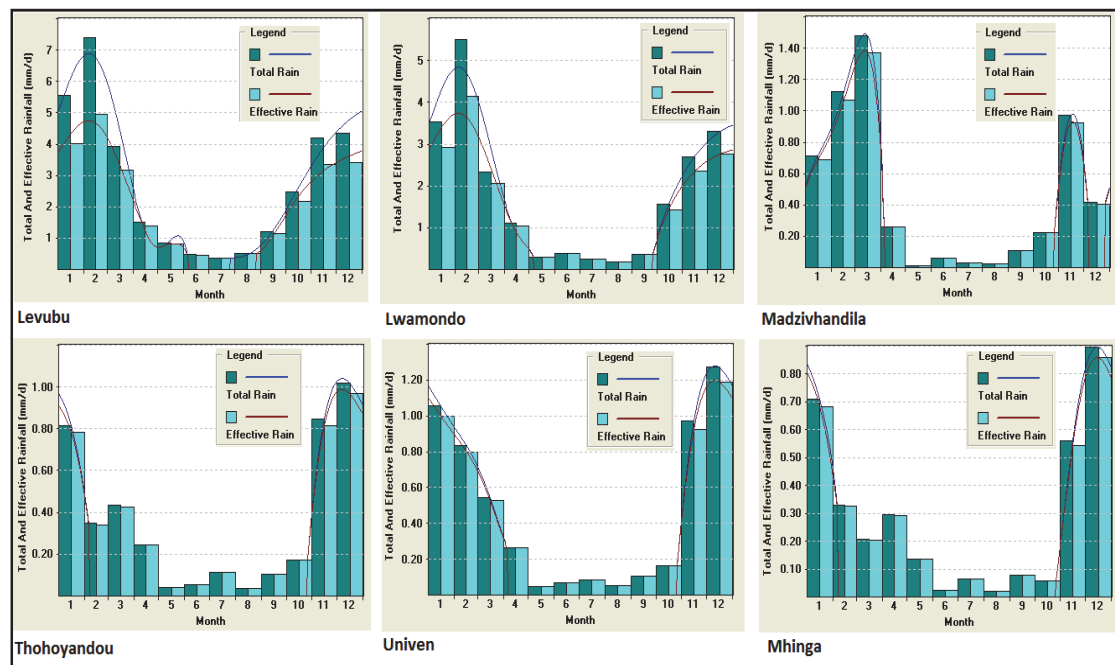


Figure 4.4: Total and effective rainfall distribution for six stations in the study area

## 4.2 Temperature and Solar radiation

Temperatures are influenced by variations in elevation, terrain, and ocean currents more than latitude. The solar radiation absorbed by the atmosphere and the heat emitted by the earth increase the air temperature. Figure 4.5 showed the solar radiation and the average monthly minimum and maximum temperatures while Figure 4.6 showed the average monthly minimum and maximum temperatures for six selected stations in the study area. Radiation is the mechanism by which solar energy reaches earth. The surface solar radiation is an important factor influencing the local energy budget. When the soil is warming or cooling, the soil heat flux for monthly periods may become significant relative to the mean monthly radiation. Today, the best-known anthropogenic effect on climate happens through emissions of carbon dioxide and other greenhouse gases. Most of the emitted anthropogenic carbon

dioxide originates from the combustion of fossil fuels which are used to produce energy. Urbanization and adoption of new live styles have led to increase in carbon emissions in the catchment.

During winter months, the solar radiation is lower than that around the summer solstice. Variation in the degree of cloud cover may create the scatter and spikes in the solar radiation data. Figure 4.5 showed that temperature corresponded to the solar radiation with a slight delay in the response of temperature to changes in solar radiation.

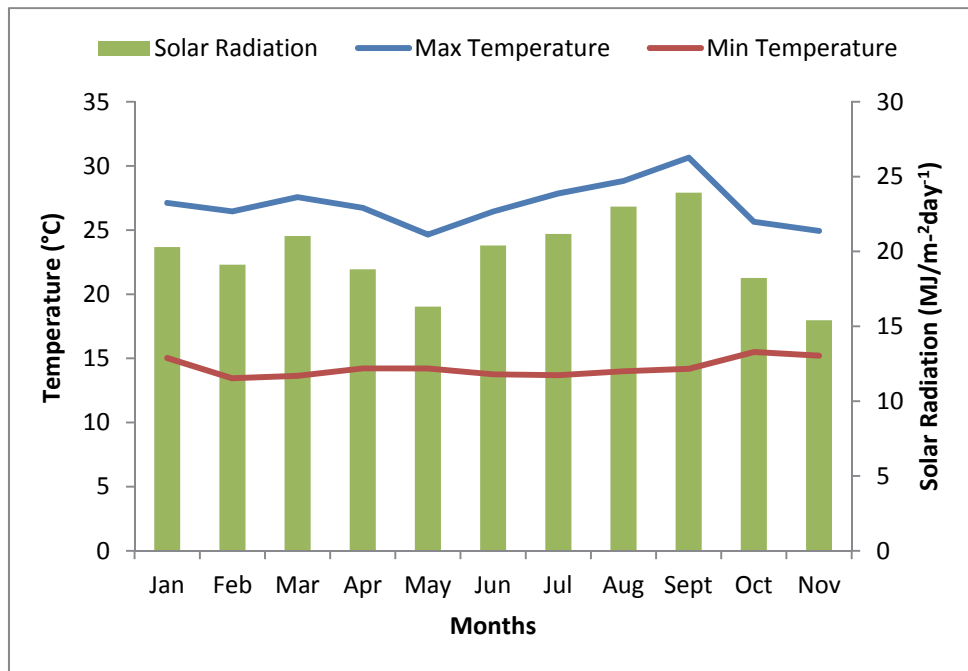


Figure 4.5: Temperature and Solar radiation

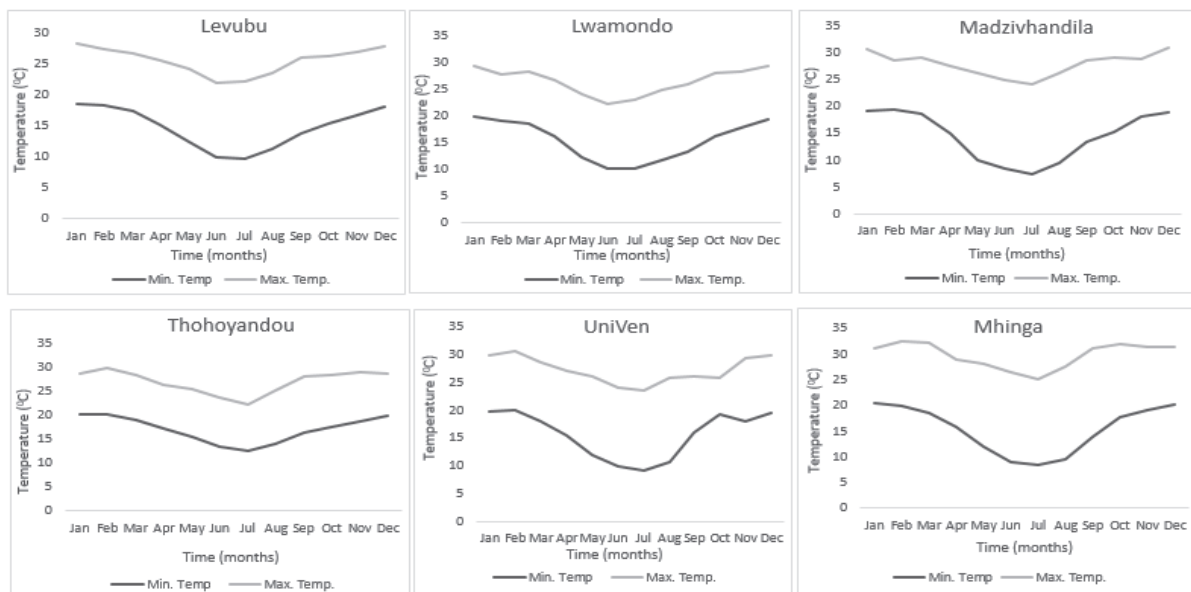


Figure 4.6: Average monthly minimum and maximum temperatures for selected stations in the study area

### 4.3 Evaporation

In the absence of rain, the amount of water evaporated during a period (mm/day) corresponds with the decrease in water depth in that period. Results showed that evaporation was highly variable during the summer season (October to March), whereas it showed a gradual decrease during the winter season (April to September). The peak evaporation months were November, December and January with mean values of 163, 193 and 159 mm respectively. During the dry season, evaporation and abstractions by plants reduce runoff and decrease the amount of subsurface and interflow that support stream flows.

Figure 4.7 showed the spatial variation of evaporation in the study area, where evaporation increased from west (upstream of the catchment) at a rate of 1 400 mm/a to east (downstream) of the catchment at a rate of 2000 mm/a. These variations could be linked to land use activities in the upstream (mostly plantations and agricultural) and downstream (mostly settlements) of the study area.

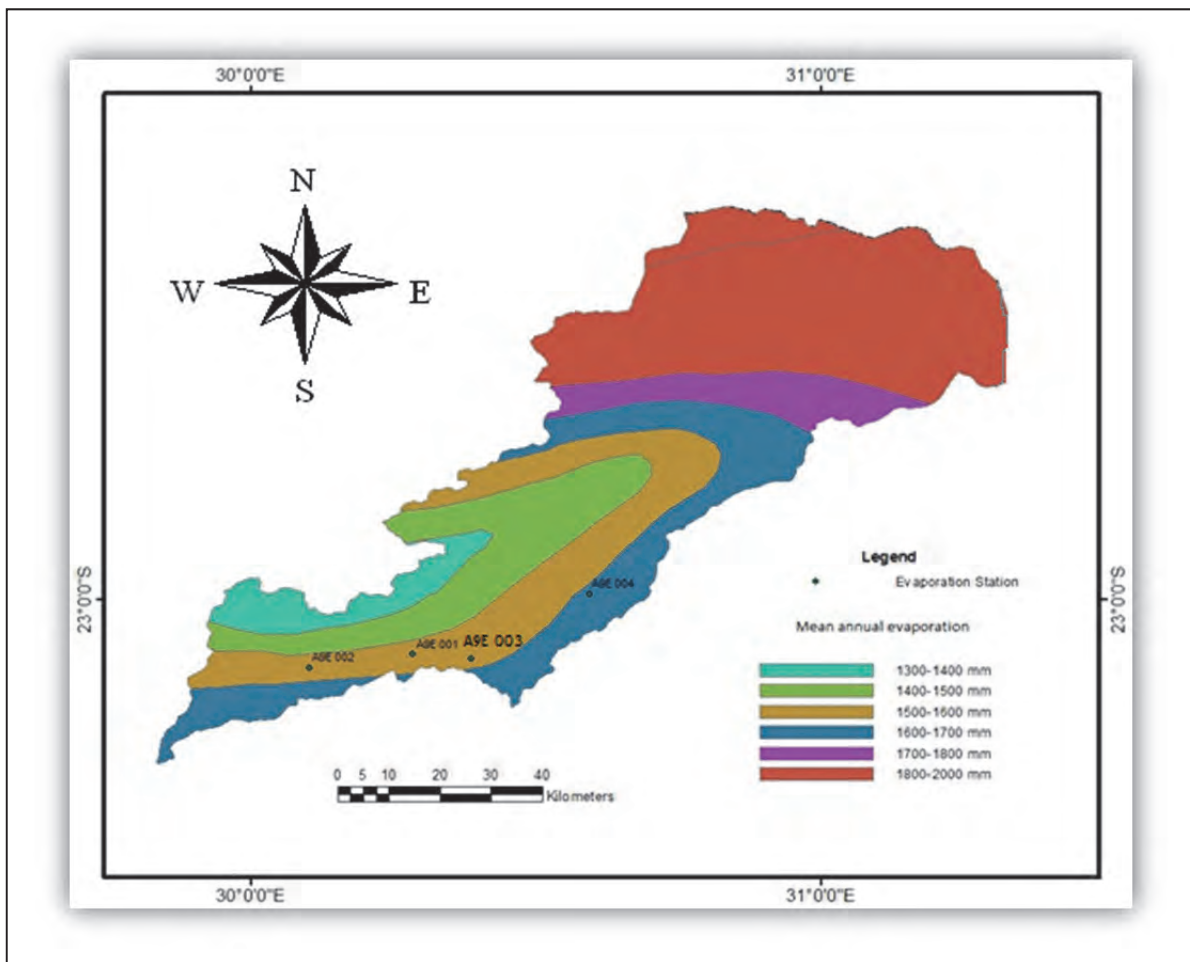


Figure 4.7: Spatial variation of evaporation

## 4.4 Evapotranspiration

Evapotranspiration is a term describing the sum of evaporation and plant transpiration from the earth's land surface to atmosphere, including soil (soil evaporation), and from vegetation (transpiration). Evaporation accounts for the movement of water to the air from sources such as the soil, canopy interception, and water bodies. Transpiration accounts for the movement of water within a plant and the subsequent loss of water as vapour through stomata in its leaves.

The evapotranspiration process is determined by the amount of energy available to vaporize water. Solar radiation is the largest energy source and is able to change large quantities of liquid water into water vapour. The sensible heat of the surrounding air transfers energy to plants and exerts a controlling influence on the rate of evapotranspiration.

### 4.4.1 Potential Evapotranspiration

The reference value denoted as the potential evapotranspiration is often taken to be the evaporation from a plant stand of short densely covered, cut grass freely supplied with water. Penman (1963) and Monteith (1981) used the term potential transpiration in as much as evaporation from the soil is truly negligible for a densely populated grass. Penman-Monteith ETo (Reference Evapotranspiration) is a function of the four main factors affecting evaporation, namely temperature, solar radiation, wind speed, and vapour pressure. Penman (1948) original derivation described evaporation from a free water surface or any surface freely covered by water such as a plant canopy immediately after rainfall. On the other hand, Thornthwaite (1948) coined the term potential evapotranspiration, assuming an unlimited supply of evaporating surfaces with free water. In Penman's original equation and in subsequent modifications, the use of a wind velocity function is probably appropriate in order to obtain ETp for integral values of a day or even somewhat longer periods. On the other hand, for diurnal computations the variation of atmospheric stability plays an important role.

Land cover changes may have impacts on the evaporation rate by either reducing or increasing it. An increase in forestry area may increase the levels of evapotranspiration from vegetation and may tend to reduce bare ground evaporation. Humidity on the other hand has a tendency of reducing evaporation rates.

### 4.4.2 Actual Evapotranspiration

Both potential and actual evapotranspiration can be measured with the soil water balance method. The water balance of the soil accounts for the incoming and outgoing fluxes of a soil compartment. The general procedure for transforming the potential evapotranspiration, to the actual evapotranspiration, follows several steps to theoretically compute the real actual evapotranspiration at a particular location. It is computed for the reference short green grass with wet surfaces and adequate water supply without advection. This reference potential evapotranspiration is transformed using specific site related values influenced by slope, land use and albedo. The site related potential evapotranspiration is adjusted to the particular type of vegetation including its stage of development. The value of actual evapotranspiration is



obtained by reducing the value of the site related potential evapotranspiration to account for the limited supply of water derived from the soil profile.

In general, the development presented by Monteith (1981) with final result often being named the Penman-Monteith equation is preferred. Here, with the stomatal resistance  $r_s$  being introduced, the Penman-Monteith equation for actual evapotranspiration is as shown in Equation 4.1.

$$E_{TA} = \frac{\frac{\phi_a}{\gamma} \left( \frac{H_Q}{\chi} \right) + \frac{\rho_A c_p d}{\chi r_A}}{\phi_a = \gamma \left( 1 + \frac{r_s}{r_A} \right)} \quad (4.1)$$

where,  $r_A$  [ $\text{s.m}^{-1}$ ] is the aerodynamic resistance against the turbulent transfer of water vapour from the evaporating surface to the atmosphere. Its values are in the range  $10 \leq r_A \leq 300$ . This equation describes the actual evapotranspiration of a particular reference plot owing to an extension of Penman's equation by Monteith (1981). It represents the entire canopy as a “big leaf” (Lynn and Carlson, 1990) and is still in agreement with the integral single layer concept of Penman.

#### 4.5 The CROPWAT Model analysis

The CROPWAT (Crop Water) model (FAO, 1992) based on the FAO (Food and Agricultural Organisation) Penman-Monteith model shown in Equation 4.2 was used to compute reference evapotranspiration for the catchment. The equation determines the evapotranspiration from the hypothetical grass reference surface and provides a standard to which evapotranspiration in different periods of the year or in other regions can be compared and to which the evapotranspiration from other crops can be related.

$$ET_o = \frac{0.408 \Delta (R_n - G) + \gamma \frac{900}{T + 273} u_2 (e_s - e_a)}{\Delta + \gamma (1 + 0.34 u_2)} \quad (4.2)$$

where,  $ET_o$  is reference evapotranspiration [ $\text{mm day}^{-1}$ ],  $R_n$  is net radiation at the crop surface [ $\text{MJ m}^{-2} \text{day}^{-1}$ ],  $G$  is soil heat flux density [ $\text{MJ m}^{-2} \text{day}^{-1}$ ],  $T$  is air temperature at 2 m height [ $^{\circ}\text{C}$ ],  $u_2$  wind speed at 2 m height [ $\text{m s}^{-1}$ ],  $e_s$  is saturation vapour pressure [ $\text{kPa}$ ],  $e_a$  is actual vapour pressure [ $\text{kPa}$ ],  $e_s - e_a$  is saturation vapour pressure deficit [ $\text{kPa}$ ],  $\Delta$  slope vapour pressure curve [ $\text{kPa } ^{\circ}\text{C}^{-1}$ ] and  $\gamma$  psychrometric constant [ $\text{kPa } ^{\circ}\text{C}^{-1}$ ].

The CROPWAT model was used to compute reference evapotranspiration for the catchment. Figure 4.8 showed the distribution of reference evapotranspiration ( $ET_o$ ) for the study area. The onset of the rainy season in October at each climate station starts with relatively high  $ET_o$  values which then increased gradually until January. Thereafter,  $ET_o$  values declined

gradually from February and reached minimum in July. It then rose again from August towards the early rainfall season in October. The peak ETo months were recorded in January, February and March, throughout for different climatic stations. The highest ETo value of 4.0 mm/day was observed at each climatic station during the wet season while the lowest ETo value of 2.5 mm/day was observed during the dry months.

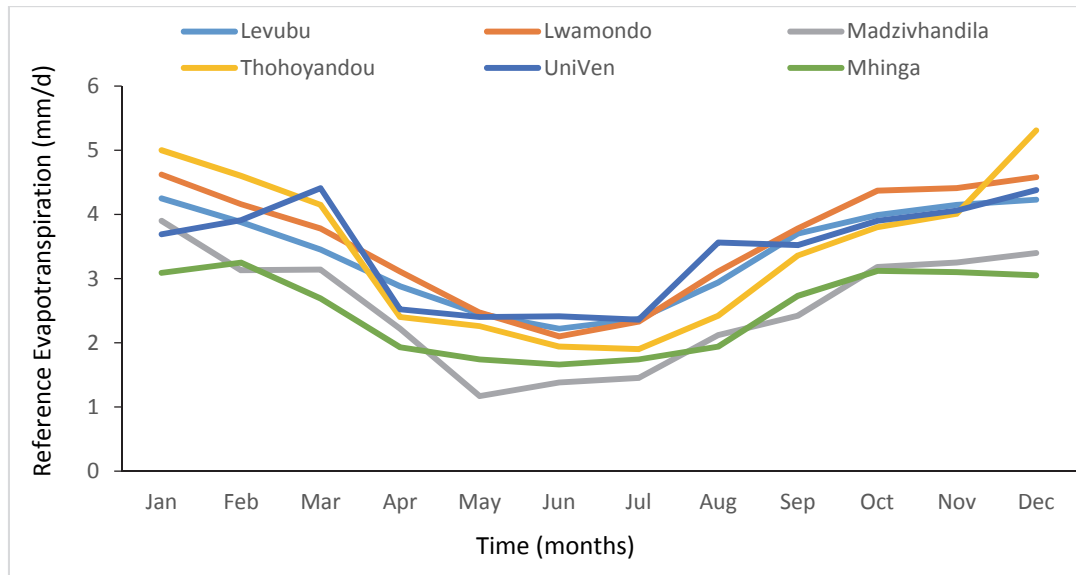


Figure 4.8: Average monthly ETo for selected stations in the study area

Schaffer (2005) noted that high evapotranspiration occurs when high available energy interacts with high soil moisture and robust plant health. Areas with the lowest ETo rates were relatively dry, where pasture and grasslands dominate the landscape. Conversely, areas with higher ETo rates were near rivers and streams, which generally have more abundant vegetation.

A study by Mölders (2011) showed that evapotranspiration was low in deforested areas due to reduced surface roughness length and it significantly decreased net radiation. Such low ETo subsequently modifies the water and energy cycles within the deforested area. In areas that are characterized by low rainfall, the rate of evapotranspiration is low as some water will be lost due to percolation and surface runoff.

#### 4.6 Humidity

The catchment is located in a semi-arid region where plants consume large amounts of water in hot dry periods due to the abundance of energy and the desiccating power of the atmosphere. But when air humidity is lifted, its ability to absorb water vapour decreases, leading to a decrease in evaporation rates. Figures 4.9, 4.10 and 4.11 showed the average monthly Humidity and average annual humidity for selected stations in the catchment respectively. Also, high temperatures may increase evaporation rates which in turn increase the water losses in rivers and dams. These can be exacerbated by land cover changes which affect local temperatures thereby increasing the rate of evaporation. It is therefore prudent

that any environmental management strategies in the catchment take into consideration the functional requirements of different plants in order to select the species that will create the best ecosystem.

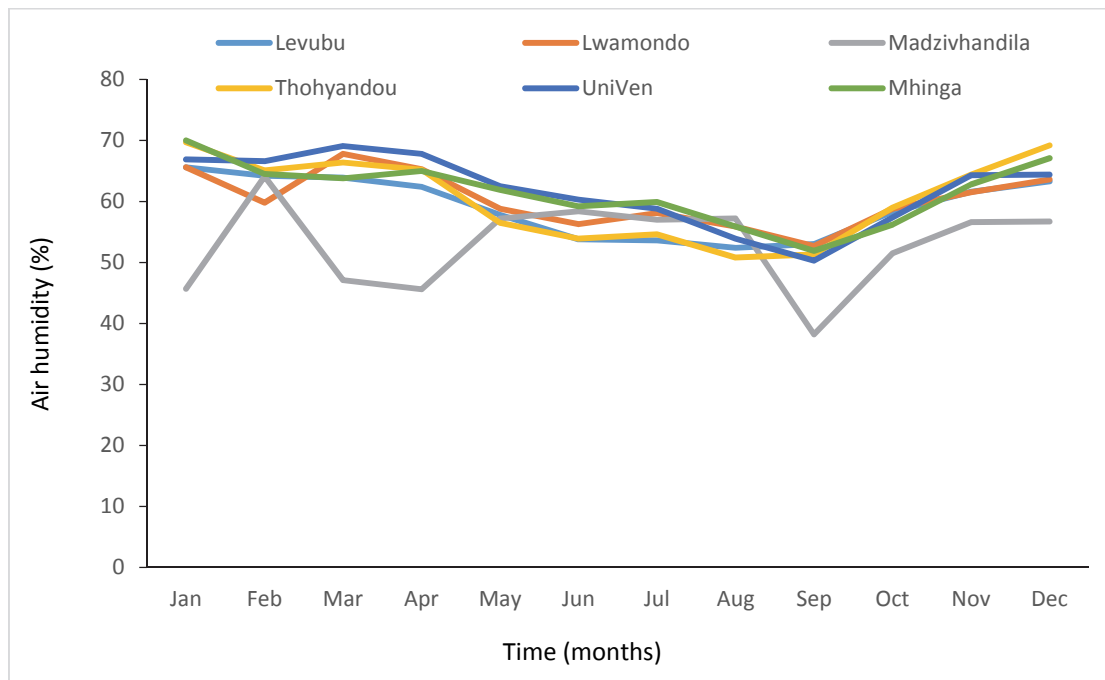


Figure 4.9: Average monthly Humidity for selected stations in the study area

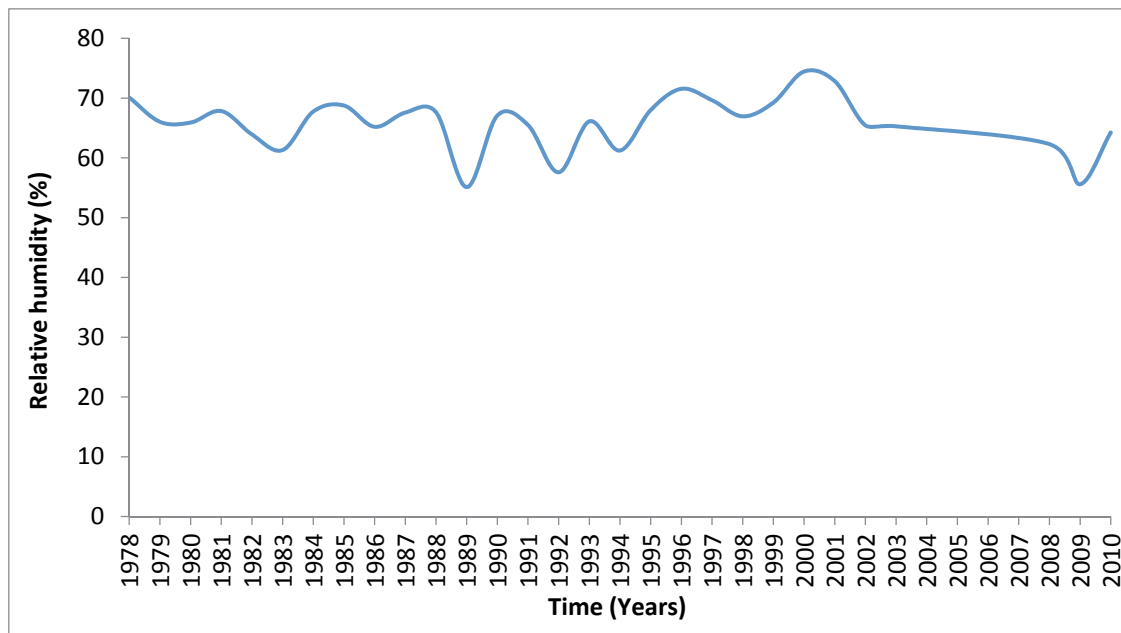


Figure 4.10: Average annual Humidity for Levubu

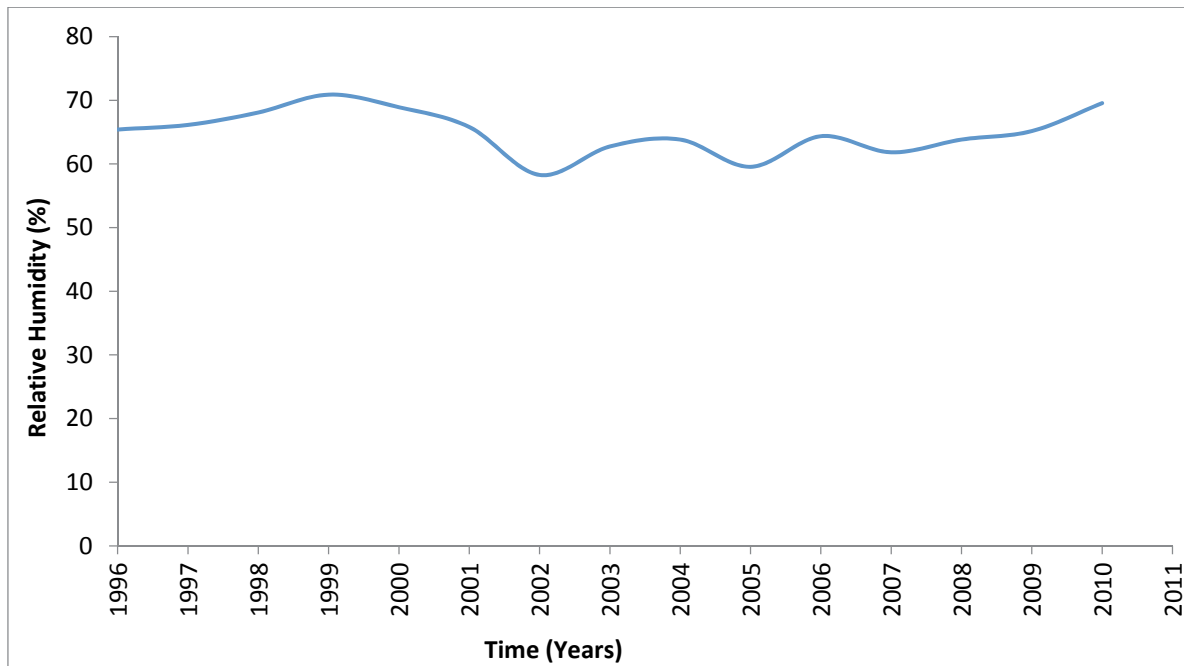


Figure 4.11: Average annual Humidity for Thohoyandou

## 4.7 Winds

Information on wind is important because the process of vapour removal depends to a large extent on wind and air turbulence which transfers large quantities of air over the evaporating surface. The evapotranspiration demand is high in hot dry weather due to the dryness of the air and the amount of energy available as direct solar radiation and latent heat. Under these circumstances, much water vapour can be stored in the air while wind may promote the transport of water allowing more water vapour to be taken up. On the other hand, under humid weather conditions, the high humidity of the air and the presence of clouds cause the evapotranspiration rate to be lower. When the level of wind speed is low, the rates of evaporation tend to decrease due to saturated air above the ground surface.

Figures 4.12, 4.13 and 4.14 showed the average monthly wind speed and the average annual wind speed for selected stations in the catchment respectively. Surface wind velocities in the study area increased gradually from May to October and declined during the rainy season from November to April as shown in Figures 4.12. The peak month was October with the least wind velocities occurring in April. About 80 km/day (0.96 m/s) to more than 129 km/day (1.5 m/s) wind velocities were experienced in the area with a maximum average of 99.1 km/day (1.2 m/s) and a minimum of 5.2 km/day (0.1 m/s). High winds tend to increase the rate of evapotranspiration as the rate of evaporation increases with the moving air. Such wind will also clear the air of any humidity produced by the plants' transpiration thereby increasing the rate of evapotranspiration. Levubu valley showed high wind velocity of more than 100 km/day during the summer months from October to December while minimal wind speed were experienced downstream of the catchment.

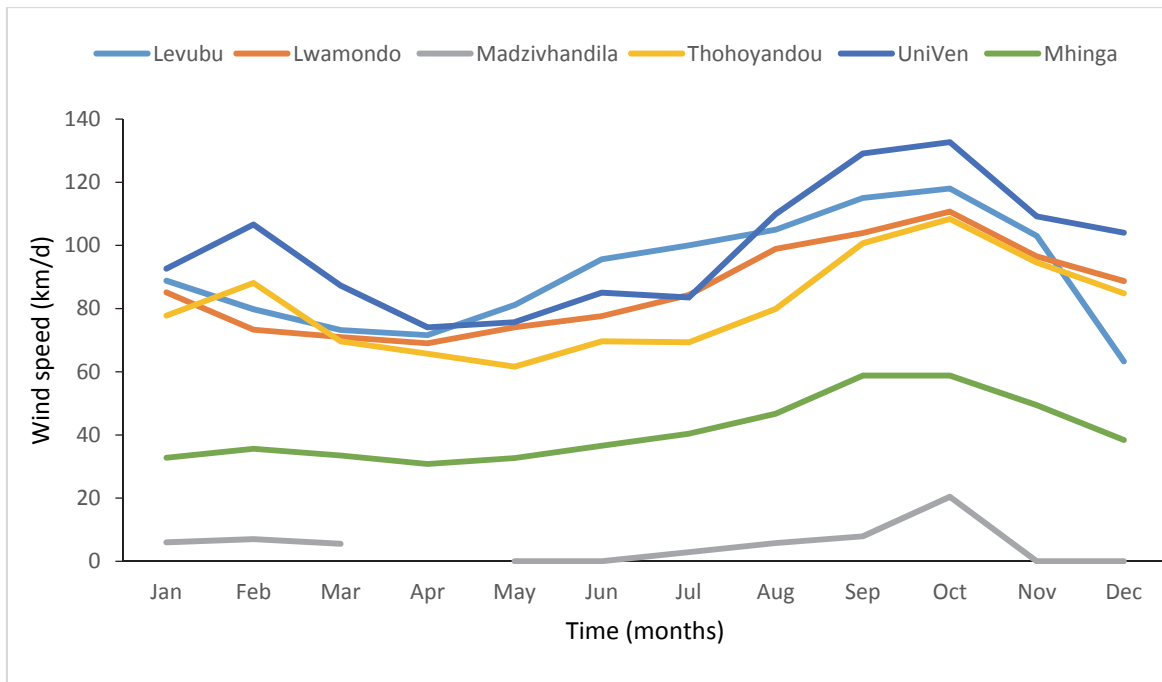


Figure 4.12: Average monthly wind speed for selected stations in the study area

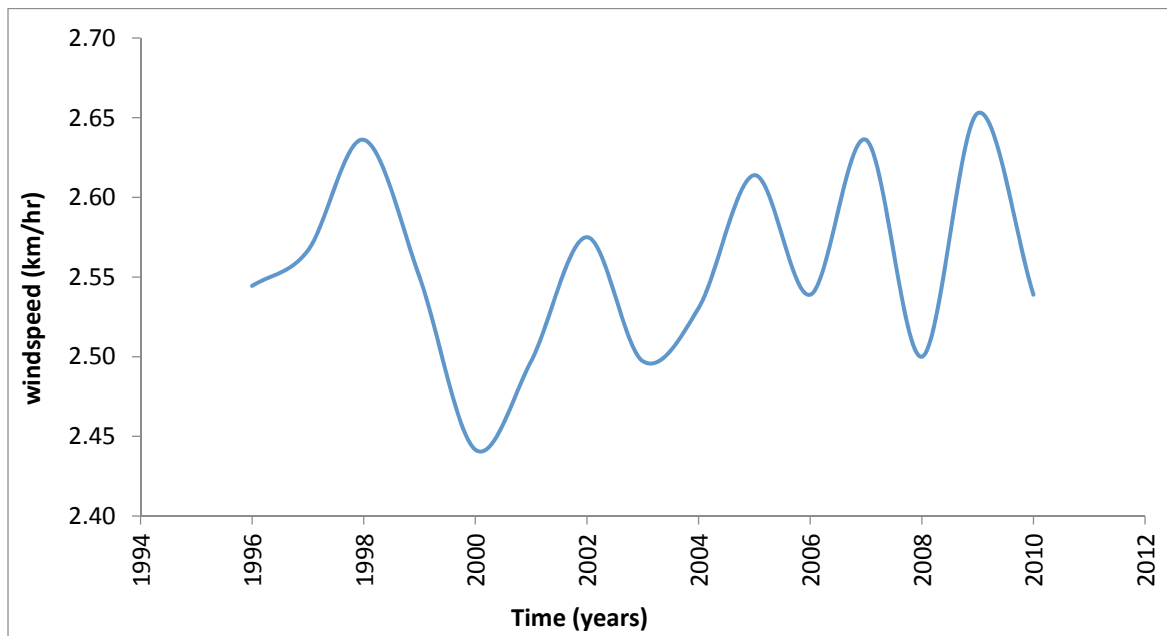


Figure 4.13: Average annual wind speed for Thohoyandou

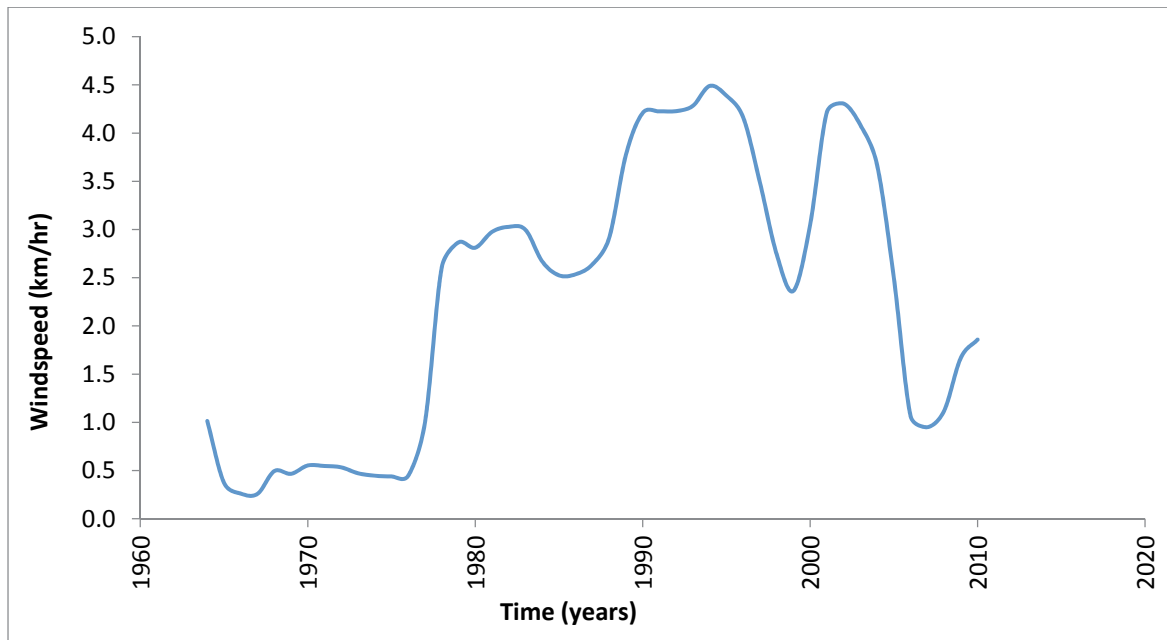


Figure 4.14: Average annual wind speed for Levubu

#### 4.8 Model Performance

The model evaluation statistics showed that Nash-Sutcliffe (NSE) ranged between 0.894 and 0.924 as shown in Figures 4.15 and 4.16. The NSE coefficient approached unity indicating that the CROPWAT estimated values and the calculated values by the Penman-Monteith method had a good correlation. The value of NSE equal to 1.0 would be the optimal value while values between zero and 1.0 would be generally viewed as acceptable levels of performance. Values less than zero from the model would indicate that the mean observed value were better predictors than the simulated values, which would depict unacceptable performance for the model.

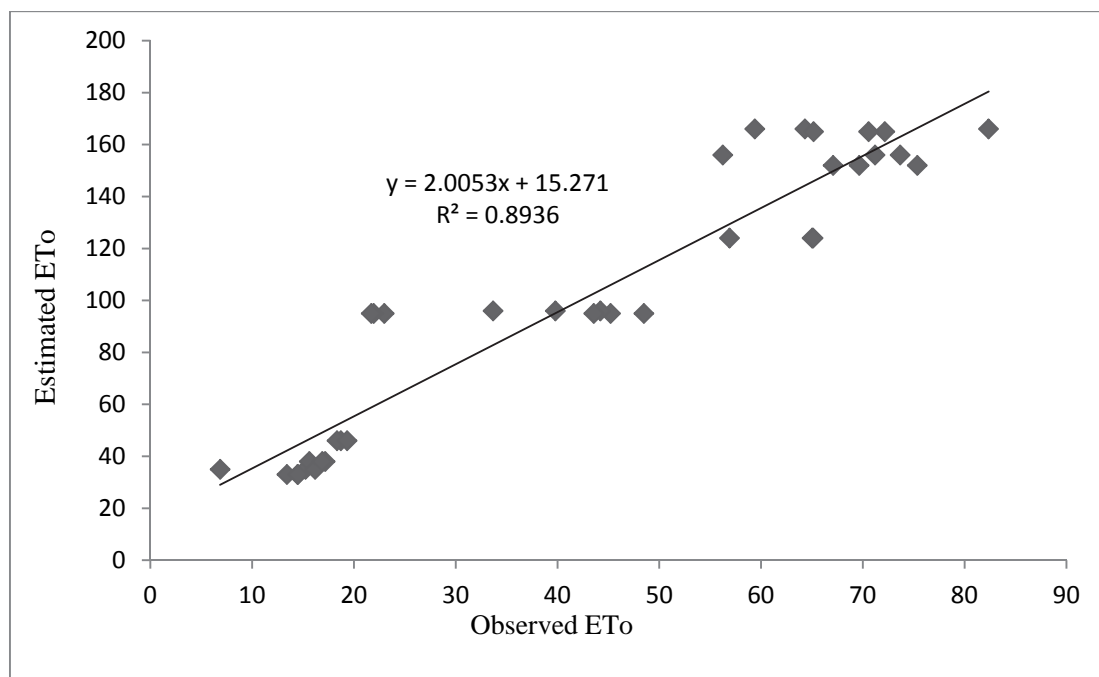


Figure 4.15: Linear regression of estimated ETo over observed ETo

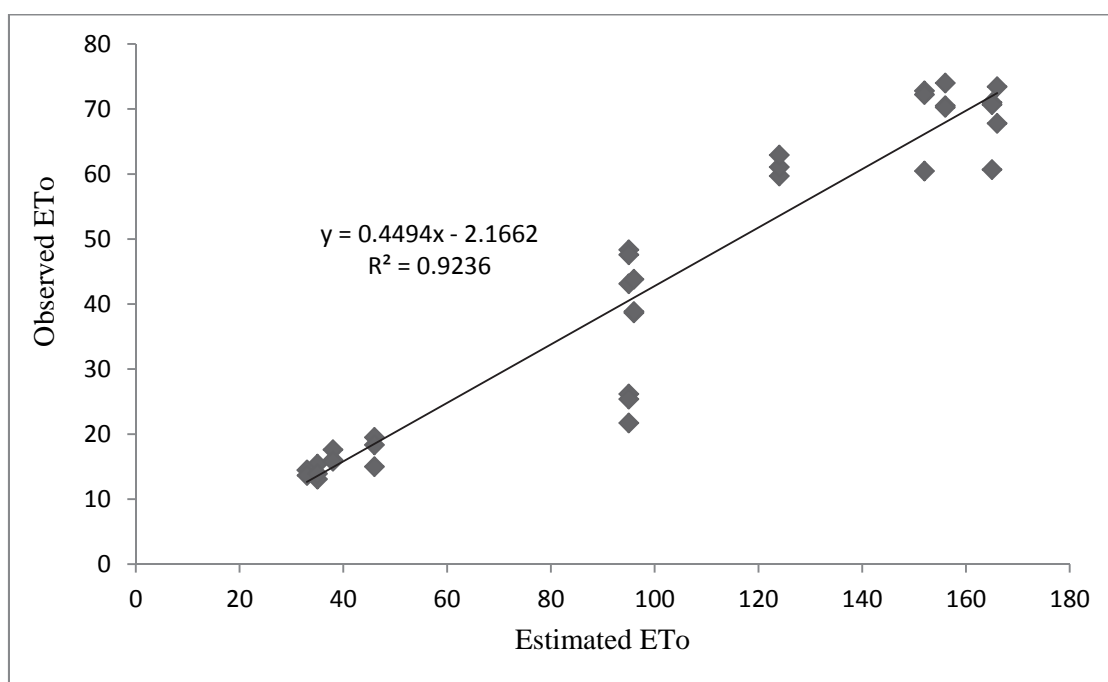


Figure 4.16: Model validation

## 4.9 Stream discharges

Luvuvhu River rises as a steep mountain stream in the southeasterly slopes of the Soutpansberg Mountain range, flows through KNP, and empties into the Limpopo River at the border with Mozambique and Zimbabwe. Daily streamflow data for eight pluviometric stations located in the catchment were obtained. Estimates for the bank full depth, width of the river channel bottom and other flow characteristics were acquired from the Department of Water Affairs (DWA). The length of the river reaches and their slopes were derived from the



DEM using ArcHydro tools. Figure 4.17 and Table 4.2 showed the spatial distribution of gauging stations in the catchment respectively. Streamflow is regarded as the main mechanism by which water moves from land to the water bodies such as oceans. It is thus regarded as the volume of water moving past a cross-section of a stream over a set period of time.

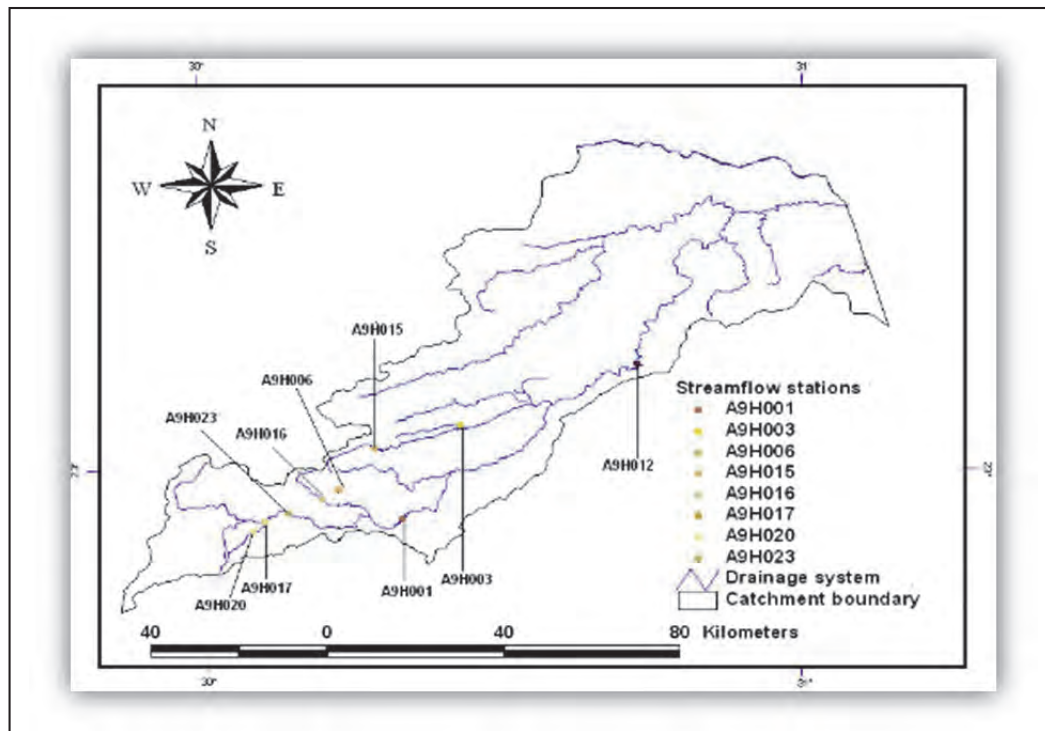


Figure 4.17: Location of gauging stations used in the study

Table 4.2: Gauging stations used in the study

Station No	Station Name	Measurement Site
A9H001	Luvuvhu River	Weltevreden
A9H003	Tshinane River	Chibase
A9H006	Canal from Livhungwa River	Barotta
A9H012	Luvuvhu River @Mhinga	Mhinga
A9H015	Canal From Livhungwa River	Barotta
A9H016	Latonanda River	Levubu Settlement
A9H017	Left Principal Canal From Dam	Goedehoop
A9H020	Luvuvhu River	Goedehoop
A9H023	Canal From Luvuvhu River	Nooitgedacht

#### 4.9.1 Changes in Flow Regimes

The flow in a river is made up of three components: base flow; interflow; and surface flow. Base flow is the water that comes from the ground discharging into the river. Interflow is the rapid subsurface flow through the channels in the soil. Plate 14 and plate 15 both showed water levels in Luvuvhu River at the KNP. Plate 15 further depicts the water levels in the river during the year 2000 flood that resulted in major damage within the catchment.



Plate 14: Luvuvhu River at KNP



Plate 15: Flooding in Luvuvhu River at KNP (Source; Kruger-2-Kalahari. 2014)

In dealing with effects of land use transformations, it is important to distinguish between effects on water yield and on flow regimes, (the seasonal distribution pattern of streamflow). Annual values of discharge and discharge to rainfall ratio give the combined effect of storm runoff and base flow and thereby conceal the actual changes that occur in the discharge pattern during the relatively wet and dry periods. To distinguish such seasonal changes within the annual cycle, changes in flow regimes were investigated to assess the variations based on mean monthly discharge. To understand the underlying causes of changing flow regimes, monthly rainfall-discharge relations, based on moving averages, were analyzed separately.

Figure 4.18 showed the annual maximum discharge for Luvuvhu River for 52 hydrological years from 1960/61 to 2012/13 in station A9H003. The 52-year mean instantaneous flow showed that the highest measured flow of  $175.61 \text{ m}^3/\text{s}$  was recorded during the 1999/00 hydrological year, while the lowest flow of  $0.17 \text{ m}^3/\text{s}$  was recorded in 1982/83. A 5-year moving average smoothed the data to highlight significant changes in the trend. The smoothed trend showed significant hydrological conditions which may suggest that erratic rainfall associated with climate variability and land use change may have caused flood peaks to increase. The coefficient of variation indicated that the distribution of flood flows was highly variable. A significant seasonality in the influence of rainfall on river discharge was identified through the analysis of seasonal rainfall and river discharge data.

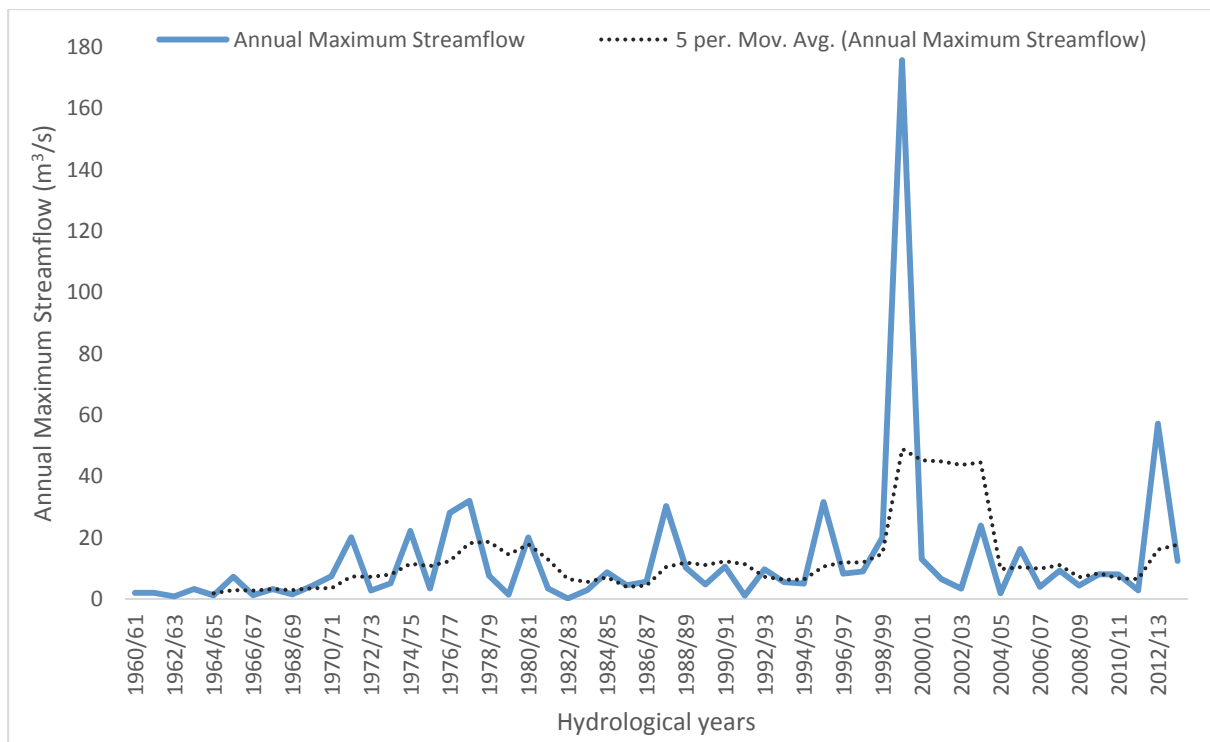


Figure 4.18: Stream discharge from 1960 to 2013

## CHAPTER 5

### SOIL ANALYSIS

Information on soil characteristics is important in catchment studies and hydrologic modelling. Specific information like soil type, texture, structure, porosity and hydraulic conductivity are essential in understanding the hydrologic cycle. A detailed soil survey for LRC was necessary but beyond the scope of this study. A physiographic soil survey approach based on landform and landscape ecology was therefore adopted. The soils were regrouped into five sub-groups due to variation in the mineralogical composition, relief and topography. Based on the data available and the characteristics of the soils from the area, the five most practical sub-groups were, Regosols (M1, Pd5), Cambisols (M11, M12), Ferrasols (Lc2), Lava, and Acrisols (L9). Regosols (M1) are shallow to moderately deep, brown to dark brown with inclusions of lava. Regosols (Pd5) are well drained, deep, pale brown to yellowish brown. Cambisols (M11) are sandy clay loam soils, Cambisols (M12) are rocky sandy clay loam soils with an acid humic topsoil. Ferrasols (Lc2) are well drained, deep, red, very friable sandy clay loam to clay. Acrisols (F15) are a complex of somewhat excessively drained to well drained, deep to very deep, dark red to brown, loose sandy loam to friable to firm clay.

The soil sampling and test sites in the catchment were selected based on specific attributes such landscape ecology, farmland, built-up and settlement. Figure 5.1 shows the spatial distribution of the soil sampling and test sites.

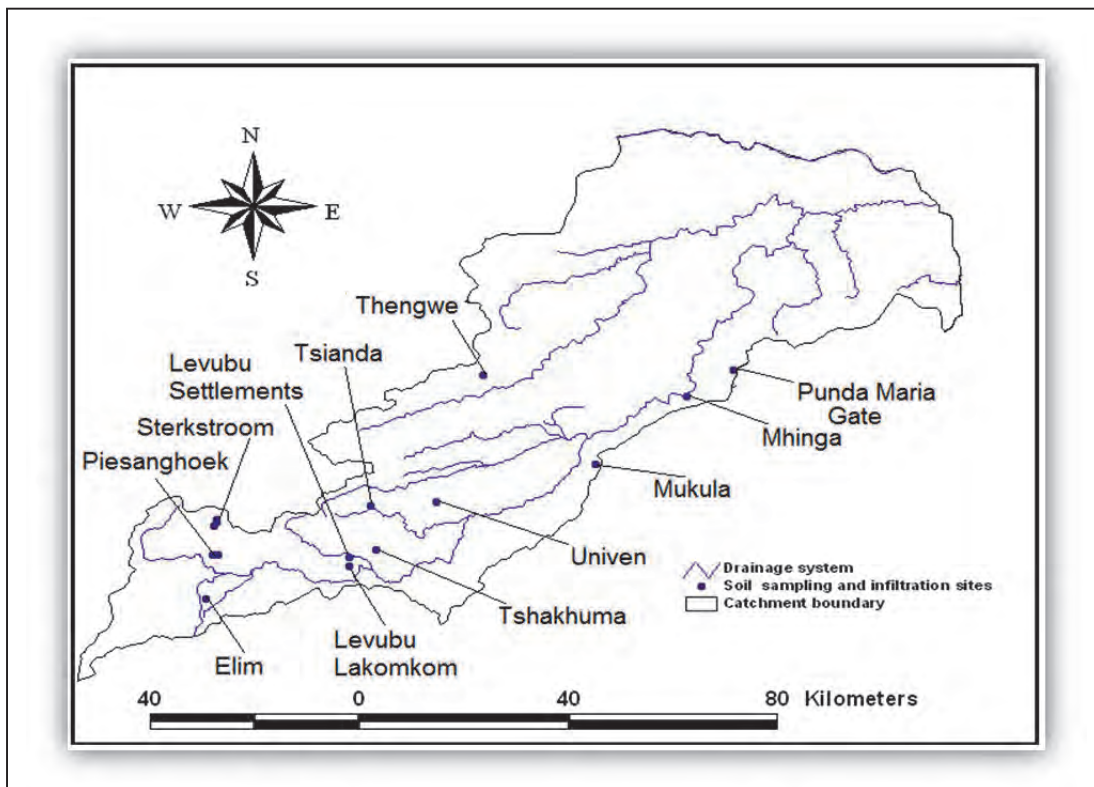


Figure 5.1: The spatial distribution of soil sampling sites

## 5.1 Soil sampling at a test site

Soil sampling and test sites were selected to represent the different land elements which included the valley bottom, the sloping land and the hill tops in different location in the catchment. Soil samples were collected at three random points around the infiltrometer by augering at 0-30 cm, 30-60 cm, 60-90 cm and 90-1000 cm depth. One set was used for initial soil moisture determination while the other was used for soil texture analysis using a mechanical sieve shaker with sieves of between 4 mm to 200  $\mu\text{m}$  sieve mesh. To determine the initial soil moisture, the soil samples were placed in a drying oven, at 105°C for 24 hours, after which the soil was removed from the oven and weighed. The weight of the container was subtracted from both the weight of moist soil and dry soil to determine the percentage of the initial soil moisture content.

To determine the particle size distribution, the mass of soil retained on each sieve was obtained by subtracting the weight of the empty sieve from the mass of the sieve plus retained soil, and this mass was recorded as the weight retained on the data sheet. The percent retained on each sieve was obtained by dividing the weight retained on each sieve by the original sample mass. Percentage passing (or percent finer) was calculated by starting with 100 percent and subtracting the percent retained on each sieve as a cumulative procedure. A semi-logarithmic graph plot of grain size versus percent finer was then made. The USDA textural triangle showing the soil texture of LRC was plotted using D-Plot computer software. Plate 16 showed soil augering and collecting of samples on a Macadamia farm after the infiltration test in Piesanghoek macadamia cropland.



Plate 16: Collecting samples for determining the texture and moisture content

## 5.2 Soil texture

The results showed a high proportion of sandy loam and silt loam, where sandy loam contained 50-88% silt, 0-27 clay, and 0-50 sand. Silt loam on the other hand contained 50% silt, 7-20% clay and more than 52% sand.

In semi-arid regions like the LRC, sandy loams are well drained soils and are good for plant growth, though the constant renewal leads to deeper, more nutrient-enriched soils which are favourable to the development of forests.

Available soil surveys in the catchment indicated that 17% of the soils of the basins (960 280 ha) were potentially suitable for afforestation. However, only 14% of this area (14 750 ha) has been planted (Hope *et al.*, 2004). Silt loams on the other hand are poorly drained and are easily eroded into streams and rivers from cultivated lands. The lowland areas are dominated by clay-rich soils which shrink and swell with changes in moisture content (Vertisols) and clay accumulation horizon, or argic B-horizon (Acrisols) (FAO-ISRIC-ISSS, 1998). In other words, soils in lowland areas are characterized by clay-enriched lower horizons and weakly developed organic horizons (IUSS, 2006). The lowveld areas however, are dominated by soil consisting of unconsolidated material from freshly deposited alluvium or sand (Regosols).

Thus, the soils in the study area vary in productivity and are also vulnerable to various forms of degradation, either physical, chemical or biological and hence appropriate management strategies are critical if productivity of the soils is to be improved and sustained

A study by Bumby (2000) found that the upland areas of the catchment were dominated by soils derived from quartzite and sandstones (Leptosols), which are generally shallow, gravely and well drained, with low nutrient content and acidic characteristics. Figure 5.2 showed the soil map for LRC (ARC, 2006).



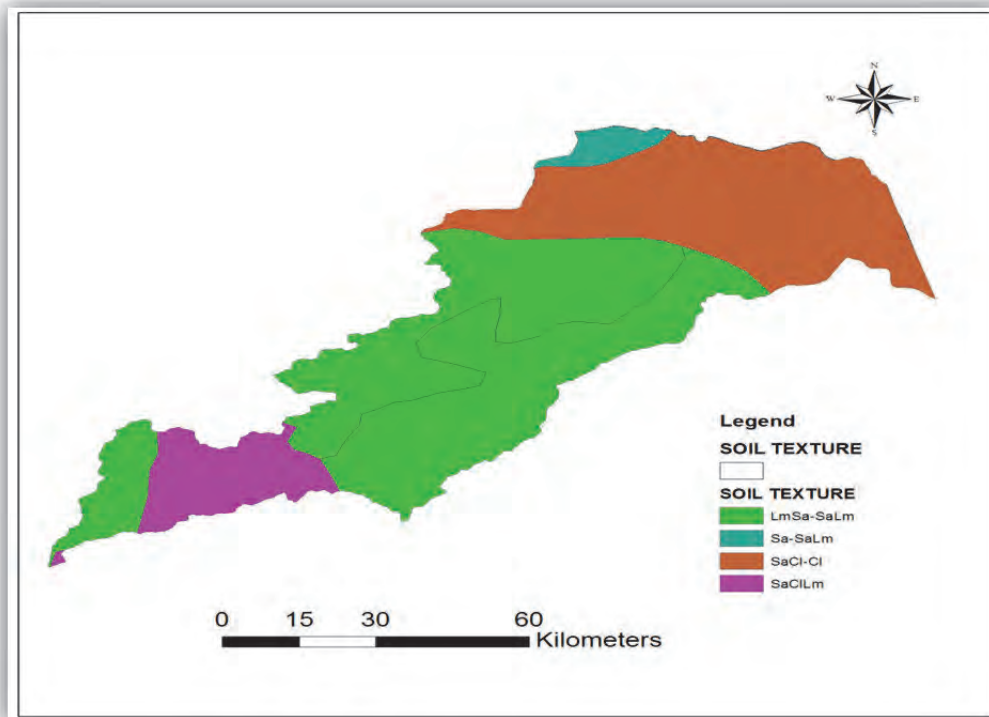


Figure 5.2: Soil map for LRC (Source: ARC, 2006).

The particle size distribution curves for Levubu settlements at various depths were as shown in Figure 5.3. The grading curves showed that the soils at the sampling sites comprised of smooth, concave distribution curves revealing well graded soils. Particle size distribution for various sites in the catchment is presented in Figure 5.4. The behaviour of the grading curves is uniform throughout the catchment.

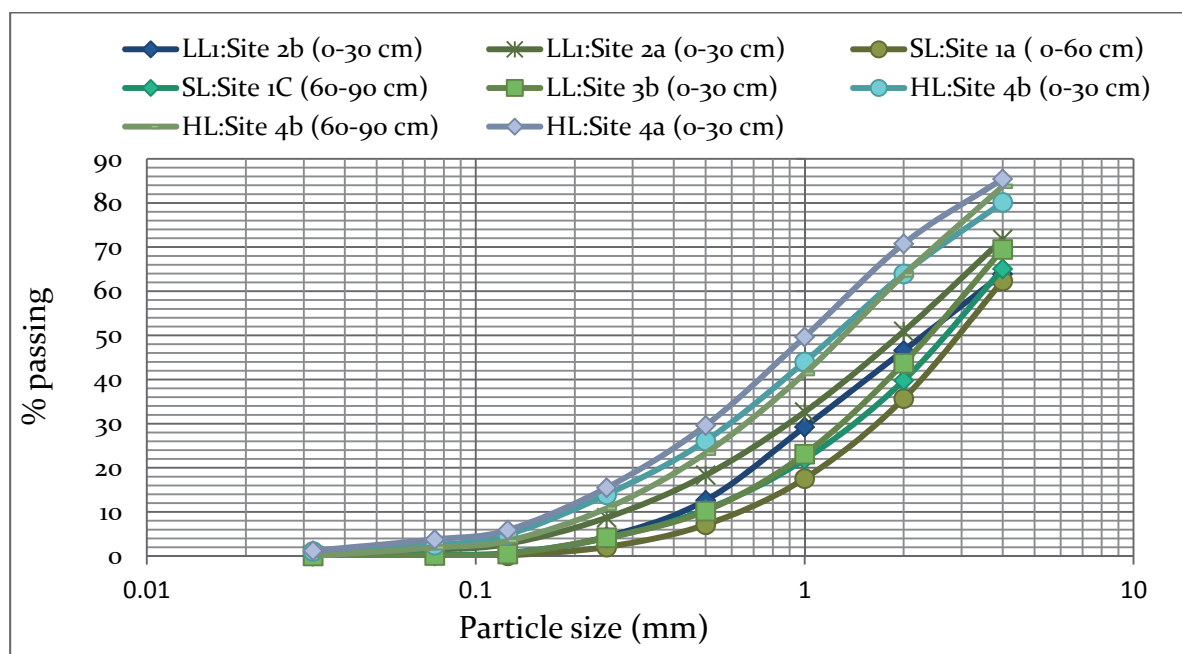


Figure 5.3: Gradational curves for Levubu settlement test site



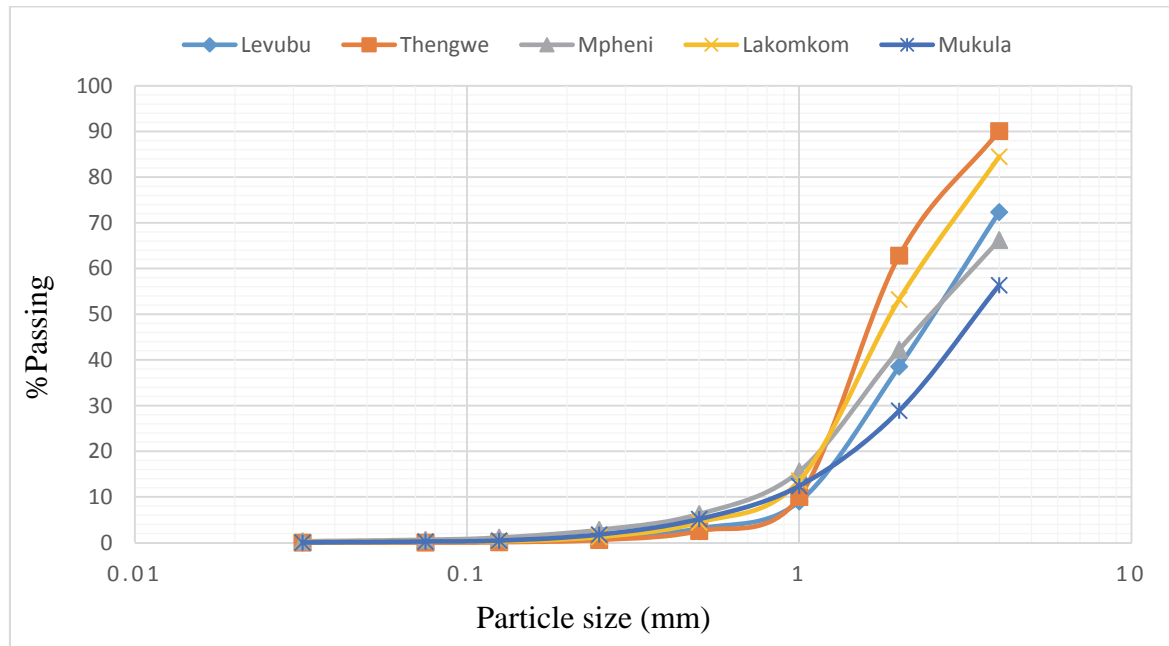


Figure 5.4: Gradational curves for various selected sites in the catchment

The soil classification triangle for the catchment was as shown in Figure 5.5. The textural results were plotted using the D-Plot version 2.0.4.7 computer software (Hydrosoft computing, 2006). The results showed a high proportion of sandy loam and silt loam, where sandy loam contained 50-88% silt, 0-27% clay, and 0-50% sand. Silt loam on the other hand contained 50% silt, 7-20% clay and more than 52% sand.

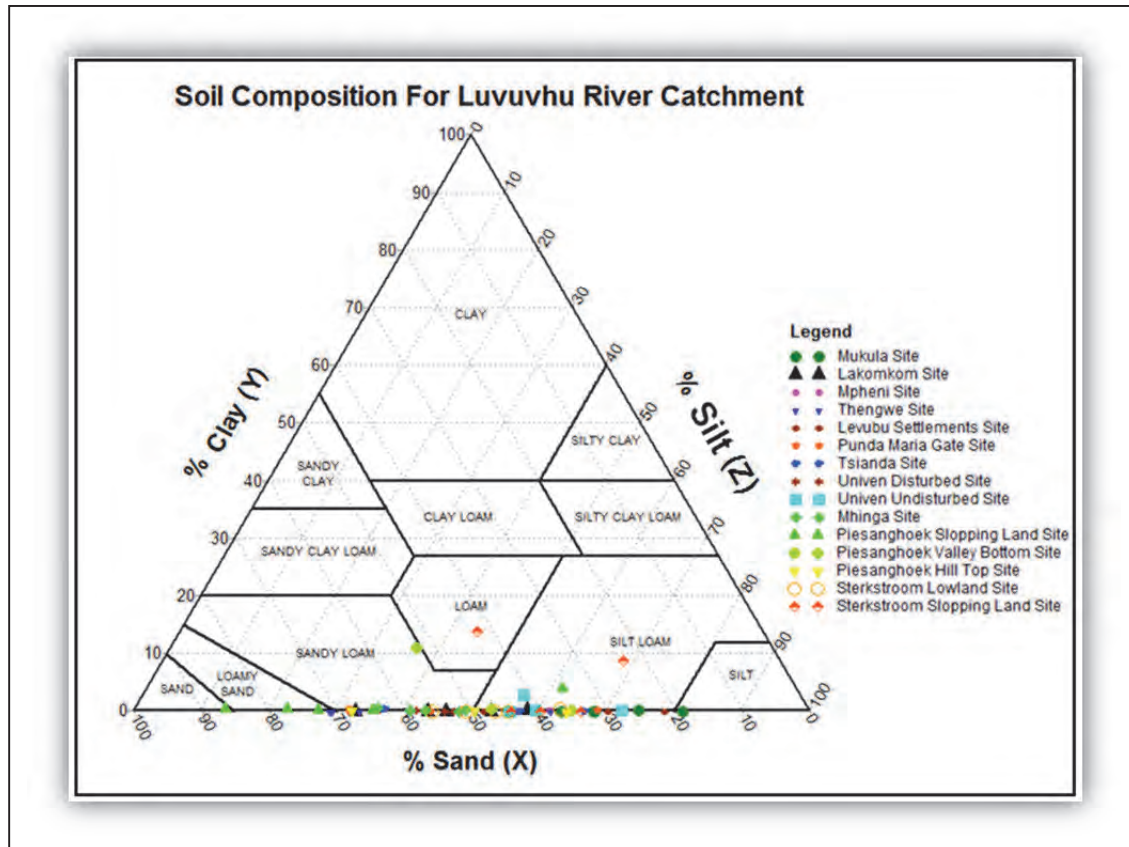


Figure 5.5: The soil triangle for LRC

### 5.3 Soil moisture

To determine soil moisture, soil samples were placed in a drying oven, at 105°C for 24 hours, after which the soil was removed from the oven and weighed. The weight of the container was subtracted from both the weight of moist soil and dry soil to determine the percentage of the initial soil moisture content. The soil moisture for the selected test sites were as shown in Figures 5.6. Initial soil moisture varied across the catchment with location and depth. From the presented results, Levubu settlements and Riverside showed high soil moisture content of 40% and 29% respectively at a depth of 90 cm to 1 m.

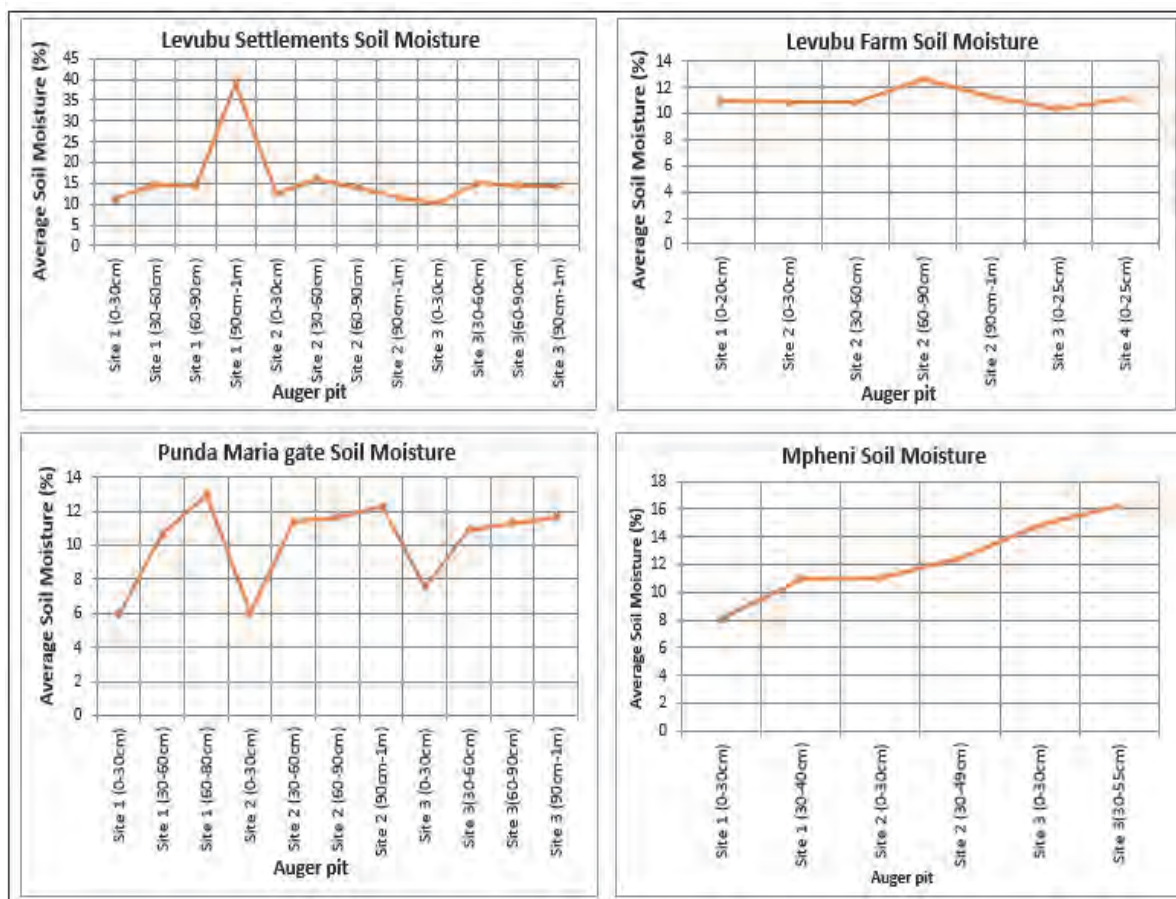


Figure 5.6: Soil moisture for selected sites in the catchment

The results showed that soil moisture was variable in space and time within the catchment being influenced by soil texture, vegetation, topography, and other hydrological components. At all sites, the soil moisture increased with an increase in soil depth up to 90 cm, and then declined to 1 m depth. An increase after 90 cm was noted at Levubu settlements site 1, Mhinga, Univen (University of Venda) disturbed site, and Piesanghoek. At Tsianda site 1 and Elim, soil moisture did not change significantly after 60 cm. The gravimetric soil moisture content was very high at Tsianda site 2 reaching an estimate of 92.64% at 60-90 cm depth. For other average values, the soil surface moisture content was less than 40% at all other sites. The lowest soil water content was found at Thengwe with a minimum average of 8.19, 7.03, and 6.48% at sites 1, 2, and 3 respectively. The higher evapotranspiration capacity associated with plantation, forest and shrub vegetation may have resulted in lower soil moisture contents in these parts.

## 5.4 Infiltration

Infiltration rates were determined in situ using a double ring infiltrometer. Tests were carried out on three different topographical locations at selected sampling sites which constituted of a valley bottom, sloping land and the hill top. The tests were run for two hours and once the values were constant, the basic infiltration rate had been reached.

#### 5.4.1 Tsianda sampling and test site

Tsianda test site lies in the headwater catchment area for Guvhevu River, whose flow was found to have reduced significantly. The landscape comprised of hilly land with saddles and shallow valleys. Figure 5.7 showed the infiltration rate and cumulative infiltration curves respectively.

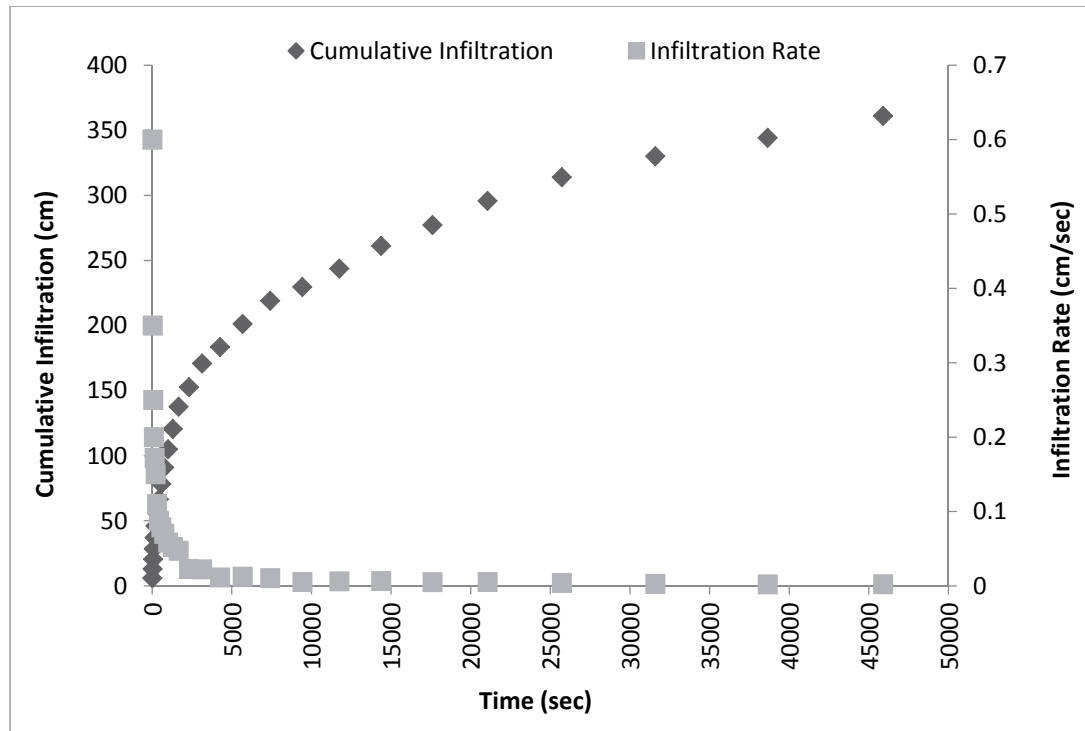


Figure 5.7: Infiltration curves for Tsianda test site

#### 5.4.2 Mhinga sampling and test site

The landscape in Mhinga comprised of rolling land and hills with shallow valleys. The vegetation ranged from open grassland with scattered trees to shrubs and thick bushes. Horticultural farming was practiced on a small scale. Sampling and test sites were selected to represent the different land elements which included the valley bottom, the sloping land and the hill tops. Plate 17 showed the infiltration test at Mhinga site, while Figure 5.8 showed infiltration rate and cumulative infiltration curves respectively.



Plate 17: Infiltration test at Mhinga site

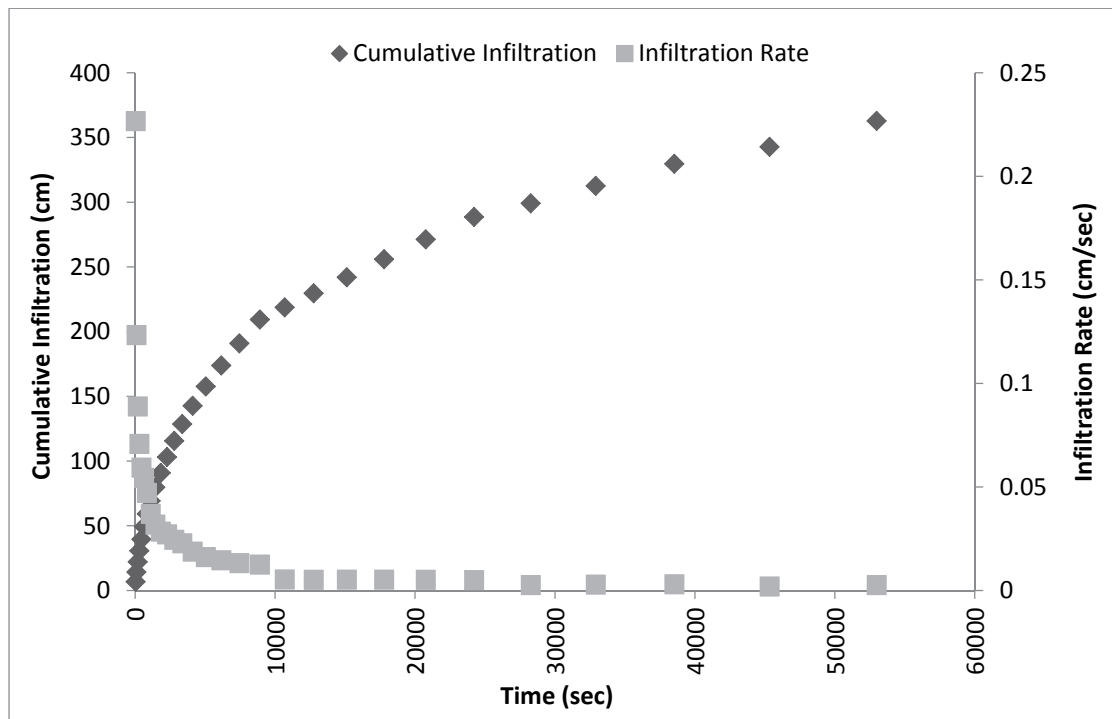


Figure 5.8: Infiltration curves for Mhinga test site

#### 5.4.3 Univen School of Agriculture test site

The farm is located on a gently sloping land and is under horticultural farming, producing cabbages and tomatoes. Figure 5.9 showed the infiltration rate and cumulative infiltration curves respectively.

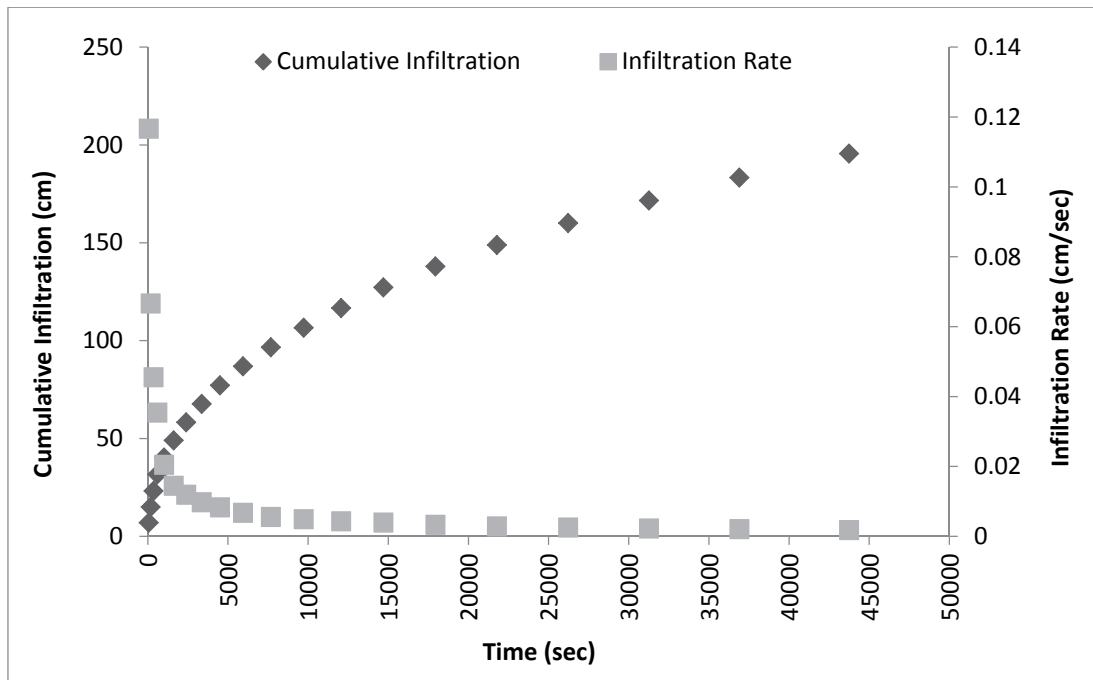


Figure 5.9: Infiltration curves for Univen school of Agriculture farm test site

#### 5.4.4 Thengwe sampling and test site

The landscape in Thengwe comprised of rolling land and hills with shallow valleys. The vegetation ranged from open grassland with scattered trees to shrubs and thick bushes. Figure 5.10 showed the infiltration rate and cumulative infiltration curves respectively.

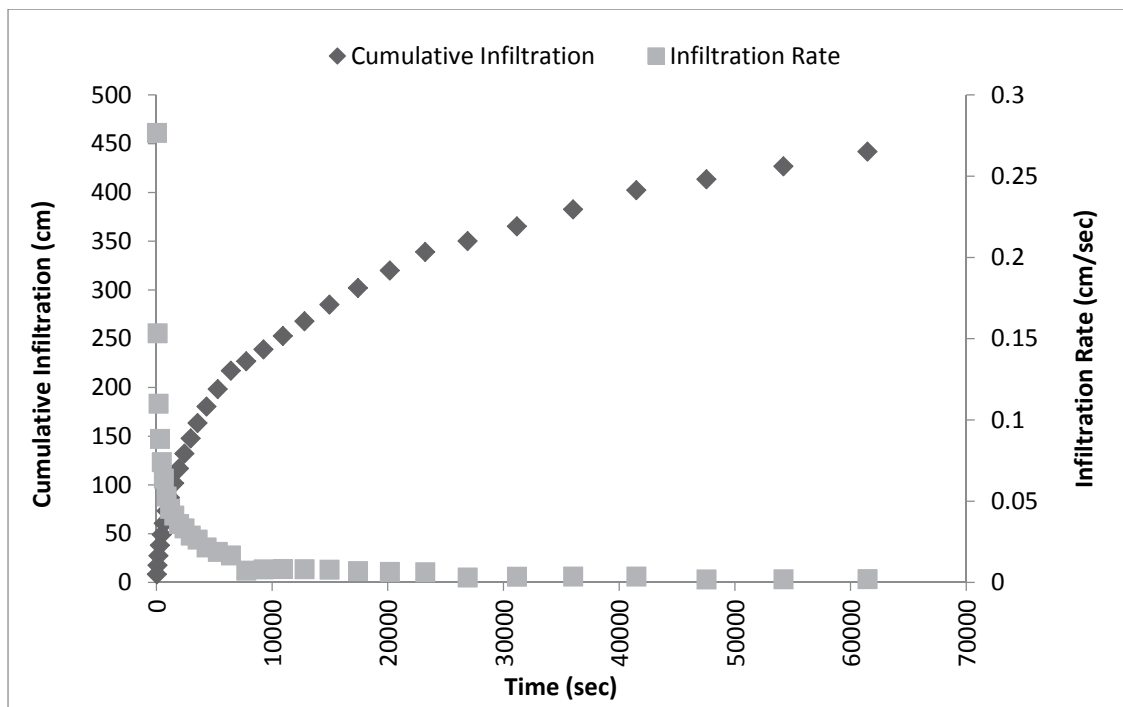


Figure 5.10: Infiltration curves for Thengwe test site



#### 5.4.5 Mukula sampling and test site

The landscape in Mukula comprised of rolling land and hills with shallow valleys. The vegetation ranged from open grassland with scattered trees to shrubs and thick bushes. Figure 5.11 showed the infiltration rate and cumulative infiltration curves respectively.

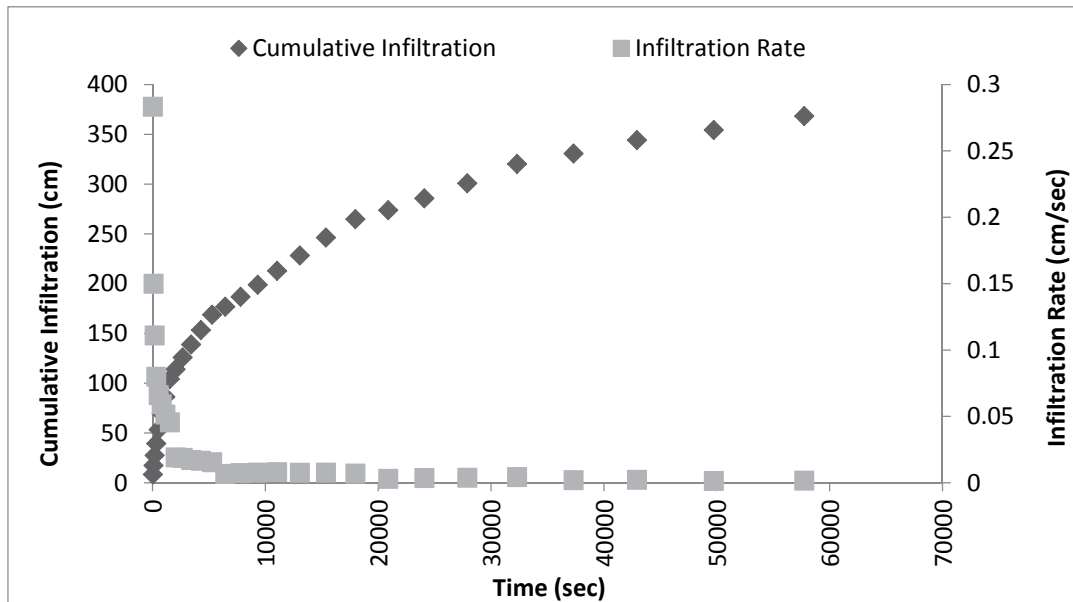


Figure 5.11: Infiltration curves for Mukula test site

#### 5.4.6 Levubu at Dandani/Lakomkom farm sampling and test site

The landscape at Dandani/Lakomkom farm comprised of rolling land and hills with shallow valleys. The vegetation ranges from open grassland with scattered trees to shrubs and thick bushes. Figure 5.12 showed the infiltration rate and cumulative infiltration curves respectively.

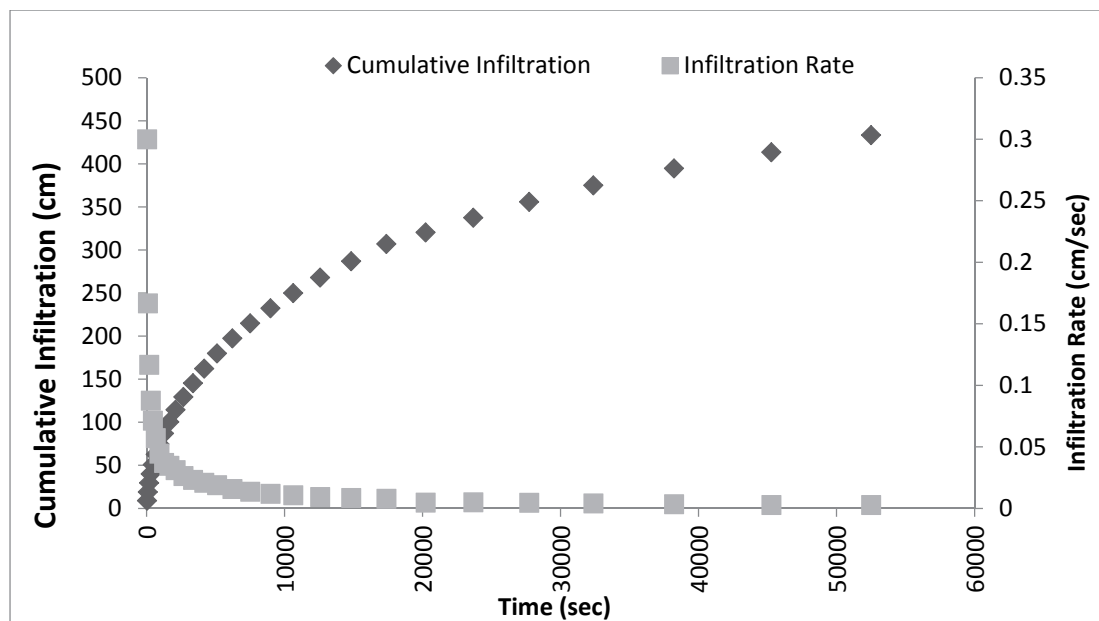


Figure 5.12: Infiltration curves for Dandani/Lakomkom test site



#### 5.4.7 Mpheni village at Elim test site

The landscape in Elim comprised of rolling land and hills with shallow valleys. The vegetation ranges from open grassland with scattered trees to shrubs and thick bushes. Figure 5.13 showed the infiltration rate and cumulative infiltration curves respectively.

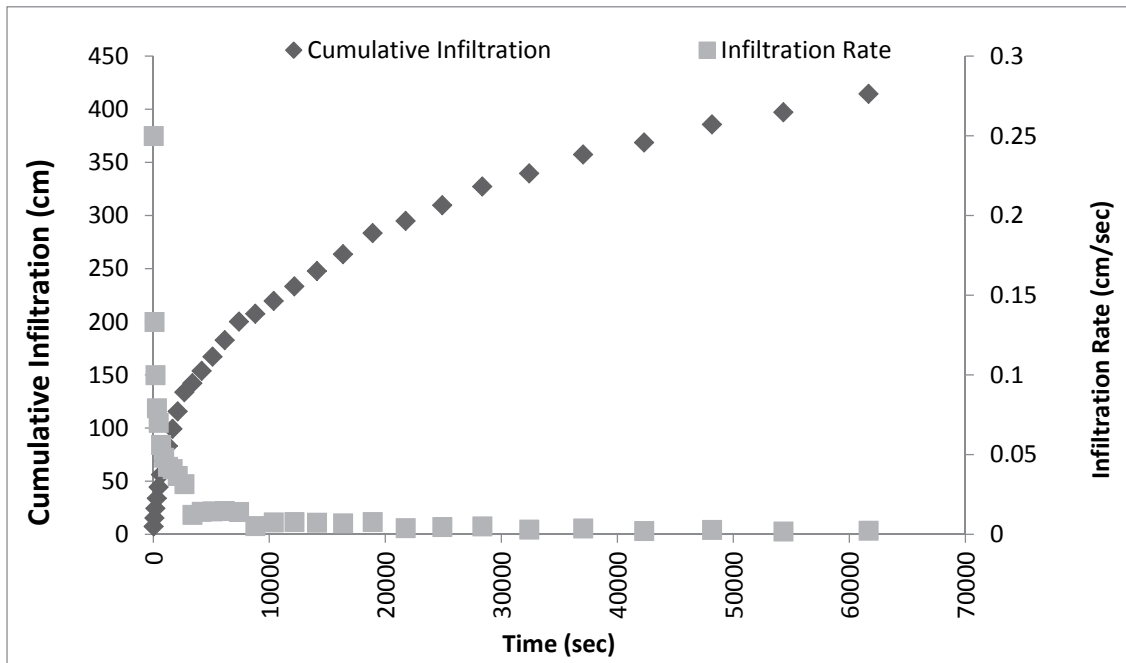


Figure 5.13: Infiltration curves for Elim test site

#### 5.4.8 Levubu Village at Tshakuma test site

The landscape in Tshakuma comprised of rolling land and hills with shallow valleys. The vegetation ranges from open grassland with scattered trees to shrubs and thick bushes. Figure 5.14 showed the infiltration rate and cumulative infiltration curves respectively.

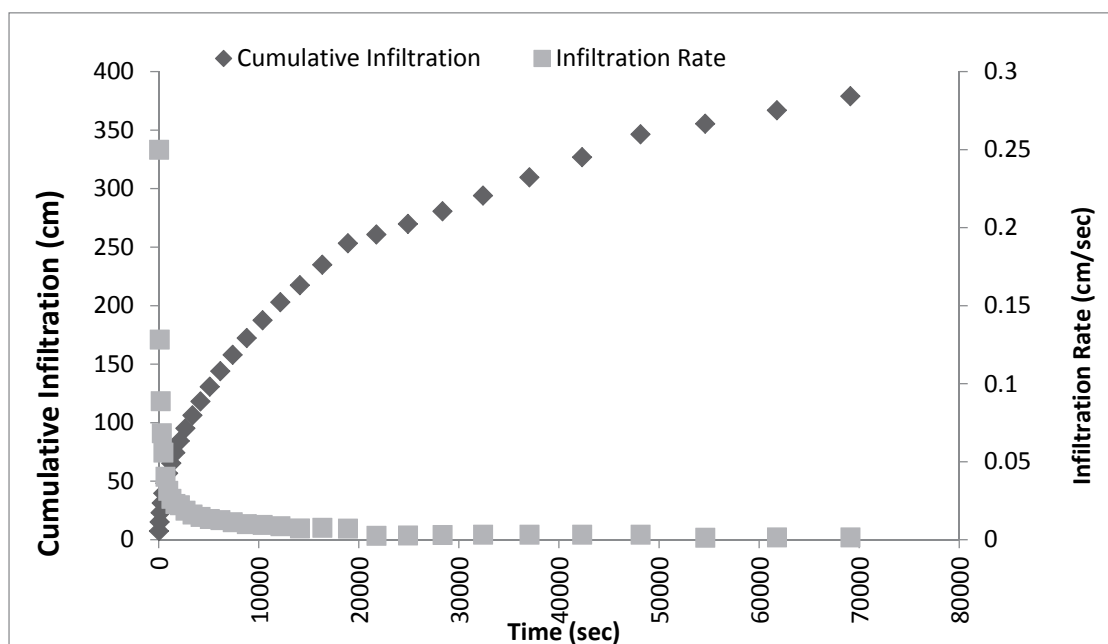


Figure 5.14: Infiltration curves for Tshakuma test site

#### 5.4.9 Matiyani village at Punda Maria test site

The landscape in Punda Maria comprised of rolling land and hills with shallow valleys. The vegetation ranged from open grassland with scattered trees to shrubs and thick bushes. Figure 5.15 showed the infiltration rate and cumulative infiltration curves respectively.

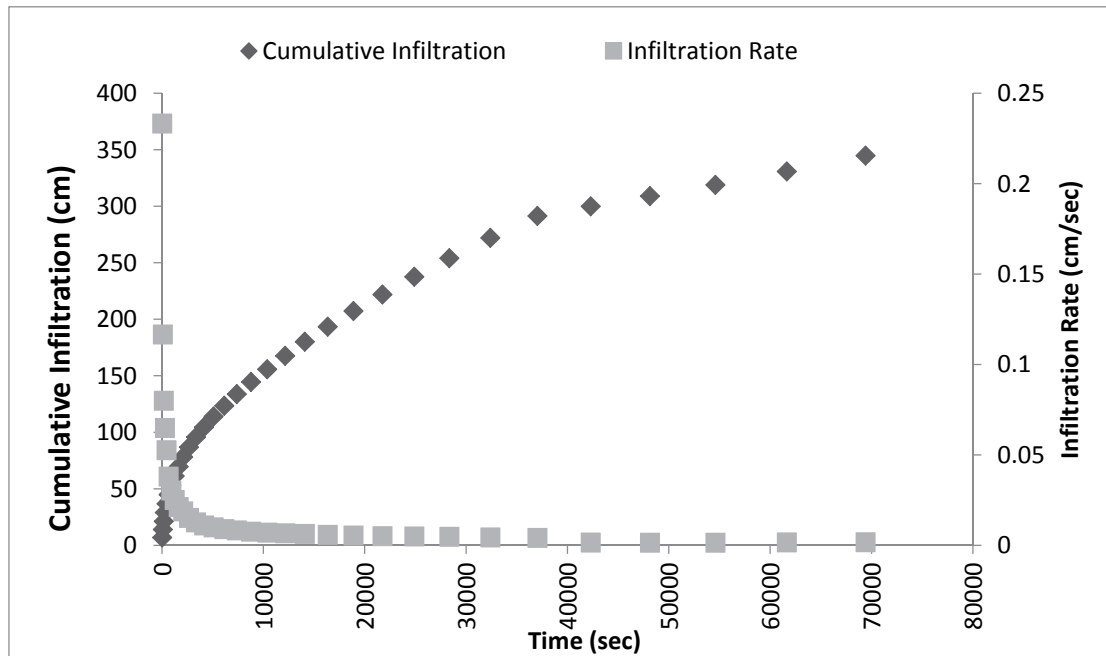


Figure 5.15: Infiltration curves for Punda Maria test site.

Cumulative infiltration indicated the variability in water intake rates of soils units within the experimental sites. In general, the initial infiltration rate was high when water was applied to dry soil. In the study area there was removal of indigenous vegetation which leaves the ground exposed to the surface. Figure 5.16 showed the combined infiltration curves for all the test sites.

Since most areas of land were used for agricultural production, a small loss in the infiltration capacity of agricultural soils may have serious impacts on flood intensity. At some sites, infiltration rates were very high exceeding 100 mm/hr. All infiltration curves showed that the initial infiltration rates for the study area were high, ranging from 72.0 mm/hr to 108.0 mm/hr. The overall measured infiltration rates ranged from 0.5 mm/hr to 108.0 mm/hr. Hillel (1980) showed that an infiltration rate of less than 15 mm/h is a low infiltration rate; medium infiltration rate ranges from 15 mm/hr to 50 mm/hr; whereas high infiltration rates are those greater than 50 mm/hr.

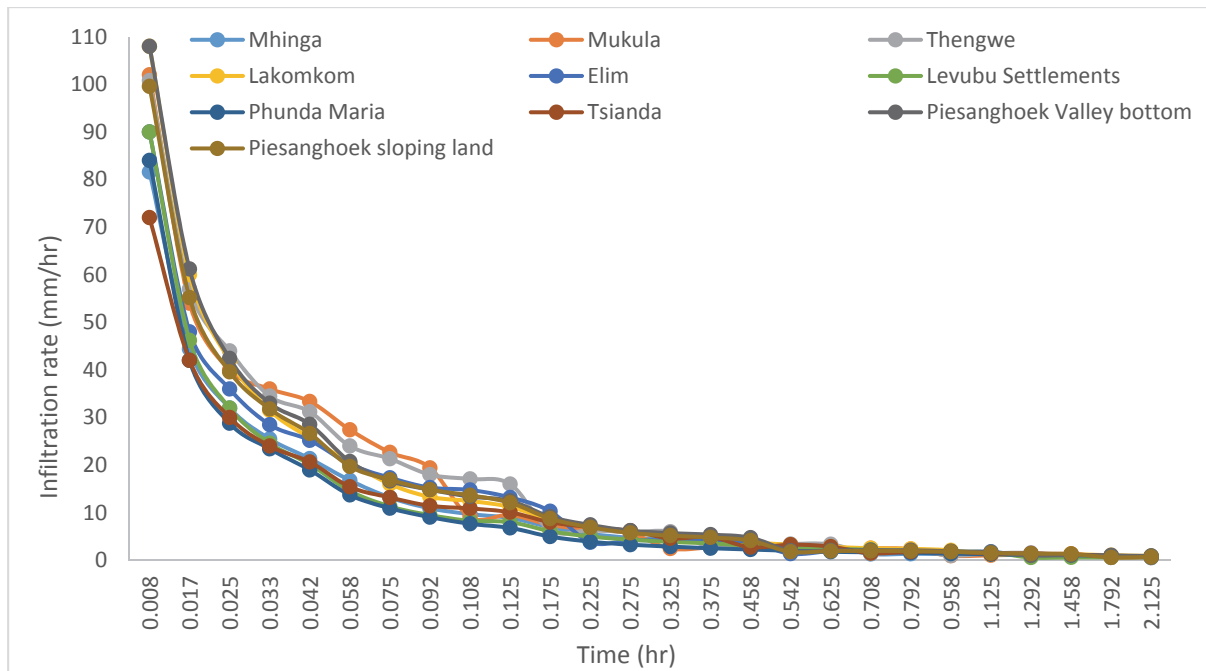


Figure 5.16: Infiltration rates at selected sampling sites

### 5.5 Spatial variability of infiltration rates

A single infiltration rate or a lumped average is often used to define the infiltration capacity of a watershed without considering the location of areas of high and low infiltration capacity (Morin and Kosovsky, 1995). Therefore, in order to differentiate these areas of low and high infiltration, the spatial variability of infiltration becomes significant for proper water and soil management in agricultural land which is a dominant land use in the upper catchment area.

Infiltrimeters and rainfall simulators are the two predominant methods which have been used to measure infiltration and its spatial variability on rangelands, though other methods have been used. Both methods have limitations in their ability to simulate infiltration as it occurs under natural rainfall conditions (Paige and Stone, 2006). A number of studies have used point measurements with geostatistics in an attempt to quantify the spatial variability of hydrologic processes (Bosch and Goodrich, 1996). Rahman *et al.* (1996) examined the spatial variability of soil properties across the landscape and concluded that the geostatistical techniques provide a better description of the nature of variability in soil properties than conventional statistical techniques such as analysis of variance and regression analysis.

Geostatistical tools for Kriging in ArcGIS were used to determine the spatial variability of infiltration in the upper reaches of the study area. The land use in part of the LRC is dominated by large scale agricultural farms. For this study, the average distance between adjacent in-situ soil moisture sites was 100 metres. The elements of each variogram model and the regression coefficient  $r^2$  of the fitting procedure were determined. The model with the higher value of  $r^2$  was selected as an appropriate model to represent the sample semi-variogram. The scatterplot of tail versus head values for a certain lag,  $h$ , is usually called an

$h$ -scattergram. With  $N(h)$  representing the number of pairs separated by lag  $h$ , the statistics for lag  $h$  were computed using Equations 5.1 to 5.3:

$$\text{Covariance: } C(h) = \frac{1}{N(h)} \sum_{\alpha=1}^{N(h)} z(u_{\alpha}) \cdot z(u_{\alpha} + h) - m_0 \cdot m_{+h} \quad 5.1$$

$$\text{Correlation: } \rho(h) = \frac{C(h)}{\sqrt{\sigma_0 \cdot \sigma_{+h}}} \quad 5.2$$

$$\text{Semi-variance: } \gamma(h) = \frac{1}{2N(h)} \sum_{\alpha=1}^{N(h)} [z(u_{\alpha} + h) - z(u_{\alpha})]^2 \quad 5.3$$

Where,  $m_0$  and  $m_{+h}$  are the means of the tail and head values:

$$m_0 = \frac{1}{N(h)} \sum_{\alpha=1}^{N(h)} z(u_{\alpha}) \quad \text{and} \quad m_{+h} = \frac{1}{N(h)} \sum_{\alpha=1}^{N(h)} z(u_{\alpha} + h)$$

And  $\sigma_0$  and  $\sigma_{+h}$  are the corresponding standard deviations:

$$\sigma_0 = \frac{1}{N(h)} \sum_{\alpha=1}^{N(h)} [z(u_{\alpha}) - m_0]^2 \quad \text{and} \quad \sigma_{+h} = \frac{1}{N(h)} \sum_{\alpha=1}^{N(h)} [z(u_{\alpha} + h) - m_{+h}]^2$$

Figure 5.17 showed the spatial variability of infiltration rates for Piesanghoek Macadamia croplands in the upper catchment. The rates were lower where the mean soil moisture values were higher after precipitation events with higher variance being observed during wet periods after precipitation. This could be due to spatially varying soil hydraulic properties such as the soil texture, bulk density and hydraulic conductivity which create differential infiltration rates during wet periods following rainfall, and causing larger variation in soil moisture.

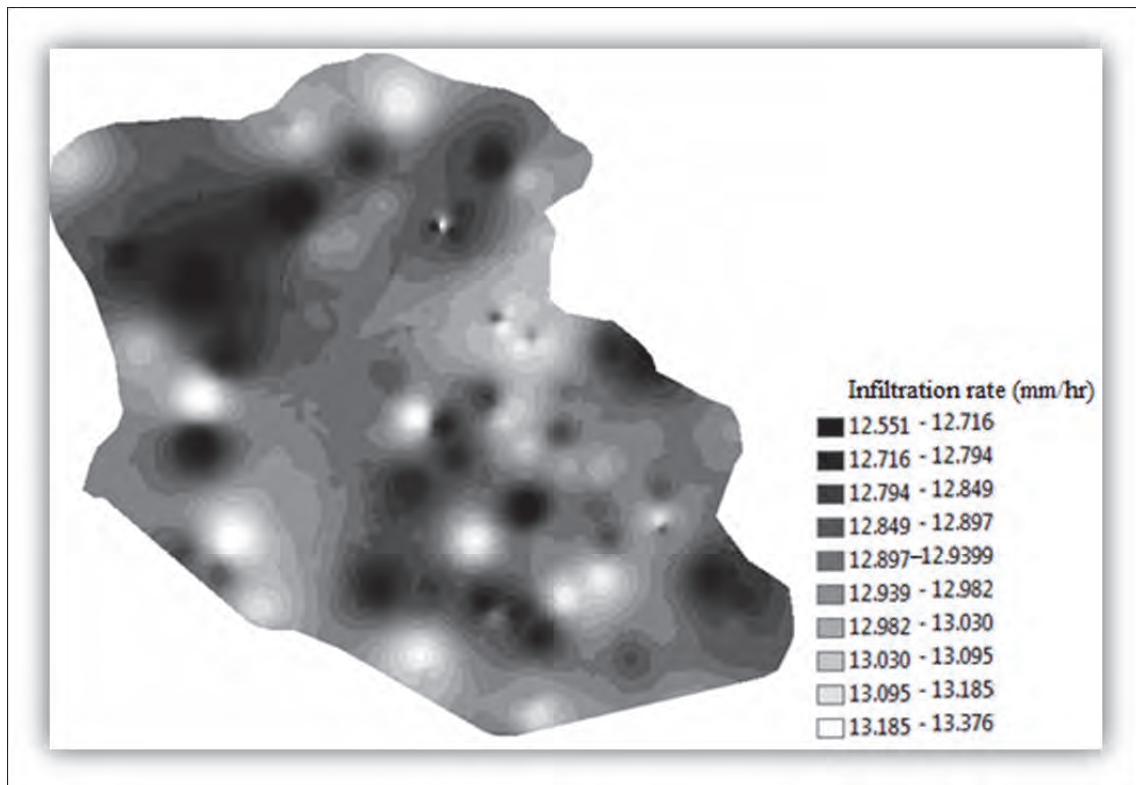


Figure 5.17: Spatial variability of infiltration rates at Piesanghoek Macadamia croplands

## **CHAPTER 6**

### **AUTOMATED CATCHMENT DELINIATION**

The automated derivation of topographic watershed data from DEMs is faster, less subjective and provides more reproducible measurements than traditional manual techniques applied to topographic maps. This approach also has the advantage that the data can be readily imported and analyzed in GIS platforms.

GIS is an important tool for hydrologic modeling as it provides consistent methods for catchment modeling using DEMs. It is a useful tool for creating databases to store geospatial information. With appropriate data it can provide valuable insights into natural systems such as floodplain environments that have been extensively modified by humans. The modeling of physical characteristics may help determine the past extent of landscape ecology and highlight suitable areas for rehabilitation or restoration. It is essential for hydrologists to depict the flow of water through the landscape in space and time.

The DEM hydro-processing procedures produced models that were found to efficiently represent the ground surface. The characteristics of the extracted network showed elevations, slope and network link lengths. The Flow direction model was consistent with the slope direction model. Using the delineated models, the effect of channel morphology on water resources can be analyzed in more detail, given that the ability of a stream to transport is directly related to the rate of energy expenditure as it flows from higher to lower elevations.

The approach provided scope for modeling and managing water resources in LRC. This technique could therefore be adopted to improve land use planning and water management and extended to all projects which take slopes and elevations in consideration for their functional, structural and aesthetic requirements.

#### **6.1 Digital Elevation Model**

DEM refers to the range of topographic variations within a given area. Since contour lines were used for DEM creation, they largely influenced the final product due to data imperfections created during capturing.

##### *6.1.1 DEM generation*

Topography plays an important role in the distribution and flux of water and energy within the natural landscape. The quantitative assessment of hydrological processes such as surface runoff, evaporation and infiltration depend on the topographic configuration of the landscape, which is one of the several controlling boundary conditions.

The ArcScene environment within ArcGIS 10.2 software was used to generate DEMs from contour maps. Arc-Macro language was used to automate the execution of multiple analytical steps in Arc-Info GIS to obtain the necessary image projections for draping on surfaces, calculate areas for land use and rectify polygons. Vertical exaggerations were varied between

3 and 10 to achieve better 3-D views. Various layers were then draped including spatial-temporal images, rivers and orthophotos for selected locations in the catchment. Interpolation is required to generate DEMs from surface specific points and from contour and stream data. The major interpolation methods for point elevation are voronoi polygons, Triangulated Irregular Network (TIN), inverse distance weighting, kriging and splines method.

The desire to describe and evaluate landscape morphology with respect to slope processes is the reason for DEMs. They provide a more systematic and cost-effective approach for slope stability analysis. The basic assumption in DEM analysis is that the shape properties including slope gradient, curvature and position within the geographic landscape are arranged in specific groupings which define the morphology facets of the landscape. These facets are in turn correlated with the behaviour of specific processes such as shallow mass movement.

Pre-processing included the filling of ‘sinks’ or ‘pits’ in the DEM. Spurious sinks or local depressions in DEMs are frequently encountered and can be a source of problems in hydrological analysis. These are a set of grid elements surrounded by higher terrain that, in terms of the DEM, do not drain. These features are extremely rare in natural topography and are generally assumed to be artifacts arising during the development of the DEM

#### *6.1.2 Threshold*

Delineation of the best-fit drainage network from a DEM requires the establishment of a threshold area. A DEM grid can be manipulated to produce many different landscape morphologic models. The first model was the slope gradient also known as the first spatial derivative of elevation. The second model was the aspect or orientation of the slope facet with the maximum gradient.

#### *6.1.3. Extraction of morphologic and hydrologic properties*

The method described by Zevenbergen and Thorne (1987) was used to derive the spatial derivatives of the DEM. The algorithm relies on the use of a third order Lagrange polynomial to obtain the derivatives. The measurable terrain and morphometric attributes shown in Table 6.1 were derived based on quadratic computations as shown in Equation 6.1:

$$h = Af^2g^2 + Bf^2g + Cfg^2 + Df^2 + Eg^2 + Ffg + Gf + Hg + I \quad (6.1)$$

where,  $f$  and  $g$  are spatial coordinates and  $h$  is elevation. The nine parameters,  $A$ ,  $B$ ,  $C$ ,  $D$ ,  $E$ ,  $F$ ,  $G$ ,  $H$  and  $I$  were determined from the nine elevations on the 3 x 3 window.



Table 6.1: Derivation of primary and secondary attributes

Attribute	Category	Calculation Method
<b>Elevation (h)</b>	<b>TIN</b>	<b>DEM</b>
Slope ( $\beta$ )	Primary	$\arctan\left[\sqrt{G^2 + H^2}\right]$
Aspect ( $\phi$ )	Primary	$180 - \arctan\left[\frac{H}{G}\right] + 90 \frac{G}{ G }$
Plan curvature ( $\Phi$ )	Primary	$-2 \frac{DG^2 + EH^2 - FGH}{G^2 + H^2}$
Profile curvature ( $\hat{w}$ )	Primary	$2 \frac{DH^2 + EG^2 - FGH}{G^2 + H^2}$
Curvature ( $\chi$ )	Primary	$2E + 2D$
Contributing area ( $A_i$ )	Primary	$\frac{1}{b} \sum_{i=1}^n a_i$
Compound Topographic Index (CTI)	Secondary	$\ln\left[\frac{A_j}{\tan \beta}\right]$
Stream Power Index (SPI)	Secondary	$A_j \tan \beta$
Slope Aspect Index (SAI)	Secondary	$\phi \tan \beta$

The deterministic eight neighbour (D-8) algorithm (Fairfield and Leymarie, 1991) was used to extract the morphologic and hydrologic properties. It was the simplest flow derivation algorithm available for use with grid DEMs and was able to rapidly extract stream networks in a straightforward and consistent manner. Flow was computed within a 3 x 3 cell kernel, with the central cell only knowing about its surrounding eight cells. This technique formed the basis of hydrological networks derived from DEMs due to its robust nature and rapid straightforward implementation.

The accuracy of the D-8 method is however directly linked to the quality of the DEM. The method had limitations in identifying the drainage pattern where there were depressions, flat areas and flow blockages in the lowland areas between Tshakhuma-Tsianda hills and Elim. It became even more difficult where the features were the result of noisy data, interpolation errors and systematic production errors in DEM elevation values. It was therefore necessary to examine and use ancillary data to remove from the data set all the sinks and problematic cells prior to drainage extraction.

Another limitation with drainage networks extracted from DEMs was the precise positioning of channels in the digital landscape. Overlays and comparisons with actual maps or remotely sensed imagery often showed discrepancies, particularly in low-relief landscapes towards KNP. The major reason being that the approximate nature of digital landscapes could not capture important topographic details below the DEM resolution. Even though the channel

position in the digital landscape was consistent with the digital topography, it sometimes did not reflect the actual drainage path in the field. To overcome this problem, it was necessary to "burn in" the path of the channels along pre-digitized waterways. This was achieved by artificially lowering the elevation of the DEM cells along digitized lines or raising the entire DEM except along stream lines.

The relief for LRC consists of a land system comprising of a landscape of plains, hills and mountains. Figure 6.1 showed the Shuttle Radar Thematic Mapper (SRTM) elevation data for the catchment. A hydrologically correct DEM was generated and used as a source of height data for modeling altitude-correlated properties.

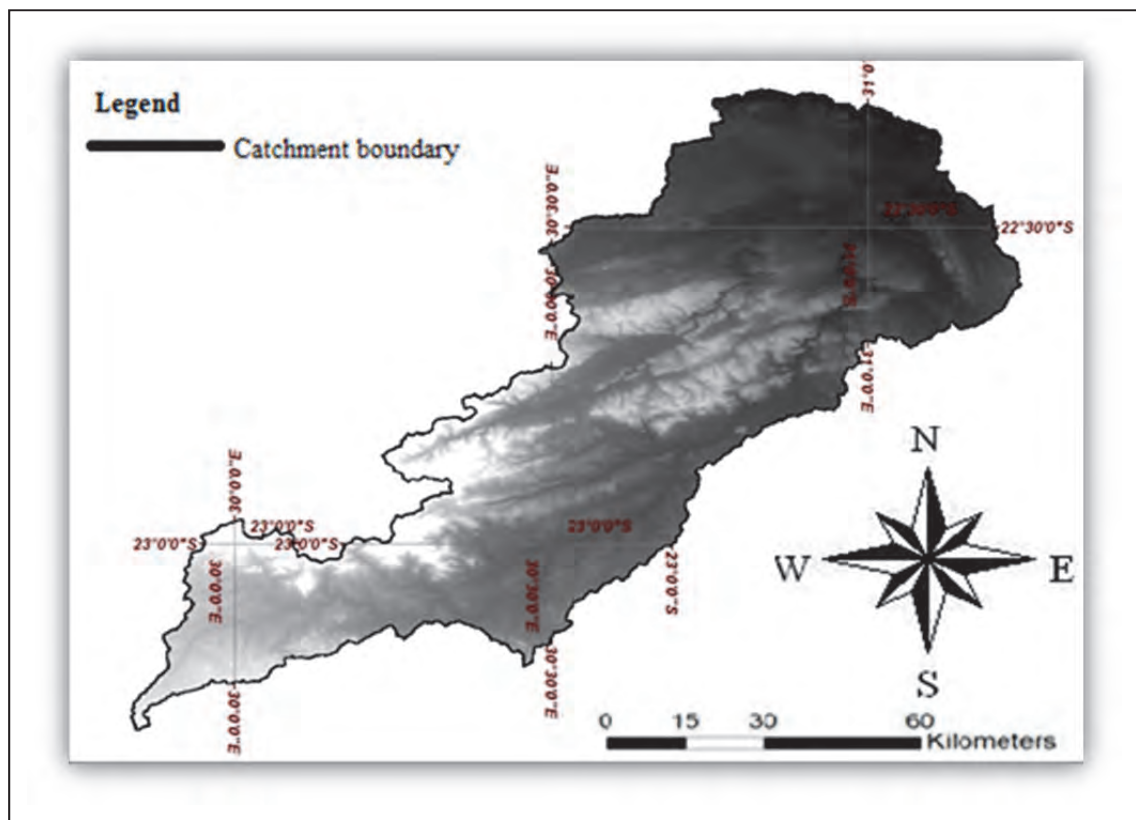


Figure 6.1: Hydrologically corrected DEM

Assessment of data quality involved extracting frequency histograms of elevations. Figure 6.2 showed the frequency distribution curve for the DEM, which indicated that the DEM had a representative number of pixels with constant Z values, and did not therefore have a large number of flat regions dominating. Imperfections contained in the DEM could directly compromise the results of analysis for hydrological modeling and should therefore be as little as possible.

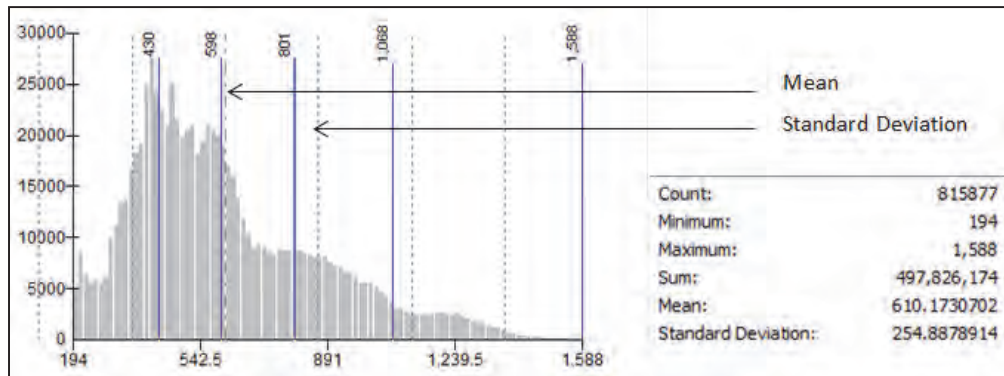


Figure 6.2: Frequency distribution of heights in the LRC

#### 6.1.4 Catchment delineation

Automated catchment delineation was done using the ArcHydro extension in ArcGIS 10.2. Simulated “Regions of hydrologic influence” and the drainage lines which were generated closely match the true ones for Luvuvhu River. Stream gauge data was used to perform spatial analysis to obtain the catchment delineation, stream segmentation, flow direction and flow accumulation. The simulated flow accumulation showed the areas where water would collect with respect to the terrain. The flow accumulation grid contained the accumulated number of cells upstream of a cell, for each cell in the input grid.

Delineation of sub-catchments can make it possible for more responsive water resources management programs encompassing assessment, planning, development, allocation, conservation, protection and monitoring to be undertaken. Management by sub-catchment approach would enhance biodiversity identification and hence enable the regeneration process and propagation. Figure 6.3 showed the delineated catchment and sub-catchments that could likely be used for water resources management in the LRC. Based on this, the technique could be used for hydrological analysis of similar catchments and thereby open the planning process to the full advantages of GIS technology. Automated catchment delineation would make it possible for more responsive water resources management programs to be taken at local micro scales.

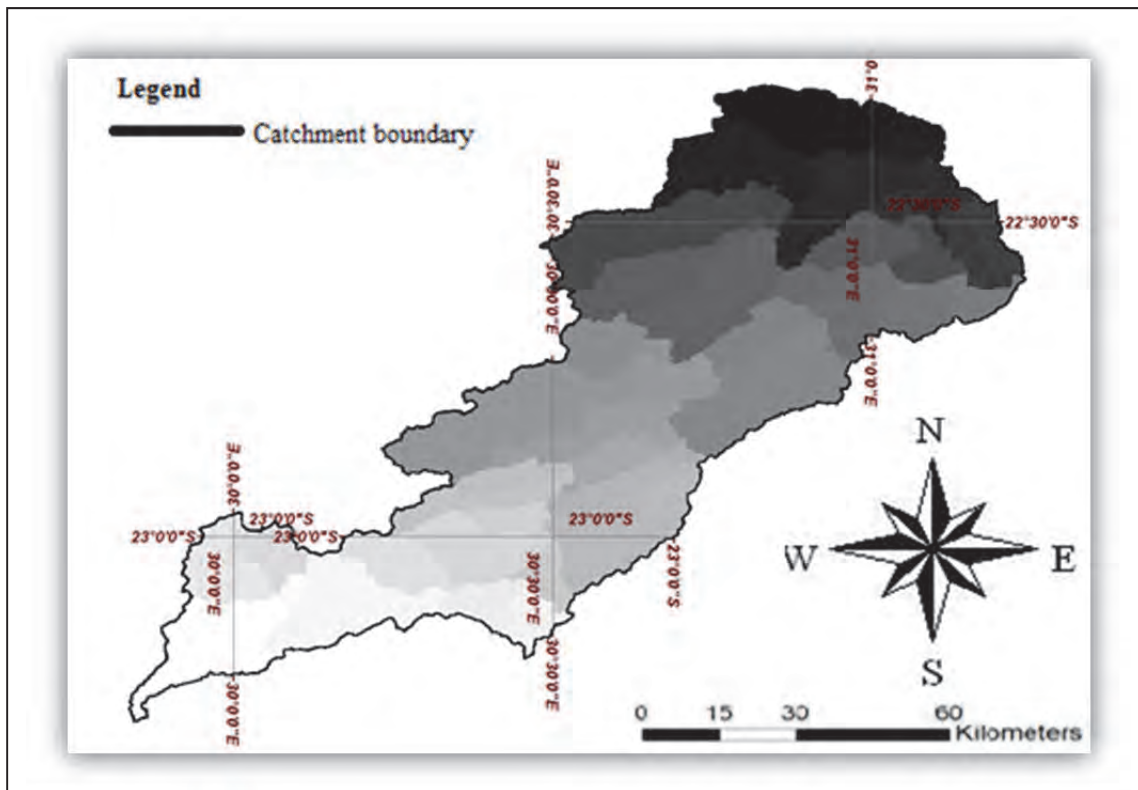


Figure 6.3: Sub-catchment delineation

The slope of terrain and direction of the steepest slope are the main parameters of all physically-based hydrological models and provide the most important information to assess how geology affects topography. Figure 6.4 showed the spatial distribution of local slope for LRC.

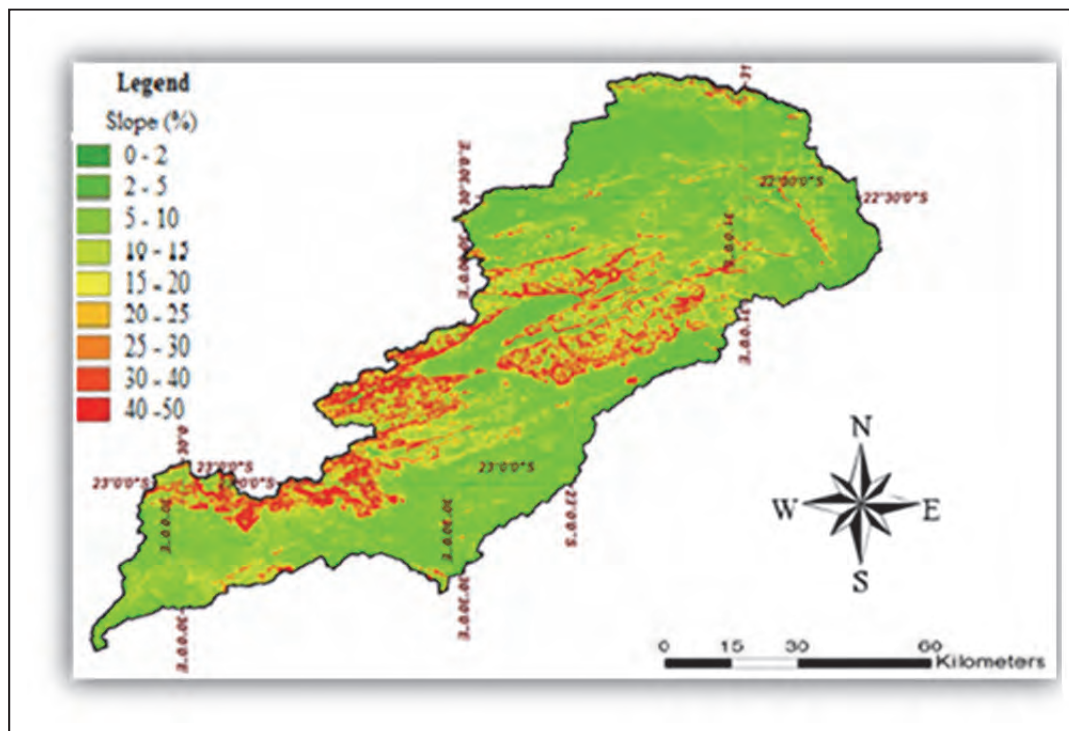


Figure 6.4: Spatial distribution of local slope for LRC

The extracted drainage pattern shown in Figure 6.5 was of the parallel type. The headwater streams were extracted to the Strahler stream order 3. The drainage network was generated using a constant-threshold method based on the evolution mechanism of Luvuvhu River and landform characteristics of the catchment. The method calculated the number of upstream cells that contributed surface flow to any cell.

The stream definition was calculated from flow accumulation, where a nominal value of river threshold was defined to determine the stream. The default threshold in ArcGIS was 36 km<sup>2</sup> and any cell which had flow accumulation of area greater than or equal to 36 km<sup>2</sup> was considered as part of the river network. The cells with greater than threshold values were assigned a value of one while the rest were assigned a value of zero. Finally all cells with the value of one were connected to provide the river network for Luvuvhu catchment. If the threshold value would decrease, the stream network would appear to be dense and would result in higher catchment delineation.

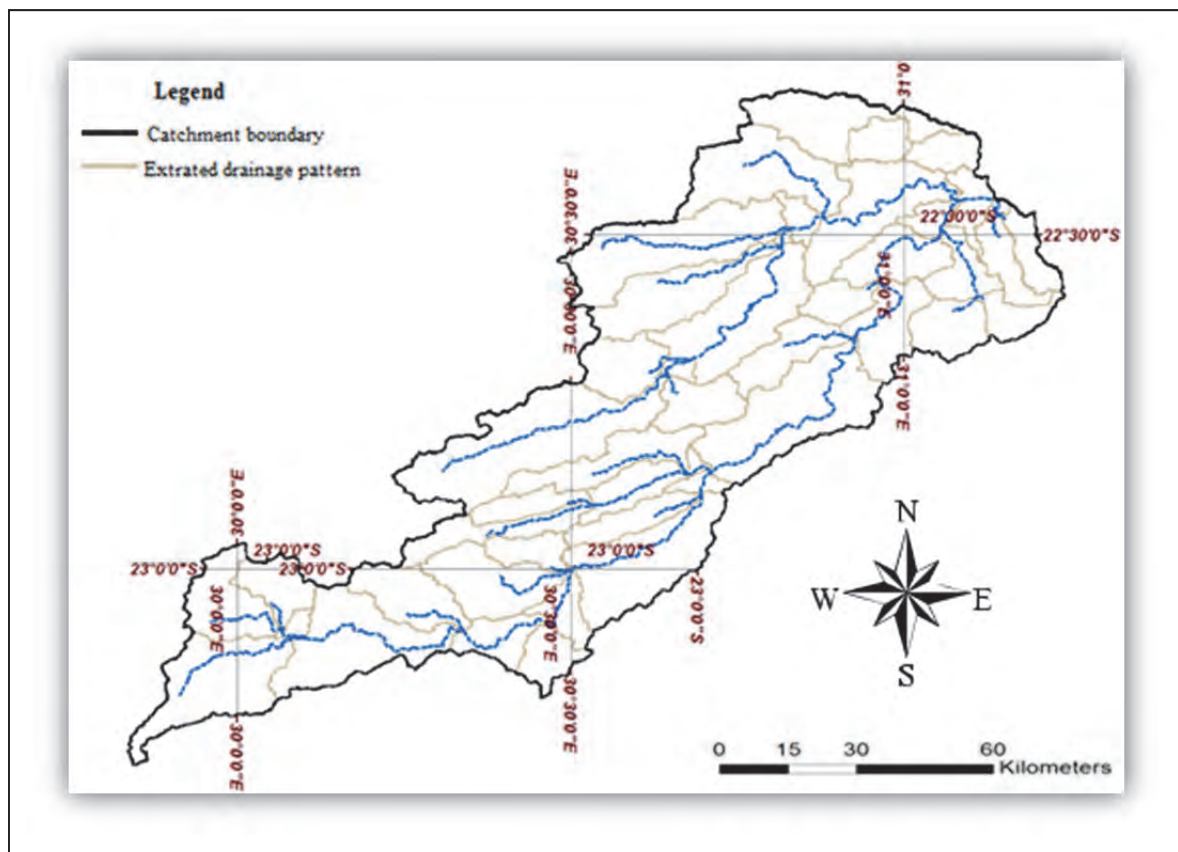


Figure 6.5: Automated extraction of the drainage pattern

Flow length is the distance travelled from any cell along the surface flow network to an outlet. This can be used to find areas that are closer to headwater locations or closer to stream outlets for better management of riparian zones.

The longest flow paths within LRC were as shown in Figure 6.6. The longest flow path is the length of catchment along the main stream from the basin outlet to the most distant ridge. The

length is used in runoff modeling to determine the time of concentration. It is also used to determine the time lag from the centroid of rainfall to peak discharge.

They are useful for inundation mapping and floodplain delineation. They have the advantage of showing drainage lines beyond what the stream lines do. They could also be used in the rainfall-runoff analysis to determine the time of concentration value necessary for computing surface runoff.

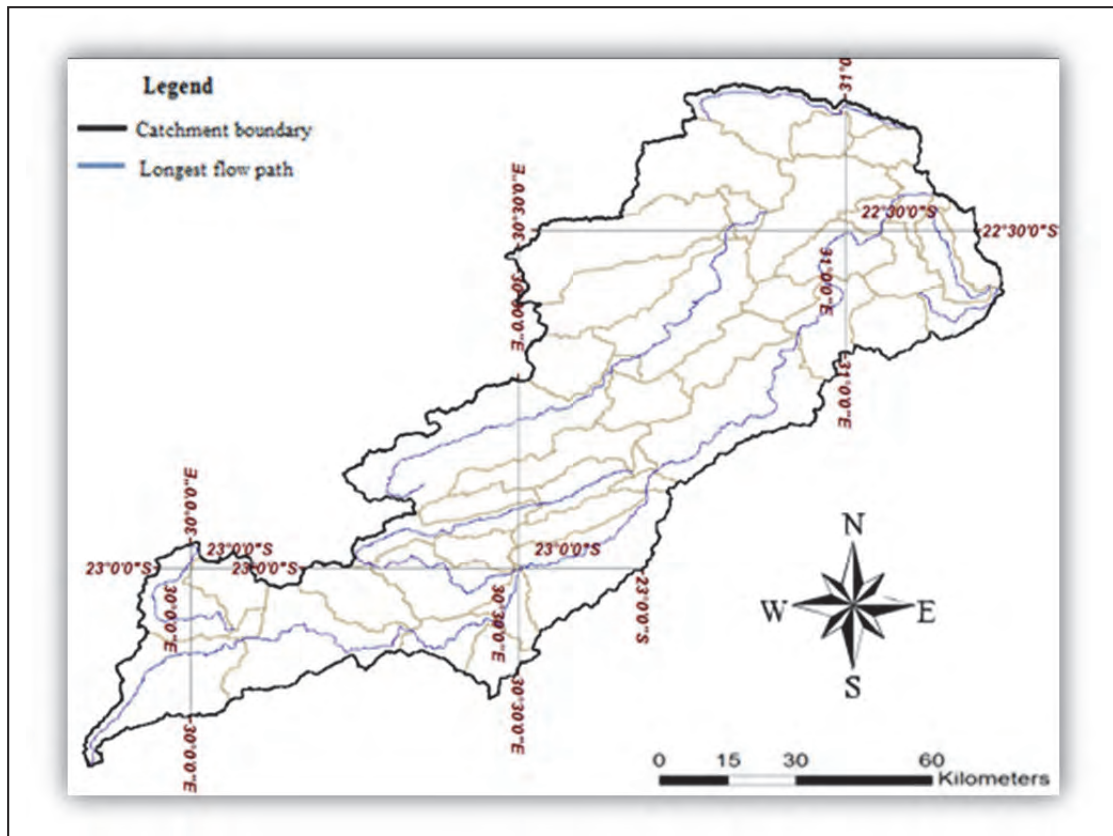


Figure 6.6: Longest flow path model for Luvuvhu River Catchment

Figure 6.7 showed the profile for Luvuvhu River. A river profile is the most significant influence of ephemeral hydrologic regime upon soils. It is related to the downstream alluvial association with hydrologic decay. The deposition increases the silt proportion of soils in the lower reaches of the rivers. Silt deposition patterns influence patterns of moisture availability and plant rooting. This helps create and maintain micro-habitats for various organisms.



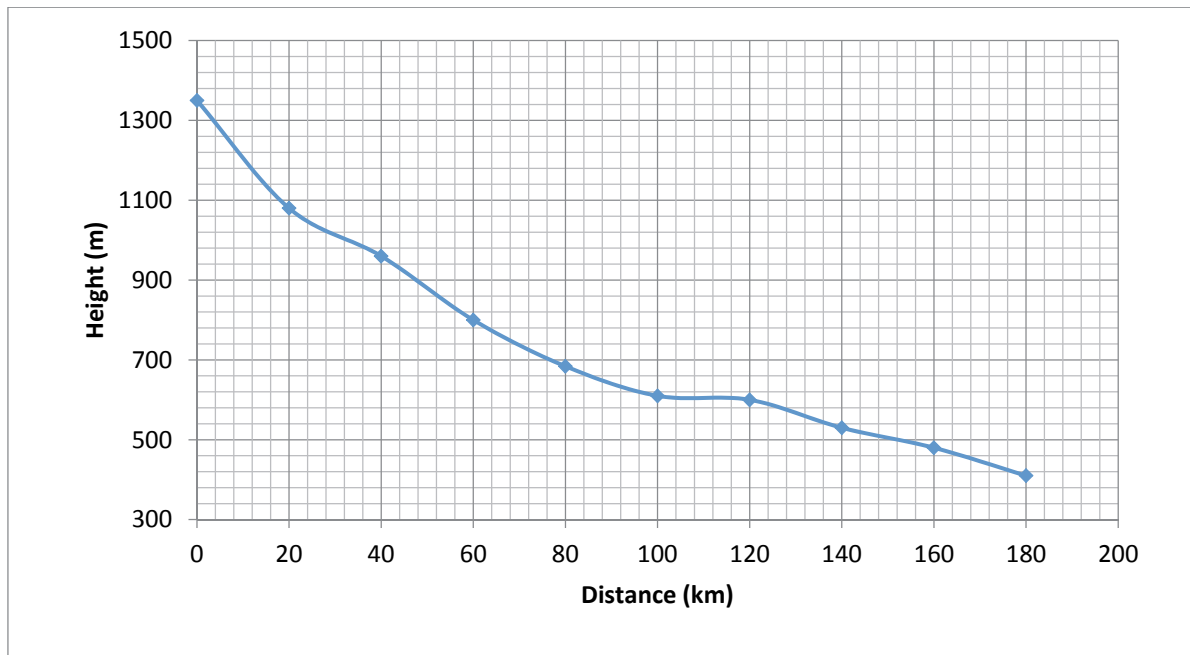


Figure 6.7: Profile for Luvuvhu River

The average slopes of the channels calculated from the upstream and downstream elevations of the longest flow path could be used to estimate the average Manning's velocity required for the channel flow routing. Stream segmentation for the catchment defined the grid for stream segments with unique identification, where all cells in a particular segment had the same grid code. The pattern formed by the values of the flow accumulation larger than the threshold will form a fully connected drainage network. Decreasing the threshold will result in an increase in the density of the network. Determination of the threshold is subjective and the synthetic channel network depends only on the DEM and not on the hydrologic characteristics. These properties are important in catchment management as they influence the effects of channel morphology on water quality through the Unit Stream Power (USP).

Stream segmentation properties are also important for restoration and conservation of aquatic life that may be sensitive to human activities. The knowledge is important in order to maintain the biodiversity and especially the sensitive aquatic flora and fauna which require flowing good quality water. In South Africa, invasive alien plants are a major threat to water resources and reduce the amount of water available while also threatening the normal biodiversity of the natural vegetation, hence monitoring could help mitigate the impacts of invading alien plants on the river systems.

Figure 6.8 showed the flow direction in the catchment. The flow direction for a cell is the direction water flows out of the cell. But provision must be made for eliminating pits and dealing with equal slopes in several directions in the software. Flow direction is important in hydrologic modeling because of its use in determining where a landscape drains. The steepest downslope neighbour for each cell was shown by colour coded direction. The model was consistent with the slope direction and was in conformity with the fact that water takes the



shortest path to find its own level. The model is important for checking non-point source pollution by agro-chemicals. It is important for farm layout for mechanized operations.

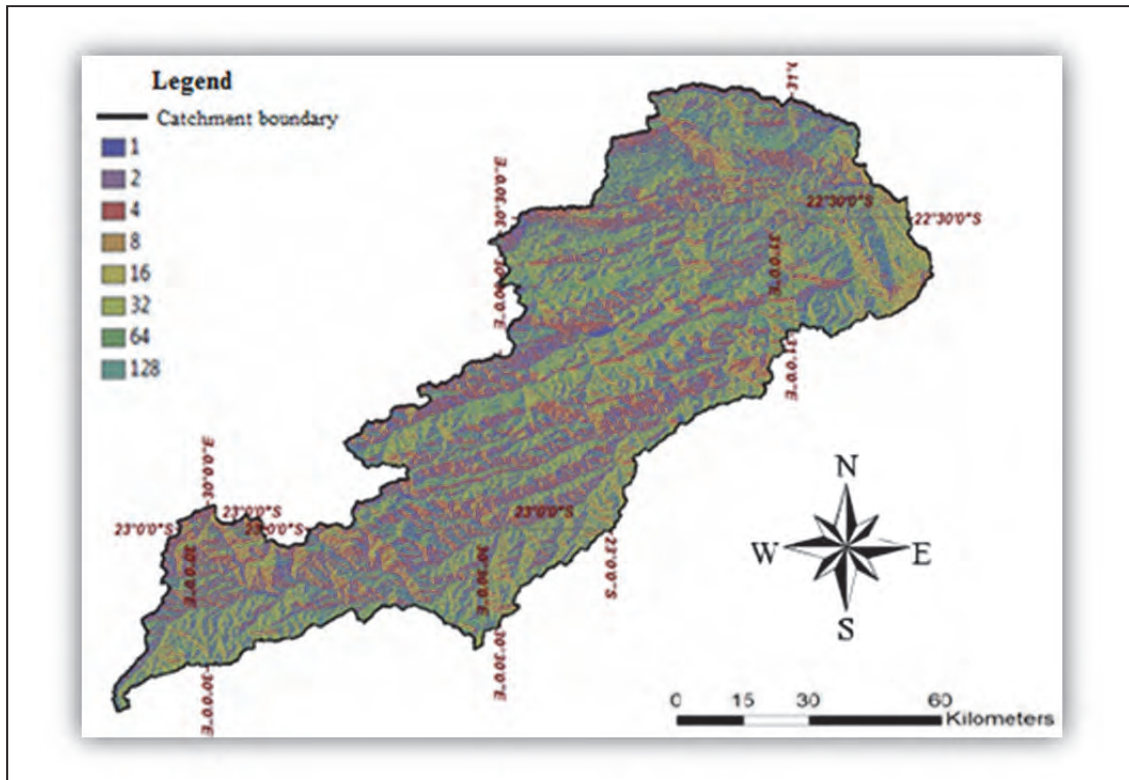


Figure 6.8: The spatial distribution of flow direction

Since watersheds are defined spatially by the geomorphological property of drainage, Flow accumulation is used to generate a drainage network, based on the direction of flow of each cell. By selecting cells with the greatest accumulated flow, we are able to create a network of high-flow cells which lie on stream channels and at valley bottoms.

The flow accumulation is calculated from the flow direction grid. It is an operator which given the flow direction and the weighting determines the resulting values such that each element represents the sum of the weights of all elements which drain to that element. Cells with a higher than a given threshold will form a connected drainage network provided that the DEM has no pits or depressions without outlet. Figure 6.9 showed the flow accumulation in the catchment reaches. These are typically points downstream of major confluences created by adding a new point layer to the project.

The flow accumulation function calculated the amount of cells situated upstream of particular point. This was so that the flow coming from all upstream cells would influence the amount of flow on one particular cell. The flow accumulation function however has the limitation that the tool does not take into account any losses such as rainfall loss by abstractions, before reaching the required node. This had the effect of showing more water accumulation in the

streams than was the case, especially at the confluence of Luvuvhu and River Limpopo, where there were many reed islands observed in the river.

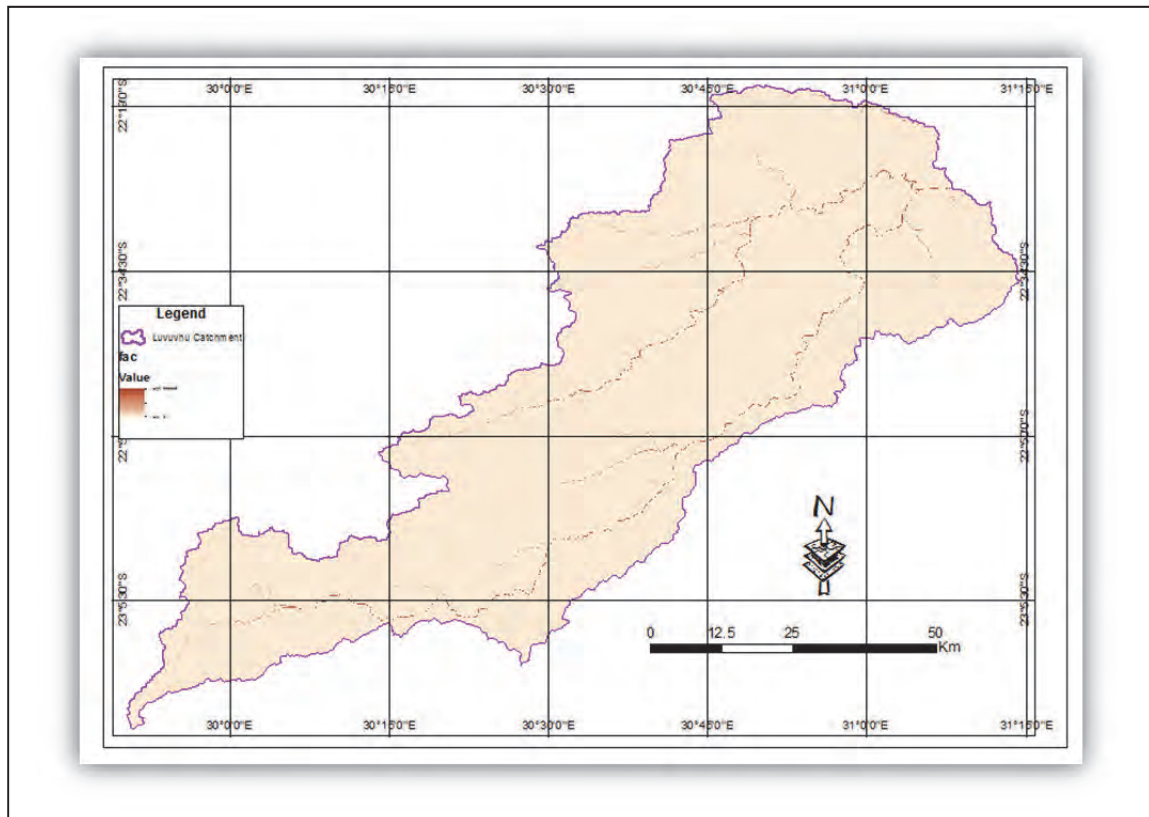


Figure 6.9: Flow accumulation

## **CHAPTER 7**

### **SOIL WATER ASSESSMENT TOOL (SWAT) ANALYSIS FOR LEVUBU-TSHAKHUMA SUB-CATCHMENT**

#### **7.1 Description of the SWAT model**

SWAT is a continuous physically-based distributed model that operates on a daily time-step (Arnold *et al.*, 2012). The model requires the following data types to operate: DEM, land use, soil, land use management, daily weather, stream flow and water quality data. It has the capability to simulate the impact of land use management on water, sediment and agricultural-chemical yields in complex catchments with varying soils, land use and management conditions over long periods of time.

SWAT simulates the entire hydrologic cycle, including surface runoff, lateral soil flow, evapotranspiration, infiltration, deep percolation, and groundwater return flows. Spatial parameterization within SWAT is performed by dividing the watershed into sub-basins based on topography. The sub-basins are further divided into Hydrologic Response Units (HRUs) based on unique combinations of land use and soil characteristics. A HRU is a unique combination of a soil and a vegetation type in a sub-basin. Surface runoff, infiltration, evaporation, plant water uptake, lateral flow, and percolation to the shallow and deep aquifer are modeled for each HRUs, and the components are summed to the sub-basin level. The components are then routed through the channel network to the watershed outlet.

For this study, surface runoff was estimated using the United States Department of Agriculture-Soil Conservation Services Curve Number (USDA-SCS CN) method (Soil Conservation Services, 1972), while evapotranspiration was estimated using the Penman-Monteith method (Penman, 1956; Monteith, 1965). SWAT divided the catchment into sub-basins, which was particularly beneficial since different areas of the catchment were dominated by different land uses and or different soils which were dissimilar enough in properties to impact on the hydrology. Each sub-basin was connected through a stream channel and further divided into HRUs.

SWAT simulates hydrology, vegetation growth, and management practices at the HRU level. The advantage is that water, nutrients, sediment, and other pollutants from each HRU are summarized in each sub-basin and then routed through the stream network to the catchment outlet. Figure 7.1 showed the hydrologically correct DEM for LRC that was used as a source of height data for modeling altitude-correlated properties.

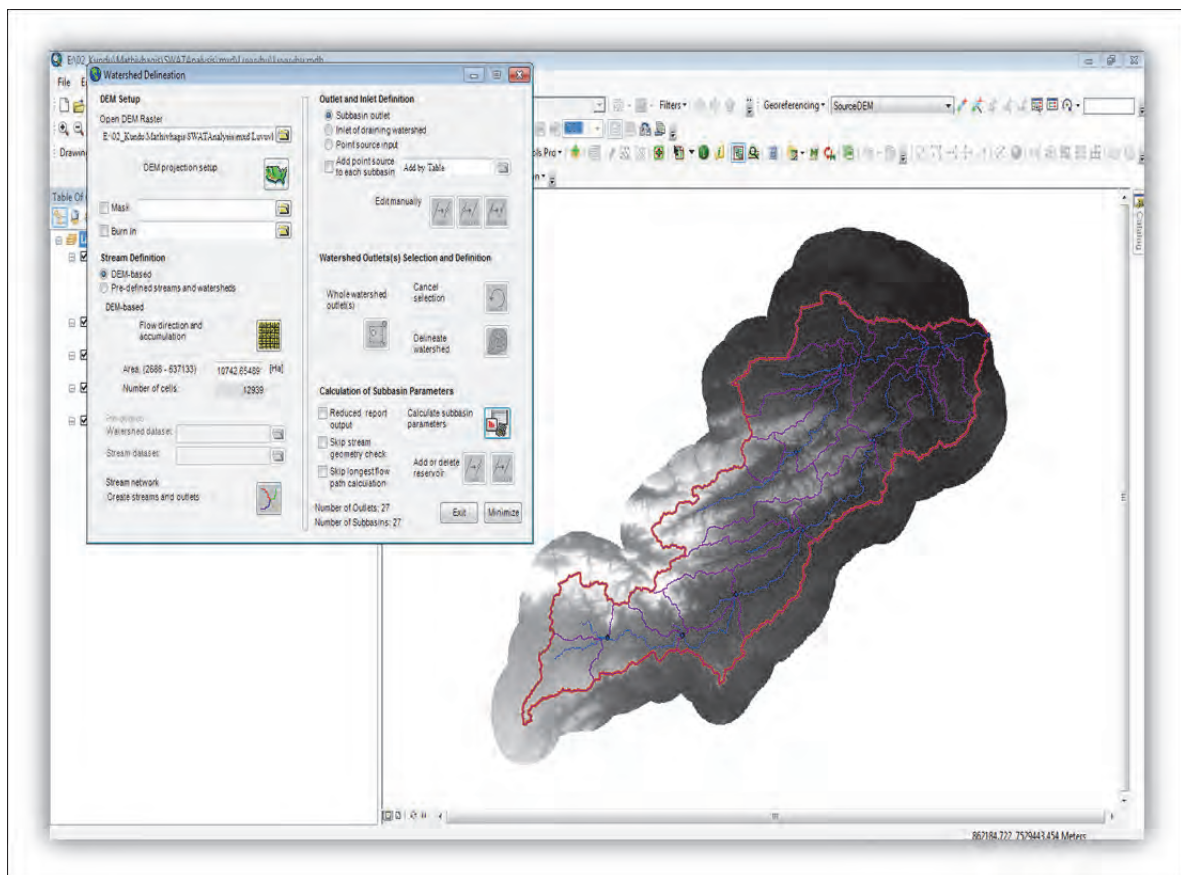


Figure 7.1: Hydrologically corrected DEM for LRC with buffer zone for the catchment

## 7.2 Levubu-Tshakhuma sub-catchment

Figure 7.2 showed the upper Luvuvhu River sub-catchment where the SWAT Tool was used to analyse the impact of land cover change for Levubu-Tshakhuma sub-catchment. The Figure is a DEM with a 3-times magnification in altimetry and draped with a 2008 Landsat image.

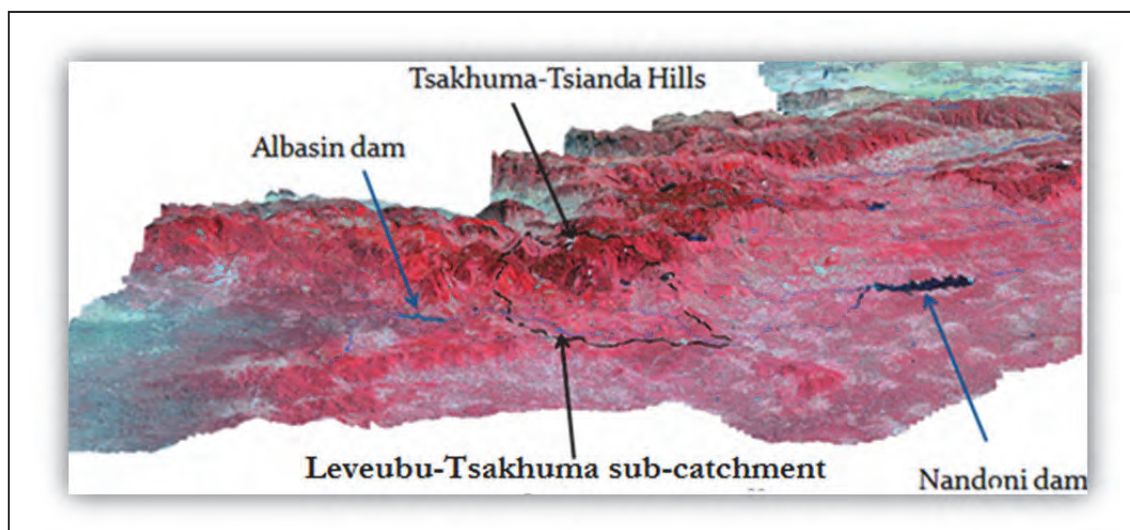


Figure 7.2: Location of Levubu-Tshakhuma sub-catchment

Figure 7.3 showed the different land cover classes from forestland, woodland and open grassland to medium size farms and built-up land. It was observed that hills around Tshakhuma and Tsianda which were covered by natural forest in the pre-change period were largely covered by small portions of trees and bushes at higher levels, interspersed agriculture at the middle and built up, mixed with agroforestry on hill-sides.

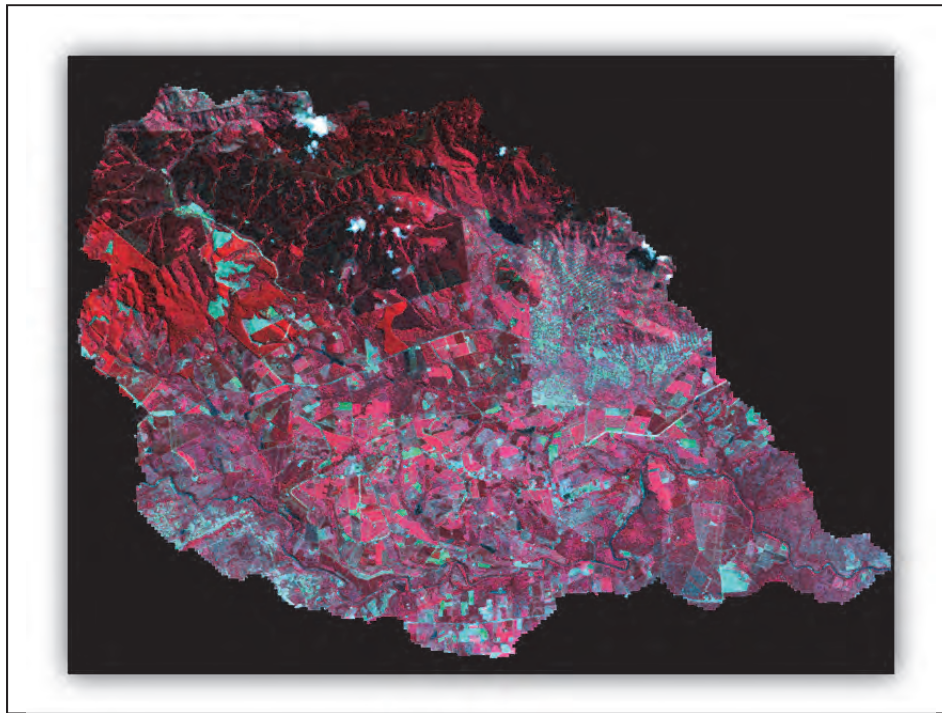


Figure 7.3: A 2008 Landsat ETM+ image clip for Levubu-Tshakhuma sub-catchment

The extracted drainage pattern shown in Figure 7.4 was of the parallel type. The flow lines showed the longest paths in upper sub-catchment, which could be used for inundation mapping and floodplain delineation. The longest flow path data could also be used in the rainfall-runoff analysis to determine the time of concentration value necessary for computing surface runoff.



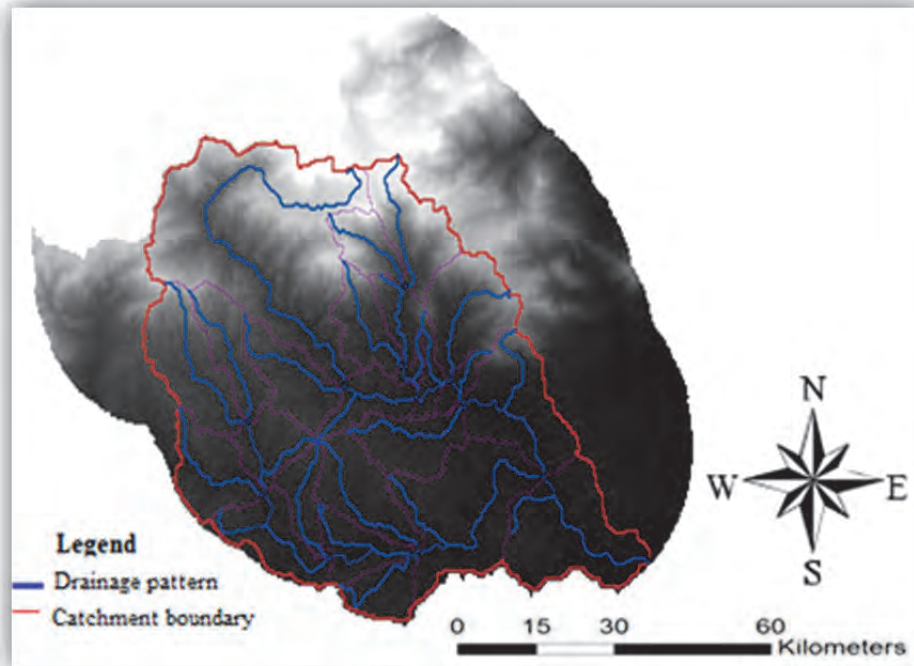


Figure 7.4: Levubu-Tshakhuma sub-catchment drainage system

The spatial distribution of local slopes for the sub-catchment was as shown in Figure 7.5. The slopes affected the overall rate of downslope movement for processes such as runoff, soil erosion, moisture balance and landslide hazards. Extraction of this property is therefore important as it allows overland and near-surface water flow to be modeled using DEMs where surface topography is the sole factor in the distribution of water. This would help check the processes of acceleration and deceleration and reduce the effects of erosion and deposition in the catchment.

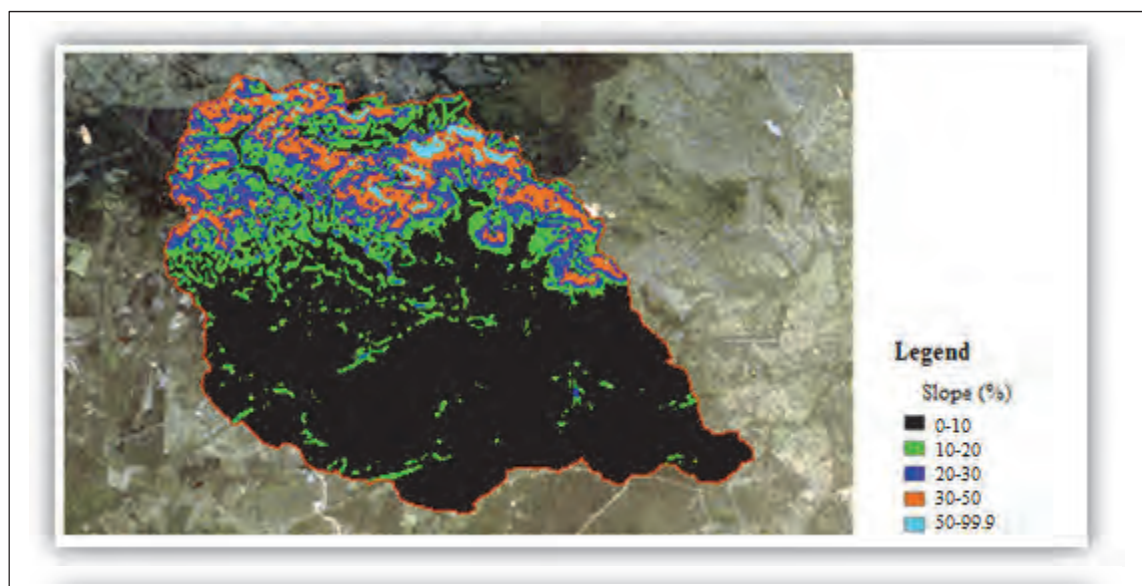


Figure 7.5: The spatial distribution of local slopes for Levubu-Tshakhuma sub-catchment

### 7.3 SWAT soil Classification

Digital soil data at a scale of 1:1 Million, were acquired from the Global Environment Facility Soil Organic Carbon database (ISRIC, 2008). This dataset was an upgraded version developed by national experts from the global Soil and Terrain (SOTER) database. The data were reclassified into the major Hydrological Soil Groups (HSG) of the catchment with the help of FAO/UNESCO revised manual for soil maps of the world based on their drainage characteristics.

The soils were classified into Hydrologic Soil Groups (A, B, C, and D) based on soil characteristics in the SOTER-ISRIC database. Soils in Group A have the lowest runoff potential and highest infiltration rates, while those in Group D have the highest runoff potential and lowest infiltration rates. The latter is because Group A is at higher elevation as compared to Group D which is at the lowest point in the sub-catchment.

The vast majority of the soils in the Levubu-Tshakhuma sub-catchment were cross-listed HSGs such as A/D, B/D and C/D which represented areas that were naturally poorly drained (D), but could be improved to the first listing (A,B or C) with appropriate management

The soil classification followed the Map Unit Key (Mukey) system, as a soil type identifier from the SOTER-ISRIC data base. The numerical key is used to join tabular data and spatial data for each soil series or complex mapped. The MUKEY dataset contained 4 soil types, although each map unit may be composed of more than one component. The Mukey system had a higher spatial resolution and showed more detailed than the ARC classification which showed that the entire area was under soil class LmSa-SaLm. Figure 7.6 showed the soil-landscape relationship for Levubu-Tsakhuma sub-catchment classified by SWAT. The soils were grouped in terms of infiltration capacity and runoff potential as opposed to the ARC classification that used the soil texture classification. For instance group A has the lowest infiltration capacity and the highest runoff potential while group D has the highest infiltration potential.



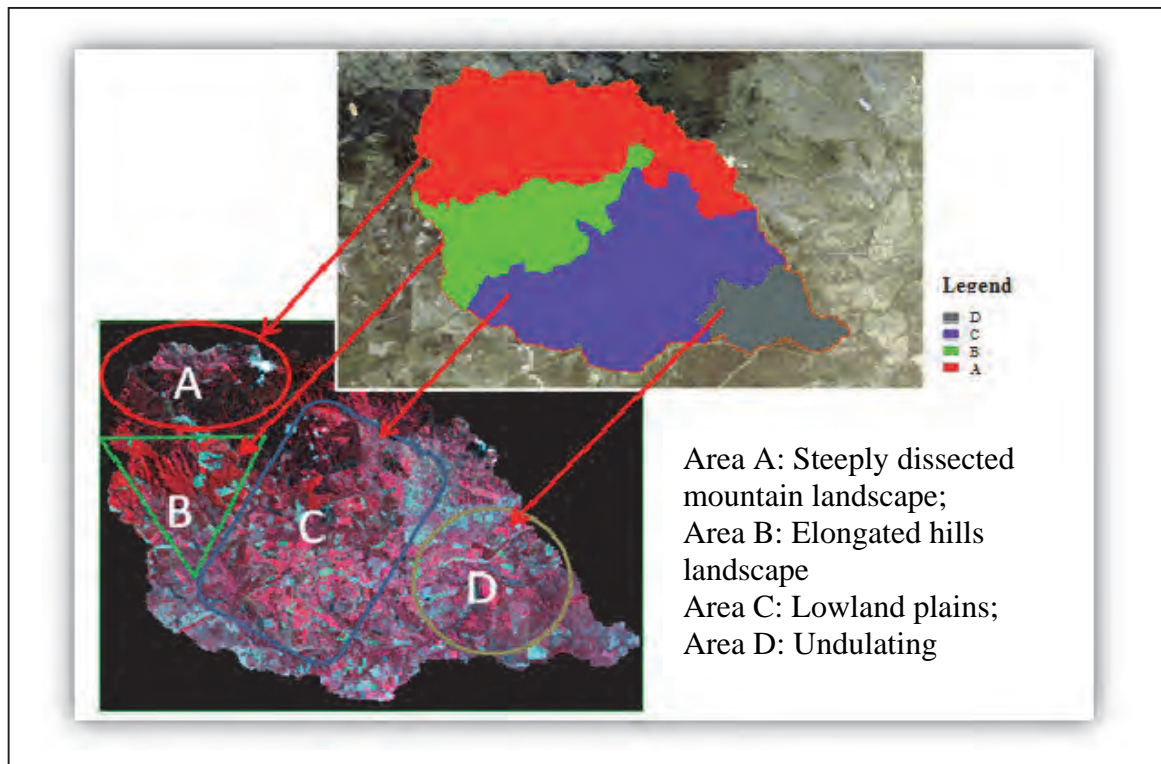


Figure 7.6: Soil-landscape relationship for Levubu-Tsakhuma sub-catchment

#### 7.4 Hydrological Response Units

The SWAT tool created 25 sub-catchments with 502 hydrologic response units (HRUs) for the catchment. Figure 7.7 showed the location of the sub-catchments while Figure 7.8 showed the 502 hydrologic response units. According to SWAT analysis the major land cover classes in the delineated sub-catchment were water, urban/ build up area, forest, agriculture and pasture. The SWAT land cover classification was comparable to Calder (2003).

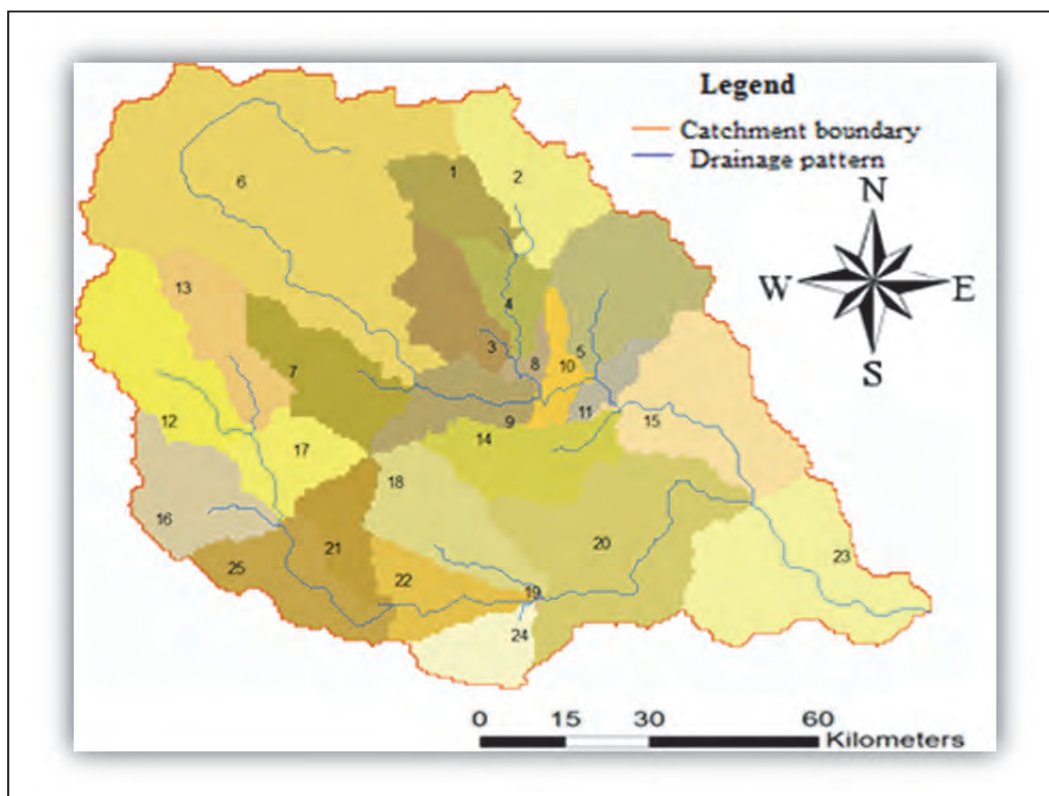


Figure 7.7: SWAT delineated sub-catchments for Levubu-Tshakhuma sub-catchment

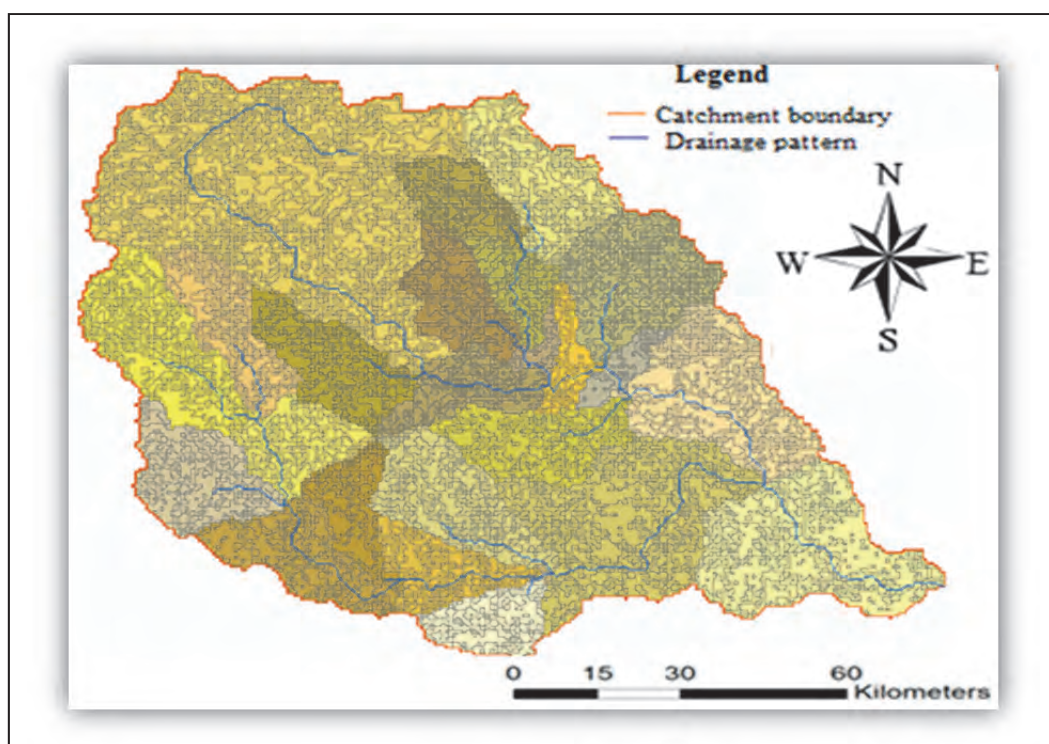
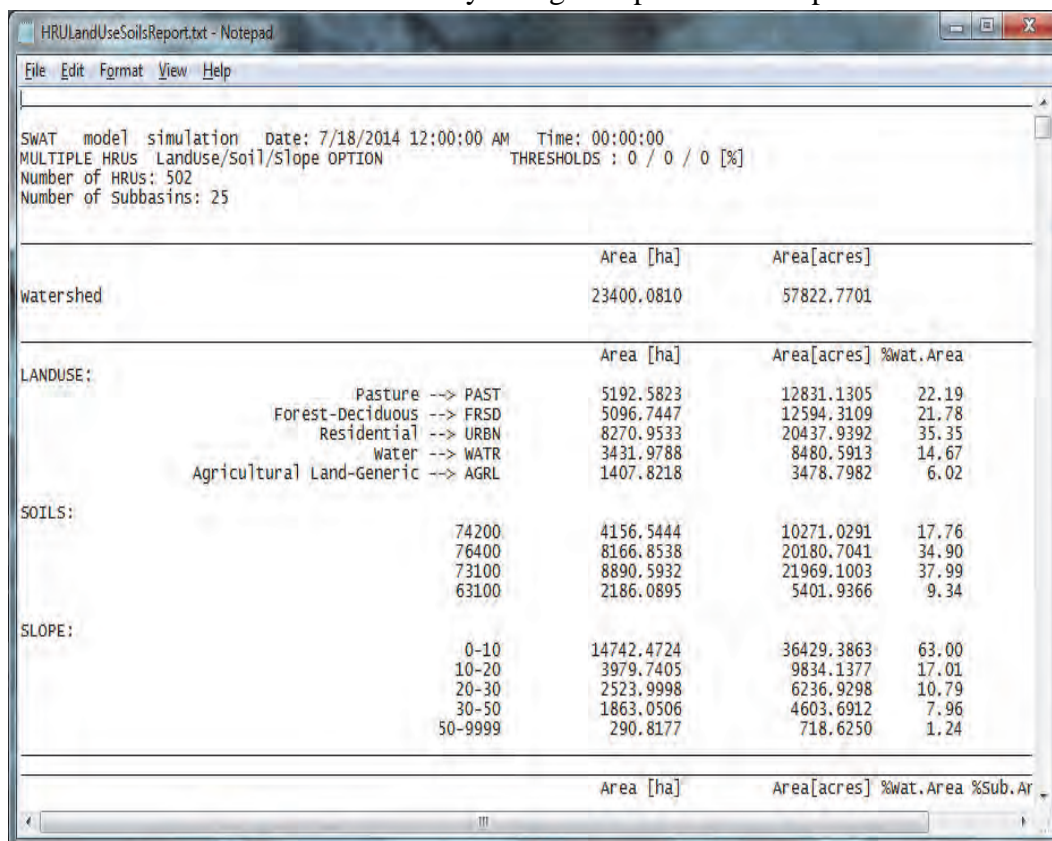


Figure 7.8: The hydrologic response units for Levubu-Tshakhuma sub-catchment.

Table 7.1 showed a typical report for the SWAT tool, provided statistics for land use, soils and slope. The five land use categories were the default classes defined by the SWAT tool.

The dominant class was found to be residential/urban followed by pasture, followed by deciduous-forest, water and generic agricultural land. Pasture represented all land under open grassland and wooded grassland. Deciduous-forest represented plantation forest and tree crops. The area under agriculture appears to be small because some was covered under pasture and deciduous forest. A limitation to recognize for the SWAT tool is that the large spatial resolution of HRUs for this study could have led to biased results.

Table 7.1: Hydrologic response units report



```

SWAT model simulation Date: 7/18/2014 12:00:00 AM Time: 00:00:00
MULTIPLE HRUS Landuse/Soil/Slope OPTION THRESHOLDS : 0 / 0 / 0 [%]
Number of HRUs: 502
Number of Subbasins: 25
  
```

		Area [ha]	Area[acres]	
watershed		23400.0810	57822.7701	
		Area [ha]	Area[acres]	%wat. Area
LANDUSE:				
	Pasture --> PAST	5192.5823	12831.1305	22.19
	Forest-Deciduous --> FRSD	5096.7447	12594.3109	21.78
	Residential --> URBN	8270.9533	20437.9392	35.35
	Water --> WATR	3431.9788	8480.5913	14.67
	Agricultural Land-Generic --> AGR1	1407.8218	3478.7982	6.02
SOILS:				
	74200	4156.5444	10271.0291	17.76
	76400	8166.8538	20180.7041	34.90
	73100	8890.5932	21969.1003	37.99
	63100	2186.0895	5401.9366	9.34
SLOPE:				
	0-10	14742.4724	36429.3863	63.00
	10-20	3979.7405	9834.1377	17.01
	20-30	2523.9998	6236.9298	10.79
	30-50	1863.0506	4603.6912	7.96
	50-9999	290.8177	718.6250	1.24
		Area [ha]	Area[acres]	%wat. Area %Sub. Ar

## 7.5 Sensitivity Analysis

A sensitivity analysis for multiple variables including stream discharges, suspended sediment and nutrients was conducted for Levubu-Tshakhuma area in the catchment so that the model could be calibrated efficiently for land quality analysis purposes. Relative sensitivity analysis was conducted to identify parameters that most influenced predicted flow, sediment, and nutrient model outputs. By means of the LH-OAT (Latin-Hypercube One-factor-At-a-Time) sensitivity analysis, the dominant hydrological parameters were determined and a reduction of the number of model parameters was performed. The sensitivity analysis was performed for 27 parameters that had the potential to influence the river flow. The ranges of variation for the parameters were based on a listing provided in the SWAT manual (Neitsch *et al.*, 2002). Figure 7.9 showed the default parameters that were checked for sensitivity analysis.

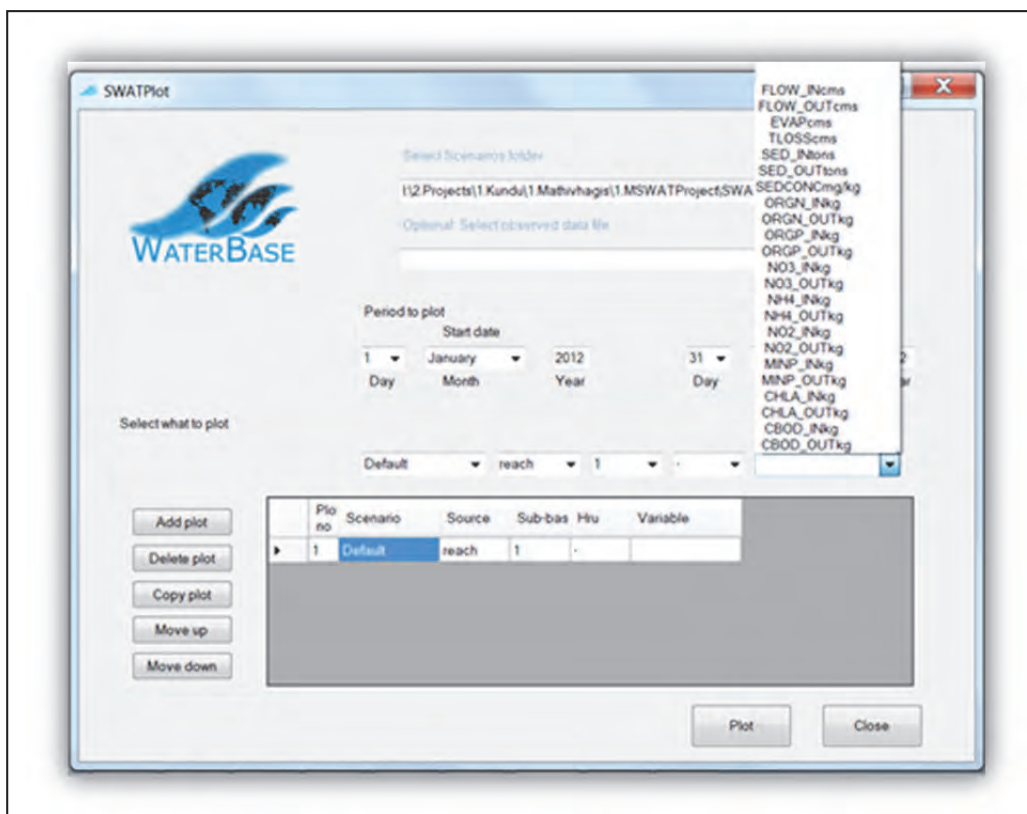


Figure 7.9: The default parameters for sensitivity analysis.

The SWAT analysis showed that agricultural activities in the sub-catchment altered the nutrient content of surface and groundwater, most notably nitrogen (N), nitrate ( $\text{NO}_3$ ), phosphorus (P) and Ammonia ( $\text{NH}_4$ ) levels. Figure 7.10 showed the trend of  $\text{NH}_4$  chemical component in the sub-catchment. Agricultural activities during the rain seasons from October to April led to increased influx of nitrogen into water bodies as a result of fertiliser application, manure from livestock production and sludge from municipal sewage treatment plants. It is known that high nutrient leaching losses can occur when fertiliser is applied to short-term crops on permeable soils, and ploughing can increase  $\text{NO}_3$  concentrations in surface and groundwater, as oxygenation of the soil causes nitrification. Application of manure from livestock production and direct runoff can lead to acidification of soils due to the volatilisation of ammonia, which in turn may increase the solubility of metals in the soil (FAO, 1996).



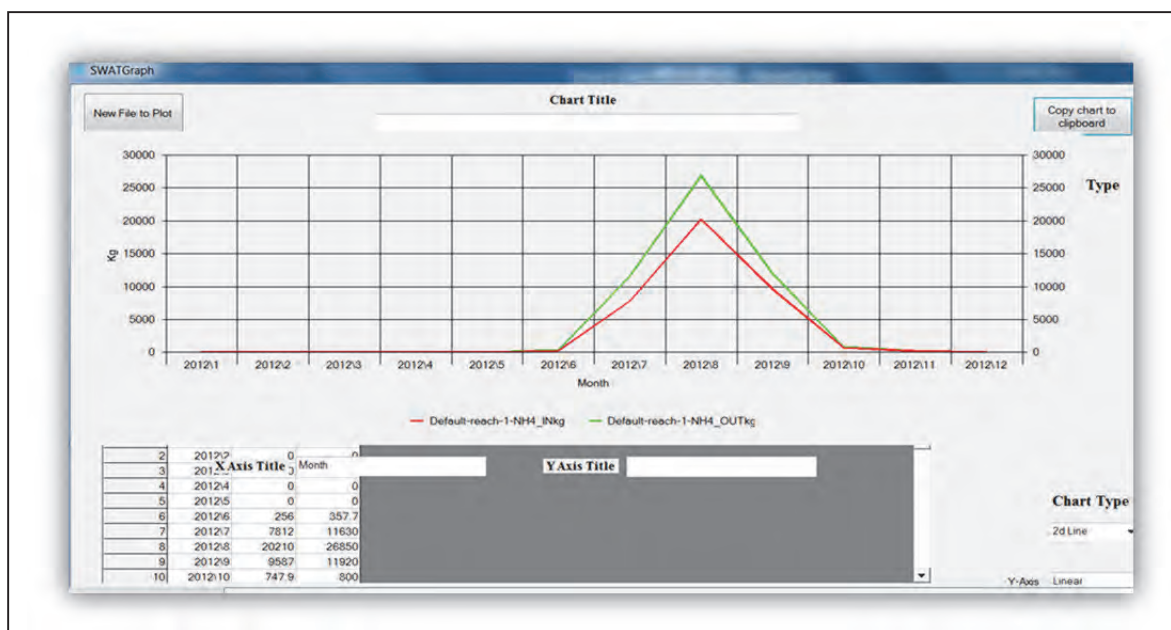


Figure 7.10: Trend of NH<sub>4</sub> chemical component in the sub-catchment

The SWAT model first delineated and divided the catchment into a number of sub-catchments, which were further subdivided into HRUs. The HRUs are the smallest units in the sub-catchment which are created by combining unique land use, soils and topography within sub-catchment and are considered to be homogenous with respect to their hydrologic properties. Over-parameterization is a major problem in the application of models for hydrologic analysis. The use of sensitivity analysis for reducing the number of parameters to be adjusted during calibration is important for simplifying the use of these models.

## **CHAPTER 8**

### **IMPACT OF LAND USE AND LAND COVER CHANGE IN THE CATCHMENT**

Hydrological effects of land use and land cover change impact catchments in several ways both directly and indirectly. There are many connections between the topography, surface characteristics and the hydrologic cycle. Land use and land cover affect both the degree of infiltration and runoff following precipitation events. The amount of vegetation cover ranging from grassland to dense forest and the albedo of the surface for example affect rates of evaporation, humidity levels and cloud formation. Land use practices such as plantation forestry, agriculture and urbanization affect amounts and rates of evapotranspiration, infiltration and surface runoff within the catchment, which in turn have significant impacts on the timing and magnitude of stream discharge events.

The conversion of land from forest to agriculture and build-up within a catchment leads to increase in hardened surface area such as roads, parking lots, sidewalks and rooftops. The impervious areas block rain from recharging groundwater, impair the ability of natural systems to cleanse runoff and protect wetlands and near shore biota from contaminants, increase the potential for flooding and erosion, and contribute to the degradation of streams and lakes.

The conversion disrupts the hydrological cycle of a drainage basin, increasing evaporation and consequently, the runoff response of the area. The higher surface albedo, the lower surface aerodynamic roughness, the lower leaf area and the shallower rooting depth of pasture reduce evapotranspiration as compared to forests which increase discharge in the long-term. In addition, low-productivity grasses like natural grassland pasture have lower leaf area and produce less litter than the original vegetation. With a lower leaf area, the pasture does not intercept as much rainfall as the forest does, making a higher fraction to reach the ground. With less litter, the capacity of surface detention is decreased, and a greater proportion of the rainfall runs off as overland flow.

If surface runoff increases substantially and infiltration is critically reduced, soil moisture may also decrease, contributing to a further reduction in the ETo. In addition, the shift from sub-surface flow to overland storm flows that often accompanies deforestation followed by adverse land use may produce dramatic changes in the catchment peak flows as well. Furthermore, if the change in infiltration associated with the land use change overrides the effect of reduced evaporation, then a shift in the river's flow regime may be expected with increased peaks during the rainy season and lowered flows during the dry season.

The earth is a finite source for land resources and as it is overused/over developed, it becomes difficult to achieve sustainable production of goods and services. As population increases, more materials and energy are required. The demand for more land leads to deforestation and draining of wetlands which lead to environmental degradation. Land use leads to land cover changes that affect radiation budgets, biodiversity, water, etc., which affect the biosphere and global climate. Land use change may contribute to climate change,

not only by altering radiation balances and evaporation, but also through increasing CO<sub>2</sub> emissions. Conversion of grassland and forests to pasture and arable land alters the hydrological regime of a catchment by modifying infiltration rates, evaporation and runoff.

Hydrometeorological data was analysed and integrated with land cover and land use data within GIS to determine the impact of change to streamflows in the catchment. In this study, the impact of change was determined from the overall effects as they affected peak runoff and the stream flow in the catchment. As land use and land cover changes, there is an increase in hardened surfaces as a results of pavements in built-up areas and soil compaction in agricultural lands. The effect of such surfaces was twofold; first, it increased the velocity of runoff, with rainwater being channelled to streams much more rapidly than under conditions of natural vegetation cover, secondly, infiltration was reduced, which reduced the groundwater levels and therefore the base flow of streams, such that the steady state streamflows that would be fed by groundwater between precipitation events were disturbed.

It was observed that subsistence agriculture had extended to the steeper slopes and in the riparian areas of the catchment. The practice of continuous cultivation in areas like Lwamondo, Tsianda and Tshakhuma was impoverishing the soils as little or no land was left to fallow even as it lost fertility. The conversion of land cover from forest to agriculture and grassland disrupted the hydrological cycle of the drainage basin, increasing evaporation and consequently, the runoff response of the area.

Sheet and rill erosion was observed in Tshakhuma and Tsianda area and gullies were beginning to develop along foot paths. Urbanization was associated with a proliferation of impervious surfaces such as paved roads, parking lots, and rooftops and created an environment whose impervious surfaces exceeded 80% of land cover in townships. The impact of land use and land cover change on hydrology was manifested in streamflow, surface runoff, suspended sediment and flood frequency and magnitudes.

## **8.1 Streamflow**

Eight gauging stations with good records of stream flow data were used to estimate average stream flow for the study area. Figure 8.1 showed the distribution of average streamflow upstream and downstream of the catchment. Gauging stations A9H001 and A9H006 represented the upper stream of catchment while A9H015 and A9H016 represented the lower catchment. The results showed that flow in the catchment was highly variable during the years.



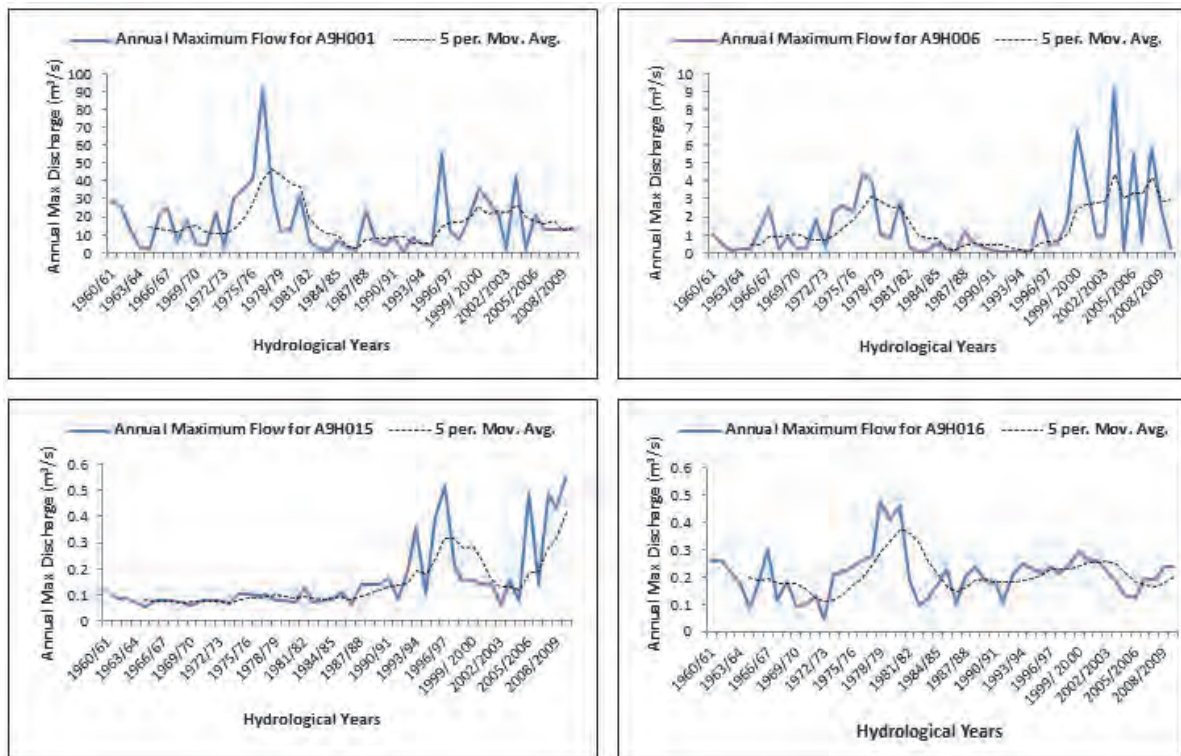


Figure 8.1: Annual maximum streamflow series for the study area

## 8.2 Surface runoff

Surface runoff during the 1960-1985 phase showed spatial and temporal variations. It could be noted from Figure 8.2 that runoff trends at each gauging station varied from year to year. Notable was the increase in runoff trends at A9H003 and A9H016 which were located upstream of the catchment. During the phase of 1985-2010 shown in Figure 8.3, trends tended to increase.

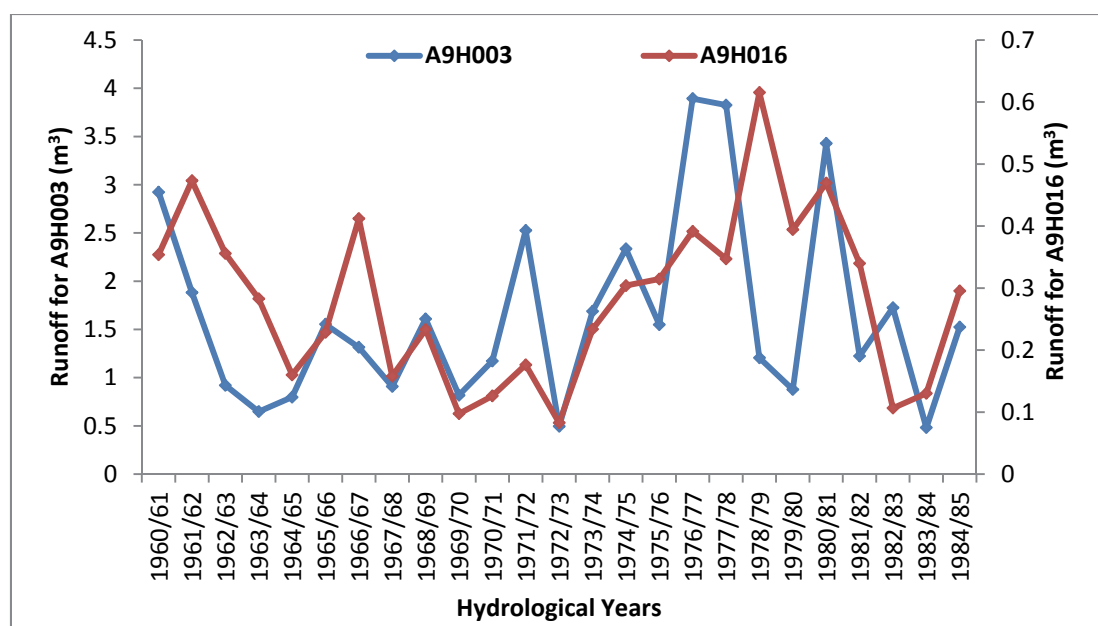


Figure 8.2: Runoff trends at A9H016 and A9H003:1960-1985

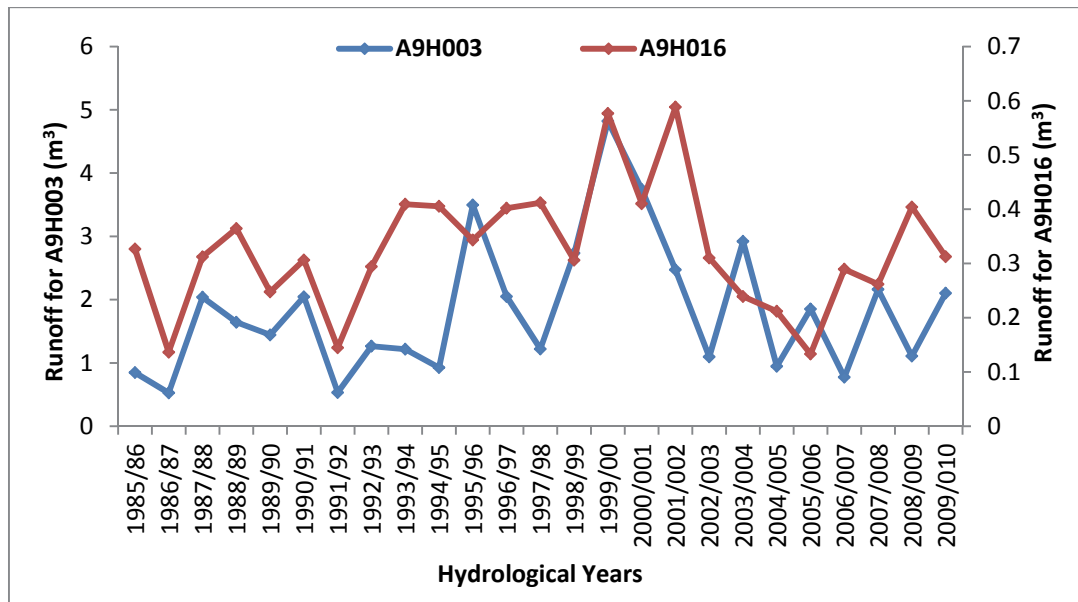


Figure 8.3: Runoff trends at A9H016 and A9H003: 1985-2010

In the post-change period, the observed reduction in baseflow during low flow periods was followed by increased storm runoff during high rainfall months compared to that observed with a high percentage of forest cover in the pre-change period. Such a variation may not have resulted from evapotranspiration by new growth but most likely due to reduced infiltration opportunities. If infiltration opportunities after forest removal were decreased to the extent that the increase in amounts of water leaving the area as storm runoff exceeded the gain in base flow associated with decreased evapotranspiration, then the result is the diminished dry season flow that is being experienced in the catchment.

#### 8.2.1 Runoff simulation by Curve Number (CN) method

Curve number estimates for antecedent moisture conditions (AMC) were obtained from standard CN table (NRCS TR-55 Table: Soil Conservation Science, 1986) where estimates for agricultural land use were used and later adjusted into AMC III. The Curve Numbers for six sub-catchments were as shown in Table 8.1.

Table 8.1: Curve Numbers for different sub-catchments

Sub-catchment	Land Use	Curve Number
A9H017	Cultivated Agricultural Land	67
A9H015	Cultivated Agricultural Land	67
A9H016	Built-up Settlements	74
A9H001	Residential and Cultivated Land	83
A9H003	Degraded, Forest	30
A9H004	Built-up Settlements	74

Figures 8.4 and 8.5 show the simulated runoff volumes and observed rainfall for 1960-1985 and 1986-2010 periods at different sub-catchments within the study area. It should be noted that runoff calculated from the CN method gives higher values than observed runoff and

streamflow. It could be seen from runoff and rainfall that there was a strong relationship between rainfall and runoff in the catchment. Notably was the increase in both runoff and rainfall during the phase of 1985-2010.

Drier areas of a catchment are widely identified by lower CN values (Suprit *et al.*, 2012). Shi *et al.* (2001) regards land use condition as an important factor to influence the storm-flood process including surface runoff formation and concentration. A study by Merz and Blöschl (2009) showed that runoff coefficients vary in space depending on the long-term controls such as climate and catchment information. They also vary in time depending on event characteristics such as AMC and rainfall depth. The AMC for the study area ranged from 72.90 mm to 201.69 mm.

To relate the amount of rainfall or storm water that appears as runoff from a surface, runoff coefficients were calculated following the rational method by dividing stream flow and rainfall. The changes in the runoff coefficients during the study period were noted in all sub-catchments. High runoff coefficients ranging from 0.1 to 0.68 were noted at sub-catchment A9H003, which is located in the downstream of the catchment. Degraded areas, such as sub-catchment A9H003, were characterized by low infiltration capacity, high runoff coefficients and high stream discharges. High runoff coefficient values are an indicator of flash flooding in an area during storms as water moves fast overland (Merz and Blöschl, 2009). The California Environmental Protection (CEP) (2011) noted that areas with permeable soils, flat slopes and dense vegetation have low runoff coefficient values. This was concurrent with the results of this study as the area was mostly dominated by relatively flat slope and dense vegetation resulting in low runoff coefficients in some areas. Such evidence was noted at sub-catchment A9H016 located upstream, which recorded low runoff coefficient values ranging from 0.01 to 0.06. A decreasing trend was noted at sub-catchment A9H017 with a mean value of 0.05. Vegetation is important, not only because it determines evapotranspiration losses from the basin, but also because it can be an important control on slowing runoff (most evident in forested versus non-forested slopes) to the river channels. Vegetation amount and type within the channels may also exercise an important control on the efficiency of stream flow.

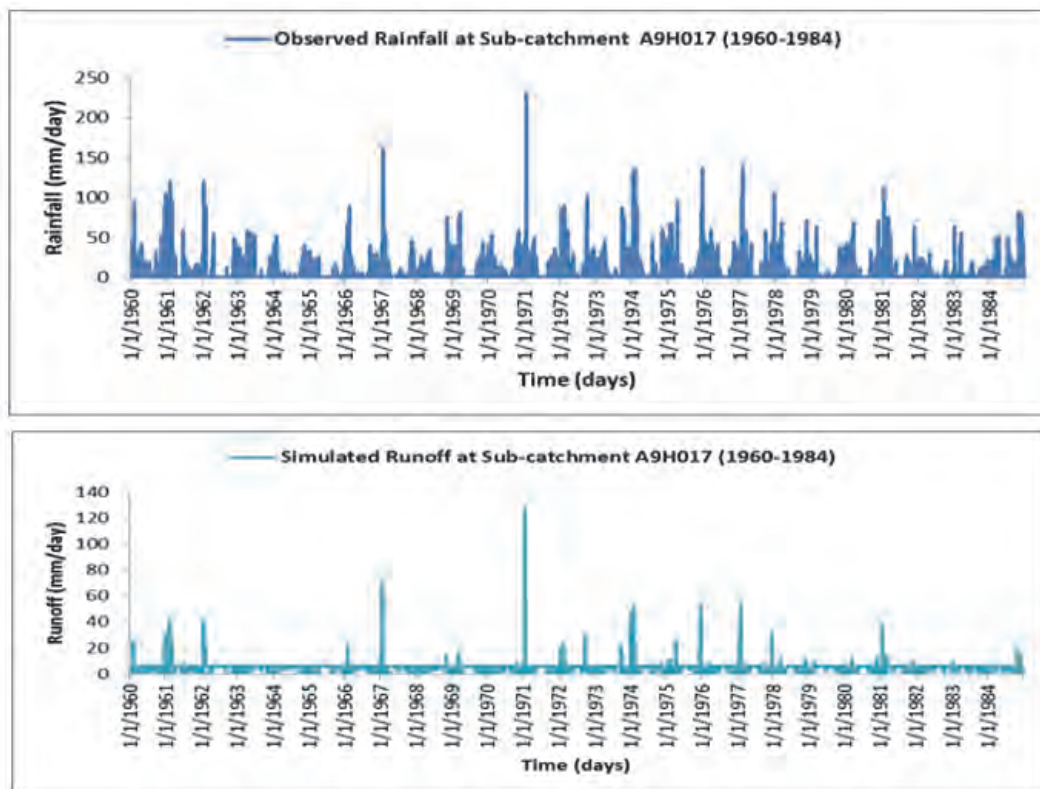


Figure 8.4: Observed rainfall and simulated runoff upstream: 1960-1984

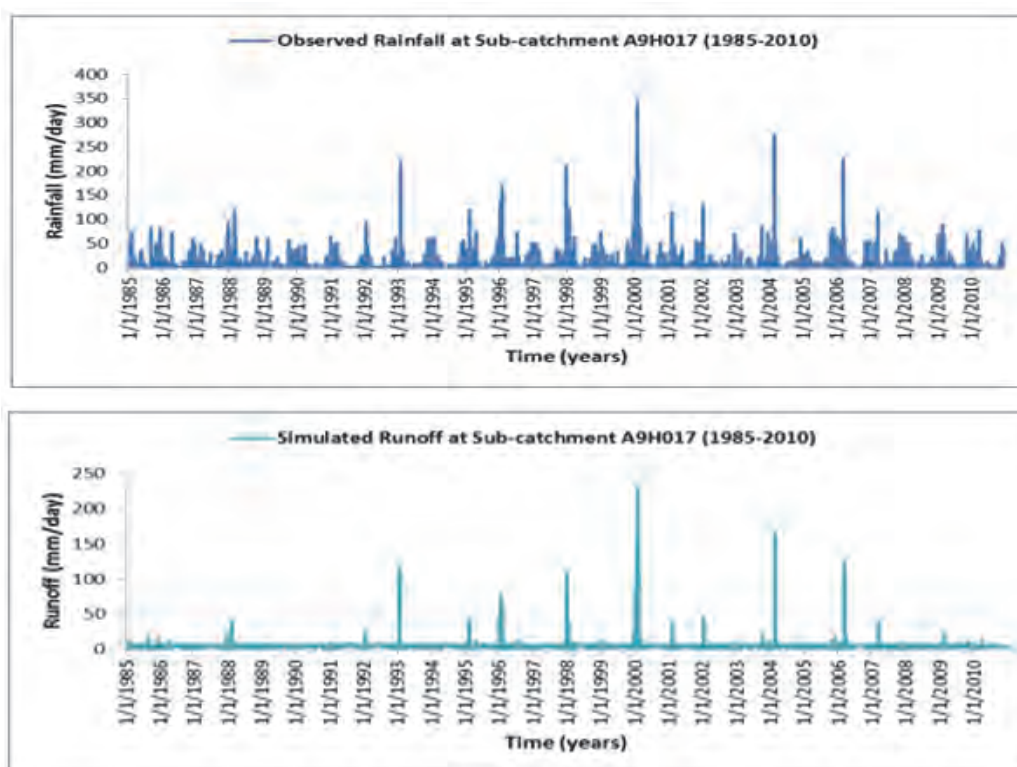


Figure 8.5: Observed rainfall and simulated runoff upstream: 1985-2010

From the simulations, the derived composite values for CN significantly changed the sub-catchments hydrologic response over the period. Increasing the CN resulted in increased

runoff which represented low infiltration, low detention and retention hence high surface runoff, while reducing it had the opposite effect. It was also noted that the two sub-catchments provided a wider collecting surface due to their size and disposed more water at the outlets in response to the degraded land cover conditions.

### **8.3 Suspended sediment discharge**

Analysis of suspended sediments on rainy days showed that sediment concentration in rivers tended to increase with the rainy season. The highest concentration of sediment transported in streams was at Mutshindudi River at Dzingahe, Mutale River at Thengwe, and Luvuvhu River at Mhinga, which showed up to 99% sediment accumulations.

Determination of total suspended-sediment load carried by overland and channel flow is critical for characterizing water quality and establishing the criteria for the maximum daily amount of sediment that aquatic vegetation can tolerate. However, sediment sources varied in the catchment with physical settings and degree of human activity. Soil erosion removes topsoil, degrades soil quality, and contributes potentially harmful substances to nearby streams. The stability and transport of sediments is central to the analysis and prediction of environmental quality and the impact on habitat stability and public health risks. Effective management of sediment requires information on the amount of sediment being transported at specific locations and how sediment transport varies with time.

Land and water are separate environmental factors which are very closely related. An important function of a catchment is to collect rainfall over large areas and deliver clean water to rivers and streams. Where vegetation is lacking, runoff erodes soil, taking suspended sediments in streams and rivers. Thus, the amount of suspended sediment can be used as an indicator of the health of a catchment ecosystem. Suspended sediments can be used as a special indicator of land quality because they integrate what is happening on the land over a large area and concentrates the results to a single location where samples may be taken.

During the onset of rainfall season, soil particles tend to become loosely attached to each other and are more erodible resulting in high chances of detachment and transportation in streams leading to high sediment concentrations. The months of December and January which exhibited a tremendous increase in sediment concentrations were dominated by tropical circulation features.

Average sediment loads in rivers revealed a decreasing trend from October 2011 to January 2012. A gradual decrease was experienced towards the end of the rainfall season. The highest loads of sediments were recorded in early November at Mutshindudi River at Phiphidi followed by Luvuvhu River at Tshino and Madanzhe River which recorded 3269.5; 2365.7; and 2313.3 mg/l respectively.



Luvuvhu River at Mhinga recorded the lowest sediment concentration of 87.07 mg/l followed by Mutale River at Thengwe, Mutshindudi River at Dzingahe, Mudaswali River at Matangari, Nyahalwe River at Thengwe and Mbwedi River at Khubvi which recorded less than 500 mg/l of sediment loads. About 500 mg/l were recorded at Dzindi River at Dzwerani and Tshinane River at Gondeni which constituted 509.2 and 535.6 mg/l respectively. A study by Kamtukule (2008) showed that sediment loads below 3000 mg/l indicated a well conserved catchment while those ranging from 3000 -10 000 mg/l indicated a catchment prone to erosion. Plate 18 showed the suspended sediment in Tshinane River at Gondeni.



Plate 18: Suspended sediment in Tshinane River at Gondeni

Mutshindudi River which runs along steep slopes where soil erosion is highly vulnerable, recorded more than 3000 mg/l of sediment load. During the time of sampling, people had been allocated empty stands and housing infrastructures were being built along the river in the riparian zone, which may have triggered the erosion and transport of sediments to the river.

Analysis of suspended sediments on rainy days showed that sediment concentration in rivers tended to increase with the rainy season. Table 8.2 showed the suspended sediment sampling sites along various rivers in the catchment.

Table 8.2: Suspended sediment sampling sites

<b>Sampling site along various rivers</b>	<b>Sampling Date</b>	<b>Sediment Load (mg/l)</b>	<b>Sediment Concentration (%)</b>
Madanzhe River	2011/10/05	2313.30	0.23
Mutshindudi River at Phiphidi	2011/11/01	3269.55	0.33
Dzindi River at Dzwerani	2011/11/02	509.243	0.05
Tshinane River at Gondeni	2011/11/15	535.61	0.05
Mutshiundudi River at Dzingahe	2011/11/15	192.22	0.02
Mbwedi River at Khubvi	2011/11/22	2291.88	0.23
Luvuvhu River at Tshino	2011/12/02	2365.70	0.24
Nyahhalwe River at Thengwe	2011/12/08	429.28	0.004
Mudaswali River at Matangari	2012/01/13	247.83	0.003
Mutale River at Thengwe	2012/01/13	99.90	0.001
Luvuvhu River at Mhinga	2012/01/24	87.07	0.01

During the onset of rainfall season, soil particles tend to become loosely attached to each other and are more erodible resulting in high chances of detachment and transportation in streams leading to high sediment concentrations.

#### **8.4 Flood frequency and magnitude**

In the recent years, the catchment has experienced floods resulting from higher than normal rainfall associated with the Intertropical Convergence Zone and cyclonic episodes. In order to understand the dynamics involved in the effects of climate change, annual maximum flow data was obtained from the South African Department of Water Affairs and used to evaluate flood frequencies in the catchment. Plate 19 showed the flood water levels in February 2000 in KNP.



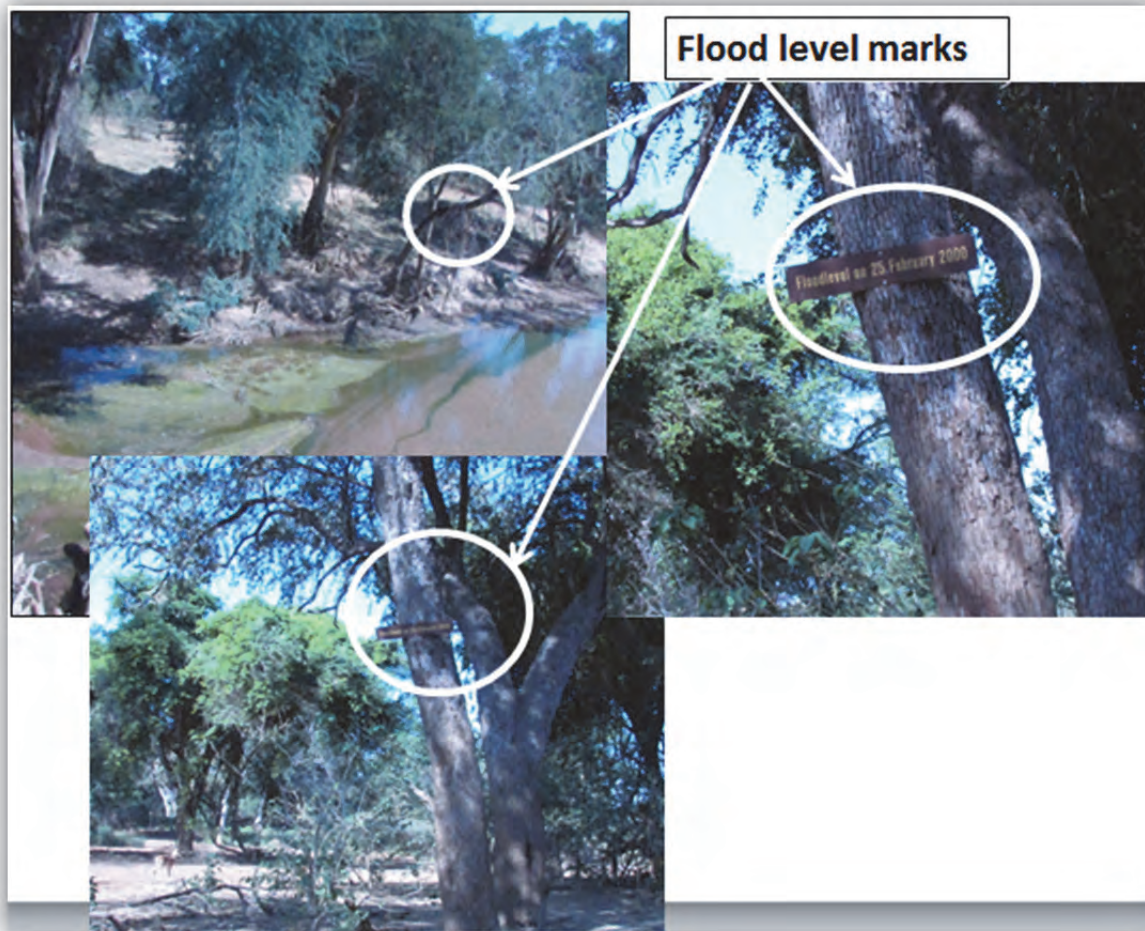


Plate 19: Flood water levels in February 2000 in KNP

Frequency distributions were used to describe historical characteristics and magnitudes of floods. The distribution models used in the study included the Generalized Extreme Value distributions (GEV), the Gumbel or Extreme Value type I distribution (EV1), the Lognormal (LN) distribution and the Log Pearson type III distribution (LP III).

The location parameter ( $\mu$ ) described the shift of the distribution on the horizontal axis. The scale parameter ( $\alpha$ ) described how spread out the distribution was, and defined where the bulk of the distribution lay. The shape parameter ( $\kappa$ ) strictly affects the shape of the distribution and governs the tail of each distribution.

Figure 8.6 showed the return periods for streamflow for stations in the upper middle reaches of catchments. A regression equation was fitted in the data to detect a relation between annual maximum series and their corresponding return periods, to test whether such a relation, either assumed or calculated, was statistically significant. The coefficient of determination ( $R^2$ ) for streamflow at gauging stations A9H002, A9H006, A9H015 and A9H016 were detected as 0.954, 0.966, 0.89 and 0.893 respectively. The highest correlation values for streamflow was detected at station A9H006 with an  $R^2$  of 0.966. The range of significant correlations for streamflow data varied from 0.893 to 0.966. The  $R^2$  values herein described the proportion of

the variance in the observed streamflow data. The  $R^2$  in streamflow had correlations of 0.8 and higher, which confirmed that a strong relationship exists between annual data and simulated return periods and were considered strong enough for flood frequency estimation.

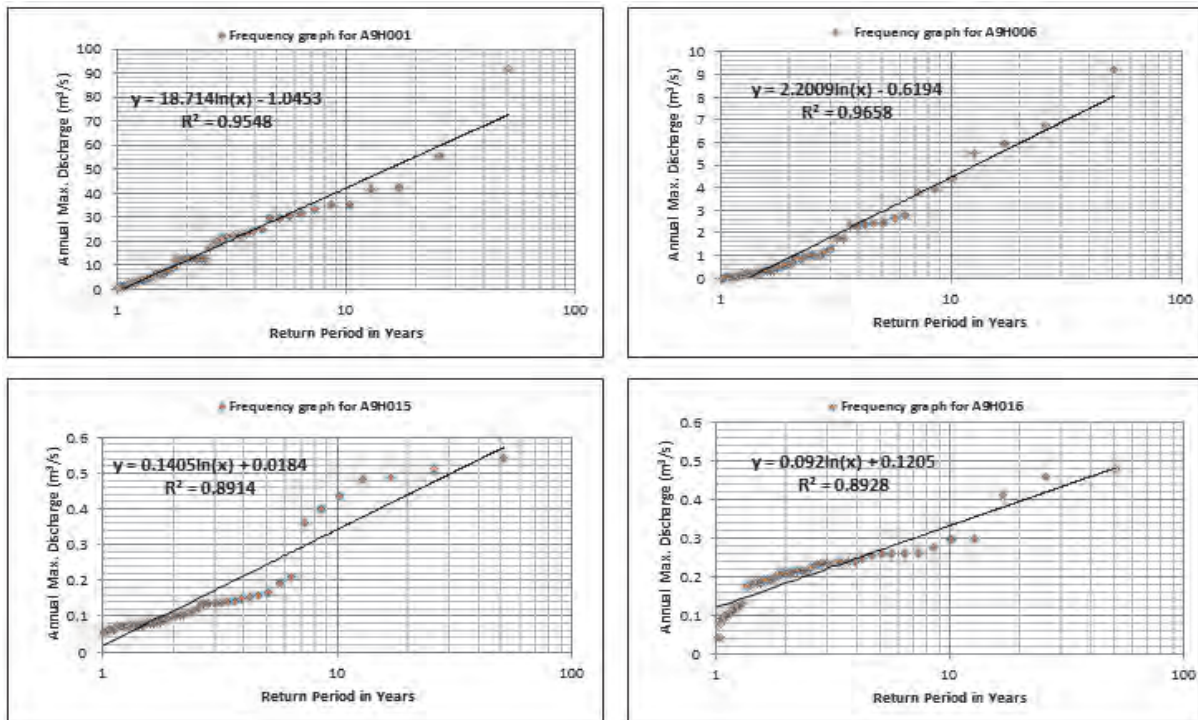


Figure 8.6: Return period of annual streamflow

Estimated flood magnitudes for various selected return periods based on Log-Pearson type III were as shown in Figures 8.7 and 8.8. Each computed flood magnitude was determined at 95-percent confidence interval. This interval was the range that contained the true flood magnitude for a particular exceedence probability. The coefficient of determinations ( $R^2$ ) at each station showed statistically significant relations between estimated flood peaks and assigned return periods.



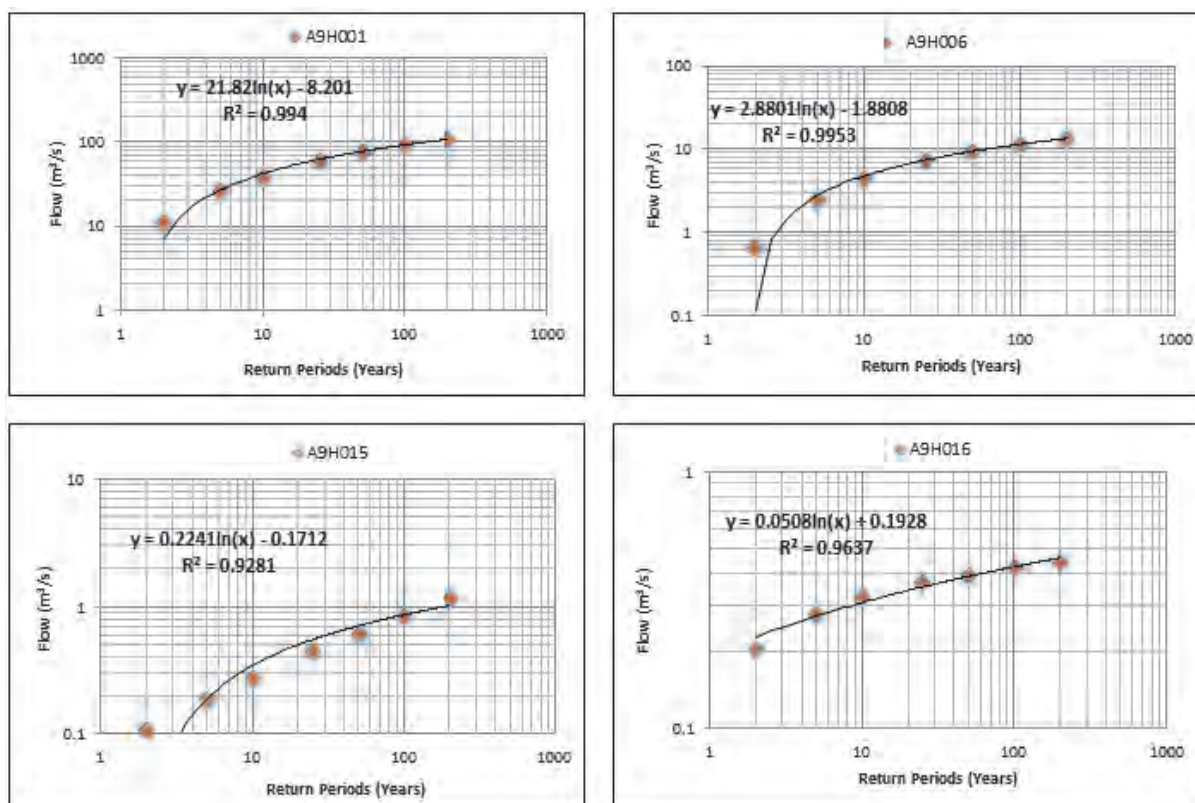


Figure 8.7: Computed peak flows for the 2, 5, 10, 25, 50, 100 and 200 year return periods

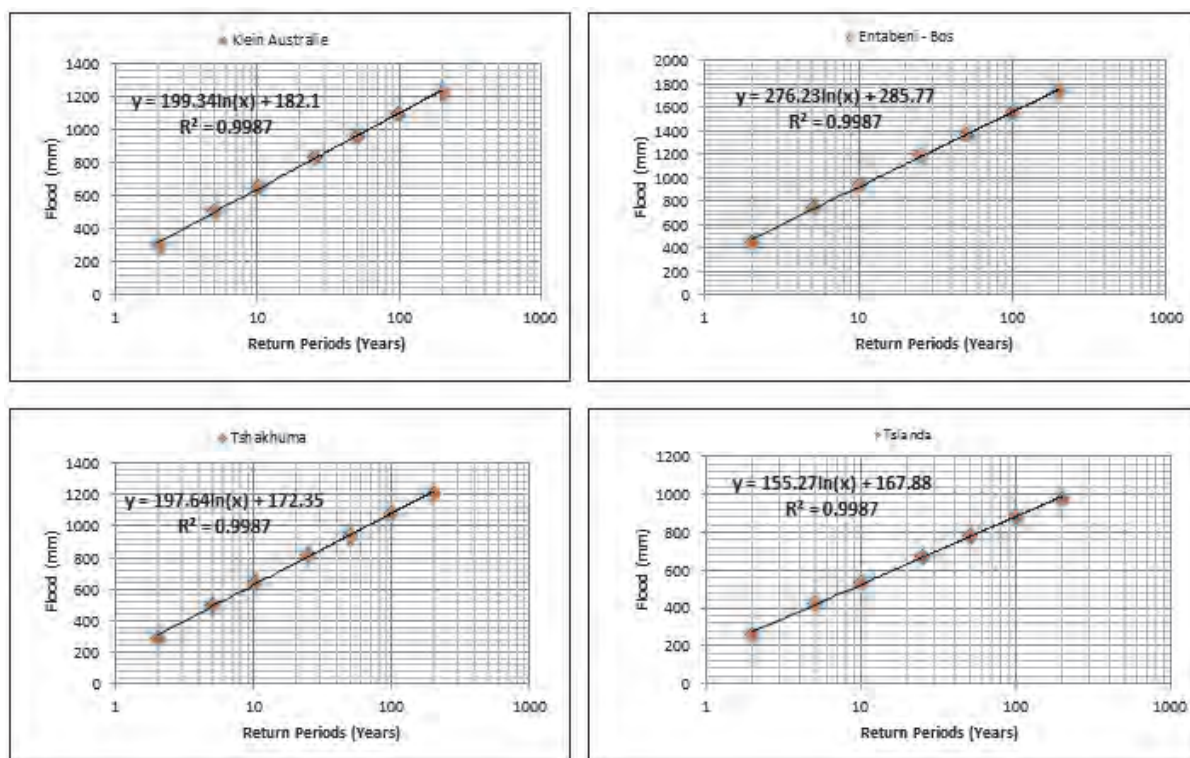


Figure 8.8: Computed peak floods for the 2, 5, 10, 25, 50, 100 and 200 year return periods

The estimated discharges using GEV, EV1, LN and LP III distributions were as shown in Tables 8.3 to 8.6 respectively. The four models showed increasing discharges at higher probabilities of exceedence for all return periods, which could be associated with the effects of climate variability and land use change.

Table 8.3: Estimated Discharges for GEV distribution

Return Period (Years)	Exceedence Probability (%)	Estimated Discharge (m <sup>3</sup> /s)	Climate-variability factor, $F_{Tijk}$	Modified peak discharge	Difference in discharge
2	50	32.28	2.12	68.43	36.15
5	20	34.32	1.87	64.18	29.86
10	10	62.33	1.41	87.89	25.56
25	4	65.34	1.38	90.17	24.83
50	2	72.30	1.23	88.93	16.63
100	1	74.02	1.15	85.12	11.10
200	0.5	76.14	1.08	82.23	6.09

Table 8.4: Estimated discharges for EV1 distribution

Return Period (Years)	Exceedence Probability (%)	Estimated Discharge (m <sup>3</sup> /s)	Climate-variability factor, $F_{Tijk}$	Modified peak discharge	Difference in discharge
2	50	27.68	2.12	58.68	31.00
5	20	30.37	1.87	56.79	26.42
10	10	50.44	1.41	71.12	20.68
25	4	53.21	1.38	73.43	20.22
50	2	59.17	1.23	72.78	13.69
100	1	61.49	1.15	70.71	9.22
200	0.5	67.51	1.08	72.91	5.40

Table 8.5: Estimated discharges for LN distribution

Return Period (Years)	Exceedence Probability (%)	Estimated Discharge (m <sup>3</sup> /s)	Climate-variability factor, $F_{Tijk}$	Modified peak discharge	Difference in discharge
2	50	29.79	2.12	63.15	33.36
5	20	31.87	1.87	59.60	27.73
10	10	51.36	1.41	72.42	21.06
25	4	55.42	1.38	76.48	21.06
50	2	58.97	1.23	72.53	13.56
100	1	63.49	1.15	73.01	9.52
200	0.5	69.07	1.08	74.60	5.53

Table 8.6: Computed Discharges for LP3 distribution

Return Period (Years)	Exceedence Probability (%)	Estimated Discharge ( $\text{m}^3/\text{s}$ )	Climate-variability factor, $F_{Tijk}$	Modified peak discharge	Difference in discharge
2	50	30.01	2.12	63.62	33.61
5	20	32.33	1.87	60.46	28.13
10	10	48.60	1.41	68.53	19.93
25	4	50.96	1.38	70.32	19.36
50	2	63.41	1.23	77.99	14.58
100	1	65.37	1.15	75.18	9.81
200	0.5	69.03	1.08	74.55	5.52

The increase in flood frequency and magnitude suggested that climate variability was having an effect on the catchment. Based on the results, the computations showed that an increase in the peak discharges was to be expected, especially for the discharge range corresponding to smaller and medium flood magnitudes. Given climate variability and the rapid land use changes in the catchment, a significant rise in water levels would lead to an increase in potential flood damage, particularly for flood events of lower to medium extremity, reducing flood security for existing protection facilities. The effect would however be less for events with a lower probability of occurrence involving large floods like the 100 and 200 year return period floods. A strategy of preserving natural forests and investing in sustainable agriculture, especially in uplands, could significantly reduce potential losses caused by the effects of degradation. The consequences of floods of such magnitudes are severe and range from shock to animals to submergence of vegetative cover to damage to infrastructure to loss of income from tourism.

## 8.5 Quality controls

Quality controls were built into the data collection process to ensure the accuracy of survey results. These safeguards included careful selection and training of enumerators on capacity building, use of detailed instruction manuals, careful field supervision, comparison of reported hectares and quantities with those measured on the orthophoto maps, and validation visits to selected segments.  $33 \text{ km}^2$  out of  $430 \text{ km}^2$  segments for the study area were sampled, representing 7.67% which is greater than the recommended 5%. In the visual analysis of the imagedettes, other existing information about the area was used to determine whether they were consistent with ground details. Hydrological data was checked for homogeneity, stationarity and normality before being analysed.

## **CHAPTER 9**

### **CONCLUSION AND RECOMMENDATIONS**

#### **9.1 CONCLUSION**

The main physical changes related to human activities that occurred in LRC included removal of natural vegetation and headwater drainage patterns, loss of natural depressions which temporarily store surface water, loss of rainfall absorbing capacity of humus on the forest floor, creation of impervious areas (rooftops, roads, parking lots, sidewalks and driveways). The effects manifested in significant modifications to several components of the hydrologic cycle including higher and more rapid peak surface discharge, increased surface runoff volume during storm events, reduced base flow rate, reduced infiltration and groundwater recharge, increase in erosion and contaminants discharged into the receiving water body.

The synergism between remote sensing and GIS for land surface analysis was utilised in this project. Through time series analysis of remotely sensed data and ground survey, it was ascertained that significant change in land cover and land use, particularly the conversion of forest and woodlands to arable and build-up land had occurred. There was a sustained conversion of rural land use to urban land use. Satellite image time series were used to analyse landscape dynamics and hence improved the knowledge of environmental processes which may lead to better development of water catchments. The use of multi-temporal remotely sensed data showed that the catchment had undergone significant changes in land cover over the decades. The satellite time series analysis of 1980s, 1990s and 2000s showed the pre-change and post-change cover types. The predominant land cover classes which were selected for the study included agriculture, natural forest, bare ground, shrub and grass lands, plantation, and water bodies.

The study made it possible to evaluate the impact of the dynamic geomorphic processes and environmental degradation due to deforestation and intensive land use on stream flows. The impacts of land use and land cover change were determined by the cause-effect relationships of human activity, landscape dynamics and hydrology. This change caused land degradation, which was impacting negatively on the catchment. Infiltration rates were declining as compared to what they were in the 1960s. Peak runoff increased while stream discharges had reduced. It was therefore concluded that integration of remotely sensed data and GIS provided information for effective routine tasks related to environmental monitoring and inventorying, especially land cover and land use change. New strategies for sustainable development in the catchment should adopt the technique and take full advantage of the capabilities of GIS as a tool for planning and decision making.

The increase in flood frequency and magnitude suggested that climate variability was having an effect on the catchment. Since flash floods in a catchment at a particular time not only depend on amount, duration and frequency of rainfall but also on the antecedent rainfall events, the delta method can be used to recapture the past and fill the gaps between events.

SWAT application to the Levubu-Tshakhuma sub-catchment divided the sub-catchment into 502 HRU. The latter aids in efficient management of water resources at catchment as each HRU is different from the next in terms of catchment properties. A crucial step in understanding the various processes resulting from anthropogenic activities was to perform a sensitivity analysis. The sensitivity analysis using the SWAT tool provided useful insight into which parameters were most sensitive concerning land use change towards rivers. In this approach, not only were long-term historical time series effects on streamflow, rainfall, evapotranspiration and land use analyzed to ascertain changes in hydrologic effects but also the landscape history and response potential were used as a guide to identify appropriate land use management options. A GIS database was created comprising of remotely sensed data, digitized data and ancillary data on land use and hydrology for purposes of planning in line with the National water strategy.

## **9.2 RECOMMENDATIONS**

1. There should be re-afforestation of hills and management of forests involving both conservation of existing patches of the forests and enrichment of degraded forests including stream buffering. Woods and villages should be improved to mimic forest ecosystems, particularly by the development of a multi-storied vertical canopy structure through agro-forestry interventions and various other conservation practices. The soil and water conservation techniques for other arable lands should be an integrated package including physical works such as drains and terraces; vegetation techniques like ground cover by crops, residue management, and vegetative hedgerows; and biological techniques such as agronomic measures.
2. Image synergism should be used as much as possible by merging multisensor image data since it has been demonstrated that, remotely sensed imagery can be used to quantify and monitor land use and land cover within catchments. A detailed soil-landscape analysis within a geodatabase structure should be carried out for purposes of spatial modelling. This will enable topographical and geological maps to be combined with aerial photos and satellite images of appropriate scale to map and identify land-scape and physiographic units.
3. Existing weather stations should be refurbished and new ones established within the catchment in order to enhance the database for climatic data. All the seven river gauging stations should be refurbished and a strict monitoring schedule to be put in place. The adoption of computer-based techniques for water catchment management should be emphasized in view of the need to build and update a database which can be queried for rapid decision making, data sharing and web services.
4. By linking the cause-effect relations revealed by the analyses, land management prescriptions should be developed for major land use categories in the catchment so that the hydrologic response would be closer to the desired conditions that existed in the pre-change period. Suitable land use management practices for agricultural land uses should be identified mainly based on their ability to mimic the forest ecosystems.



5. Concurrent application of biological and physical measures should be promoted depending on the validation of such combinations under given circumstances from engineering, agronomic, and socioeconomic points of view. The suggested techniques of soil and water conservation should include those well known to the farmers in the area and accepted by them. In the case of plantation tree seedlings on afforestation land, it is important either to replant or to diversify with other tree species if in order to achieve a good ground cover.

6. Cultural practices to minimize soil loss should be practiced by selecting vegetative plant materials such as Vetiver grass (*Vetiveria zizanioides*) that can thrive in the same ecosystem. Besides increasing soil fertility, such techniques would aid in the addition of organic matter and improve the soil structure and reduce soil erodibility. The selection of species for such plantations could be based on demand for timber, fodder, fuelwood, fruits, biomass for organic manure, biodiversity needs and so on. It is of great importance to stabilize the slopes and protect the exposed land surface from rain drop impact and scouring runoff in case of house building and road construction, to reduce heavy sediment supply to the streams.

7. The hedgerows in the area should be improved to double hedgerow planting of leguminous trees which have benefits similar to those of grass hedgerows while providing biomass for mulching. Such hedgerows provide a variety of other benefits such as fixing of atmospheric nitrogen for soil replenishment agricultural land uses. The conservation strategy must involve a package of conservation measures that are economically beneficial to the land owners. It should include the type of vegetation and or crop suitable for the given location, appropriate land and water saving and conservation practices, as well as user rights to benefit from conservation of natural resources. Under such circumstances, the aggregated impact of such initiatives as a whole could be expected to have a role upon the quality and quantity of water including its temporal and spatial distribution so that the water cycle could revert and be closer to that which existed with a higher percentage of land area under natural forests.

8. The impact on forest ecosystem should be reduced by substituting wood products with steel and plastic products in many applications. The impact on arable land should be reduced by planning settlements and build up areas to mimic natural functions and minimize disruption to hydrologic processes. There should be elaborate soil and water management projects in headwater catchment areas, riparian zones and wetlands.

## REFERENCES

- Anderson J.R. (1977) Land use and land cover changes-A framework for monitoring: *US Geol. Survey, Jour. Research*, **5**(2) p.223-224.
- ARC-ISCW (2006) Land types and soil inventory databases of South Africa. (Agricultural Research Council's Institute for Soil Climate and Water: Pretoria, South Africa)
- Arnold, J.G., Moriasi, D.N., Gassman, P.W., Abbaspour, K.G., White, M.J., Srinivasan, R., Santhi, C., Harmel, R.D., van Griensven, A., van Liew, M.V., Kannan, N. and Jha, M.K. (2012) SWAT: Model use, calibration and validation, *America. Soc. Of Agric. And Biol. Eng.*, **55**(5) p.1491-1508.
- Bate, R.R., Tren, R. and Mooney, L. (1999) An econometric and institutional economic analysis of water use in the Crocodile River Catchment, Mpumalanga province, South Africa, WRC report No. 885/1/99, Pretoria, RSA.
- Bithell, M. and Brasington, J. (2009) Coupling agent-based models of subsistence farming with individual-based forest models and dynamic models of water distribution, *Environmental Modeling & Software*, **24** p.173-190.
- Bosch, D.D. and Goodrich, D.C. (1996) Statistical and geostatistical characterization of spatial variability, USDAARS Infiltration Conference, Pingree Park, CO, July 22-25.
- Bumby, A.J. (2000) The geology of the Blouberg formation: Waterberg and Soutpansberg groups in the area of Blouberg mountain, Northern Province, South Africa. Published PhD Thesis, University of Pretoria, South Africa, p.323.
- Calder, I.R. (1992) Hydrological effects of land use change: In Handbook of Hydrology. D.R Maidment (Eds.), McGraw Hill, New York, p.13.11-13.15.
- Calder, I.R. (2003) Assessing the water use of vegetation and forests – development of the HYLUC, Hydrological Land Use Change model. *Water Resour. Res.*, **39**(11) p.1318.
- Chow, V.T., Maidment, D.R. and Mays, L.W. (2010) Applied hydrology, Tata McGraw-Hill Edition, New Dehli, India, p.572
- Congalton, R.G. and Green, K. (1999) Assessing accuracy of remotely sensed data: Principles and practices, Lewis publishers, Boca Roton, Florida, p.137.
- DWAF (2002) A proposed National Water Resources Strategy for South Africa. Department of Water Affairs and Forestry, South Africa.

- DWAF (2004) Directorate: National Water Resource Planning (North) Internal strategic perspective: Luvuvhu/Letaba water management areas, Goba Moahloli Keeve Steyn and Tlou & Matji Engineering & Management Services, Department of Water Affairs and Forestry, DWAF Report no: *PWMA 02/000/00/0304*.
- FAO. (1992) CROPWAT: A computer program for irrigation planning and management. Smith M. (Ed.), Irrigation and Drainage Paper 46, Rome, Italy.
- FAO. (1996) Steps towards a participatory and integrated approach to watershed management. Report of the Inter-regional Project for Participatory Upland Conservation and Development, FAO/Italy Cooperative Programme. Tunis, Eds. Fé d'Ostiani, L. & Warren, P.
- FAO-ISSS-ISRIC. (1998) World reference base for soil resources. World Soil Resources Report No. 84. Rome.
- Fairfield, J. and Leymarie, P. (1991) Drainage Networks from Grid Digital Elevation Models. *Water Resources Res.*, **30**(6) p.1681-1692.
- Gallego, F.J. (1995) Sampling frames of square segments, Institute for Remote Sensing application, Ispra, Italy. P.55.
- Gibson, D.J.D. (2006) Land degradation in Limpopo Province, South Africa, Masters Dissertation, University of Witwatersrand, Johannesburg, South Africa, p.51
- Griscom, H.R., Miller, S.N., Gyedu-Ababio, T. and Sivanpillai, R. (2009) Mapping land cover change of the Luvuvhu catchment, South Africa for environmental modeling, *Springer, Geo. Journal*, **75** p.163-173.
- Haith, D. A. and Shoemaker, I. L. (1987) Generalized watershed loading functions for stream flow nutrients, *Water Resources Bulletin*, **107** p.121-137
- Hillel, D. (1980) Fundamentals of Soil Physics. Academic Press, New York, p.413.
- Hope, R.A. Jewitt, G.P.W. and Gowing, J.W. (2004) Linking the hydrological cycle and rural livelihoods: A case study in the Luvuvhu catchment, South Africa. *Physics and chemistry of the Earth*, **29** p.1209-1217.
- Hydrosoft Computing, LLC (2006) D-Plot ver. 2.0.4.7.: Graph software for scientists and Engineers.
- ISRIC (2008) SOTER database for Kenya (version 2.0). Accessed on 12<sup>th</sup> January 2008, <http://www.isric.org>.

- IUSS. (2006) World Reference base for soil resources. 2nd Ed, World Soil Resources Report No 103, FAO, Rome.
- Jensen, J. R. (2005) Introductory Digital Image Processing: A Remote Sensing Perspective, 3rd Edition, Upper Saddle River: Prentice-Hall, p.526.
- Jewitt, G.P.W., Garratt, J.A., Calder, I.R. and Fuller, L. (2004) Water resources planning and modeling tools for the assessment of land use change in the Luvuvhu catchment, South Africa, *Physics and chemistry of the earth*, Vol: **29** p.1233-12410.
- Jury, M.R., Weeks, S. and Gondwe, M.P. (1997) Satellite-observed vegetation as an indicator of climate variability over southern Africa. *South. Afr. J. Sci*, **93** p.34-38.
- Kruger-2-Kalahari (2014) Pafuri river Camp, Accessed on 22<sup>nd</sup> July 2005 <http://www.kruger-2-kalahari.com/pafuri-river-camp.html>.
- Kamtukule, S.L. (2008) Investigating impacts of sedimentation on water availability in small dams: Case study of Chamakala II Small Earth dam, Malawi. Published Thesis.
- Kundu, P.M. and Olang, L.O. (2011) Automated extraction of morphologic and hydrologic properties for River Njoro catchment in Eastern Mau, Kenya. In Proc. 4th International Conference of Applied Geoinformatics for Science and Environment, at JKUAT, Kenya. AGSE: Publishing, <http://appliedgeoinformatics.org/publications>.
- Lin, Y. P., Hong, N. M., Wu, P. J., Wu, C. F. and Verburg, P. H. (2006) Impacts of land use change scenarios on hydrology and land use patterns in the Wu-Tu watershed in Northern Taiwan, *Landscape and Urban Planning*, **80** p.111-126
- Lynn, B.H. and Carlson, T.N. (1990) A stomatal resistance model illustrating plant vs. external control of transpiration, *Agricultural and Forest Meteorology*, **52** p.5-43.
- Merz, R. and Blöschl, G. (2009) A regional analysis of event runoff coefficients with respect to climate and catchment characteristics in Austria, *Water Resour. Res.*, 45, W01405, doi:10.1029/2008WR007163.
- Miller, S. N., Kepner, W. G., Mehaffey, M. H., Hernandez, M., Miller, R. C. and Goodrich, D. C. (2002) Integrating landscape assessment and hydrological modeling for land cover change analysis, *Journal of the American Water Resources Association*, **38** p.915-929.
- Monteith, J.L. (1965) Evaporation and environment: the state and movement of water in living organisms. *Symp. Soc. Exp. Biol.* **19** p.205-234.

- Monteith, J.L. (1981) Evaporation and surface temperature. *Quart. J. Roy. Meteorology. Soc.*, **107** p.1-27.
- Morin, J. and Kosovsky, A. (1995) The surface infiltration model. *Journal of Soil and Water Conservation* 50(5) p.470-476.
- Mukheibir, P. (2005) Local Water Resource Management Strategies for Adaptation to Climate Induced Impacts in South Africa. Energy Research Centre. University of Cape Town.
- Mukheibir, P. and Sparks, D. (2003) Water resource management and climate change in South Africa: visions, driving factors and sustainable development indicators; report for Phase I of the Sustainable Development and Climate Change Project. University of Cape Town, Rondebosch, South Africa.
- Mölders, N. (2011) Land use and Land-Cover Changes: Impact on Climate and Air Quality. *Springer*, p.210.
- Neitsch, S.L., Arnold, J.G., Kiniry, J.R., Williams, J.R. and King, K.W. (2002) Soil and Water Assessment Tool Theoretical documentation: Version 2000. TWRI Report TR-191, Texas Water Resources Institute, in USA.
- Paige, G. and Stone, J. (1996) Measurement Methods to Identify and Quantify Spatial variability of infiltration on Rangelands, In: Ahuja, L.R. and Garrison, A. (Eds), Proceedings of the USDS-ARS workshop “Real world” infiltration, July 22-25, Water resources institute, Colorado State University, p.109-121.
- Penman, H.L. (1948) Natural evaporation from open water, bare soil, and grass. *Proc. of the Royal Society, London* **193**, p.120-146.
- Penman, H.L. (1956) Evaporation. An introductory survey. *Neth. J. Agric. Sci*: **4** p.9-29.
- Penman, H.L. (1963) Vegetation and Hydrology. Tech. Comm. No. 53, Commonwealth Bureau of Soils, Harpenden, England, p.125.
- Rahman, S., Munn, L.C., Zhang, R. and Vance, G.F. (1996) Wyoming Rocky Mountain forest soils: Evaluating variability using statistics and geostatistics, *Canadian Journal of Soil Science* **75** p.501-507.
- Reddy, S.J. (1985) Suggested farming systems and associated risks over southern Mozambique. Comunicação No. 24, Série Terra e Água, INIA. Maputo.

- Rudd, S. (2006) *Environment: An illustrated guide to science*, The Diagram Group, Chelsea House, New York, p.208.
- Schaffer, C.H. (2005) *Investigating the Importance of Land Cover on Evapotranspiration*. Published MSc Thesis in Geography, Northern Illinois University, p.85.
- Scott, E.M. and Dixon, P.M. (2008) Statistical sampling design for radionuclides, In: Povinec P.P. (Eds). *Analysis of environmental radionuclides*, Elsevier, Amsterdam, p.3-15.
- Shi, J., Blundell, T. L. and Mizuguchi, K. (2001) FUGUE: sequence-structure homology recognition using environment-specific substitution tables and structure-dependent gap penalties. *J. Mol. Biol.* **310** p.243-257.
- Soil Conservation Services. (1972) *National Engineering Handbook*. Section 4: Hydrology. Soil Conservation Service, USDA, Washington, DC, USA.
- Suprit K., Shankar D., Venugopal V. and Bhatkar N.V. (2012) Simulating the daily discharge of the Mandovi River, west coast of India. *Hydrological Sciences Journal*, **57**(4), p.686-704.
- Taylor, C.M., Lambin, E.F., Stephenne, N., Harding, R.J. and Essery R.L.H. (2002) The Influence of Land Use Change on Climate in the Sahel. *Journal of Climate*, **15**, p.3615-3629.
- Thornthwaite, C. W. (1948) “An approach toward a rational classification of climate.” *Geography*. Rev. 38.
- Yuan, F., Sawaya, K. E., Loeffelholz, B. C., Bauer, M. E. (2005) Land cover classification and changes analysis of the twin cities (Minnesota) Metropolitan Area by multitemporal Landsat remote sensing. *Journal of Remote Sensing and Environment*, **98** p.317-328.
- Zevenbergen, L.W., Thorne, C.R. (1987) Quantitative analysis of land surface topography. *Earth Surface Processes and Landforms*, **12** p.47-56.



## Appendix 1: SWAT Report Statistics

SUB-BASIN	LU NUM	LU CODE	SOIL NUM	SOIL CODE	SLOPE NUM	SLOPE CODE	MEAN SLOPE	AREA	UNIQUE COMB	HRU GIS
6	7	URBN	76400	76400	3	20-30	24.74914932	312.2985067	6_URBN_76400_20-30	000060025
6	1	FRSD	76400	76400	4	30-50	36.35853577	676.6467645	6_FRSD_76400_30-50	000060015
6	7	URBN	76400	76400	4	30-50	37.85795975	238.7679059	6_URBN_76400_30-50	000060026
6	7	URBN	76400	76400	2	10-20	15.31677914	385.8291075	6_URBN_76400_10-20	000060022
6	0	PAST	76400	76400	2	10-20	15.36203194	12.39279789	6_PAST_76400_10-20	000060007
6	7	URBN	76400	76400	1	0-10	6.371501446	141.2778959	6_URBN_76400_0-10	000060023
6	1	FRSD	76400	76400	999	50-9999	53.69930267	48.74500502	6_FRSD_76400_50-9999	000060016
6	8	WATR	76400	76400	4	30-50	38.24328232	63.61636248	6_WATR_76400_30-50	000060033
6	0	PAST	76400	76400	1	0-10	6.541261196	8.261865257	6_PAST_76400_0-10	000060005
6	8	WATR	76400	76400	3	20-30	24.29169083	84.27102562	6_WATR_76400_20-30	000060032
6	1	FRSD	76400	76400	3	20-30	24.56929207	893.9338208	6_FRSD_76400_20-30	000060012
6	7	URBN	76400	76400	999	50-9999	55.83336639	45.44025891	6_URBN_76400_50-9999	000060024
6	0	PAST	76400	76400	4	30-50	39.20331955	8.261865257	6_PAST_76400_30-50	000060006
6	8	WATR	76400	76400	2	10-20	15.49032307	103.2733157	6_WATR_76400_10-20	000060034
6	8	WATR	76400	76400	1	0-10	6.498269081	45.44025891	6_WATR_76400_0-10	000060036
6	9	AGRL	76400	76400	2	10-20	16.2140007	16.52373051	6_AGRL_76400_10-20	000060042
6	0	PAST	76400	76400	3	20-30	24.60250473	9.914238308	6_PAST_76400_20-30	000060008
6	9	AGRL	76400	76400	4	30-50	37.22189713	0.826186526	6_AGRL_76400_30-50	000060041
6	8	WATR	76400	76400	999	50-9999	52.75195313	7.435678731	6_WATR_76400_50-9999	000060035
6	1	FRSD	76400	76400	2	10-20	15.56116009	943.5050123	6_FRSD_76400_10-20	000060014
2	1	FRSD	76400	76400	1	0-10	6.745839596	89.22814477	2_FRSD_76400_0-10	000020006
2	1	FRSD	76400	76400	2	10-20	14.59139729	150.3659477	2_FRSD_76400_10-20	000020007
6	1	FRSD	76400	76400	1	0-10	6.979185104	253.6392634	6_FRSD_76400_0-10	000060013

SUBBASIN	LU_NUM	LU_CODE	SOIL_NUM	SOIL_CODE	SLOPE_NUM	SLOPE_CODE	MEAN_SLOPE	AREA	UNIQUECOMB	HRUGIS
2	1	FRSD	76400	76400	3	20-30	24.93777084	139.6255228	2_FRSD_76400_20-30	000020008
2	7	URBN	76400	76400	2	10-20	15.38166714	57.00687027	2_URBN_76400_10-20	000020014
2	0	PAST	76400	76400	1	0-10	5.628733635	3.304746103	2_PAST_76400_0-10	000020005
2	7	URBN	76400	76400	1	0-10	7.185574532	15.69754399	2_URBN_76400_0-10	000020013
2	7	URBN	76400	76400	3	20-30	24.84830475	81.79246604	2_URBN_76400_20-30	000020017
2	7	URBN	76400	76400	4	30-50	37.5188446	58.65924332	2_URBN_76400_30-50	000020016
2	1	FRSD	76400	76400	999	50-9999	60.77750015	71.87822773	2_FRSD_76400_50-9999	000020010
2	1	FRSD	76400	76400	4	30-50	38.22308731	171.8467973	2_FRSD_76400_30-50	000020009
2	7	URBN	76400	76400	999	50-9999	59.64506912	25.6117823	2_URBN_76400_50-9999	000020015
2	8	WATR	76400	76400	2	10-20	14.46236992	22.30703619	2_WATR_76400_10-20	000020023
1	1	FRSD	76400	76400	3	20-30	24.60365486	101.6209427	1_FRSD_76400_20-30	000010009
1	1	FRSD	76400	76400	4	30-50	38.75659943	88.40195825	1_FRSD_76400_30-50	000010006
1	1	FRSD	76400	76400	2	10-20	16.06549454	39.65695323	1_FRSD_76400_10-20	000010007
1	1	FRSD	76400	76400	999	50-9999	63.62866211	44.61407239	1_FRSD_76400_50-9999	000010008
1	7	URBN	76400	76400	1	0-10	6.312716961	4.957119154	1_URBN_76400_0-10	000010013
1	7	URBN	76400	76400	4	30-50	38.37302399	52.04975112	1_URBN_76400_30-50	000010014
1	1	FRSD	76400	76400	1	0-10	6.208319187	7.435678731	1_FRSD_76400_0-10	000010010
1	8	WATR	76400	76400	999	50-9999	62.23616409	6.609492206	1_WATR_76400_50-9999	000010020
1	7	URBN	76400	76400	3	20-30	23.80220222	54.5283107	1_URBN_76400_20-30	000010017
1	7	URBN	76400	76400	999	50-9999	63.06406021	22.30703619	1_URBN_76400_50-9999	000010015

2	8	WATR	76400	76400	76400	4	30-50	37.0172348	3.304746103	2_WATR_76400_30-50	000020022
1	7	URBN	76400	76400	76400	2	10-20	16.00311661	33.04746103	1_URBN_76400_10-20	000010016
1	8	WATR	76400	76400	76400	4	30-50	34.72918701	6.609492206	1_WATR_76400_30-50	000010021
1	8	WATR	76400	76400	76400	3	20-30	23.59565735	11.56661136	1_WATR_76400_20-30	000010022
1	0	PAST	76400	76400	76400	3	20-30	26.23765564	5.78330568	1_PAST_76400_20-30	000010005
6	9	AGRL	76400	76400	76400	1	0-10	6.237411499	3.304746103	6_AGRL_76400_0-10	000060040
2	8	WATR	76400	76400	76400	3	20-30	24.56759834	14.87135746	2_WATR_76400_20-30	000020020
1	8	WATR	76400	76400	76400	1	0-10	7.53761673	1.652373051	1_WATR_76400_0-10	000010023

SUBBASIN	LU_NUM	LU_CODE	SOIL_NUM	SOIL_CODE	SLOPE_NUM	SLOPE_CODE	MEAN_SLOPE	AREA	UNIQUECOMB	HRUGIS
1	0	PAST	76400	76400	2	10-20	16.39425659	2.478559577	1_PAST_76400_10-20	000010003
5	1	FRSD	76400	76400	1	0-10	8.238577843	5.78330568	5_FRSD_76400_0-10	000050008
1	8	WATR	76400	76400	2	10-20	16.54545021	4.957119154	1_WATR_76400_10-20	000010024
2	0	PAST	76400	76400	2	10-20	16.60237122	10.74042483	2_PAST_76400_10-20	000020004
5	1	FRSD	76400	76400	3	20-30	25.58501625	22.30703619	5_FRSD_76400_20-30	000050010
5	1	FRSD	76400	76400	2	10-20	16.65188789	12.39279789	5_FRSD_76400_10-20	000050011
5	0	PAST	76400	76400	2	10-20	15.35625648	68.57348163	5_PAST_76400_10-20	000050007
5	8	WATR	76400	76400	1	0-10	7.961884022	5.78330568	5_WATR_76400_0-10	000050024
5	7	URBN	76400	76400	2	10-20	15.78131771	131.3636576	5_URBN_76400_10-20	000050015
5	8	WATR	76400	76400	2	10-20	16.49311638	66.92110858	5_WATR_76400_10-20	000050020
1	0	PAST	76400	76400	1	0-10	8.089263916	0.826186526	1_PAST_76400_0-10	000010004
5	7	URBN	76400	76400	3	20-30	24.08622169	142.1040824	5_URBN_76400_20-30	000050014
5	0	PAST	76400	76400	1	0-10	8.111859322	13.21898441	5_PAST_76400_0-10	000050004

2	9	AGRL	76400	76400	76400	3	20-30	20.14398193	0.826186526	2_AGRL_76400_20-30	000020024
2	7	URBN	74200	74200	74200	1	0-10	5.855240822	7.435678731	2_URBN_74200_0-10	000020011
5	1	FRSD	76400	76400	76400	4	30-50	37.07060623	47.09263196	5_FRSD_76400_30-50	000050009
5	7	URBN	76400	76400	76400	4	30-50	37.639431	80.14009299	5_URBN_76400_30-50	000050016
6	9	AGRL	76400	76400	76400	3	20-30	24.87836456	18.17610357	6_AGRL_76400_20-30	000060039
3	1	FRSD	76400	76400	76400	3	20-30	24.58267021	50.39737807	3_FRSD_76400_20-30	000030012
3	7	URBN	76400	76400	76400	3	20-30	25.83029175	7.435678731	3_URBN_76400_20-30	000030022
1	9	AGRL	76400	76400	76400	2	10-20	19.53520966	1.652373051	1_AGRL_76400_10-20	000010026
1	9	AGRL	76400	76400	76400	1	0-10	6.804193497	0.826186526	1_AGRL_76400_0-10	000010027
1	0	PAST	74200	74200	74200	2	10-20	12.31303024	1.652373051	1_PAST_74200_10-20	000010002
1	7	URBN	74200	74200	74200	2	10-20	14.77587605	9.088051783	1_URBN_74200_10-20	000010012
1	8	WATR	74200	74200	74200	2	10-20	18.74536133	0.826186526	1_WATR_74200_10-20	000010019
2	0	PAST	74200	74200	74200	2	10-20	13.24371433	9.914238308	2_PAST_74200_10-20	000020002
2	8	WATR	74200	74200	74200	1	0-10	2.562536478	24.78559577	2_WATR_74200_0-10	000020018
2	8	WATR	74200	74200	74200	2	10-20	12.7144146	5.78330568	2_WATR_74200_10-20	000020019

SUBBASIN	LU_NUM	LU_CODE	SOIL_NUM	SOIL_CODE	SLOPE_NUM	SLOPE_CODE	MEAN_SLOPE	AREA	UNIQUECOMB	HRUGIS
5	8	WATR	76400	76400	3	20-30	24.07413864	83.44483909	5_WATR_76400_20-30	000050022
3	7	URBN	76400	76400	4	30-50	38.03154373	21.48084967	3_URBN_76400_30-50	000030021
3	7	URBN	76400	76400	2	10-20	14.96576881	9.914238308	3_URBN_76400_10-20	000030019
1	7	URBN	74200	74200	1	0-10	6.456262589	9.088051783	1_URBN_74200_0-10	000010011
2	0	PAST	74200	74200	1	0-10	6.088763237	15.69754399	2_PAST_74200_0-10	000020001
5	8	WATR	76400	76400	4	30-50	36.95073318	54.5283107	5_WATR_76400_30-50	000050021
3	1	FRSD	76400	76400	4	30-50	37.00744629	47.91881849	3_FRSD_76400_30-50	000030009
3	1	FRSD	76400	76400	2	10-20	15.68915749	67.74729511	3_FRSD_76400_10-20	000030008

1	8	WATR	74200	74200	1	0-10	4.667506218	4.957119154	1_WATR_74200_0-10	000010018
1	0	PAST	74200	74200	1	0-10	6.216853619	7.435678731	1_PAST_74200_0-10	000010001
2	8	WATR	76400	76400	1	0-10	6.710885525	4.130932628	2_WATR_76400_0-10	000020021
5	0	PAST	76400	76400	3	20-30	24.19716263	53.70212417	5_PAST_76400_20-30	000050005
3	1	FRSD	76400	76400	1	0-10	7.637341499	9.914238308	3_FRSD_76400_0-10	000030011
5	0	PAST	76400	76400	4	30-50	34.70657349	16.52373051	5_PAST_76400_30-50	000050003
1	9	AGRL	74200	74200	1	0-10	6.534809589	0.826186526	1_AGRL_74200_0-10	000010025
4	7	URBN	76400	76400	3	20-30	23.90825462	11.56661136	4_URBN_76400_20-30	000040022
4	7	URBN	76400	76400	2	10-20	14.2738018	8.261865257	4_URBN_76400_10-20	000040020
4	1	FRSD	76400	76400	2	10-20	14.81335926	28.9165284	4_FRSD_76400_10-20	000040011
4	1	FRSD	76400	76400	3	20-30	24.89234543	21.48084967	4_FRSD_76400_20-30	000040012
5	7	URBN	76400	76400	1	0-10	7.226109028	15.69754399	5_URBN_76400_0-10	000050017
4	7	URBN	76400	76400	4	30-50	35.81201935	9.088051783	4_URBN_76400_30-50	000040021
4	1	FRSD	76400	76400	4	30-50	32.48502731	7.435678731	4_FRSD_76400_30-50	000040013
2	7	URBN	74200	74200	2	10-20	12.04521084	5.78330568	2_URBN_74200_10-20	000020012
2	0	PAST	76400	76400	3	20-30	24.37618256	3.304746103	2_PAST_76400_20-30	000020003
3	1	FRSD	76400	76400	999	50-9999	53.82156372	8.261865257	3_FRSD_76400_50-9999	000030010
3	7	URBN	76400	76400	999	50-9999	53.66599655	1.652373051	3_URBN_76400_50-9999	000030020
5	0	PAST	76400	76400	999	50-9999	54.01256561	0.826186526	5_PAST_76400_50-9999	000050006
5	8	WATR	76400	76400	999	50-9999	50.49010086	0.826186526	5_WATR_76400_50-9999	000050023

SUBBASIN	LU_NUM	LU_CODE	SOIL_NUM	SOIL_CODE	SLOPE_NUM	SLOPE_CODE	MEAN_SLOPE	AREA	UNIQUECOMB	HRUGIS
12	7	URBN	76400	76400	1	0-10	7.315024376	26.43796882	12_URBN_76400_0-10	000120018
12	9	AGRL	76400	76400	3	20-30	25.78922844	5.78330568	12_AGRL_76400_20-30	000120030
12	1	FRSD	76400	76400	3	20-30	24.4957962	85.09721215	12_FRSD_76400_20-30	000120010

12	1	FRSD	76400	76400	2	10-20	14.65969276	112.3613675	12_FRSD_76400_10-20	000120009
13	7	URBN	76400	76400	3	20-30	23.26452827	27.26415535	13_URBN_76400_20-30	000130014
13	7	URBN	76400	76400	2	10-20	14.30097961	48.74500502	13_URBN_76400_10-20	000130015
4	7	URBN	74200	74200	2	10-20	11.31860638	6.609492206	4_URBN_74200_10-20	000040018
5	9	AGRL	76400	76400	4	30-50	34.7933197	6.609492206	5_AGRL_76400_30-50	000050028
12	1	FRSD	76400	76400	4	30-50	37.91930008	62.79017595	12_FRSD_76400_30-50	000120008
13	7	URBN	76400	76400	1	0-10	7.410364628	9.914238308	13_URBN_76400_0-10	000130013
13	1	FRSD	76400	76400	2	10-20	14.6783123	119.7970462	13_FRSD_76400_10-20	000130009
13	1	FRSD	76400	76400	4	30-50	36.15491486	23.95940924	13_FRSD_76400_30-50	000130008
13	7	URBN	76400	76400	4	30-50	38.93674469	6.609492206	13_URBN_76400_30-50	000130016
13	1	FRSD	76400	76400	3	20-30	24.7573967	54.5283107	13_FRSD_76400_20-30	000130007
4	8	WATR	76400	76400	1	0-10	7.306204319	4.130932628	4_WATR_76400_0-10	000040027
4	8	WATR	74200	74200	2	10-20	10.87786865	2.478559577	4_WATR_74200_10-20	000040025
4	0	PAST	74200	74200	2	10-20	11.70821285	5.78330568	4_PAST_74200_10-20	000040004
4	7	URBN	74200	74200	1	0-10	7.224271774	21.48084967	4_URBN_74200_0-10	000040017
4	0	PAST	74200	74200	1	0-10	6.07464838	5.78330568	4_PAST_74200_0-10	000040003
12	7	URBN	76400	76400	4	30-50	38.2656517	12.39279789	12_URBN_76400_30-50	000120016
13	1	FRSD	76400	76400	1	0-10	7.378173351	42.96169934	13_FRSD_76400_0-10	000130010
4	7	URBN	76400	76400	1	0-10	9.74174118	1.652373051	4_URBN_76400_0-10	000040019
12	7	URBN	76400	76400	2	10-20	13.97417927	61.1378029	12_URBN_76400_10-20	000120017
13	7	URBN	76400	76400	999	50-9999	52.46517181	0.826186526	13_URBN_76400_50-9999	000130017
4	1	FRSD	76400	76400	1	0-10	8.489882469	5.78330568	4_FRSD_76400_0-10	000040010
4	8	WATR	74200	74200	1	0-10	7.059341908	9.914238308	4_WATR_74200_0-10	000040026
5	9	AGRL	76400	76400	3	20-30	25.38903236	10.74042483	5_AGRL_76400_20-30	000050027
5	9	AGRL	76400	76400	2	10-20	15.02286816	7.435678731	5_AGRL_76400_10-20	000050029

SUBBASIN	LU_NUM	LU_CODE	SOIL_NUM	SOIL_CODE	SLOPE_NUM	SLOPE_CODE	MEAN_SLOPE	AREA	UNIQUECOMB	HRUGIS
12	1	FRSD	76400	76400	999	50-9999	52.51914597	4.130932628	12_FRSD_76400_50-9999	000120011
13	8	WATR	76400	76400	2	10-20	14.04267979	7.435678731	13_WATR_76400_10-20	000130022
3	8	WATR	76400	76400	2	10-20	16.18530464	10.74042483	3_WATR_76400_10-20	000030029
4	1	FRSD	74200	74200	1	0-10	8.204228401	17.34991704	4_FRSD_74200_0-10	000040009
12	7	URBN	76400	76400	3	20-30	24.72428894	23.95940924	12_URBN_76400_20-30	000120020
3	8	WATR	76400	76400	3	20-30	25.32730103	3.304746103	3_WATR_76400_20-30	000030027
4	1	FRSD	74200	74200	2	10-20	10.30953598	0.826186526	4_FRSD_74200_10-20	000040008
4	7	URBN	73100	73100	1	0-10	4.710899353	56.18068375	4_URBN_73100_0-10	000040016
4	7	URBN	73100	73100	2	10-20	13.28799248	7.435678731	4_URBN_73100_10-20	000040014
4	0	PAST	76400	76400	2	10-20	15.37717438	1.652373051	4_PAST_76400_10-20	000040006
4	8	WATR	76400	76400	2	10-20	16.35502052	10.74042483	4_WATR_76400_10-20	000040029
4	0	PAST	73100	73100	1	0-10	4.321280479	65.26873553	4_PAST_73100_0-10	000040001
4	8	WATR	73100	73100	2	10-20	13.51903343	6.609492206	4_WATR_73100_10-20	000040023
4	0	PAST	73100	73100	2	10-20	12.46844482	13.21898441	4_PAST_73100_10-20	000040002
4	8	WATR	76400	76400	3	20-30	24.3569603	13.21898441	4_WATR_76400_20-30	000040030
12	8	WATR	76400	76400	4	30-50	31.26855659	0.826186526	12_WATR_76400_30-50	000120025
12	7	URBN	76400	76400	999	50-9999	51.31049347	0.826186526	12_URBN_76400_50-9999	000120019
3	8	WATR	76400	76400	4	30-50	36.40677261	1.652373051	3_WATR_76400_30-50	000030028
4	8	WATR	73100	73100	1	0-10	4.217155933	33.04746103	4_WATR_73100_0-10	000040024
4	0	PAST	76400	76400	3	20-30	24.02341652	2.478559577	4_PAST_76400_20-30	000040005
5	9	AGRL	73100	73100	1	0-10	5.473267555	8.261865257	5_AGRL_73100_0-10	000050026



13	9	AGRL	76400	76400	2	10-20	14.41519356	4.957119154	13_AGRL_76400_10-20	000130026
5	7	URBN	73100	73100	1	0-10	6.445450306	134.6684037	5_URBN_73100_0-10	000050012
5	0	PAST	73100	73100	1	0-10	5.577049255	74.35678731	5_PAST_73100_0-10	000050001
5	7	URBN	73100	73100	2	10-20	12.96645164	58.65924332	5_URBN_73100_10-20	000050013
12	1	FRSD	76400	76400	1	0-10	7.537539005	35.5260206	12_FRSD_76400_0-10	000120012
3	1	FRSD	74200	74200	2	10-20	13.23026943	33.87364755	3_FRSD_74200_10-20	000030007
3	8	WATR	74200	74200	2	10-20	11.50294113	8.261865257	3_WATR_74200_10-20	000030026

SUBBASIN	LU_NUM	LU_CODE	SOIL_NUM	SOIL_CODE	SLOPE_NUM	SLOPE_CODE	MEAN_SLOPE	AREA	UNIQUECOMB	HRUGIS
3	1	FRSD	74200	74200	1	0-10	6.428304195	50.39737807	3_FRSD_74200_0-10	000030005
5	8	WATR	73100	73100	2	10-20	12.62694454	9.914238308	5_WATR_73100_10-20	000050018
3	8	WATR	76400	76400	1	0-10	7.083821297	4.130932628	3_WATR_76400_0-10	000030030
3	8	WATR	74200	74200	1	0-10	6.034276485	50.39737807	3_WATR_74200_0-10	000030025
5	0	PAST	73100	73100	2	10-20	12.74878502	15.69754399	5_PAST_73100_10-20	000050002
12	0	PAST	76400	76400	4	30-50	32.20355606	0.826186526	12_PAST_76400_30-50	000120004
3	7	URBN	76400	76400	1	0-10	7.219280243	4.957119154	3_URBN_76400_0-10	000030018
3	0	PAST	74200	74200	1	0-10	6.17919445	20.65466314	3_PAST_74200_0-10	000030002
4	9	AGRL	74200	74200	1	0-10	6.558956623	1.652373051	4_AGRL_74200_0-10	000040033
4	8	WATR	76400	76400	4	30-50	32.48422241	0.826186526	4_WATR_76400_30-50	000040028
10	8	WATR	76400	76400	2	10-20	16.19254875	0.826186526	10_WATR_76400_10-20	000100015
10	7	URBN	76400	76400	1	0-10	6.941777229	0.826186526	10_URBN_76400_0-10	000100011
5	8	WATR	73100	73100	1	0-10	6.766801834	11.56661136	5_WATR_73100_0-10	000050019
12	8	WATR	76400	76400	3	20-30	22.03952789	0.826186526	12_WATR_76400_20-30	000120023
13	8	WATR	76400	76400	3	20-30	20.99176407	0.826186526	13_WATR_76400_20-30	000130021

13	9	AGRL	76400	76400	1	0-10	9.135457993	2.478559577	13_AGRL_76400_0-10	000130025
7	1	FRSD	76400	76400	2	10-20	12.77251339	18.17610357	7_FRSD_76400_10-20	000070007
6	7	URBN	74200	74200	1	0-10	6.159007072	123.1017923	6_URBN_74200_0-10	000060020
6	1	FRSD	74200	74200	2	10-20	14.60021877	56.18068375	6_FRSD_74200_10-20	000060009
6	1	FRSD	74200	74200	1	0-10	5.963002682	66.09492206	6_FRSD_74200_0-10	000060010
3	7	URBN	74200	74200	1	0-10	5.776879787	99.96856961	3_URBN_74200_0-10	000030015
3	7	URBN	74200	74200	2	10-20	12.47356319	5.78330568	3_URBN_74200_10-20	000030016
4	9	AGRL	73100	73100	1	0-10	6.600067616	17.34991704	4_AGRL_73100_0-10	000040031
10	1	FRSD	76400	76400	4	30-50	35.07214355	5.78330568	10_FRSD_76400_30-50	000100005
10	1	FRSD	76400	76400	3	20-30	23.1685791	4.130932628	10_FRSD_76400_20-30	000100006
12	8	WATR	76400	76400	2	10-20	14.33825302	12.39279789	12_WATR_76400_10-20	000120024
6	8	WATR	74200	74200	1	0-10	5.644897938	74.35678731	6_WATR_74200_0-10	000060030
6	7	URBN	74200	74200	2	10-20	13.75133896	71.87822773	6_URBN_74200_10-20	000060021

SUBBASIN	LU_NUM	LU_CODE	SOIL_NUM	SOIL_CODE	SLOPE_NUM	SLOPE_CODE	MEAN_SLOPE	AREA	UNIQUECOMB	HRUGIS
5	9	AGRL	73100	73100	2	10-20	15.75207901	0.826186526	5_AGRL_73100_10-20	000050025
7	1	FRSD	76400	76400	1	0-10	6.136982918	20.65466314	7_FRSD_76400_0-10	000070008
6	8	WATR	74200	74200	2	10-20	13.75041485	28.09034187	6_WATR_74200_10-20	000060029
6	0	PAST	74200	74200	1	0-10	4.288314819	18.17610357	6_PAST_74200_0-10	000060004
6	1	FRSD	74200	74200	3	20-30	22.68525505	18.17610357	6_FRSD_74200_20-30	000060011
4	9	AGRL	76400	76400	3	20-30	25.64400101	0.826186526	4_AGRL_76400_20-30	000040034
10	8	WATR	76400	76400	3	20-30	27.75075722	0.826186526	10_WATR_76400_20-30	000100014
10	7	URBN	76400	76400	4	30-50	32.53860474	1.652373051	10_URBN_76400_30-50	000100010

12	9	AGRL	76400	76400	2	10-20	13.03763962	10.74042483	12_AGRL_76400_10-20	000120029
6	7	URBN	74200	74200	3	20-30	24.02370644	4.130932628	6_URBN_74200_20-30	000060019
3	1	FRSD	74200	74200	3	20-30	20.93107796	2.478559577	3_FRSD_74200_20-30	000030006
3	7	URBN	74200	74200	3	20-30	21.19885826	0.826186526	3_URBN_74200_20-30	000030017
3	9	AGRL	74200	74200	1	0-10	6.072983742	3.304746103	3_AGRL_74200_0-10	000030032
4	9	AGRL	73100	73100	2	10-20	10.55847168	2.478559577	4_AGRL_73100_10-20	000040032
4	7	URBN	73100	73100	3	20-30	20.02439308	0.826186526	4_URBN_73100_20-30	000040015
10	0	PAST	76400	76400	3	20-30	25.08881187	4.130932628	10_PAST_76400_20-30	000100004
12	9	AGRL	76400	76400	4	30-50	30.82079887	0.826186526	12_AGRL_76400_30-50	000120031
12	0	PAST	76400	76400	2	10-20	13.59636688	7.435678731	12_PAST_76400_10-20	000120003
7	7	URBN	76400	76400	2	10-20	12.80693626	6.609492206	7_URBN_76400_10-20	000070012
7	7	URBN	76400	76400	1	0-10	7.184961796	14.87135746	7_URBN_76400_0-10	000070013
6	0	PAST	74200	74200	3	20-30	23.25248337	1.652373051	6_PAST_74200_20-30	000060003
6	8	WATR	74200	74200	3	20-30	21.01058388	2.478559577	6_WATR_74200_20-30	000060031
6	0	PAST	74200	74200	2	10-20	12.50656223	11.56661136	6_PAST_74200_10-20	000060002
10	0	PAST	76400	76400	2	10-20	16.4933548	1.652373051	10_PAST_76400_10-20	000100003
10	7	URBN	76400	76400	3	20-30	20.09510231	0.826186526	10_URBN_76400_20-30	000100009
7	9	AGRL	76400	76400	1	0-10	7.282155991	0.826186526	7_AGRL_76400_0-10	000070020
10	0	PAST	73100	73100	2	10-20	13.42997551	10.74042483	10_PAST_73100_10-20	000100002
10	7	URBN	73100	73100	2	10-20	13.25065136	11.56661136	10_URBN_73100_10-20	000100008
SUBBASIN	LU_NUM	LU_CODE	SOIL_NUM	SOIL_CODE	SLOPE_NUM	SLOPE_CODE	MEAN_SLOPE	AREA	UNIQUECOMB	HRUGIS
13	0	PAST	76400	76400	3	20-30	22.08667374	0.826186526	13_PAST_76400_20-30	000130004
7	7	URBN	74200	74200	2	10-20	12.11643505	53.70212417	7_URBN_74200_10-20	000070010
7	7	URBN	74200	74200	1	0-10	6.325574875	260.2487556	7_URBN_74200_0-10	000070011

4	1	FRSD	73100	73100	73100	1	0-10	2.784600496	0.826186526	4_FRSD_73100_0-10	000040007
8	0	PAST	73100	73100	73100	1	0-10	4.358106136	16.52373051	8_PAST_73100_0-10	000080001
10	0	PAST	73100	73100	73100	1	0-10	4.490996838	87.57577172	10_PAST_73100_0-10	000100001
10	9	AGRL	73100	73100	73100	2	10-20	11.50855732	6.609492206	10_AGRL_73100_10-20	000100017
15	0	PAST	76400	76400	76400	1	0-10	7.340294838	2.478559577	15_PAST_76400_0-10	000150004
15	0	PAST	76400	76400	76400	2	10-20	14.71715641	18.17610357	15_PAST_76400_10-20	000150005
15	7	URBN	76400	76400	76400	2	10-20	15.60087013	40.48313976	15_URBN_76400_10-20	000150016
15	8	WATR	76400	76400	76400	2	10-20	16.25168037	12.39279789	15_WATR_76400_10-20	000150024
15	7	URBN	76400	76400	76400	1	0-10	8.033660889	4.130932628	15_URBN_76400_0-10	000150017
12	7	URBN	74200	74200	74200	2	10-20	12.73715973	36.35220713	12_URBN_74200_10-20	000120015
12	9	AGRL	76400	76400	76400	1	0-10	8.572976112	4.130932628	12_AGRL_76400_0-10	000120032
12	8	WATR	76400	76400	76400	1	0-10	8.19178009	11.566661136	12_WATR_76400_0-10	000120026
13	7	URBN	74200	74200	74200	2	10-20	12.94087982	38.00458018	13_URBN_74200_10-20	000130011
3	0	PAST	74200	74200	74200	2	10-20	14.28922081	3.304746103	3_PAST_74200_10-20	000030003
3	0	PAST	73100	73100	73100	1	0-10	4.738981724	28.9165284	3_PAST_73100_0-10	000030001
8	9	AGRL	73100	73100	73100	1	0-10	4.889980316	5.78330568	8_AGRL_73100_0-10	000080007
8	7	URBN	73100	73100	73100	1	0-10	4.290745735	58.65924332	8_URBN_73100_0-10	000080003
15	0	PAST	76400	76400	76400	3	20-30	25.16662788	25.6117823	15_PAST_76400_20-30	000150006
12	8	WATR	74200	74200	74200	2	10-20	12.47626495	28.9165284	12_WATR_74200_10-20	000120022
12	1	FRSD	74200	74200	74200	2	10-20	12.9887495	23.13322272	12_FRSD_74200_10-20	000120007
13	1	FRSD	74200	74200	74200	2	10-20	13.84435368	8.261865257	13_FRSD_74200_10-20	000130005
13	7	URBN	74200	74200	74200	1	0-10	6.613930702	154.4968803	13_URBN_74200_0-10	000130012
7	8	WATR	76400	76400	76400	1	0-10	9.723148346	1.652373051	7_WATR_76400_0-10	000070017
7	0	PAST	74200	74200	74200	1	0-10	6.276529312	137.1469633	7_PAST_74200_0-10	000070002

3	7	URBN	73100	73100	1	0-10	5.452144146	57.00687027	3_URBN_73100_0-10	000030013
---	---	------	-------	-------	---	------	-------------	-------------	-------------------	-----------

SUBBASIN	LU_NUM	LU_CODE	SOIL_NUM	SOIL_CODE	SLOPE_NUM	SLOPE_CODE	MEAN_SLOPE	AREA	UNIQUECOMB	HRUGIS
10	9	AGRL	73100	73100	1	0-10	5.855266571	16.52373051	10_AGRL_73100_0-10	000100016
10	7	URBN	73100	73100	1	0-10	5.070593834	101.6209427	10_URBN_73100_0-10	000100007
15	9	AGRL	76400	76400	3	20-30	25.08268929	8.261865257	15_AGRL_76400_20-30	000150030
15	7	URBN	76400	76400	3	20-30	23.9320755	52.04975112	15_URBN_76400_20-30	000150015
12	0	PAST	74200	74200	2	10-20	11.83616543	14.04517094	12_PAST_74200_10-20	000120001
12	7	URBN	74200	74200	1	0-10	5.250293732	299.0795223	12_URBN_74200_0-10	000120013
13	8	WATR	74200	74200	3	20-30	20.36063194	0.826186526	13_WATR_74200_20-30	000130019
13	8	WATR	74200	74200	2	10-20	13.00876904	33.87364755	13_WATR_74200_10-20	000130020
13	1	FRSD	74200	74200	1	0-10	7.045173645	3.304746103	13_FRSD_74200_0-10	000130006
7	0	PAST	74200	74200	2	10-20	12.62316322	15.69754399	7_PAST_74200_10-20	000070003
7	1	FRSD	74200	74200	1	0-10	7.009054184	52.87593764	7_FRSD_74200_0-10	000070006
3	8	WATR	73100	73100	2	10-20	11.58666039	3.304746103	3_WATR_73100_10-20	000030023
3	1	FRSD	73100	73100	1	0-10	5.390263081	4.957119154	3_FRSD_73100_0-10	000030004
15	9	AGRL	76400	76400	4	30-50	32.17316055	1.652373051	15_AGRL_76400_30-50	000150032
15	1	FRSD	76400	76400	4	30-50	42.17801666	4.130932628	15_FRSD_76400_30-50	000150010
15	7	URBN	76400	76400	4	30-50	36.76099396	57.8330568	15_URBN_76400_30-50	000150018
12	8	WATR	74200	74200	1	0-10	5.278337955	185.0657818	12_WATR_74200_0-10	000120021
12	0	PAST	76400	76400	1	0-10	7.436666012	2.478559577	12_PAST_76400_0-10	000120005
7	9	AGRL	74200	74200	1	0-10	6.354238987	69.39966816	7_AGRL_74200_0-10	000070018
6	9	AGRL	74200	74200	1	0-10	6.226631641	4.130932628	6_AGRL_74200_0-10	000060038
6	9	AGRL	74200	74200	2	10-20	15.3061552	2.478559577	6_AGRL_74200_10-20	000060037

3	7	URBN	73100	73100	2	10-20	12.01507759	5.78330568	3_URBN_73100_10-20	000030014
15	8	WATR	76400	76400	1	0-10	5.116099834	0.826186526	15_WATR_76400_0-10	000150026
15	8	WATR	76400	76400	4	30-50	36.22229767	10.74042483	15_WATR_76400_30-50	000150027
12	9	AGRL	74200	74200	1	0-10	5.037649155	29.74271492	12_AGRL_74200_0-10	000120027
12	1	FRSD	74200	74200	1	0-10	7.490503311	24.78559577	12_FRSD_74200_0-10	000120006
7	8	WATR	74200	74200	2	10-20	11.85225105	31.39508798	7_WATR_74200_10-20	000070015
7	1	FRSD	74200	74200	2	10-20	12.2441082	23.95940924	7_FRSD_74200_10-20	000070004

SUBBASIN	LU_NUM	LU_CODE	SOIL_NUM	SOIL_CODE	SLOPE_NUM	SLOPE_CODE	MEAN_SLOPE	AREA	UNIQUECOMB	HRUGIS
7	8	WATR	74200	74200	1	0-10	5.913402081	122.2756058	7_WATR_74200_0-10	000070016
8	8	WATR	73100	73100	1	0-10	3.998637676	24.78559577	8_WATR_73100_0-10	000080006
10	8	WATR	73100	73100	1	0-10	3.424379587	14.04517094	10_WATR_73100_0-10	000100013
15	0	PAST	76400	76400	4	30-50	33.59246063	9.088051783	15_PAST_76400_30-50	000150007
15	7	URBN	76400	76400	999	50-9999	50.57543182	0.826186526	15_URBN_76400_50-9999	000150019
12	0	PAST	74200	74200	1	0-10	5.547374725	85.09721215	12_PAST_74200_0-10	000120002
13	8	WATR	74200	74200	1	0-10	6.421627522	87.57577172	13_WATR_74200_0-10	000130018
7	9	AGRL	74200	74200	2	10-20	12.05522537	4.957119154	7_AGRL_74200_10-20	000070019
3	8	WATR	73100	73100	1	0-10	7.049059868	5.78330568	3_WATR_73100_0-10	000030024
3	9	AGRL	73100	73100	1	0-10	4.187679291	23.13322272	3_AGRL_73100_0-10	000030031
15	8	WATR	76400	76400	3	20-30	25.55091667	5.78330568	15_WATR_76400_20-30	000150025
13	0	PAST	74200	74200	2	10-20	12.06483841	7.435678731	13_PAST_74200_10-20	000130002
7	1	FRSD	74200	74200	3	20-30	20.57959366	0.826186526	7_FRSD_74200_20-30	000070005
15	9	AGRL	76400	76400	2	10-20	14.96061325	3.304746103	15_AGRL_76400_10-20	000150031
12	9	AGRL	74200	74200	2	10-20	11.04788971	3.304746103	12_AGRL_74200_10-20	000120028

13	0	PAST	74200	74200	74200	1	0-10	6.184608936	29.74271492	13_PAST_74200_0-10	000130001
11	0	PAST	73100	73100	73100	1	0-10	2.904619455	52.04975112	11_PAST_73100_0-10	000110001
11	0	PAST	76400	76400	76400	1	0-10	9.393843651	0.826186526	11_PAST_76400_0-10	000110006
11	7	URBN	76400	76400	76400	2	10-20	15.80116272	5.78330568	11_URBN_76400_10-20	000110010
11	7	URBN	76400	76400	76400	3	20-30	23.55706787	5.78330568	11_URBN_76400_20-30	000110009
11	0	PAST	76400	76400	76400	3	20-30	25.20258904	4.957119154	11_PAST_76400_20-30	000110005
11	0	PAST	76400	76400	76400	4	30-50	35.43951035	0.826186526	11_PAST_76400_30-50	000110004
11	7	URBN	73100	73100	73100	1	0-10	4.975299358	105.7518753	11_URBN_73100_0-10	000110007
11	8	WATR	73100	73100	73100	2	10-20	11.26634502	2.478559577	11_WATR_73100_10-20	000110013
11	0	PAST	76400	76400	76400	2	10-20	14.52303028	3.304746103	11_PAST_76400_10-20	000110003
11	8	WATR	76400	76400	76400	3	20-30	21.29013252	1.652373051	11_WATR_76400_20-30	000110017
11	9	AGRL	76400	76400	76400	3	20-30	29.58537102	0.826186526	11_AGRL_76400_20-30	000110021
11	7	URBN	76400	76400	76400	4	30-50	35.59127426	0.826186526	11_URBN_76400_30-50	000110012

SUBBASIN	LU_NUM	LU_CODE	SOIL_NUM	SOIL_CODE	SLOPE_NUM	SLOPE_CODE	MEAN_SLOPE	AREA	UNIQUECOMB	HRUGIS
15	1	FRSD	76400	76400	3	20-30	25.36444473	0.826186526	15_FRSD_76400_20-30	000150009
13	0	PAST	74200	74200	3	20-30	21.40571594	0.826186526	13_PAST_74200_20-30	000130003
11	7	URBN	76400	76400	1	0-10	9.811326027	1.652373051	11_URBN_76400_0-10	000110011
12	7	URBN	74200	74200	3	20-30	21.73537636	0.826186526	12_URBN_74200_20-30	000120014
8	1	FRSD	73100	73100	1	0-10	2.729726076	0.826186526	8_FRSD_73100_0-10	000080002
11	7	URBN	73100	73100	2	10-20	13.13968754	9.088051783	11_URBN_73100_10-20	000110008
11	8	WATR	76400	76400	1	0-10	9.77274704	0.826186526	11_WATR_76400_0-10	000110018
11	9	AGRL	76400	76400	2	10-20	11.50752735	0.826186526	11_AGRL_76400_10-20	000110020
9	9	AGRL	73100	73100	1	0-10	5.424289703	15.69754399	9_AGRL_73100_0-10	000090018



9	0	PAST	73100	73100	1	0-10	5.09322691	67.74729511	9_PAST_73100_0-10	000090001
11	8	WATR	76400	76400	2	10-20	14.50005436	1.652373051	11_WATR_76400_10-20	000110016
15	7	URBN	73100	73100	3	20-30	26.53990364	3.304746103	15_URBN_73100_20-30	000150012
15	8	WATR	73100	73100	3	20-30	23.274086	0.826186526	15_WATR_73100_20-30	000150022
11	0	PAST	73100	73100	2	10-20	14.01819706	3.304746103	11_PAST_73100_10-20	000110002
15	7	URBN	73100	73100	2	10-20	12.96882915	38.83076671	15_URBN_73100_10-20	000150014
15	0	PAST	73100	73100	2	10-20	13.49127483	14.04517094	15_PAST_73100_10-20	000150002
9	7	URBN	74200	74200	1	0-10	6.25428915	42.13551281	9_URBN_74200_0-10	000090010
9	7	URBN	73100	73100	1	0-10	6.079500675	143.7564555	9_URBN_73100_0-10	000090008
11	8	WATR	73100	73100	1	0-10	4.703540325	4.957119154	11_WATR_73100_0-10	000110014
11	8	WATR	73100	73100	3	20-30	20.38383865	0.826186526	11_WATR_73100_20-30	000110015
15	9	AGRL	73100	73100	2	10-20	12.72846317	2.478559577	15_AGRL_73100_10-20	000150029
15	7	URBN	73100	73100	1	0-10	4.368513584	470.1001331	15_URBN_73100_0-10	000150013
13	9	AGRL	74200	74200	1	0-10	6.149064541	20.65466314	13_AGRL_74200_0-10	000130023
9	8	WATR	74200	74200	1	0-10	6.441800117	46.26644544	9_WATR_74200_0-10	000090015
9	0	PAST	73100	73100	2	10-20	11.19424248	15.69754399	9_PAST_73100_10-20	000090002
11	9	AGRL	73100	73100	1	0-10	3.853217363	4.130932628	11_AGRL_73100_0-10	000110019
15	0	PAST	73100	73100	1	0-10	3.939149618	345.3459677	15_PAST_73100_0-10	000150003
9	7	URBN	74200	74200	2	10-20	13.00621033	12.39279789	9_URBN_74200_10-20	000090012

SUBBASIN	LU_NUM	LU_CODE	SOIL_NUM	SOIL_CODE	SLOPE_NUM	SLOPE_CODE	MEAN_SLOPE	AREA	UNIQUECOMB	HRUGIS
9	7	URBN	73100	73100	2	10-20	11.59835339	31.39508798	9_URBN_73100_10-20	000090009
8	7	URBN	73100	73100	2	10-20	11.46603394	3.304746103	8_URBN_73100_10-20	000080004

8	8	WATR	73100	73100	2	10-20	13.36824226	3.304746103	8_WATR_73100_10-20	000080005
15	9	AGRL	73100	73100	1	0-10	3.358319759	131.3636576	15_AGRL_73100_0-10	000150028
9	0	PAST	74200	74200	1	0-10	5.802567959	19.00229009	9_PAST_74200_0-10	000090004
9	8	WATR	74200	74200	2	10-20	13.24768829	23.13322272	9_WATR_74200_10-20	000090017
9	1	FRSD	73100	73100	1	0-10	6.411670208	2.478559577	9_FRSD_73100_0-10	000090005
15	8	WATR	73100	73100	2	10-20	17.41085625	1.652373051	15_WATR_73100_10-20	000150023
15	8	WATR	73100	73100	1	0-10	4.078407288	107.4042483	15_WATR_73100_0-10	000150021
6	8	WATR	73100	73100	1	0-10	5.614761353	3.304746103	6_WATR_73100_0-10	000060027
8	9	AGRL	73100	73100	2	10-20	12.38000107	0.826186526	8_AGRL_73100_10-20	000080008
6	7	URBN	73100	73100	1	0-10	6.473570347	2.478559577	6_URBN_73100_0-10	000060017
6	7	URBN	73100	73100	2	10-20	10.73171425	1.652373051	6_URBN_73100_10-20	000060018
9	9	AGRL	74200	74200	1	0-10	6.402322769	37.17839366	9_AGRL_74200_0-10	000090020
9	9	AGRL	74200	74200	2	10-20	11.27279758	12.39279789	9_AGRL_74200_10-20	000090021
9	8	WATR	73100	73100	1	0-10	5.761154175	76.83534689	9_WATR_73100_0-10	000090014
9	8	WATR	73100	73100	2	10-20	11.25201988	12.39279789	9_WATR_73100_10-20	000090013
7	8	WATR	73100	73100	1	0-10	6.083657265	3.304746103	7_WATR_73100_0-10	000070014
6	8	WATR	73100	73100	2	10-20	10.68074703	0.826186526	6_WATR_73100_10-20	000060028
9	0	PAST	74200	74200	2	10-20	11.98512745	2.478559577	9_PAST_74200_10-20	000090003
6	0	PAST	73100	73100	1	0-10	6.594091415	1.652373051	6_PAST_73100_0-10	000060001
7	7	URBN	73100	73100	1	0-10	6.183091164	4.130932628	7_URBN_73100_0-10	000070009
7	0	PAST	73100	73100	1	0-10	5.735423565	2.478559577	7_PAST_73100_0-10	000070001
9	8	WATR	74200	74200	3	20-30	21.5128212	1.652373051	9_WATR_74200_20-30	000090016
9	1	FRSD	74200	74200	3	20-30	23.10454941	1.652373051	9_FRSD_74200_20-30	000090007
9	7	URBN	74200	74200	3	20-30	23.25132179	0.826186526	9_URBN_74200_20-30	000090011
9	9	AGRL	73100	73100	2	10-20	12.08835411	1.652373051	9_AGRL_73100_10-20	000090019

9	1	FRSD	74200	74200	2	10-20	17.88627052	0.826186526	9_FRSD_74200_10-20	000090006
---	---	------	-------	-------	---	-------	-------------	-------------	--------------------	-----------

SUBBASIN	LU_NUM	LU_CODE	SOIL_NUM	SOIL_CODE	SLOPE_NUM	SLOPE_CODE	MEAN_SLOPE	AREA	UNIQUECOMB	HRUGIS
13	9	AGRL	74200	74200	2	10-20	10.47333431	0.826186526	13_AGRL_74200_10-20	000130024
17	7	URBN	74200	74200	1	0-10	5.395232201	191.675274	17_URBN_74200_0-10	000170008
17	0	PAST	74200	74200	1	0-10	5.580621243	109.8828079	17_PAST_74200_0-10	000170002
17	8	WATR	74200	74200	1	0-10	5.161157608	79.31390647	17_WATR_74200_0-10	000170012
10	8	WATR	73100	73100	2	10-20	14.00426579	0.826186526	10_WATR_73100_10-20	000100012
16	1	FRSD	74200	74200	1	0-10	6.251170158	3.304746103	16_FRSD_74200_0-10	000160006
14	7	URBN	73100	73100	2	10-20	11.91293049	4.957119154	14_URBN_73100_10-20	000140004
14	0	PAST	73100	73100	1	0-10	4.597045898	247.0297712	14_PAST_73100_0-10	000140001
14	7	URBN	73100	73100	1	0-10	4.440386295	356.9125791	14_URBN_73100_0-10	000140005
16	1	FRSD	74200	74200	2	10-20	13.38871574	2.478559577	16_FRSD_74200_10-20	000160005
16	8	WATR	74200	74200	2	10-20	12.67965984	17.34991704	16_WATR_74200_10-20	000160014
16	7	URBN	74200	74200	1	0-10	5.941447258	215.6346832	16_URBN_74200_0-10	000160009
17	8	WATR	74200	74200	2	10-20	10.45526123	0.826186526	17_WATR_74200_10-20	000170011
14	8	WATR	73100	73100	1	0-10	4.370391369	40.48313976	14_WATR_73100_0-10	000140006
16	7	URBN	74200	74200	2	10-20	11.21445847	9.088051783	16_URBN_74200_10-20	000160010
17	1	FRSD	74200	74200	1	0-10	4.760839462	10.74042483	17_FRSD_74200_0-10	000170005
17	9	AGRL	74200	74200	1	0-10	6.232929707	37.17839366	17_AGRL_74200_0-10	000170015
16	0	PAST	74200	74200	2	10-20	11.85914135	9.914238308	16_PAST_74200_10-20	000160003
16	0	PAST	74200	74200	1	0-10	5.41710186	221.4179889	16_PAST_74200_0-10	000160004
16	9	AGRL	74200	74200	1	0-10	5.145849705	14.04517094	16_AGRL_74200_0-10	000160017
16	8	WATR	74200	74200	1	0-10	5.522319794	154.4968803	16_WATR_74200_0-10	000160015

14	9	AGRL	73100	73100	73100	1	0-10	4.477087498	174.3253569	14_AGRL_73100_0-10	000140007
14	0	PAST	73100	73100	73100	2	10-20	10.4445858	1.652373051	14_PAST_73100_10-20	000140002
17	7	URBN	74200	74200	74200	2	10-20	13.4914856	1.652373051	17_URBN_74200_10-20	000170009
15	1	FRSD	73100	73100	73100	1	0-10	3.745824337	8.261865257	15_FRSD_73100_0-10	000150008
14	1	FRSD	73100	73100	73100	1	0-10	7.412657261	2.478559577	14_FRSD_73100_0-10	000140003
18	7	URBN	74200	74200	74200	1	0-10	6.052785873	5.78330568	18_URBN_74200_0-10	000180007
18	0	PAST	73100	73100	73100	1	0-10	4.272297382	326.3436776	18_PAST_73100_0-10	000180001

SUBBASIN	LU_NUM	LU_CODE	SOIL_NUM	SOIL_CODE	SLOPE_NUM	SLOPE_CODE	MEAN_SLOPE	AREA	UNIQUECOMB	HRUGIS
18	8	WATR	73100	73100	1	0-10	4.294044018	71.05204121	18_WATR_73100_0-10	000180010
18	9	AGRL	73100	73100	1	0-10	4.331044674	197.4585796	18_AGRL_73100_0-10	000180012
18	7	URBN	73100	73100	1	0-10	4.37850523	324.6913046	18_URBN_73100_0-10	000180005
18	9	AGRL	74200	74200	1	0-10	7.319918156	5.78330568	18_AGRL_74200_0-10	000180014
18	9	AGRL	74200	74200	2	10-20	11.59952736	4.130932628	18_AGRL_74200_10-20	000180015
18	9	AGRL	73100	73100	2	10-20	11.06601524	5.78330568	18_AGRL_73100_10-20	000180013
17	9	AGRL	74200	74200	2	10-20	13.34504509	3.304746103	17_AGRL_74200_10-20	000170014
17	0	PAST	74200	74200	2	10-20	11.62513733	3.304746103	17_PAST_74200_10-20	000170003
20	0	PAST	73100	73100	1	0-10	4.351595879	719.6084639	20_PAST_73100_0-10	000200004
20	9	AGRL	73100	73100	1	0-10	4.55146265	127.232725	20_AGRL_73100_0-10	000200019
20	7	URBN	73100	73100	1	0-10	4.43090868	556.8497183	20_URBN_73100_0-10	000200009
21	7	URBN	74200	74200	1	0-10	7.988515854	5.78330568	21_URBN_74200_0-10	000210009
18	8	WATR	74200	74200	2	10-20	13.48833942	0.826186526	18_WATR_74200_10-20	000180011
18	7	URBN	74200	74200	2	10-20	10.3587389	1.652373051	18_URBN_74200_10-20	000180008
21	0	PAST	74200	74200	2	10-20	12.73425007	4.130932628	21_PAST_74200_10-20	000210003

21	1	FRSD	74200	74200	74200	2	10-20	19.7495594	0.826186526	21_FRSD_74200_10-20	000210006
21	0	PAST	74200	74200	74200	3	20-30	23.29534149	1.652373051	21_PAST_74200_20-30	000210004
21	9	AGRL	74200	74200	74200	2	10-20	13.87806034	1.652373051	21_AGRL_74200_10-20	000210018
18	0	PAST	74200	74200	74200	1	0-10	7.806447029	1.652373051	18_PAST_74200_0-10	000180003
20	8	WATR	73100	73100	73100	1	0-10	4.56362772	235.4631598	20_WATR_73100_0-10	000200015
17	7	URBN	73100	73100	73100	1	0-10	4.24554491	69.39966816	17_URBN_73100_0-10	000170007
17	0	PAST	73100	73100	73100	1	0-10	4.07757835	26.43796882	17_PAST_73100_0-10	000170001
17	8	WATR	73100	73100	73100	1	0-10	4.017542362	44.61407239	17_WATR_73100_0-10	000170010
21	7	URBN	74200	74200	74200	2	10-20	14.75542164	2.478559577	21_URBN_74200_10-20	000210010
21	8	WATR	74200	74200	74200	3	20-30	20.96628189	1.652373051	21_WATR_74200_20-30	000210013
21	8	WATR	74200	74200	74200	2	10-20	16.28697205	1.652373051	21_WATR_74200_10-20	000210015
21	0	PAST	73100	73100	73100	2	10-20	13.1674757	5.78330568	21_PAST_73100_10-20	000210001
21	9	AGRL	73100	73100	73100	2	10-20	11.48910522	3.304746103	21_AGRL_73100_10-20	000210016

SUBBASIN	LU_NUM	LU_CODE	SOIL_NUM	SOIL_CODE	SLOPE_NUM	SLOPE_CODE	MEAN_SLOPE	AREA	UNIQUECOMB	HRUGIS
21	7	URBN	73100	73100	2	10-20	11.96339512	7.435678731	21_URBN_73100_10-20	000210007
15	7	URBN	63100	63100	1	0-10	4.327886581	25.6117823	15_URBN_63100_0-10	000150011
15	0	PAST	63100	63100	1	0-10	4.756542683	18.17610357	15_PAST_63100_0-10	000150001
17	9	AGRL	73100	73100	1	0-10	2.174407721	0.826186526	17_AGRL_73100_0-10	000170013
21	0	PAST	73100	73100	1	0-10	3.761469126	113.187554	21_PAST_73100_0-10	000210002
21	9	AGRL	73100	73100	1	0-10	3.853456259	57.00687027	21_AGRL_73100_0-10	000210017
15	8	WATR	63100	63100	1	0-10	4.484158993	4.130932628	15_WATR_63100_0-10	000150020
21	8	WATR	74200	74200	1	0-10	5.4062953	1.652373051	21_WATR_74200_0-10	000210014
21	7	URBN	73100	73100	1	0-10	3.335642576	238.7679059	21_URBN_73100_0-10	000210008

20	0	PAST	73100	73100	2	10-20	11.28048229	10.74042483	20_PAST_73100_10-20	000200003
20	7	URBN	73100	73100	2	10-20	12.17825413	10.74042483	20_URBN_73100_10-20	000200010
23	0	PAST	63100	63100	1	0-10	4.088802338	880.7148364	23_PAST_63100_0-10	000230002
17	1	FRSD	73100	73100	1	0-10	3.540690422	1.652373051	17_FRSD_73100_0-10	000170004
21	0	PAST	74200	74200	1	0-10	7.235257626	0.826186526	21_PAST_74200_0-10	000210005
23	8	WATR	63100	63100	1	0-10	4.179887772	384.1767344	23_WATR_63100_0-10	000230007
21	8	WATR	73100	73100	1	0-10	3.970623255	28.09034187	21_WATR_73100_0-10	000210012
23	7	URBN	63100	63100	1	0-10	4.03524828	420.5289416	23_URBN_63100_0-10	000230006
21	8	WATR	73100	73100	2	10-20	11.55345249	0.826186526	21_WATR_73100_10-20	000210011
16	8	WATR	73100	73100	1	0-10	5.497669697	57.8330568	16_WATR_73100_0-10	000160011
20	9	AGRL	73100	73100	2	10-20	10.63926697	1.652373051	20_AGRL_73100_10-20	000200018
16	0	PAST	73100	73100	1	0-10	5.258874893	69.39966816	16_PAST_73100_0-10	000160001
16	7	URBN	73100	73100	1	0-10	6.384429455	70.22585468	16_URBN_73100_0-10	000160007
20	8	WATR	73100	73100	2	10-20	11.48289871	11.56661136	20_WATR_73100_10-20	000200014
23	1	FRSD	63100	63100	1	0-10	6.840231419	0.826186526	23_FRSD_63100_0-10	000230004
20	9	AGRL	63100	63100	1	0-10	5.654926777	41.30932628	20_AGRL_63100_0-10	000200016
20	8	WATR	63100	63100	1	0-10	4.772564888	73.53060079	20_WATR_63100_0-10	000200011
23	8	WATR	73100	73100	1	0-10	3.721534014	4.130932628	23_WATR_73100_0-10	000230009
18	1	FRSD	73100	73100	1	0-10	6.657605648	8.261865257	18_FRSD_73100_0-10	000180004
SUBBASIN	LU_NUM	LU_CODE	SOIL_NUM	SOIL_CODE	SLOPE_NUM	SLOPE_CODE	MEAN_SLOPE	AREA	UNIQUECOMB	HRUGIS
20	0	PAST	63100	63100	1	0-10	4.78449297	95.83763698	20_PAST_63100_0-10	000200001
20	7	URBN	63100	63100	1	0-10	4.930670738	97.49001003	20_URBN_63100_0-10	000200007
16	8	WATR	73100	73100	2	10-20	13.38708305	9.088051783	16_WATR_73100_10-20	000160012

16	0	PAST	73100	73100	2	10-20	12.8063488	4.957119154	16_PAST_73100_10-20	000160002
20	1	FRSD	73100	73100	1	0-10	3.431736708	3.304746103	20_FRSD_73100_0-10	000200006
20	0	PAST	63100	63100	2	10-20	12.23087978	4.130932628	20_PAST_63100_10-20	000200002
23	0	PAST	73100	73100	1	0-10	4.332868099	1.652373051	23_PAST_73100_0-10	000230003
16	7	URBN	73100	73100	2	10-20	12.72063446	14.04517094	16_URBN_73100_10-20	000160008
20	8	WATR	63100	63100	3	20-30	23.4160881	5.78330568	20_WATR_63100_20-30	000200012
20	7	URBN	63100	63100	2	10-20	11.68840027	5.78330568	20_URBN_63100_10-20	000200008
23	8	WATR	63100	63100	2	10-20	11.27189159	4.957119154	23_WATR_63100_10-20	000230008
17	7	URBN	73100	73100	2	10-20	11.07027626	0.826186526	17_URBN_73100_10-20	000170006
25	0	PAST	73100	73100	1	0-10	5.185009956	358.5649521	25_PAST_73100_0-10	000250003
25	7	URBN	73100	73100	1	0-10	4.863267422	194.9800201	25_URBN_73100_0-10	000250006
20	9	AGRL	63100	63100	2	10-20	12.12106133	2.478559577	20_AGRL_63100_10-20	000200017
23	9	AGRL	63100	63100	1	0-10	4.383247852	57.8330568	23_AGRL_63100_0-10	000230010
25	8	WATR	73100	73100	1	0-10	5.499306202	216.4608697	25_WATR_73100_0-10	000250009
23	7	URBN	63100	63100	2	10-20	13.05037498	16.52373051	23_URBN_63100_10-20	000230005
25	8	WATR	73100	73100	2	10-20	12.0798502	15.69754399	25_WATR_73100_10-20	000250008
20	8	WATR	63100	63100	2	10-20	11.58944225	5.78330568	20_WATR_63100_10-20	000200013
23	0	PAST	63100	63100	2	10-20	11.32360363	14.87135746	23_PAST_63100_10-20	000230001
18	7	URBN	73100	73100	2	10-20	11.14765072	4.130932628	18_URBN_73100_10-20	000180006
23	9	AGRL	63100	63100	2	10-20	11.34625816	1.652373051	23_AGRL_63100_10-20	000230011
18	8	WATR	73100	73100	2	10-20	12.44703579	0.826186526	18_WATR_73100_10-20	000180009
16	9	AGRL	73100	73100	1	0-10	4.562345505	2.478559577	16_AGRL_73100_0-10	000160016



22	9	AGRL	73100	73100	73100	1	0-10	4.185602665	62.79017595	22_AGRL_73100_0-10	000220014
18	0	PAST	73100	73100	73100	2	10-20	11.24986649	3.304746103	18_PAST_73100_10-20	000180002
22	0	PAST	73100	73100	73100	1	0-10	4.154452801	185.0657818	22_PAST_73100_0-10	000220004

SUBBASIN	LU_NUM	LU_CODE	SOIL_NUM	SOIL_CODE	SLOPE_NUM	SLOPE_CODE	MEAN_SLOPE	AREA	UNIQUECOMB	HRUGIS
25	0	PAST	73100	73100	2	10-20	11.72938442	28.09034187	25_PAST_73100_10-20	000250002
25	7	URBN	73100	73100	2	10-20	11.14050293	12.39279789	25_URBN_73100_10-20	000250007
22	7	URBN	73100	73100	1	0-10	4.173524857	181.7610357	22_URBN_73100_0-10	000220008
16	8	WATR	74200	74200	3	20-30	20.81079674	0.826186526	16_WATR_74200_20-30	000160013
25	9	AGRL	73100	73100	1	0-10	5.703619003	4.957119154	25_AGRL_73100_0-10	000250010
22	8	WATR	73100	73100	1	0-10	4.464113235	89.22814477	22_WATR_73100_0-10	000220011
25	1	FRSD	73100	73100	1	0-10	5.658372879	5.78330568	25_FRSD_73100_0-10	000250005
22	1	FRSD	73100	73100	1	0-10	3.595410347	1.652373051	22_FRSD_73100_0-10	000220005
20	1	FRSD	63100	63100	1	0-10	2.70201993	1.652373051	20_FRSD_63100_0-10	000200005
22	7	URBN	73100	73100	2	10-20	11.81997967	15.69754399	22_URBN_73100_10-20	000220009
22	8	WATR	73100	73100	2	10-20	12.58462715	10.74042483	22_WATR_73100_10-20	000220012
19	7	URBN	73100	73100	1	0-10	3.361471891	5.78330568	19_URBN_73100_0-10	000190002
19	0	PAST	73100	73100	1	0-10	2.980882168	2.478559577	19_PAST_73100_0-10	000190001
19	8	WATR	73100	73100	1	0-10	2.507208347	3.304746103	19_WATR_73100_0-10	000190003
22	0	PAST	73100	73100	2	10-20	11.0212574	9.088051783	22_PAST_73100_10-20	000220003
24	7	URBN	73100	73100	1	0-10	3.240068913	235.4631598	24_URBN_73100_0-10	000240004
24	9	AGRL	73100	73100	1	0-10	3.261425018	57.8330568	24_AGRL_73100_0-10	000240007
24	8	WATR	73100	73100	1	0-10	3.055503607	38.00458018	24_WATR_73100_0-10	000240006

24	0	PAST	73100	73100	73100	1	0-10	3.00006628	169.3682378	24_PAST_73100_0-10	000240002
22	9	AGRL	73100	73100	73100	2	10-20	10.77873421	2.478559577	22_AGRL_73100_10-20	000220015
22	8	WATR	63100	63100	63100	1	0-10	8.342769623	3.304746103	22_WATR_63100_0-10	000220010
22	0	PAST	63100	63100	63100	1	0-10	8.122470856	1.652373051	22_PAST_63100_0-10	000220002
22	7	URBN	63100	63100	63100	1	0-10	7.662526131	1.652373051	22_URBN_63100_0-10	000220007
22	0	PAST	63100	63100	63100	2	10-20	14.57079601	5.78330568	22_PAST_63100_10-20	000220001
22	7	URBN	63100	63100	63100	2	10-20	16.52616501	5.78330568	22_URBN_63100_10-20	000220006
25	0	PAST	74200	74200	74200	2	10-20	18.68342781	1.652373051	25_PAST_74200_10-20	000250004
22	8	WATR	74200	74200	74200	2	10-20	19.53097343	0.826186526	22_WATR_74200_10-20	000220013
24	8	WATR	63100	63100	63100	1	0-10	4.747982025	0.826186526	24_WATR_63100_0-10	000240005

SUBBASIN	LU_NUM	LU_CODE	SOIL_NUM	SOIL_CODE	SLOPE_NUM	SLOPE_CODE	MEAN_SLOPE	AREA	UNIQUECOMB	HRUGIS
24	7	URBN	63100	63100	1	0-10	5.897895336	2.478559577	24_URBN_63100_0-10	000240003
25	0	PAST	73100	73100	3	20-30	21.2336216	0.826186526	25_PAST_73100_20-30	000250001
24	0	PAST	63100	63100	1	0-10	9.529761314	0.826186526	24_PAST_63100_0-10	000240001

## Appendix 2: Climate/ ETO data for selected stations in the catchment

***** Cropwat 4 windows ver 4.3 Climate and ETo (grass) Data *****						
Country : South Africa		Station : Levubu				
Altitude: 610 meter(s) above M.S.L.		Longitude: 30.28 Deg. (East)				
Latitude: -23.08 Deg. (South)						
Month	MaxTemp (deg.C)	MinTemp (deg.C)	Humidity (%)	wind Spd. (km/d)	Sunshine (Hours)	Solar Rad. (MJ/m2/d)
January	28.4	18.6	65.6	88.8	5.4	19.2
February	27.4	18.4	64.2	79.8	5.0	17.9
March	26.7	17.4	63.9	73.2	5.1	16.5
April	25.6	15.2	62.4	71.6	5.5	14.8
May	24.2	12.4	57.8	81.1	6.1	13.2
June	21.9	9.8	53.8	95.6	5.9	11.8
July	22.1	9.6	53.6	100.0	6.1	12.5
August	23.6	11.2	52.4	105.0	6.0	14.4
September	26.0	13.7	53.0	115.0	5.8	16.5
October	26.3	15.4	58.3	118.5	5.2	17.5
November	27.0	16.7	61.6	103.4	5.2	18.6
December	27.8	18.0	63.3	96.3	5.1	18.8
Average	25.6	14.7	59.2	94.0	5.5	16.0
-----						
Pen-Mon equation was used in ETo calculations with the following values for Angstrom's Coefficients: a = 0.25      b = 0.5						
*****						

***** Cropwat 4 windows ver 4.3 climate and Eto (grass) Data *****							
Country : South Africa				Station : Lwamondo			
Altitude: 648 meter(s) above M.S.L.				Longitude: 30.37 Deg. (East)			
Latitude: -23.04 Deg. (South)							
Month	MaxTemp (deg.C)	MinTemp (deg.C)	Humidity (%)	wind spd. (km/d)	sunshine (Hours)	Solar Rad. (MJ/m2/d)	ETo (mm/d)
January	29.5	19.9	65.6	85.1	6.6	21.1	4.62
February	27.7	19.1	59.8	73.3	6.1	19.6	4.16
March	28.3	18.7	67.8	71.0	6.4	18.5	3.78
April	26.8	16.1	65.3	69.0	6.8	16.5	3.11
May	24.1	12.2	58.8	74.1	7.3	14.6	2.47
June	22.2	10.2	56.3	77.6	6.7	12.7	2.10
July	23.0	10.1	58.1	84.3	7.4	13.9	2.33
August	25.0	11.8	55.9	98.9	7.7	16.5	3.11
September	25.9	13.4	52.7	103.9	7.1	18.3	3.78
October	28.0	16.3	58.8	110.7	6.7	19.8	4.37
November	28.4	17.9	61.5	96.5	6.0	19.9	4.41
December	29.4	19.3	63.6	88.7	6.2	20.6	4.58
Average	26.5	15.4	60.4	86.1	6.8	17.7	3.57
Pen-Mon equation was used in Eto calculations with the following values for Angstrom's Coefficients: a = 0.25      b = 0.5							
*****							

Cropwat 4 windows Ver 4.3 Climate and ETo (grass) Data							
Country : South Africa				Station : Madzivhandila			
Altitude: 517 meter(s) above M.S.L.				Longitude: 30.55 Deg. (East)			
Latitude: -22.98 Deg. (South)							
Month	MaxTemp (deg.C)	MinTemp (deg.C)	Humidity (%)	wind spd. (km/d)	Sunshine (Hours)	Solar Rad. (MJ/m2/d)	ETo (mm/d)
January	30.6	19.1	45.7	6.0	6.5	21.0	3.90
February	28.5	19.4	64.1	7.0	3.7	15.8	3.13
March	29.0	18.7	47.1	5.5	6.1	18.0	3.14
April	27.5	15.0	45.6	0.0	5.6	14.9	2.22
May	26.3	10.0	57.2	0.0	6.6	13.8	1.71
June	24.9	8.4	58.4	2.9	6.0	12.0	1.38
July	24.0	7.5	57.0	5.8	5.6	12.0	1.45
August	26.2	9.5	57.2	6.8	6.8	15.4	2.12
September	28.5	13.4	38.2	7.9	4.4	14.6	2.42
October	29.0	15.2	51.5	20.4	4.6	16.6	3.18
November	28.9	18.2	56.6	0.0	4.3	17.2	3.25
December	30.9	18.9	56.7	0.0	4.2	17.4	3.40
Average	27.9	14.4	52.9	5.2	5.4	15.7	2.61
pen-Mon equation was used in ETo calculations with the following values for Angstrom's coefficients: a = 0.25      b = 0.5							

***** Cropwat 4 windows ver 4.3 Climate and ETo (grass) Data *****							
Country : South Africa				Station : Thohoyandou			
Altitude: 730 meter(s) above M.S.L.				Longitude: 30.49 Deg. (East)			
Latitude: -22.94 Deg. (South)							
Month	MaxTemp (deg.C)	MinTemp (deg.C)	Humidity (%)	wind spd. (km/d)	Sunshine (Hours)	Solar Rad. (MJ/m2/d)	ETo (mm/d)
January	28.8	20.3	69.7	77.8	8.6	24.3	5.00
February	29.9	20.3	65.1	88.1	7.0	21.0	4.60
March	28.4	19.1	66.4	69.6	8.1	21.0	4.15
April	26.3	17.1	65.2	65.7	2.2	10.4	2.40
May	25.5	15.4	56.5	61.6	4.6	11.5	2.26
June	23.6	13.5	53.9	69.6	3.1	8.9	1.94
July	22.2	12.5	54.6	69.3	2.6	8.7	1.90
August	25.2	13.9	50.8	79.9	1.8	9.2	2.42
September	28.2	16.3	51.3	100.7	3.0	12.6	3.36
October	28.5	17.6	59.0	108.4	3.6	15.1	3.80
November	28.9	18.6	64.4	94.6	4.2	17.0	4.01
December	28.7	19.9	69.2	84.8	1.0	12.3	5.31
Average	27.0	17.0	60.5	80.8	4.2	14.3	3.43
-----							
Pen-Mon equation was used in ETo calculations with the following values for Angstrom's coefficients: a = 0.25                      b = 0.5 *****							

\*\*\*\*\*

Cropwat 4 windows ver 4.3 Climate and ETo (grass) Data

\*\*\*\*\*

Country : South Africa  
Altitude: 712 meter(s) above M.S.L.  
Latitude: -22.97 Deg. (South)

Station : university of venda (univen)  
Longitude: 30.44 Deg. (East)

Month	MaxTemp (deg.C)	MinTemp (deg.C)	Humidity (%)	wind spd. (km/d)	sunshine (Hours)	Solar Rad. (MJ/m2/d)	ETo (mm/d)
January	29.6	19.8	66.9	92.6	2.6	14.7	3.69
February	30.6	20.0	66.6	106.6	3.4	15.4	3.91
March	28.7	18.1	69.1	87.3	9.0	22.3	4.41
April	27.0	15.4	67.8	74.1	2.6	11.0	2.52
May	26.1	11.9	62.5	75.7	5.3	12.3	2.40
June	24.1	9.9	60.3	85.0	9.8	16.0	2.41
July	23.5	9.2	58.8	83.5	7.6	14.2	2.36
August	25.9	10.7	53.9	109.9	0.1	7.1	2.56
September	26.0	16.0	50.3	129.1	3.2	12.9	3.52
October	25.9	19.4	57.4	132.7	3.9	15.6	3.90
November	29.3	18.0	64.3	109.2	3.9	16.6	4.06
December	29.8	19.5	64.4	104.0	4.8	18.3	4.38
-----							
Average	27.2	15.7	61.9	99.1	4.7	14.7	3.34
-----							
pen-mon equation was used in ETo calculations with the following values							
for Angstrom's coefficients:							
a = 0.25      b = 0.5							
*****							



\*\*\*\*\*  
Cropwat 4 windows Ver 4.3 Climate and ETo (grass) Data  
\*\*\*\*\*

Country : South Africa		Station : Mhinga					
Altitude: 460 meter(s) above M.S.L.		Longitude: 30.84 Deg. (East)					
Latitude: -22.79 Deg. (South)							
Month	MaxTemp (deg.C)	MinTemp (deg.C)	Humidity (%)	wind spd. (Km/d)	sunshine (Hours)	solar Rad. (MJ/m2/d)	ETo (mm/d)
January	31.1	20.5	70.0	32.8	1.7	13.3	3.09
February	32.6	19.8	64.5	35.6	2.5	14.0	3.25
March	32.2	18.5	63.8	33.5	1.6	11.4	2.69
April	29.0	15.8	65.0	30.8	0.4	8.1	1.93
May	28.2	12.0	61.9	32.7	1.5	8.0	1.74
June	26.5	8.9	59.2	36.6	3.0	8.8	1.66
July	25.0	8.4	59.9	40.4	3.4	9.6	1.74
August	27.6	9.6	55.9	46.7	0.0	7.0	1.94
September	31.1	14.0	51.9	58.8	1.0	9.8	2.73
October	31.9	17.8	56.2	58.8	1.4	11.7	3.12
November	31.5	19.0	62.8	49.4	1.2	12.3	3.10
December	31.3	20.2	67.1	38.4	1.2	12.6	3.05
Average	29.8	15.4	61.5	41.2	1.6	10.5	2.50

Pen-Mon equation was used in ETo calculations with the following values  
for Angstrom's Coefficients:

a = 0.25      b = 0.5

\*\*\*\*\*